

SANDIA REPORT

SAND86-2311 • UC-70

Unlimited Release

Printed March 1987

RS-8232-2/65322

C.1



8232-2//065322



00000001 -

Analysis of Pumping Tests of the Culebra Dolomite Conducted at the H-3 Hydropad at the Waste Isolation Pilot Plant (WIPP) Site

Richard L. Beauheim

Prepared by
Sandia National Laboratories
Albuquerque, New Mexico 87185 and Livermore, California 94550
for the United States Department of Energy
under Contract DE-AC04-76DP00789

1051581

Issued by Sandia National Laboratories, operated for the United States Department of Energy by Sandia Corporation.

NOTICE: This report was prepared as an account of work sponsored by an agency of the United States Government. Neither the United States Government nor any agency thereof, nor any of their employees, nor any of their contractors, subcontractors, or their employees, makes any warranty, express or implied, or assumes any legal liability or responsibility for the accuracy, completeness, or usefulness of any information, apparatus, product, or process disclosed, or represents that its use would not infringe privately owned rights. Reference herein to any specific commercial product, process, or service by trade name, trademark, manufacturer, or otherwise, does not necessarily constitute or imply its endorsement, recommendation, or favoring by the United States Government, any agency thereof or any of their contractors or subcontractors. The views and opinions expressed herein do not necessarily state or reflect those of the United States Government, any agency thereof or any of their contractors or subcontractors.

Printed in the United States of America
Available from
National Technical Information Service
U.S. Department of Commerce
5285 Port Royal Road
Springfield, VA 22161

NTIS price codes
Printed copy: A08
Microfiche copy: A01

Analysis of Pumping Tests of the Culebra Dolomite Conducted at the H-3 Hydropad at the Waste Isolation Pilot Plant (WIPP) Site

Richard L. Beauheim
Earth Sciences Division
Sandia National Laboratories
Albuquerque, NM 87185

Abstract

Two pumping tests were conducted in the Culebra Dolomite Member of the Rustler Formation at the H-3 hydropad at the Waste Isolation Pilot Plant (WIPP) site. The first test was in 1984, with well H-3b3 pumped for 14 days at an average rate of 4 gpm. The second test, the H-3 multipad test, was in late 1985 and early 1986, with well H-3b2 pumped for 62 days at an average rate of 4.8 gpm. Both tests provided information on the hydraulic properties of the Culebra at the H-3 hydropad. The second test provided information on average Culebra hydraulic properties on a much larger scale; responses were observed up to 8000 ft from the pumping well.

The interpretation of these tests had three principal objectives. The first was to determine the most appropriate conceptualization of the nature of the Culebra flow system around the H-3 hydropad. The pumping well responses during the H-3 tests appear to be those of wells completed in a double-porosity medium with unrestricted interporosity flow. In such a system, fractures provide the bulk of the permeability, while matrix pores provide the majority of the storage capacity. The importance of fracture flow is indicated by the speed with which the observation

Abstract (concluded)

wells on the H-3 hydropad respond to pumping, and the nearly identical behaviors of these wells and the pumping well. The similarity between pumping- and observation-well behavior on the H-3 hydropad is so pronounced that the responses of all three wells on the hydropad can be interpreted only by using pumping-well analytical techniques, not observation-well analytical techniques. H-3b1 and H-3b3, in particular, appear to be very well connected by fractures.

The second objective was to quantify the hydraulic properties of the Culebra in the vicinity of the H-3 hydropad. The total-system (fractures plus matrix) transmissivity of the Culebra derived from the first test is $2.9 \text{ ft}^2/\text{day}$; that from the second test is $1.7 \text{ ft}^2/\text{day}$. The lower value derived from the second test probably represents lower transmissivity (lower fracture connectivity) at H-3b2 than at H-3b3, and/or lower average transmissivity of the volume of Culebra stressed in the multipad test as opposed to the smaller volume stressed in the first test. The fracture-to-total-system storativity ratios derived from the various analyses range from 0.03 to 0.25, indicating a relatively high degree of storage within the fractures. The highest storativity ratios were consistently found at H-3b1. Wellbore skin values are highly negative, indicating direct wellbore connection with fractures.

The third objective was to quantify the average hydraulic properties of the Culebra between the H-3 hydropad and more-distant observation wells. Meeting this objective was complicated by the effects of an apparent increase in groundwater leakage from the Culebra into the Waste-Handling Shaft on the data from wells near that shaft, and by water-level/pressure trends already existing at many of the observation wells when the multipad test began. Between H-3 and wells DOE-1 and H-11 to the southeast, the average apparent Culebra transmissivity is between 5.5 and $13 \text{ ft}^2/\text{day}$, and the apparent storativity is between 6.6×10^{-6} and 1.0×10^{-5} . The rapid responses observed at DOE-1 and H-11 during the multipad test, and the associated relatively high transmissivities, indicate a preferential hydraulic connection, probably related to fractures, between H-3 and the southeast portion of the WIPP site.

Between H-3 and wells H-1 and H-2 to the north-northwest, the apparent transmissivity is between 0.46 and $2.5 \text{ ft}^2/\text{day}$, and the apparent storativity is between 2.7×10^{-5} and 4.5×10^{-5} . If the possible shaft-leakage effects are ignored, the apparent transmissivity between H-3 and wells WIPP-19, 21, and 22 to the north is between 1.1 and $2.9 \text{ ft}^2/\text{day}$, and the apparent storativity is between 9.0×10^{-6} and 2.9×10^{-5} . If shaft leakage did, as is believed, affect the responses observed at WIPP-19, 21, and 22, then the transmissivity values listed above are not representative. The wells to the north of H-3 are not so well connected hydraulically to H-3 as are DOE-1 and H-11, and provided no indications that groundwater flow was occurring primarily through fractures.

The interpretations presented in this report represent an analytical approach to the understanding of large-scale tests. In an aquifer with considerable areal heterogeneity, an analytical approach has significant limitations. Calculated transmissivities and storativities are only "apparent" values, representing the average response of large volumes of aquifer to a stress imposed at a certain location. These interpretations are most useful in qualitatively defining areas of "higher" and "lower" transmissivity. Quantitative evaluation/simulation of heterogeneous systems on a large scale is best attempted with numerical models, an effort now under way.

Acknowledgments

The author thanks Wayne Stensrud, George Saulnier, Kent Lantz, Jeff Palmer, Michael Bame, and Geoff Freeze for their help in performing the H-3 multipad test. Dave Tomasko, Al Lappin, Jerry Mercer, John Pickens, and George Saulnier provided helpful review comments on the original manuscript of this document. Mary Gonzalez's help with the data preparation is also greatly appreciated.

Contents

1. Introduction.....	11
2. Site Hydrogeology.....	13
3. Monitoring Wells	15
3.1 Test 1	15
3.2 Test 2 (Multipad Test)	15
4. Test Instrumentation	18
4.1 Test 1	18
4.2 Test 2 (Multipad Test)	18
5. Test Data	28
5.1 Test 1	28
5.2 Test 2 (Multipad Test)	32
5.2.1 Observed Data	32
5.2.2 Extraneous Trends and Modified Data	49
6. Test Results.....	54
6.1 Test 1.....	54
6.1.1 H-3b3 (Pumping Well)	54
6.1.2 H-3b1 and H-3b2	57
6.1.3 DOE-1	60
6.2 Test 2 (Multipad Test)	62
6.2.1 H-3 Hydropad	62
6.2.2 Observation Wells	72
6.3 Comparison of 1984 and Multipad Test Results	88
7. Summary and Conclusions	89
APPENDIX A—1984 H-3 Pumping Test Data	91
APPENDIX B—H-3 Multipad Pumping Test Data	101
APPENDIX C—Techniques for Analyzing Multiwell Pumping Test Data	135
References	148

Figures

1-1 Location of the H-3 Test Site Relative to the WIPP Site Observation-Well Network	12
2-1 WIPP Area Stratigraphic Column	14
3-1 Plan View of the Wells at the H-3 Hydropad.....	16
3-2 Stratigraphy and Well-Construction Details for the H-3 Hydropad	17
4-1 Configuration of Downhole and Surface Equipment for the 1984 Pumping Test at the H-3 Hydropad	20
4-2 H-3 Data-Acquisition System	21
4-3 Configuration of the Test Equipment in the Wells at the H-3 Hydropad During the H-3 Multipad Pumping Test	22
4-4 Flow-Regulation and Discharge-Measurement System for the H-3 Multipad Pumping Test.....	23

Figures (continued)

4-5	Configuration of the Test Equipment in Observation Well H-2c During the H-3 Multipad Pumping Test.....	24
4-6	Configuration of the Test Equipment in Observation Well H-4b During the H-3 Multipad Pumping Test.....	25
4-7	Configuration of the Test Equipment in Observation Well H-11b3 During the H-3 Multipad Pumping Test.....	26
4-8	Configuration of the Test Equipment in Observation Well DOE-1 During the H-3 Multipad Pumping Test.....	27
5-1	Pressure Responses in Wells H-3b1, H-3b2, and H-3b3 During the 1984 H-3 Pumping Test.....	29
5-2	Water-Level Response in Well H-1 During the 1984 H-3 Pumping Test.....	30
5-3	Water-Level Response in Well DOE-1 During the 1984 H-3 Pumping Test.....	31
5-4	Pressure Responses in Wells H-3b1, H-3b2, and H-3b3 During the H-3 Multipad Pumping Test.....	33
5-5	Pressure Response in Observation Well H-2c During the H-3 Multipad Pumping Test.....	34
5-6	Pressure Response in Observation Well H-4b During the H-3 Multipad Pumping Test.....	35
5-7	Pressure Response in Observation Well H-11b3 During the H-3 Multipad Pumping Test.....	36
5-8	Pressure Response in Observation Well DOE-1 During the H-3 Multipad Pumping Test.....	37
5-9	Water Levels Measured in Observation Well H-1 (Culebra) During the H-3 Multipad Pumping Test.....	38
5-10	Water Levels Measured in Observation Well H-2b2 During the H-3 Multipad Pumping Test.....	39
5-11	Water Levels Measured in Observation Well H-6b During the H-3 Multipad Pumping Test.....	40
5-12	Water Levels Measured in Observation Wells H-11b1 and H-11b2 During the H-3 Multipad Pumping Test.....	41
5-13	Water Levels Measured in Observation Well WIPP-18 During the H-3 Multipad Pumping Test.....	42
5-14	Water Levels Measured in Observation Well WIPP-19 During the H-3 Multipad Pumping Test.....	43
5-15	Water Levels Measured in Observation Well WIPP-21 During the H-3 Multipad Pumping Test.....	44
5-16	Water Levels Measured in Observation Well WIPP-22 During the H-3 Multipad Pumping Test.....	45
5-17	Water Levels Measured in Observation Well P-14 During the H-3 Multipad Pumping Test.....	46
5-18	Water Levels Measured in Observation Well P-15 During the H-3 Multipad Pumping Test.....	47
5-19	Water Levels Measured in Observation Well P-17 During the H-3 Multipad Pumping Test.....	48
5-20	Pressure Response of the Culebra Transducer in the Waste-Handling Shaft During the H-3 Multipad Pumping Test.....	51
5-21	Water Levels Measured in Observation Well H-1 (Magenta) During the H-3 Multipad Pumping Test.....	52
5-22	Water Levels Measured in Observation Well H-2b1 (Magenta) During the H-3 Multipad Pumping Test.....	53
6-1	1984 H-3 Pumping Test—H-3b3 Sequence Plot With INTERPRET Simulation.....	55
6-2	1984 H-3 Pumping Test—H-3b3 Drawdown Log-Log Plot With INTERPRET Simulation.....	56
6-3	1984 H-3 Pumping Test—H-3b1 Drawdown Log-Log Plot With INTERPRET Simulation.....	58
6-4	1984 H-3 Pumping Test—H-3b2 Drawdown Log-Log Plot With INTERPRET Simulation.....	59
6-5	1984 H-3 Pumping Test—DOE-1 Pressure Response With INTERPRET Simulation.....	61
6-6	H-3 Multipad Pumping Test—H-3b2 Drawdown Log-Log Plot With INTERPRET Simulation.....	63
6-7	H-3 Multipad Pumping Test—H-3b2 Sequence Plot With INTERPRET Simulation.....	64
6-8	H-3 Multipad Pumping Test—H-3b2 Recovery Log-Log Plot With INTERPRET Simulation.....	65
6-9	H-3 Multipad Pumping Test—H-3b2 Drawdown Dimensionless Horner Plot With INTERPRET Simulation.....	67
6-10	H-3 Multipad Pumping Test—H-3b2 Recovery Dimensionless Horner Plot With INTERPRET Simulation.....	68
6-11	H-3 Multipad Pumping Test—H-3b1 Drawdown Log-Log Plot With INTERPRET Simulation.....	69
6-12	H-3 Multipad Pumping Test—H-3b3 Drawdown Log-Log Plot With INTERPRET Simulation.....	70
6-13	H-3 Multipad Pumping Test—H-3b3 Recovery Dimensionless Horner Plot With INTERPRET Simulation.....	71
6-14	H-3 Multipad Pumping Test—H-1 Pressure Response With INTERPRET Simulation.....	73

Figures (continued)

6-15	H-3 Multipad Pumping Test—H-1 Pressure Response Modified for 1.3 Ft/15 Days Water-Level Trend With INTERPRET Simulation	74
6-16	H-3 Multipad Pumping Test—H-2b2 Pressure Response With INTERPRET Simulation	75
6-17	H-3 Multipad Pumping Test—H-2b2 Pressure Response Modified for 0.57 Ft/15 Days Water-Level Trend With INTERPRET Simulation	76
6-18	H-3 Multipad Pumping Test—H-11b1 Pressure Response With INTERPRET Simulation	78
6-19	H-3 Multipad Pumping Test—H-11b1 Pressure Response Modified for 0.425 Ft/15 Days Water-Level Trend With INTERPRET Simulation	79
6-20	H-3 Multipad Pumping Test—DOE-1 Pressure Response With INTERPRET Simulation	80
6-21	H-3 Multipad Pumping Test—DOE-1 Pressure Response Modified for 0.27 psi/15 Days Pressure Trend With INTERPRET Simulation	81
6-22	H-3 Multipad Pumping Test—WIPP-19 Pressure Response With INTERPRET Simulation	82
6-23	H-3 Multipad Pumping Test—WIPP-21 Pressure Response With INTERPRET Simulation	83
6-24	H-3 Multipad Pumping Test—WIPP-22 Pressure Response With INTERPRET Simulation	84
6-25	Comparison of Culebra Pressure Trends at the Waste-Handling Shaft and WIPP-21	86

Tables

3-1	Positions of Observation Wells Relative to Pumping Well H-3b2	15
5-1	Response Times and Maximum Drawdowns at Multipad-Test Observation Wells	49
6-1	Summary of Interpretive Results From 1984 H-3 Pumping Test	54
6-2	1985 H-3b2 Pumping History	62
6-3	Summary of Multipad-Test Interpretive Results From H-3 Wells	66
6-4	Summary of Multipad-Test Observation-Well Response Interpretations	72

Analysis of Pumping Tests of the Culebra Dolomite Conducted at the H-3 Hydropad at the Waste Isolation Pilot Plant (WIPP) Site

1. Introduction

This report presents the results of two pumping tests on the Culebra Dolomite Member of the Rustler Formation at the H-3 hydropad south of the Waste Isolation Pilot Plant (WIPP) site in southeastern New Mexico (Figure 1-1). The WIPP is a US Department of Energy research and development facility designed to demonstrate the safe disposal of transuranic radioactive wastes resulting from the nation's defense programs. The WIPP facility will lie in bedded halite in the lower Salado Formation. The tests reported here were conducted in the Rustler Formation, which overlies the Salado Formation, under the technical direction of Sandia National Laboratories (SNL), Albuquerque, NM.

The H-3 hydropad lies in the southeast quarter of Section 29, Township 22 South, Range 31 East, ~4300 ft south of the WIPP Construction and Salt-Handling Shaft. The hydropad contains three wells,

H-3b1, H-3b2, and H-3b3, which are completed in the Culebra dolomite.

Two long-term pumping tests have been conducted at the H-3 hydropad. Well H-3b3 was pumped at a rate of ~4 gallons per minute (gpm) from April 23 to May 7, 1984 (Julian days 114 to 128) to provide data on the hydraulic properties of the Culebra at the H-3 hydropad and to create a stable flow field for a subsequent tracer test. From October 15 to December 16, 1985 (Julian days 288 to 350), well H-3b2 was pumped at a rate of ~4.8 gpm to create a hydraulic stress that would be felt over the southern part of the WIPP site. This test, known as the H-3 (or southern) multipad test, caused observable responses up to 8000 ft from the pumping well. The interpretation of these two tests is the subject of this report.

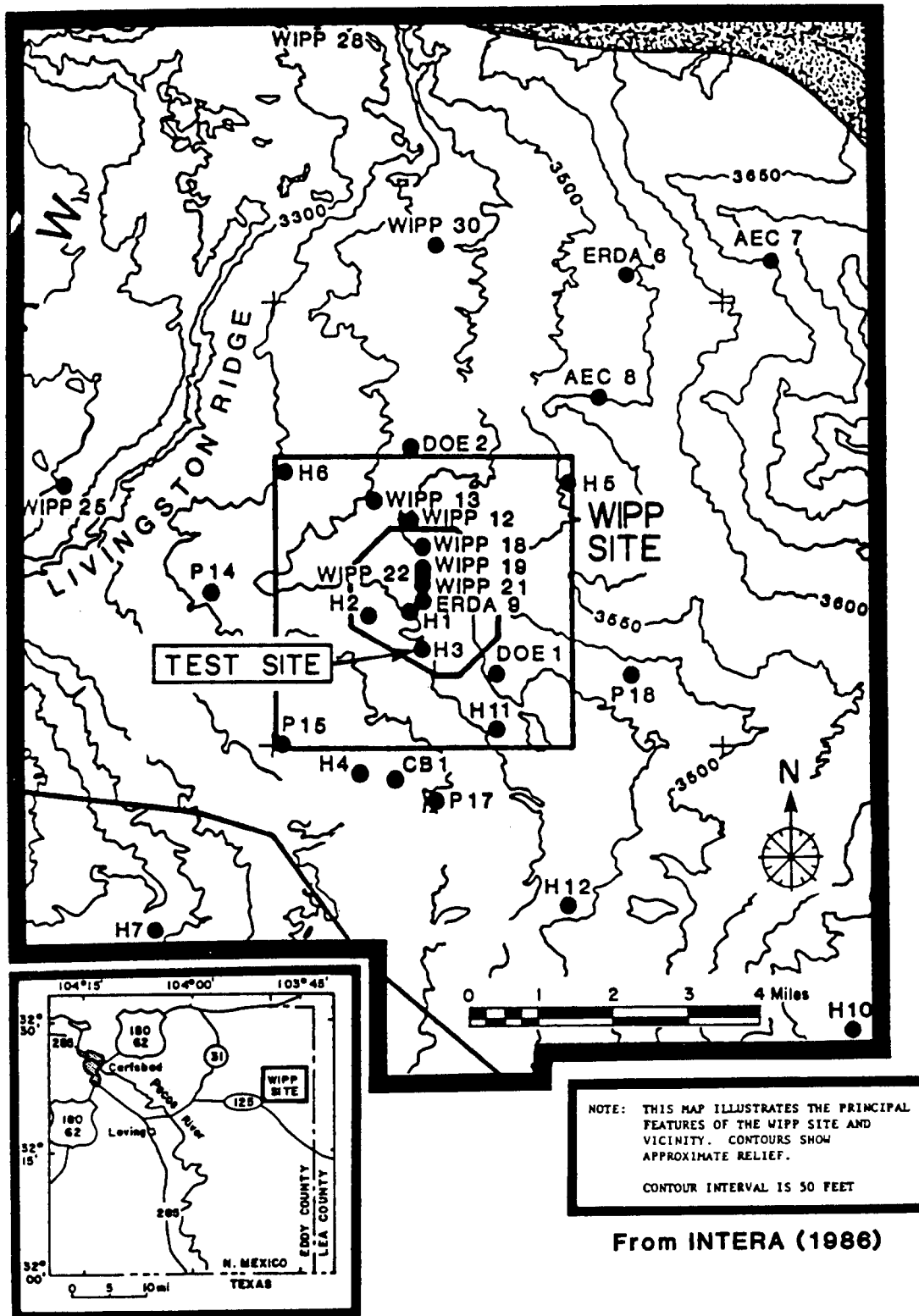


Figure 1-1. Location of the H-3 Test Site Relative to the WIPP Site Observation-Well Network

2. Site Hydrogeology

The WIPP site is located in the northern part of the Delaware Basin in southeastern New Mexico. WIPP-site geologic investigations have concentrated on the upper seven formations typically found in that part of the Delaware Basin: in ascending order, the Bell Canyon Formation, the Castile Formation, the Salado Formation, the Rustler Formation, the Dewey Lake Red Beds, the Dockum Group, and the Gatuña Formation (Figure 2-1). All these formations are of Permian age, except for the Dockum Group, which is of Triassic age, and the Gatuña, a Quaternary deposit. Of these formations, only the Bell Canyon and the Rustler contain saturated intervals that are regionally continuous and permeable enough to allow testing by standard hydrogeological techniques.

The Rustler Formation lies from 502 to 821 ft below ground surface at the H-3 hydropad (Mercer, 1983). At this location, the Rustler consists of five mappable members (in ascending order): the unnamed lower member, the Culebra Dolomite Member, the Tamarisk Member, the Magenta Dolomite Member, and the Forty-niner Member. The Culebra dolomite, which lies from 672 to 694 ft deep at H-3b1 (Mercer, 1983), is the principal water-bearing member of the Rustler. At H-3, the Culebra is a light olive-gray, fine-grained, vuggy silty dolomite. Poor core

recovery at H-3b2 (~15%) may be related, in part, to extensive fracturing of the Culebra. The Culebra is considered to be the most important potential groundwater-transport pathway for radionuclides that may escape from the WIPP facility to reach the accessible environment. The vast majority of hydrologic tests performed at the WIPP site have examined the hydraulic properties of the Culebra.

The Culebra is confined by the underlying unnamed member, composed of a layered sequence of clayey silt, anhydrite, and halite, and by the overlying Tamarisk Member, composed of anhydrite and gypsum with a single clayey silt interbed. The stabilized Culebra water level in September 1977 at H-3b1 was ~405 ft below ground surface (Mercer and Orr, 1979), or ~267 ft above the top of the unit. The water level was ~11 ft lower in September 1985 (INTERA Technologies, 1986) before the H-3 multipad test, apparently in response to the continued drainage of Culebra water into the WIPP shafts since 1981.

The Culebra fluid at H-3 has a total dissolved solids concentration of ~56,000 mg/L, primarily because of sodium and chloride (Robinson, in preparation), and a specific gravity of ~1.037 at 23°C (INTERA Technologies, 1986).

SYSTEM	SERIES	GROUP	FORMATION	MEMBER
RECENT	RECENT		SURFICIAL DEPOSITS	
QUATERNARY	PLEISTOCENE		MESCALERO CALICHE	
			GATUÑA	
TRIASSIC		DOCKUM	UNDIVIDED	
PERMIAN	OCHOAN		DEWEY LAKE RED BEDS	
			RUSTLER	Forty-niner
				Magenta
				Tamarisk
				Culebra
				Unnamed
	SALADO	Upper		
		McNutt		
		Lower		
	CASTILE			
	GUADALUPIAN	DELAWARE MOUNTAIN	BELL CANYON	
			CHERRY CANYON	
BRUSHY CANYON				

From Kelley and Pickens (1986)

Figure 2-1. WIPP Area Stratigraphic Column

3. Monitoring Wells

Different pumping and observation wells were used for the two H-3 pumping tests. The second test, the H-3 multipad test, was designed on a larger scale and involved a much greater number of observation wells than the first, including several wells that did not exist at the time of the first test. The well networks used for each test are discussed below.

3.1 Test 1

The primary monitoring wells for the first H-3 test were the three on the H-3 hydropad itself. H-3b3 was the pumping well for this test, and H-3b1 and H-3b2 were the principal observation wells. The wells on the H-3 hydropad form a roughly equilateral triangle with 100-ft sides (Figure 3-1). Well H-3b1 (originally known simply as H-3) was drilled and cased to the top of the Salado Formation in 1976 (Mercer and Orr, 1979). The casing was perforated across the Rustler-Salado contact, the Culebra dolomite (perforation interval 675 to 703 ft deep; see Figure 3-2), and the Magenta dolomite in 1977. After bailing tests, a bridge plug was set in the casing below the Culebra, and a production-injection packer (PIP) on 2.375-in. tubing was set between the Culebra and the Magenta (Figure 3-2), allowing access to the Culebra through the tubing. Wells H-3b2 and H-3b3 were drilled through the Culebra, and cased to above the Culebra, in 1983 and 1984 (HydroGeoChem, 1985; Figure 3-2).

Water levels were also measured in wells H-1 and DOE-1 (Figure 1-1) during the first H-3 test. H-1 is completed in the same manner as H-3b1, with access to the Culebra through tubing and a PIP (Mercer and Orr, 1979). H-1 is ~2775 ft from H-3b3 in the direction N18°W. Well DOE-1 is cased from the surface to the upper Salado Formation and perforated across the Culebra interval, with a bridge plug set ~15 ft below the Culebra (HydroGeoChem, 1985). DOE-1 is ~5220 ft from H-3b3 in the direction S69°E.

3.2 Test 2 (Multipad Test)

H-3b2 was the pumping well for the second test, and H-3b1 and H-3b3 were observation wells. An automated data-acquisition system (DAS) measured pressures in these wells during the test (Section 4).

Pressures were also measured in wells H-2c, H-4b, H-11b3, and DOE-1 (Figure 1-1) during the test with

automated DASs (Section 4). Inflatable packers isolated the Culebra intervals in all the wells instrumented with DASs. Water levels were measured regularly in H-1, H-2b2, H-6b, H-11b1, WIPP-18, WIPP-19, WIPP-21, WIPP-22, P-14, P-15, and P-17 (Figure 1-1) throughout the test, although not all these wells showed clear responses. The rest of the wells at the WIPP site were monitored approximately every 2 wk during the test as part of the ongoing regional water-level monitoring. In addition, pressure transducers installed in the Culebra dolomite in the Waste-Handling Shaft at the WIPP site were also monitored during the test. Distances and directions from H-3b2 to all the observation wells are listed in Table 3-1.

Table 3-1. Positions of Observation Wells Relative to Pumping Well H-3b2

Observation Well	Distance From H-3b2 (ft)	Direction From H-3b2
H-1	2675	N19°W
H-2b2	4165	N54°W
H-2c	4185	N53°W
H-3b1	91.3*	S69°E*
H-3b3	87.9*	S1°E*
H-4b	9050	S29°W
H-6b	16820	N37°W
H-11b1	7950	S42°E
H-11b3	8005	S42°E
DOE-1	5270	S68°E
P-14	15390	N77°W
P-15	12315	S55°W
P-17	11345	S3°E
WIPP-18	7460	N2°E
WIPP-19	6150	N2°E
WIPP-21	4715	N3°E
WIPP-22	5705	N2°E
W-H Shaft	3840	N5°W
C&SH Shaft	4240	N5°W

*Deviated hole locations at the middle of the Culebra.

H-3 Hydropad

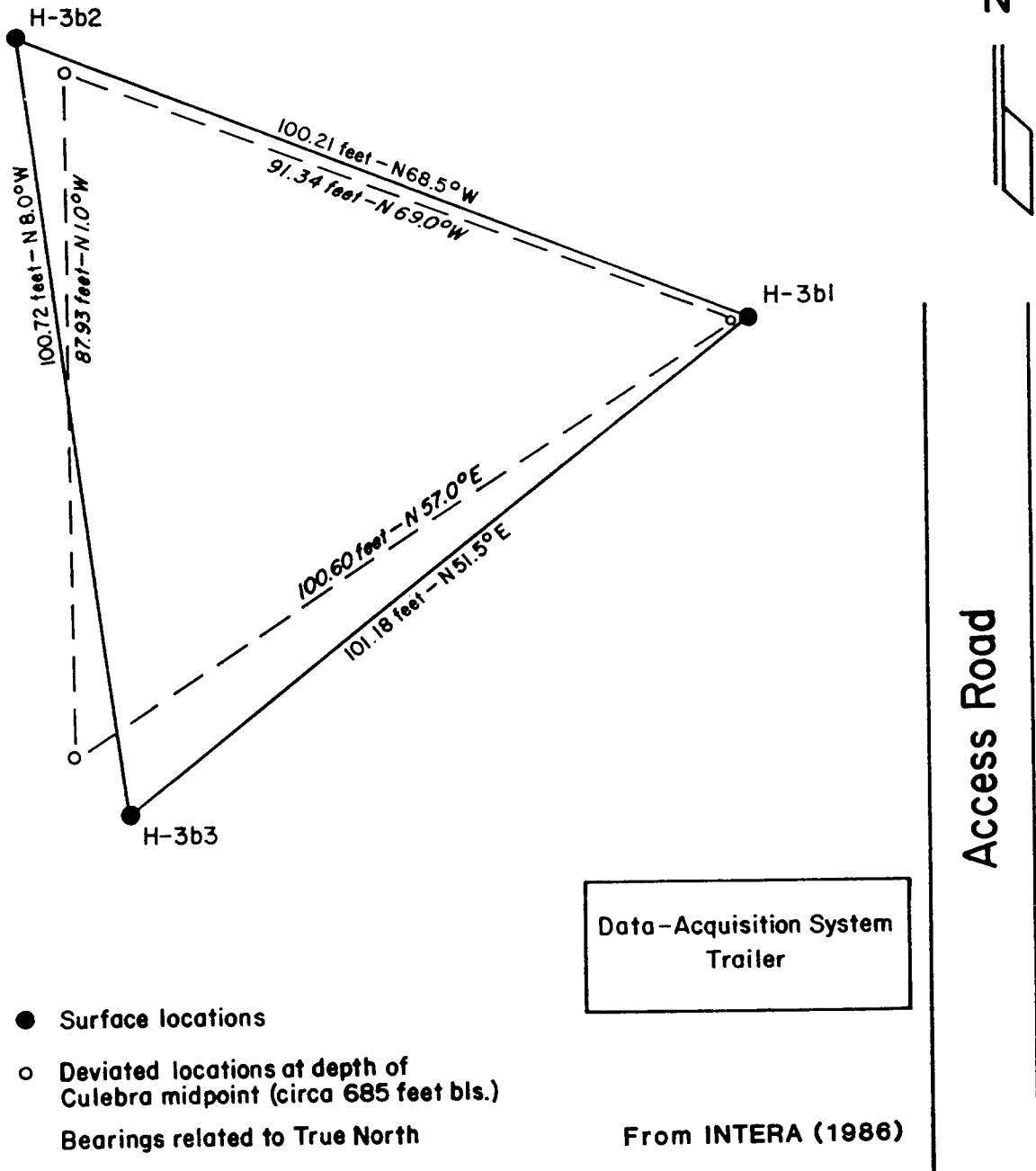


Figure 3-1. Plan View of the Wells at the H-3 Hydropad

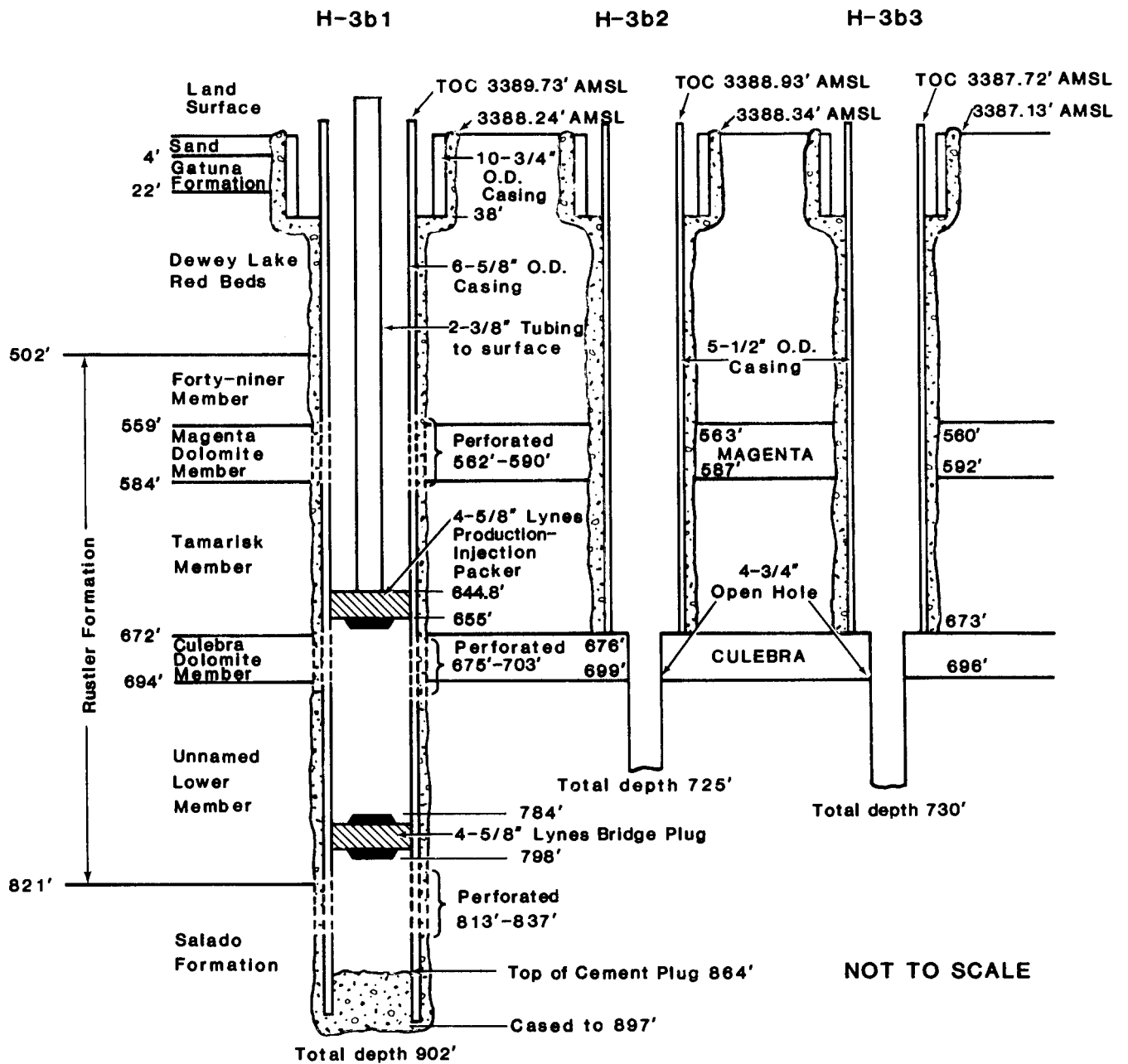


Figure 3-2. Stratigraphy and Well-Construction Details for the H-3 Hydropad

4. Test Instrumentation

The instrumentation used for the two H-3 pumping tests is described in detail in INTERA Technologies (1986). A brief discussion is also presented below. (NOTE: The use of brand names in this report is for identification only, and does not imply endorsement of specific products by Sandia National Laboratories.)

4.1 Test 1

The first H-3 pumping test was fielded by HydroGeoChem, Inc., of Tucson, AZ. The downhole equipment in H-3b3 consisted of a 3-hp Red Jacket 32B pump suspended below a Baski air-inflatable packer, with a Druck PDCR-10 strain-gage transducer strapped to the tubing above the packer (Figure 4-1). The transducer was connected to the test interval below the packer by means of a feedthrough line through the packer. The uphole equipment consisted of a backpressure ball valve and a Precision totalizing flowmeter.

Well H-3b1 had a Druck PDCR-10 transducer suspended in the open 2.375-in. tubing above the PIP isolating the Culebra from the Magenta (Figure 4-1). Well H-3b2 had a similar transducer suspended in the open well casing (Figure 4-1).

The DAS at the surface for the H-3 hydropad consisted of Tektronix PS503A dual power supplies to provide power to the transducers, an HP-3495A signal scanner for channel switching, an HP-3456A digital voltmeter (DVM) to measure the transducer output, an EDC-501J programmable voltage standard to verify the accuracy of the DVM, an HP-9845B desktop computer for system control, and HP-9885M and S floppy disk drives for data storage (Figure 4-2). The HP-3456A DVM and EDC-501J voltage standard are calibrated by the Sandia Standards Laboratory every 6 mo, and the transducers were calibrated in the field with a Heise gage before installation in the wells. The data-acquisition software was written and is maintained by SNL. Additional information on this DAS can be found in INTERA Technologies and HydroGeoChem (1985).

For data storage, the system software for this test automatically converted the millivolt output from the transducers to water levels instead of pressures. This

was done by (1) assigning an initial water level to the initial transducer reading, (2) calculating changes in pressure from the changes in millivolt output using the calibrated sensitivity coefficients, and (3) converting these changes in pressure to changes in water level using an assumed borehole fluid density of 1.00 g/cm³ (HydroGeoChem, 1985).

Water levels in the more distant observation wells, H-1 and DOE-1, were measured with a steel tape and the Iron Horse water-level sounder, respectively (INTERA Technologies and HydroGeoChem, 1985).

4.2 Test 2 (Multipad Test)

The H-3 multipad pumping test was fielded by INTERA Technologies, Inc., of Austin, TX. The downhole equipment at H-3b2 consisted of a 3-hp Red Jacket 32B pump suspended below a Baski air-inflatable packer on 1.5-in. galvanized iron pipe, with two Druck PDCR-10 strain-gage transducers strapped to the tubing above the packer (Figure 4-3). The transducers were connected to the test interval below the packer by means of a feedthrough line through the packer. One of the transducers was used to monitor the test-interval pressure during the test; the second served as a backup transducer that would have been activated if the primary transducer had failed during the test.

The uphole equipment consisted of a backpressure ball valve, a Flow Technology FT-12 analog flowmeter wired to the DAS, a Precision totalizing flowmeter, a Dole orifice valve, and a calibrated standpipe to provide a backup means of measuring flow rate (Figure 4-4). A Weathertronics Model 7105-A analog-output barometer was also connected to the DAS, and provided a record of the barometric pressure at the H-3 hydropad for the duration of the test.

Wells H-3b1 and H-3b3 were also outfitted with packers and transducers. In H-3b1, a Druck PDCR-10 transducer was suspended above a Baski minipacker inside the 2.375-in. tubing above the PIP that isolated the Culebra from the Magenta. A feedthrough line through the minipacker provided a pressure connection for the transducer to the Culebra (Figure 4-3). An additional transducer was suspended in the H-3b1 annulus (Figure 4-3). This transducer measured the

pressure in the Magenta during the test. In H-3b3, a Druck PDCR-10 transducer was suspended above a Baski packer, and accessed the Culebra by means of a feedthrough line (Figure 4-3).

The DAS at the surface for the H-3 hydropad was identical to that used for the first pumping test at the H-3 pad (Section 4.1). For this test, however, the system software did not calculate and store water levels, but instead stored both raw millivolt output from the transducers and calculated pressures.

DASs identical to that used at H-3 were used at the DOE-1 and H-11b3 observation wells during the multipad test. The system controllers at the H-2c and H-4b observation wells were HP-85 computers. The HP-85 records data on tape cartridges instead of floppy disks. Otherwise, the DASs at H-2c and H-4b

were identical to that used at H-3. The downhole equipment configurations for H-2c, H-4b, H-11b3, and DOE-1 are shown in Figures 4-5 through 4-8, respectively.

Water levels in wells were measured with a variety of equipment during the test. A dedicated Solinst water-level meter (INTERA Technologies and Hydro-GeoChem, 1985) was mounted in a box on the H-1 wellhead for the duration of the test. Between readings the probe was kept in the well several inches above the water surface. The Iron Horse was used to make water-level measurements in H-2b2, H-6b, H-11b1, WIPP-18, WIPP-19, WIPP-22, and P-14 (sometimes). Another Solinst meter was used to measure water levels at WIPP-21, P-14 (sometimes), P-15, and P-17.

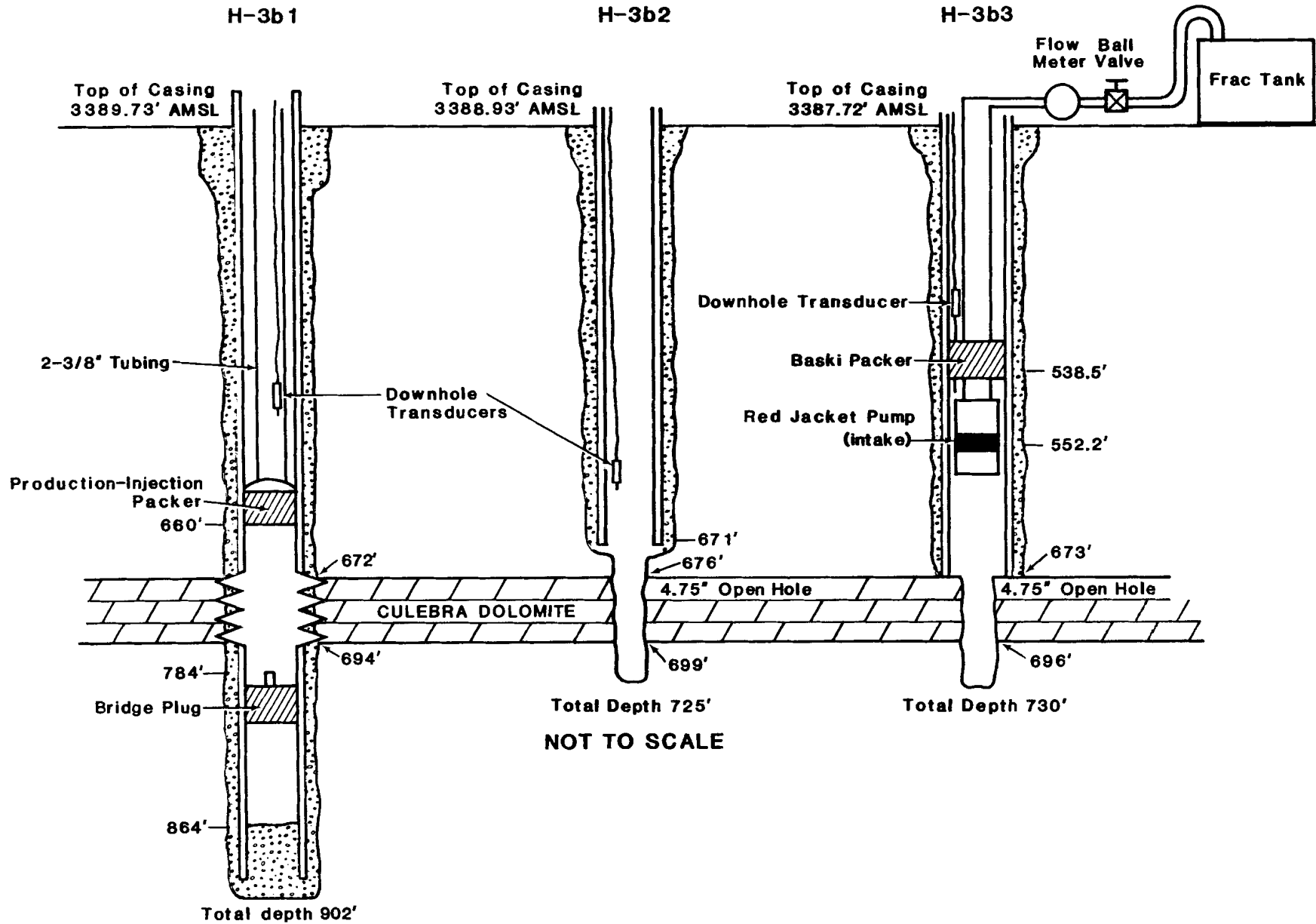


Figure 4-1. Configuration of Downhole and Surface Equipment for the 1984 Pumping Test at the H-3 Hydropad

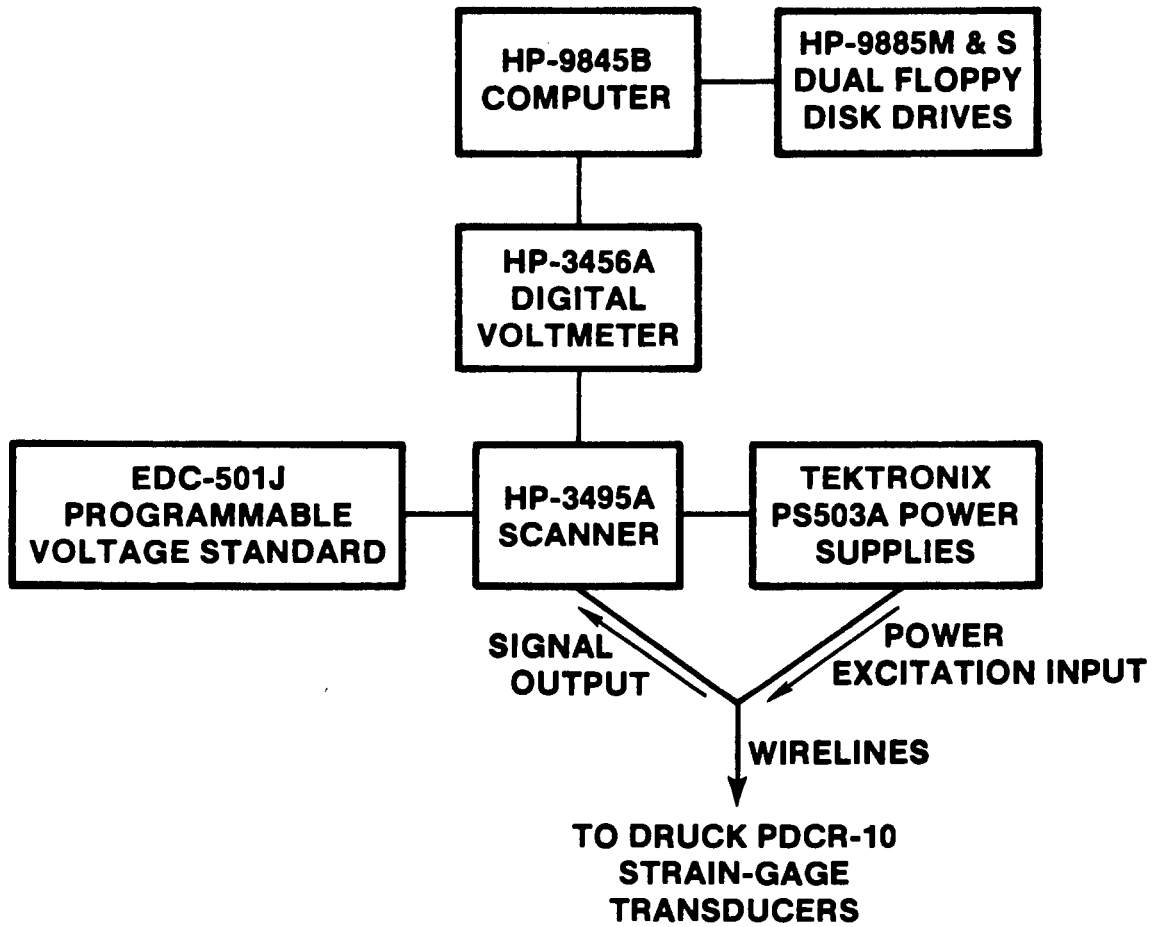


Figure 4-2. H-3 Data-Acquisition System

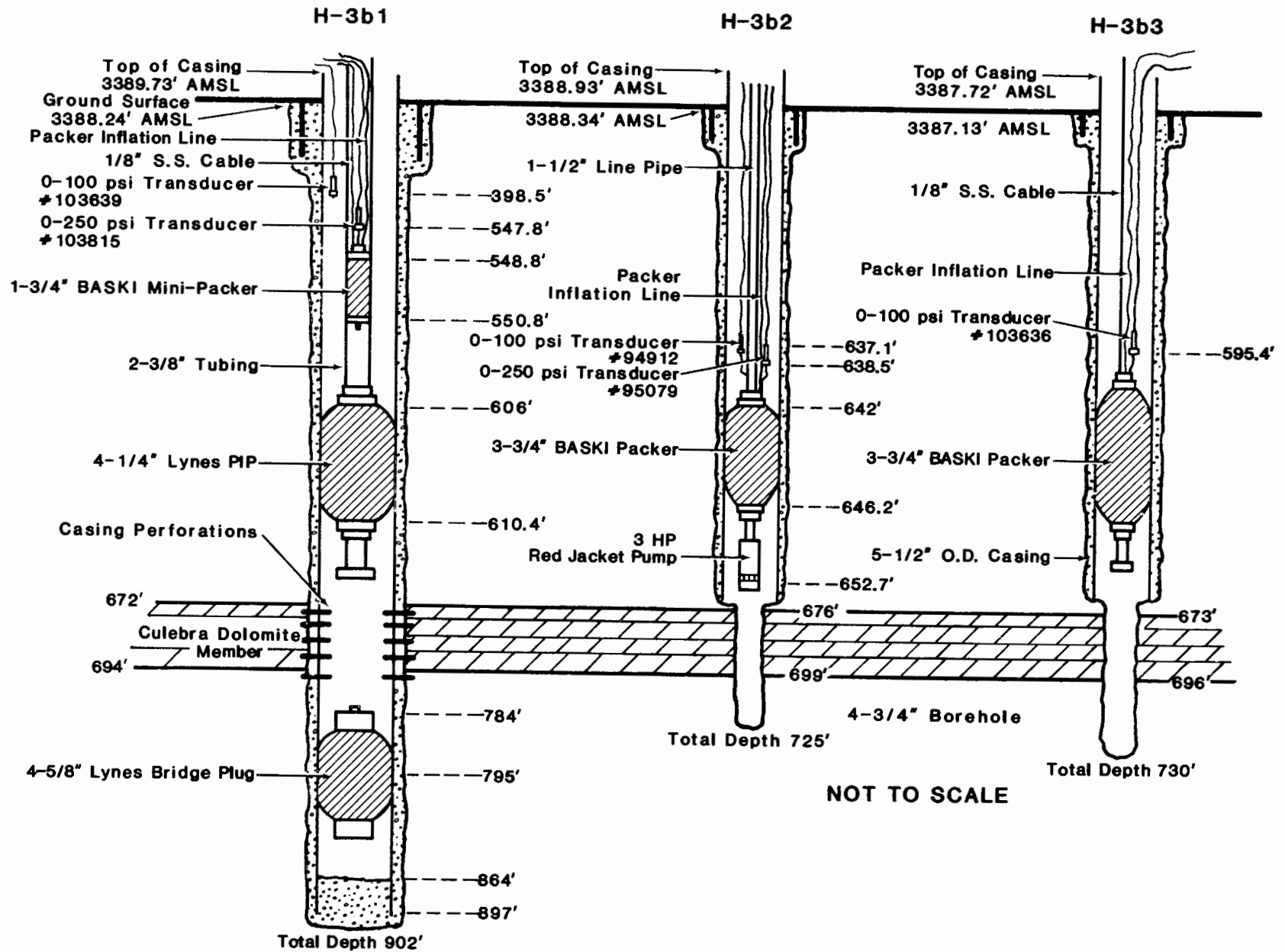
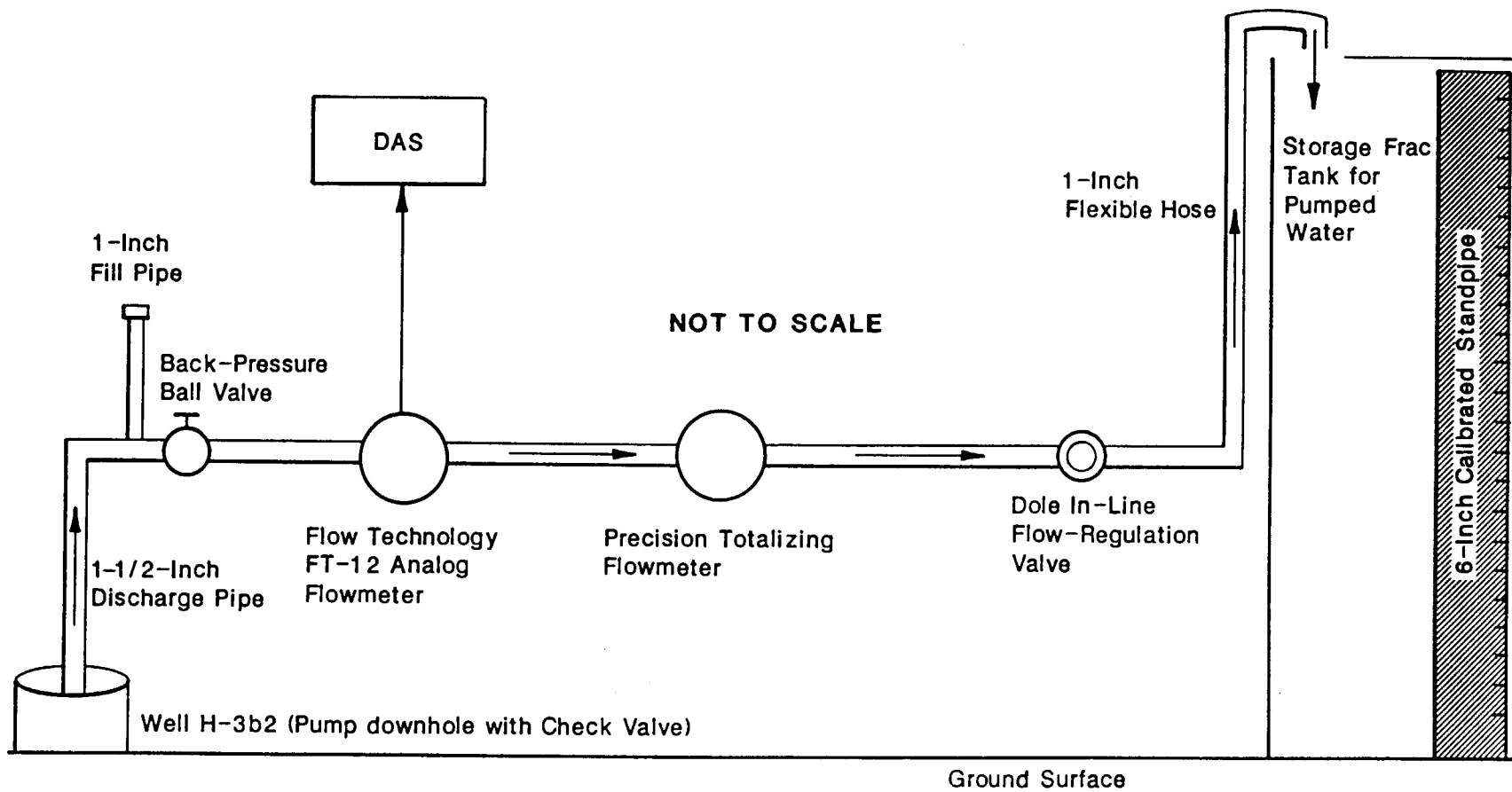


Figure 4-3. Configuration of the Test Equipment in the Wells at the H-3 Hydropad During the H-3 Multipad Pumping Test



From INTERA (1986)

Figure 4-4. Flow-Regulation and Discharge-Measurement System for the H-3 Multipad Pumping Test

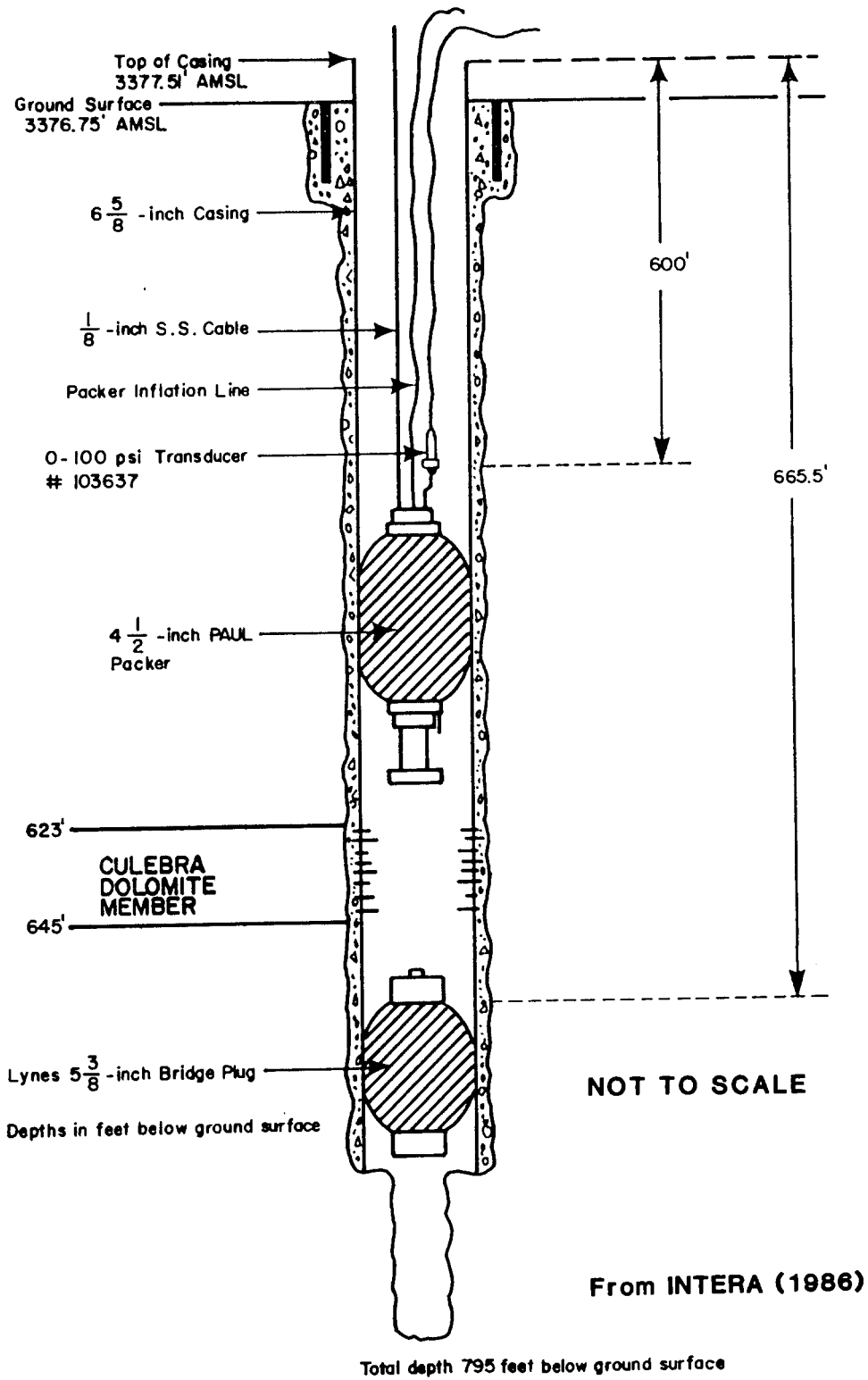


Figure 4-5. Configuration of the Test Equipment in Observation Well H-2c During the H-3 Multipad Pumping Test

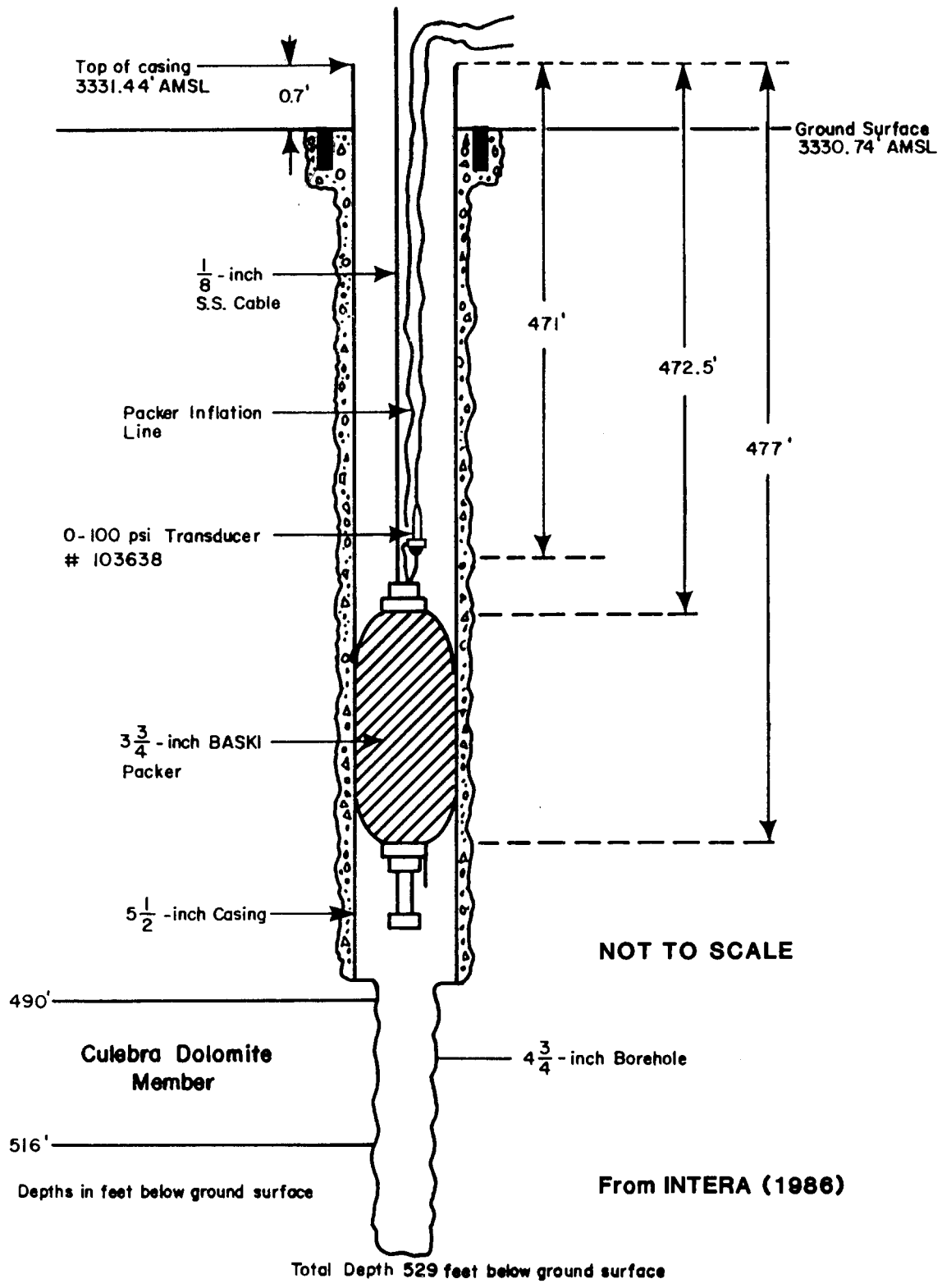


Figure 4-6. Configuration of the Test Equipment in Observation Well H-4b During the H-3 Multipad Pumping Test

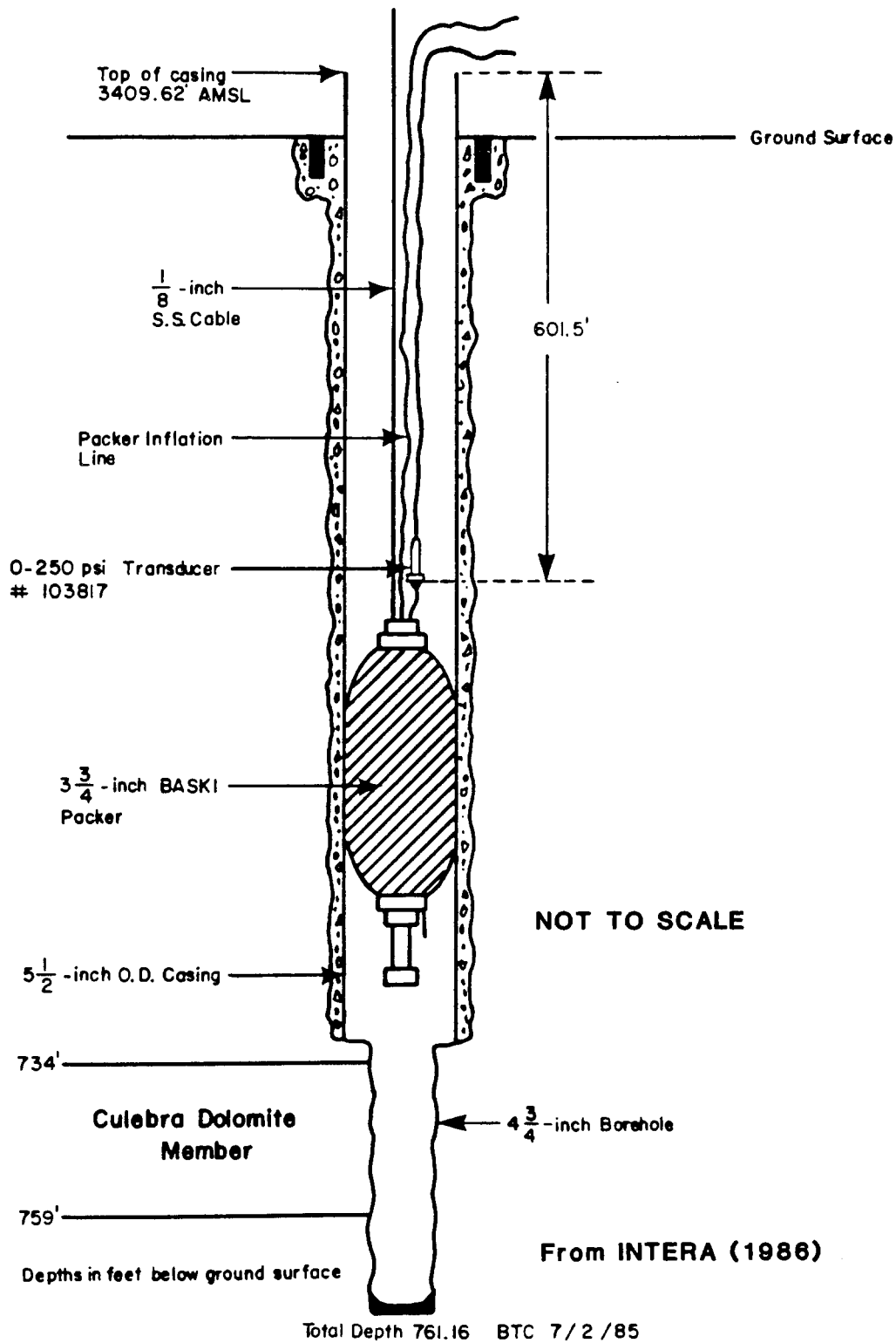


Figure 4-7. Configuration of the Test Equipment in Observation Well H-11b3 During the H-3 Multipad Pumping Test

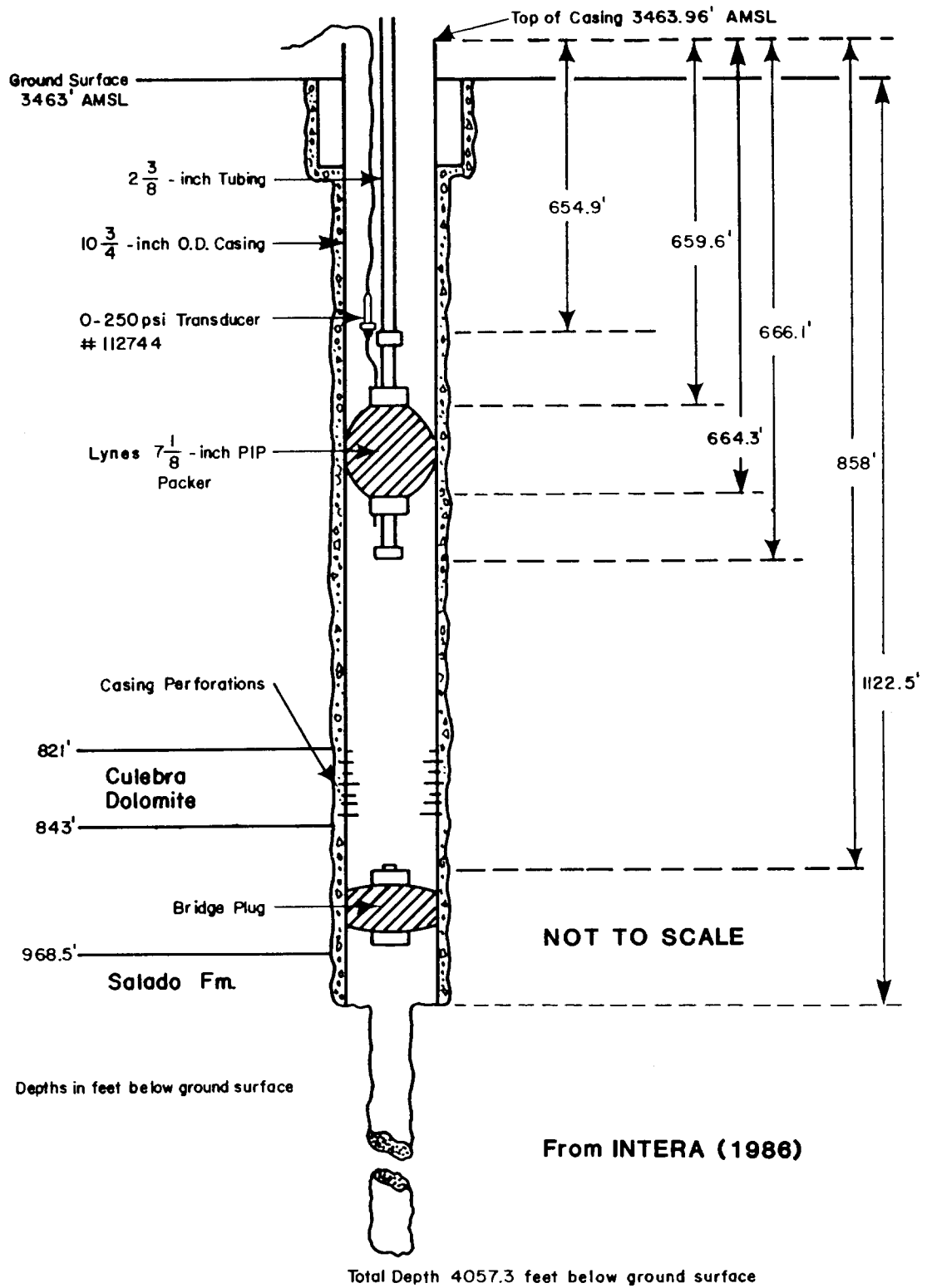


Figure 4-8. Configuration of the Test Equipment in Observation Well DOE-1 During the H-3 Multipad Pumping Test

5. Test Data

Extensive pressure and/or water-level data were collected from the pumping wells and observation wells during the two H-3 pumping tests. In many instances, the observed data were affected not only by the pumping tests, but also by residual hydraulic stresses from earlier hydraulic tests at other locations, well completions, shaft drainage, and other factors. Consequently, some of the data required modifications to remove the effects of the pressure trends existing at the beginning of the tests. Also, because the analytical techniques employed to interpret the data require the use of pressures rather than water levels, water-level data had to be converted to pressure data. The observed data, extraneous trends in the data, and modifications made to the data to aid analysis are discussed below.

For most wells, more data were collected than needed for analysis. Hence, abridged data sets were created by selecting points to give an adequate distribution of data through time for analysis. No other criteria were involved in the data abridgment. The abridged data sets used in the analyses presented in this report, both as measured and as modified, are tabulated in Appendixes A and B for the first and second tests, respectively. More extensive tabulations of the data collected are contained in INTERA Technologies (1986).

5.1 Test 1

As discussed in Section 4.1, the DAS at the H-3 hydropad during the 1984 test calculated and recorded water levels instead of pressures. For analysis, these water levels were converted to pressures by subtracting the depths to water from an arbitrary datum of 600 ft, and then multiplying the remainders by 0.433 psi/ft (Table A-1), the conversion factor for fresh water used by the DAS software for the original water-level calculations. This procedure was applied to the data from all three wells on the H-3 hydropad. Plots of these pressure data are shown in Figure 5-1.

A second modification was required for the data from the pumping well H-3b3 and from observation

well H-3b1. When a pump is turned on, an initial pressure drop occurs that is related to turbulence in the wellbore caused by the pump instead of to the aquifer response. This turbulence-related pressure drop is maintained until the moment when the pump is turned off. Additional pressure fluctuations may occur during the first few minutes of pumping if the discharge line is not fully filled before the pump is turned on. Analyses using pressure-change data must compensate for these pressure surges. In the case of the beginning of pumping at H-3b3, 4.45 psi was subtracted from the prepumping pressure to provide the starting point to calculate test-related drawdowns. For the same reason, 0.23 psi was subtracted from the prepumping pressure at H-3b1 (see discussion of H-3b1 response below and in Section 6.1.2). No other modifications were made to the H-3 data.

Responses of the three wells on the H-3 hydropad are strikingly similar (Figure 5-1). Total drawdowns at the end of the test for H-3b3 (including pump loss), H-3b2, and H-3b1 were 29.4, 27.0, and 26.6 psi, respectively. Of note also is how quickly H-3b1 and H-3b2 responded to the onset of pumping at H-3b3. At the beginning of the test, the DAS was set to scan and record transducer readings every 20 s. By the first scan after the pump was turned on, drawdown had begun at the two observation wells, 100.6 and 87.9 ft away (Figure 3-1).

The water-level data from H-1 before and during the H-3 pumping test are shown in Figure 5-2 and listed in Table A-2. The general water-level trend shown is upward, not downward, indicating that H-1 did not respond appreciably during pumping.

The water-level data from DOE-1 before and during the H-3 pumping test are shown in Figure 5-3. About 3 ft of drawdown were observed during the pumping. These water-level data required conversion to pressures before analysis. The conversion was performed by subtracting the depths to water from an arbitrary 600 ft, and multiplying the remainders by 0.473 psi/ft (Table A-3), the conversion factor for DOE-1 water having a specific gravity of 1.092 (Fischer, 1985).

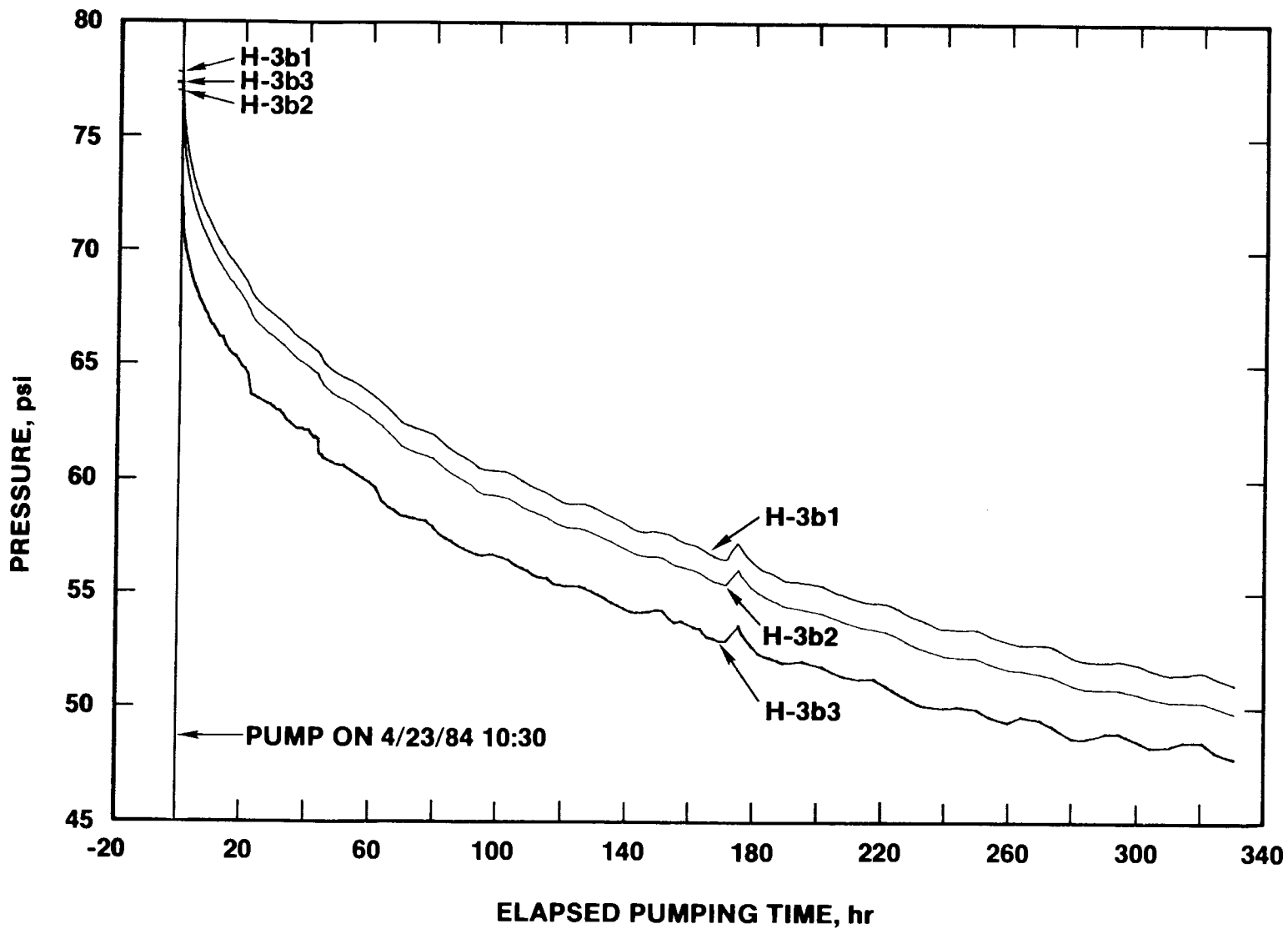


Figure 5-1. Pressure Responses in Wells H-3b1, H-3b2, and H-3b3 During the 1984 H-3 Pumping Test

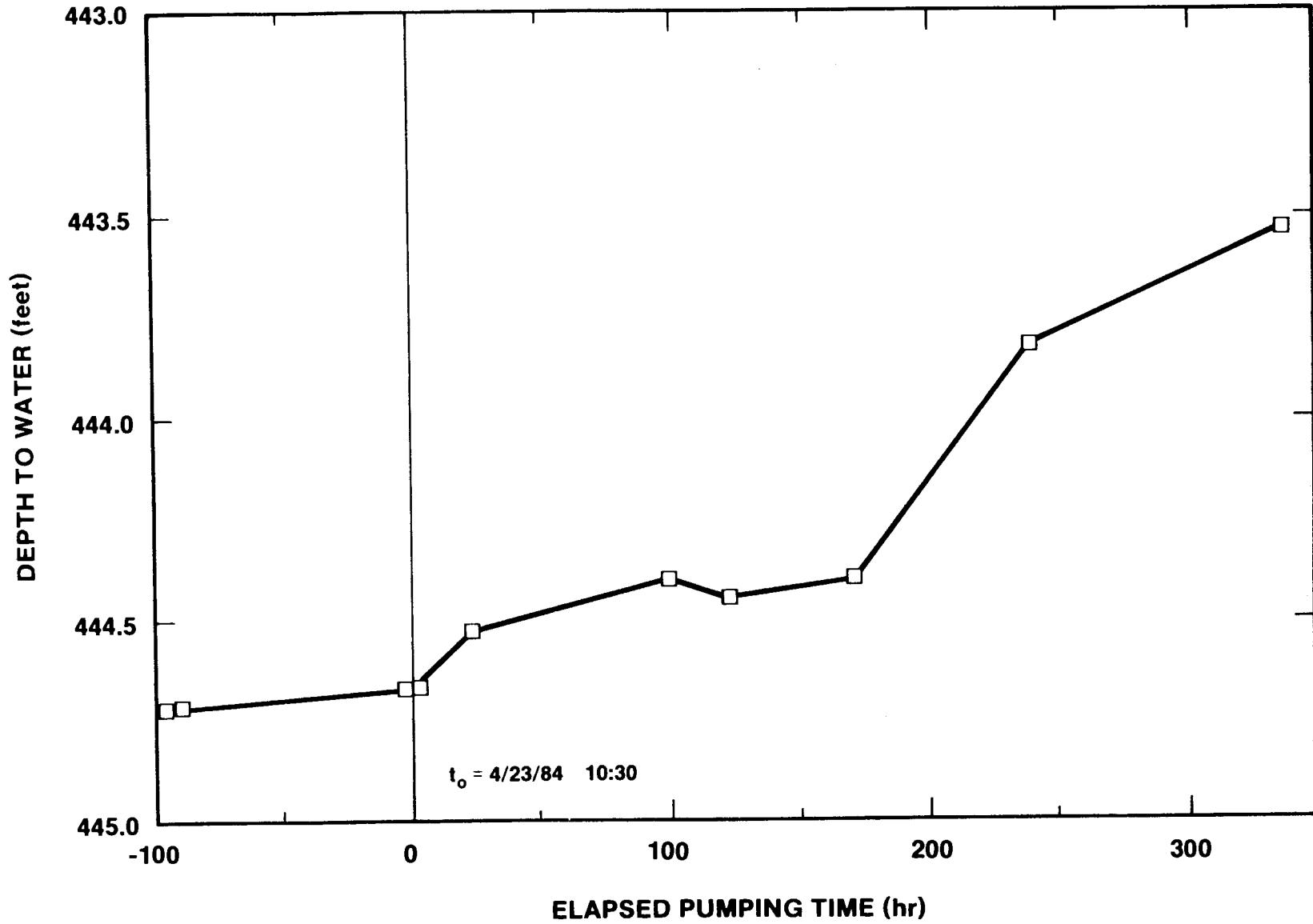


Figure 5-2. Water-Level Response in Well H-1 During the 1984 H-3 Pumping Test

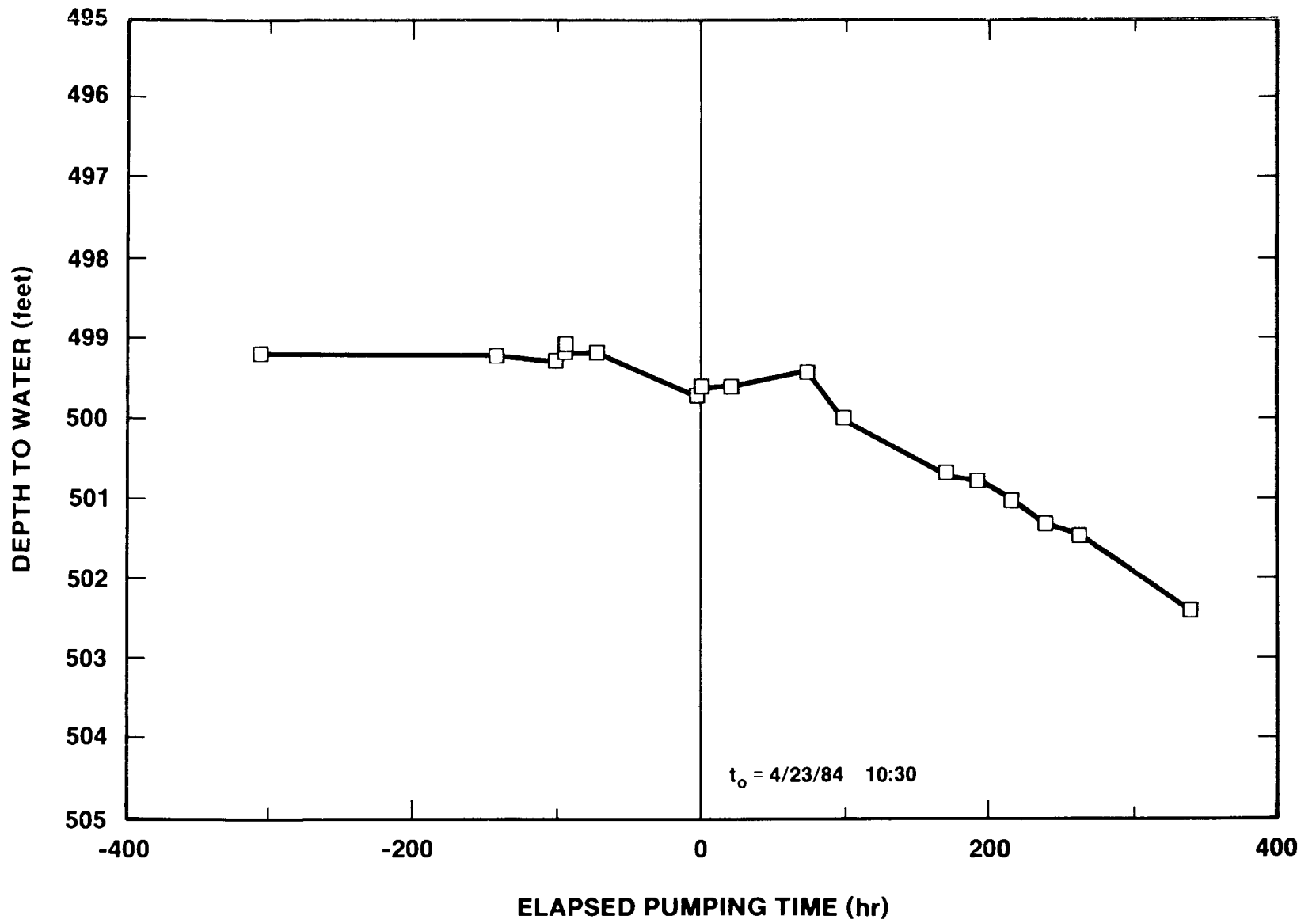


Figure 5-3. Water-Level Response in Well DOE-1 During the 1984 H-3 Pumping Test

5.2 Test 2 (Multipad Test)

Automated DASs collected pressure data from wells H-3b2, H-3b1 (Culebra and Magenta), H-3b3, H-2c, H-4b, H-11b3, and DOE-1 during the H-3 multipad test. Water levels were measured regularly in H-1 (Culebra and Magenta), H-2b1 (Magenta), H-2b2, H-6b, H-11b1, WIPP-18, WIPP-19, WIPP-21, WIPP-22, P-14, P-15, and P-17 during the test. The rest of the wells at the WIPP site were monitored about every 2 wk during the test as part of the ongoing regional water-level monitoring. Clear drawdown responses were observed in the Culebra in wells at the H-3 hydropad, the H-2 hydropad, the H-11 hydropad, DOE-1, H-1, WIPP-19, WIPP-21, and WIPP-22. Small, ambiguous responses were noted at P-14, P-15, P-17, H-6b, and WIPP-18. The Culebra pressure in the Waste-Handling Shaft also decreased during the pumping of H-3b2. No Magenta responses were observed that could be attributed to the Culebra pumping at H-3b2.

5.2.1 Observed Data

The complete DAS records of pressures measured at the H-3 hydropad, H-2c, H-4b, H-11b3, and DOE-1 are presented in Figures 5-4 through 5-8, respectively. Of these wells, only H-4b (Figure 5-6) showed no response to the multipad test. All three wells on the H-3 hydropad responded very similarly. The pressure in the pumping well, H-3b2, after compensating for the initial pump loss of ~ 10.7 psi, decreased by ~ 55.9 psi (Figure 5-4). Pressures in H-3b1 and H-3b3 decreased by ~ 53.0 and 52.5 psi, respectively (Figure 5-4). As noted during the 1984 H-3 test, the observation wells on the H-3 hydropad responded very quickly to the onset and end of pumping. The DAS was set to make 5-s scans when the pump was turned

on and off for the multipad test. By the first scans after the pump was turned on and off, the two observation wells, 91.3 and 87.9 ft away, had responded (Table B-1).

Of the other DAS-equipped wells, H-2c showed a pressure drop of almost 4 psi (Figure 5-5), H-11b3 pressure decreased by ~ 3 psi (Figure 5-7), and DOE-1 pressure dropped ~ 6.7 psi (Figure 5-8). Drawdown was observed at these wells beginning ~ 400 , 80, and 60 hr, respectively, after the pump was turned on at H-3b2. After the pump had been turned off for ~ 117 days, the pressure at H-11b3 appeared to have recovered to a level ~ 2 psi higher than its pretest level. As discussed below, this apparent over-recovery was not confirmed by water-level measurements in the other wells on the H-11 hydropad.

The water-level records for wells H-1, H-2b2, H-6b, H-11b1, WIPP-18, WIPP-19, WIPP-21, WIPP-22, P-14, P-15, and P-17 during the period of the H-3 multipad test are shown in Figures 5-9 through 5-19, respectively. Drawdowns at the wells showing a clear response ranged from a low of ~ 6 ft (~ 3 psi) at WIPP-19 to a high of ~ 32 ft (~ 14 psi) at WIPP-21. Table 5-1 summarizes the maximum observed drawdowns, the times at which drawdown responses were first observed, and the times at which maximum drawdowns were observed for each well. Because of data noise, a degree of subjectivity is involved in defining response times for the various wells. Also, for wells exhibiting rising water-level trends before the test, drawdown was considered to begin when water levels actually started declining, even though the effects of pumping must have been felt sooner to reverse the upward trend. Consequently, the response times presented in Table 5-1 should be considered approximations, and are most likely overestimates.

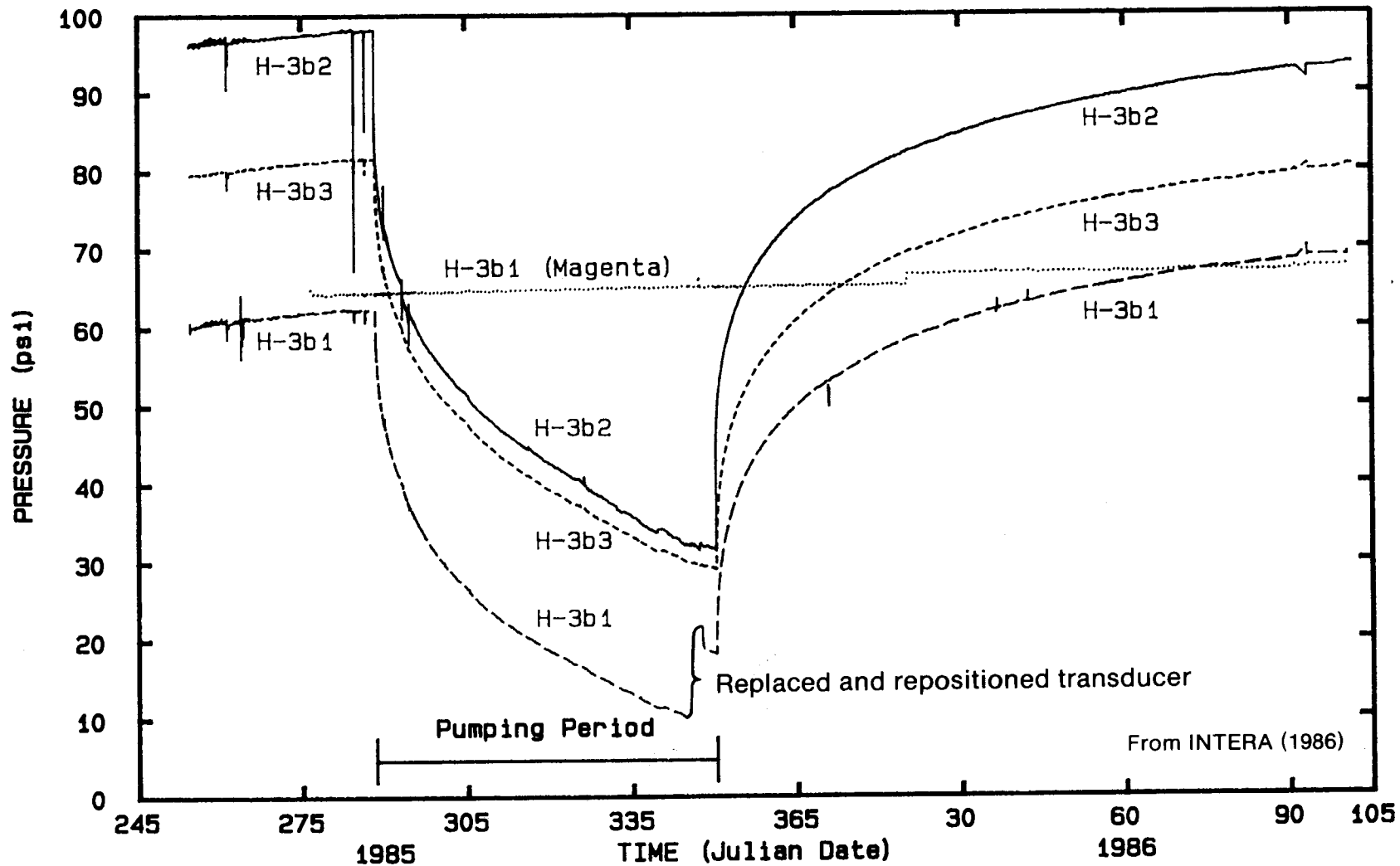


Figure 5-4. Pressure Responses in Wells H-3b1, H-3b2, and H-3b3 During the H-3 Multipad Pumping Test

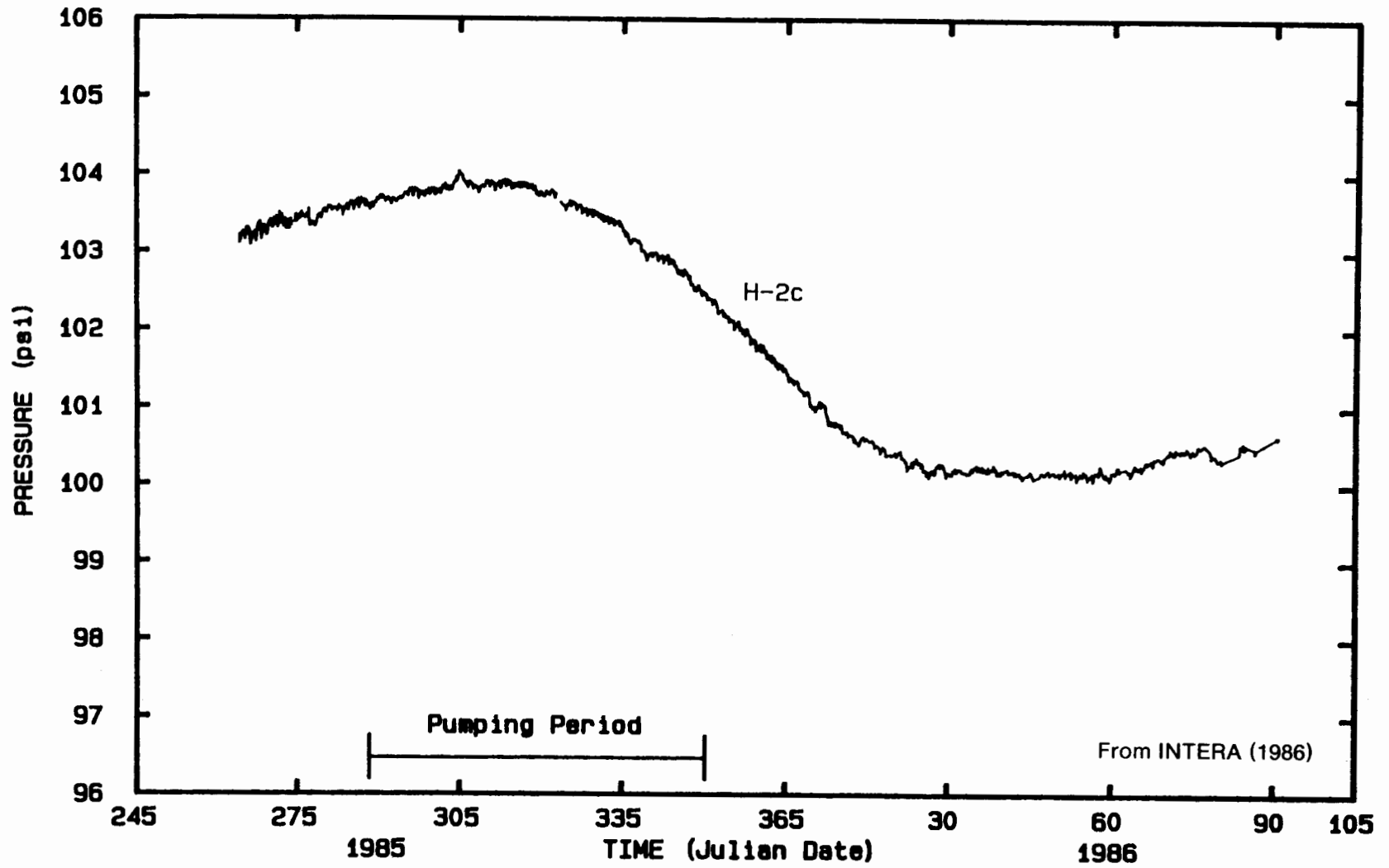


Figure 5-5. Pressure Response in Observation Well H-2c During the H-3 Multipad Pumping Test

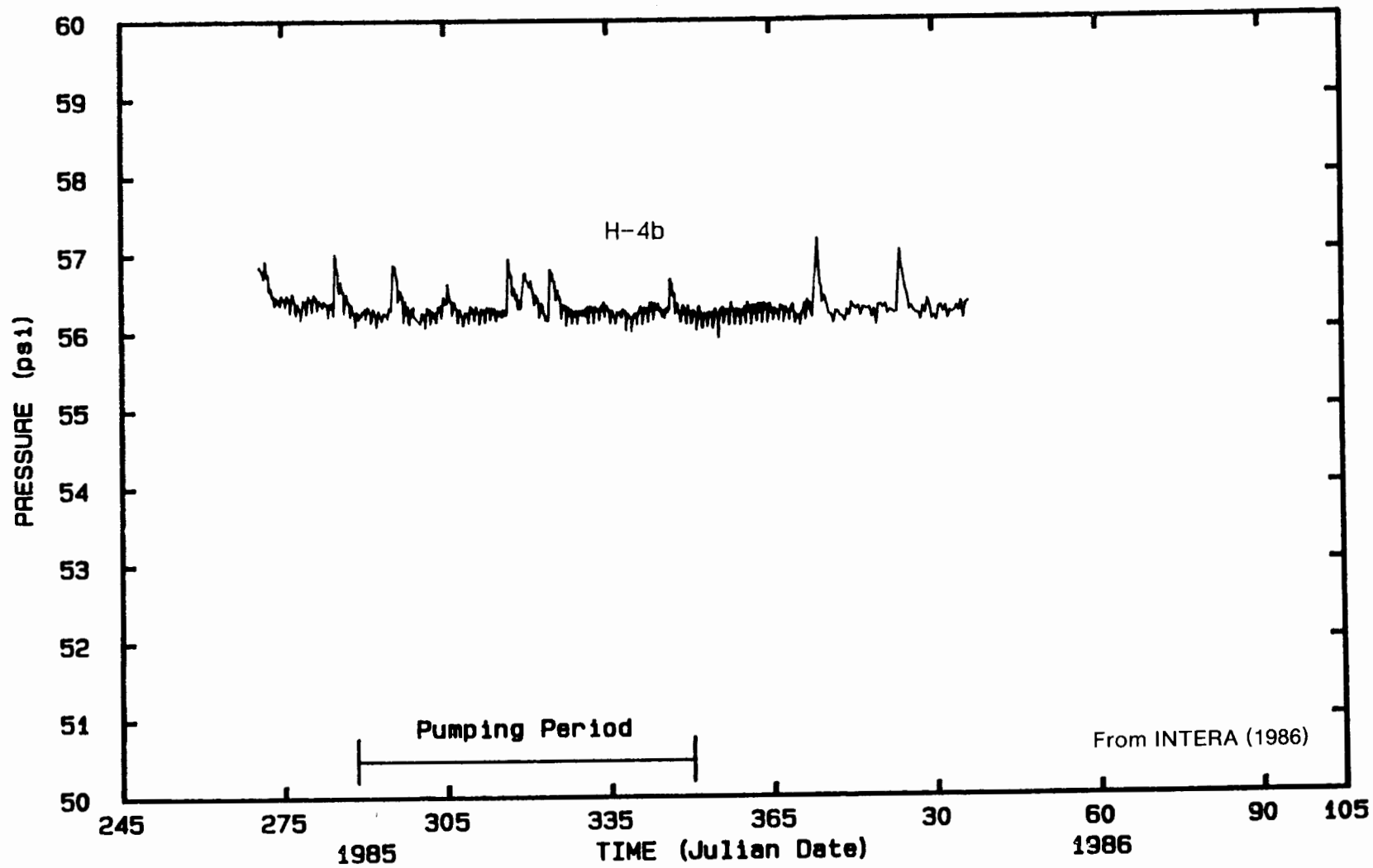


Figure 5-6. Pressure Response in Observation Well H-4b During the H-3 Multipad Pumping Test

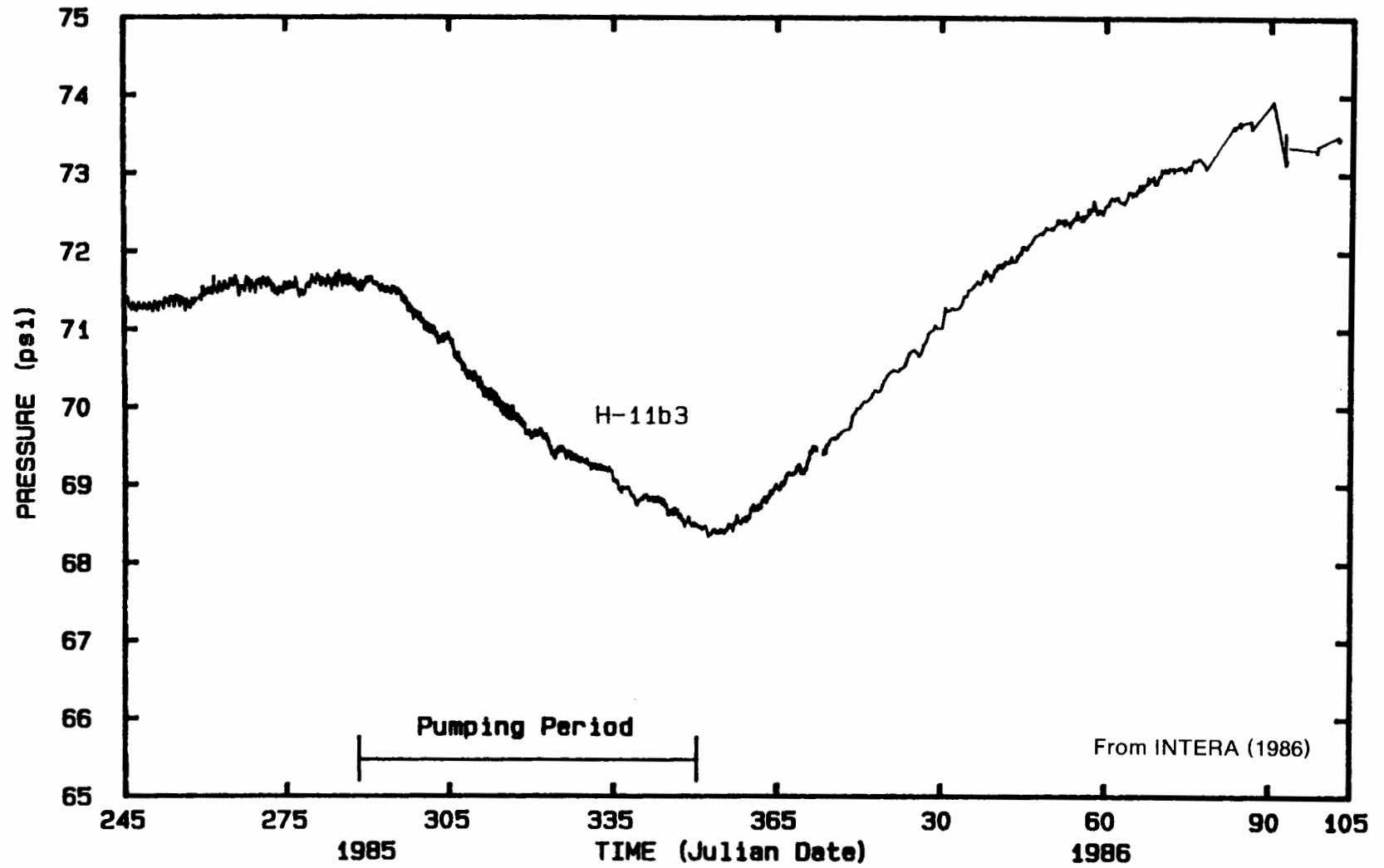


Figure 5-7. Pressure Response in Observation Well H-11b3 During the H-3 Multipad Pumping Test

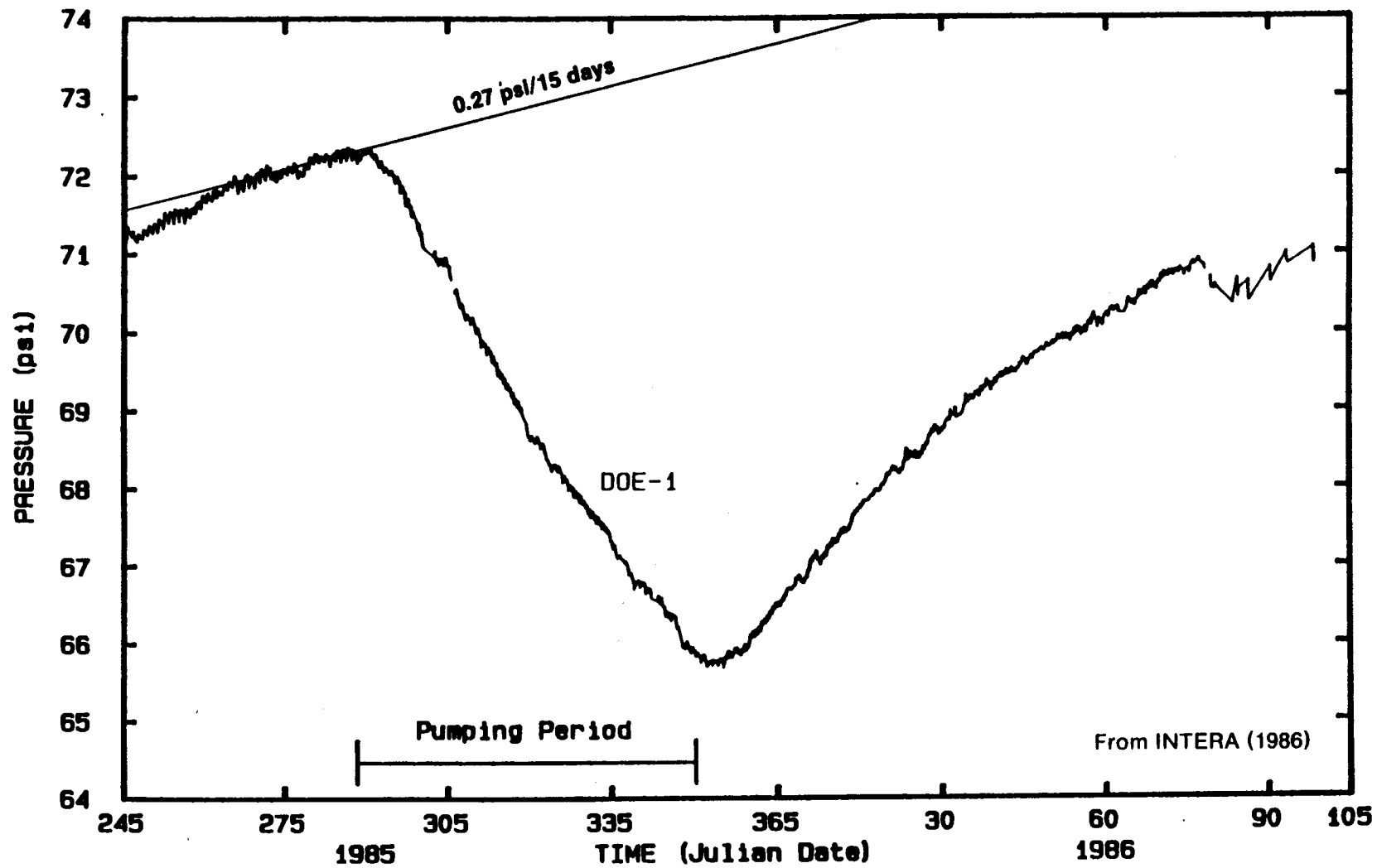


Figure 5-8. Pressure Response in Observation Well DOE-1 During the H-3 Multipad Pumping Test

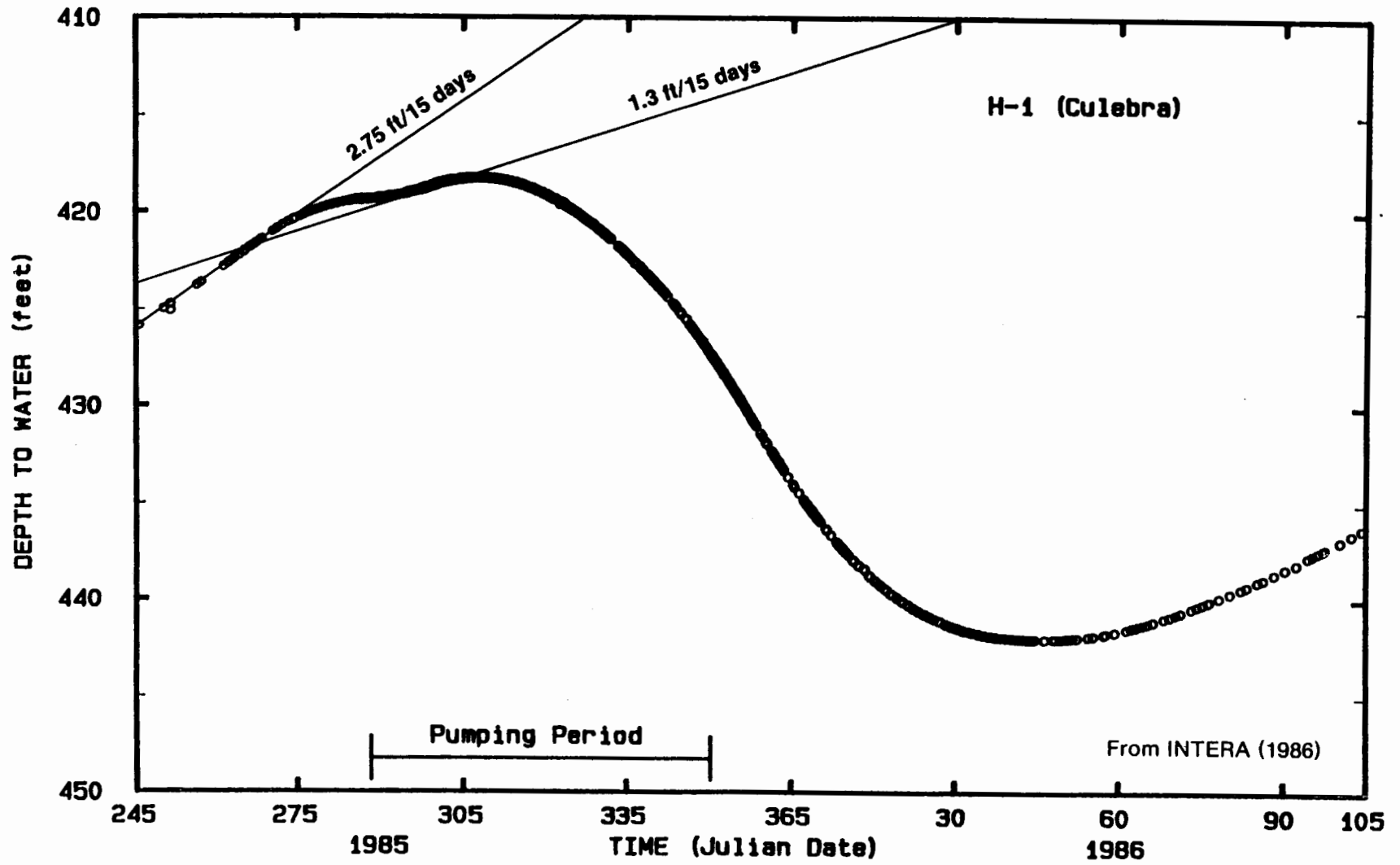


Figure 5-9. Water Levels Measured in Observation Well H-1 (Culebra) During the H-3 Multipad Pumping Test

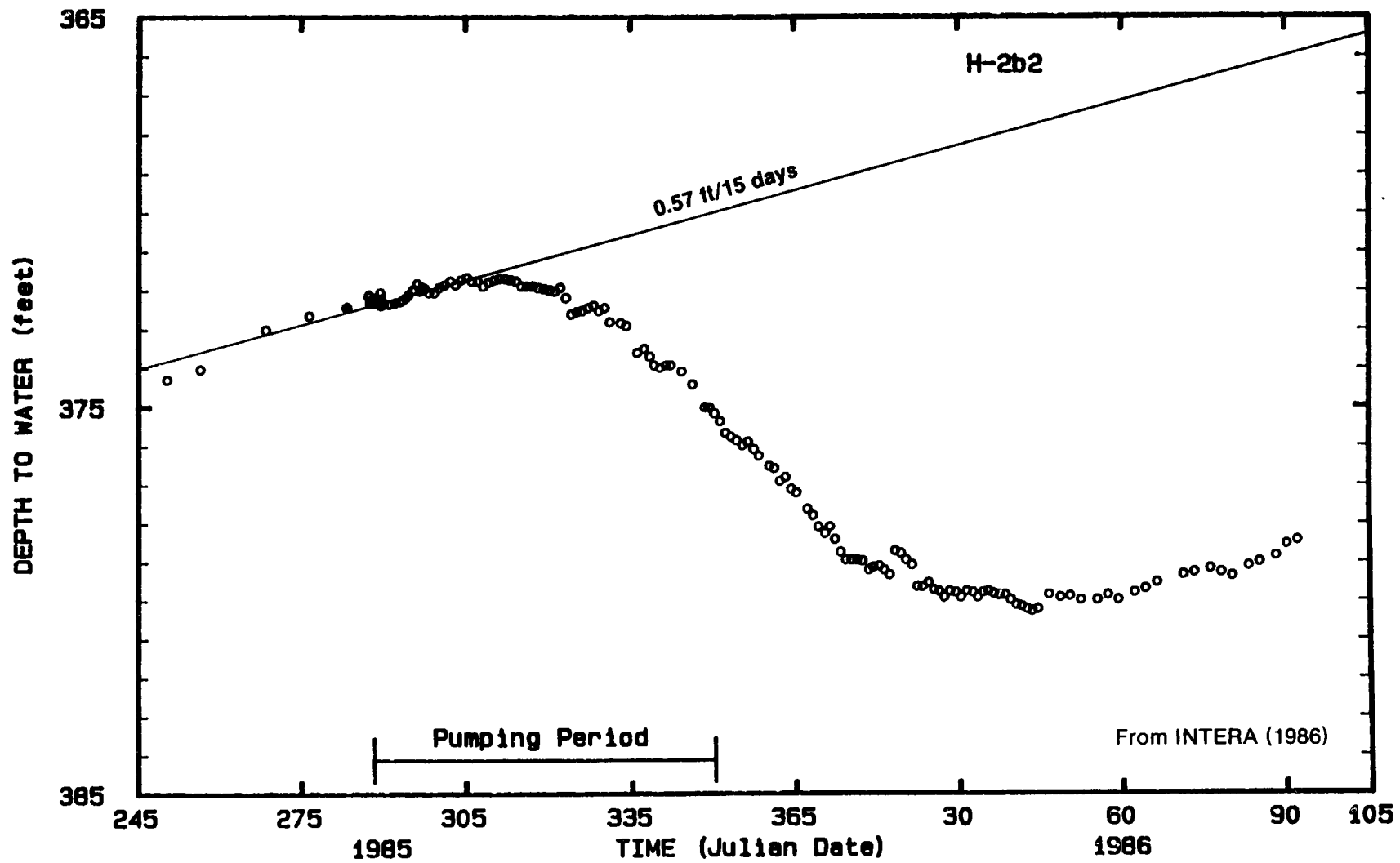
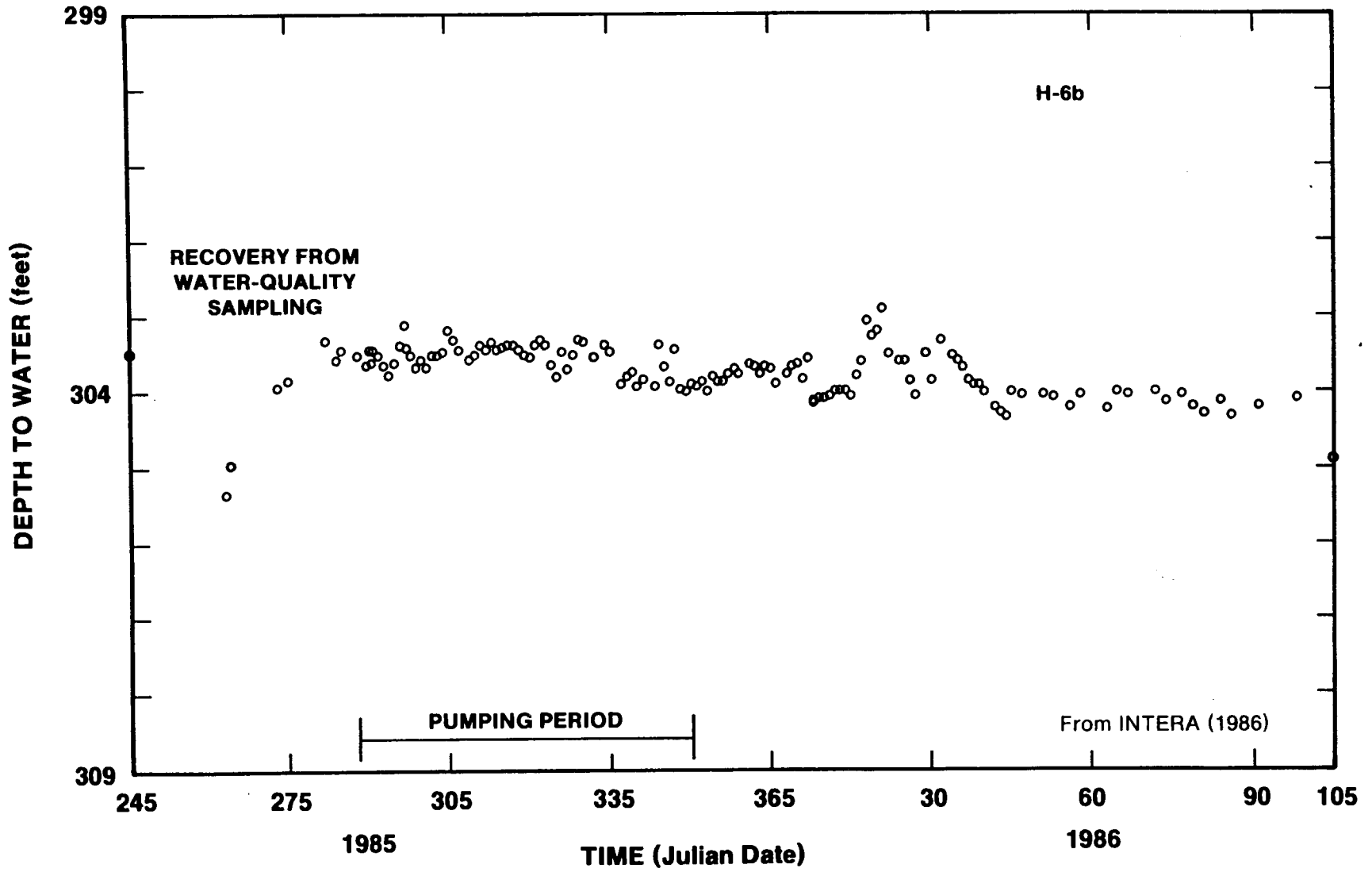
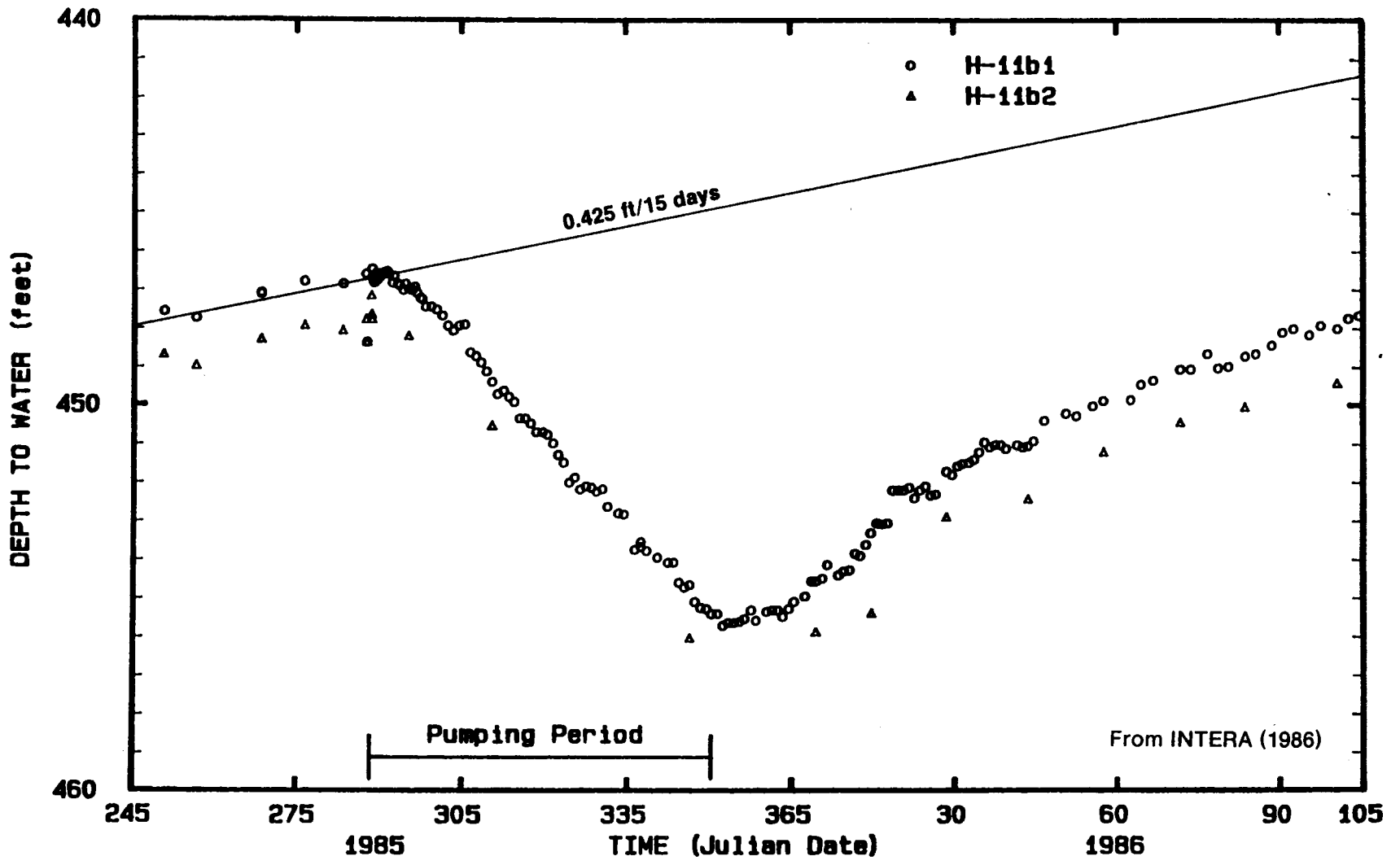


Figure 5-10. Water Levels Measured in Observation Well H-2b2 During the H-3 Multipad Pumping Test





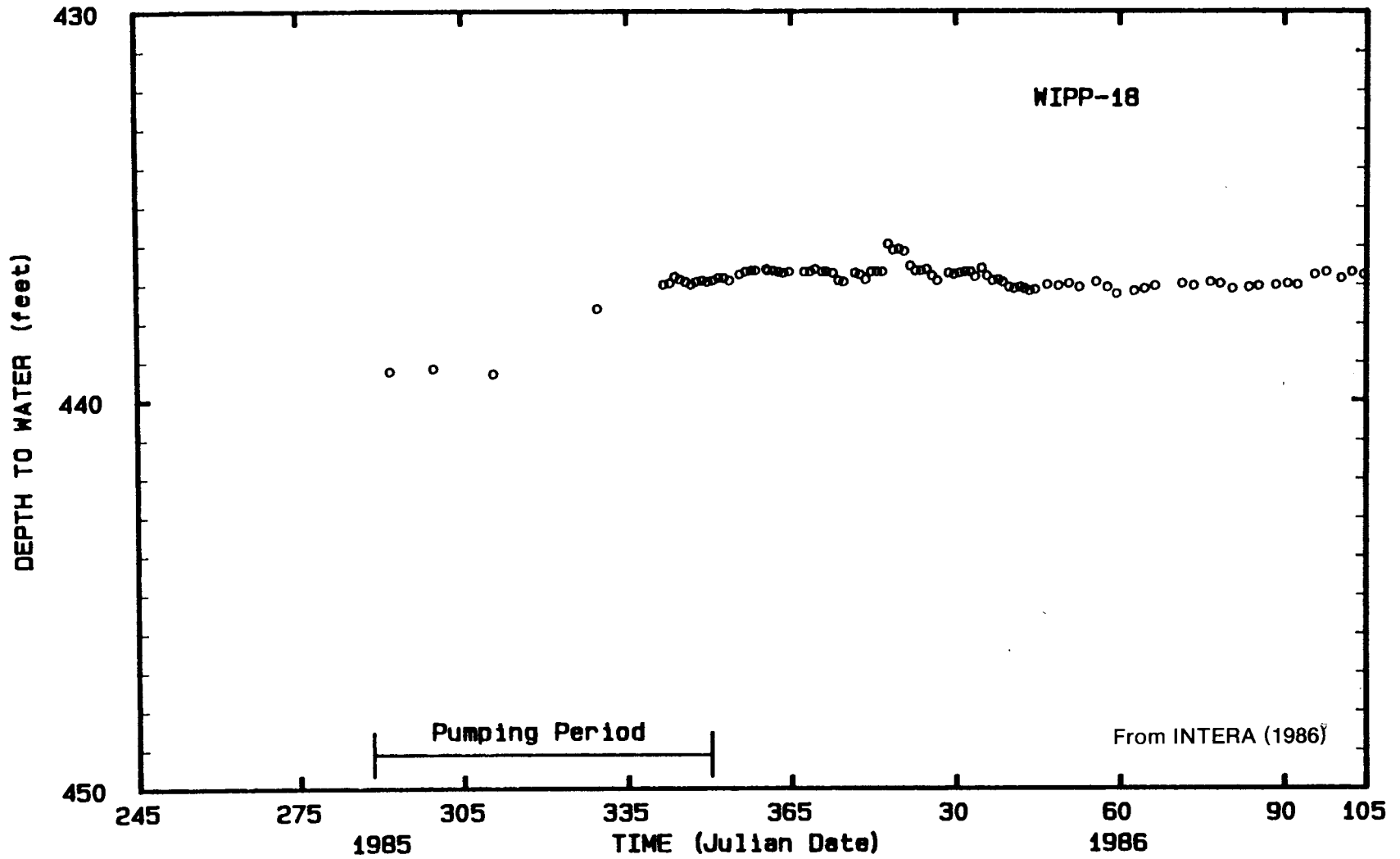


Figure 5-13. Water Levels Measured in Observation Well WIPP-18 During the H-3 Multipad Pumping Test

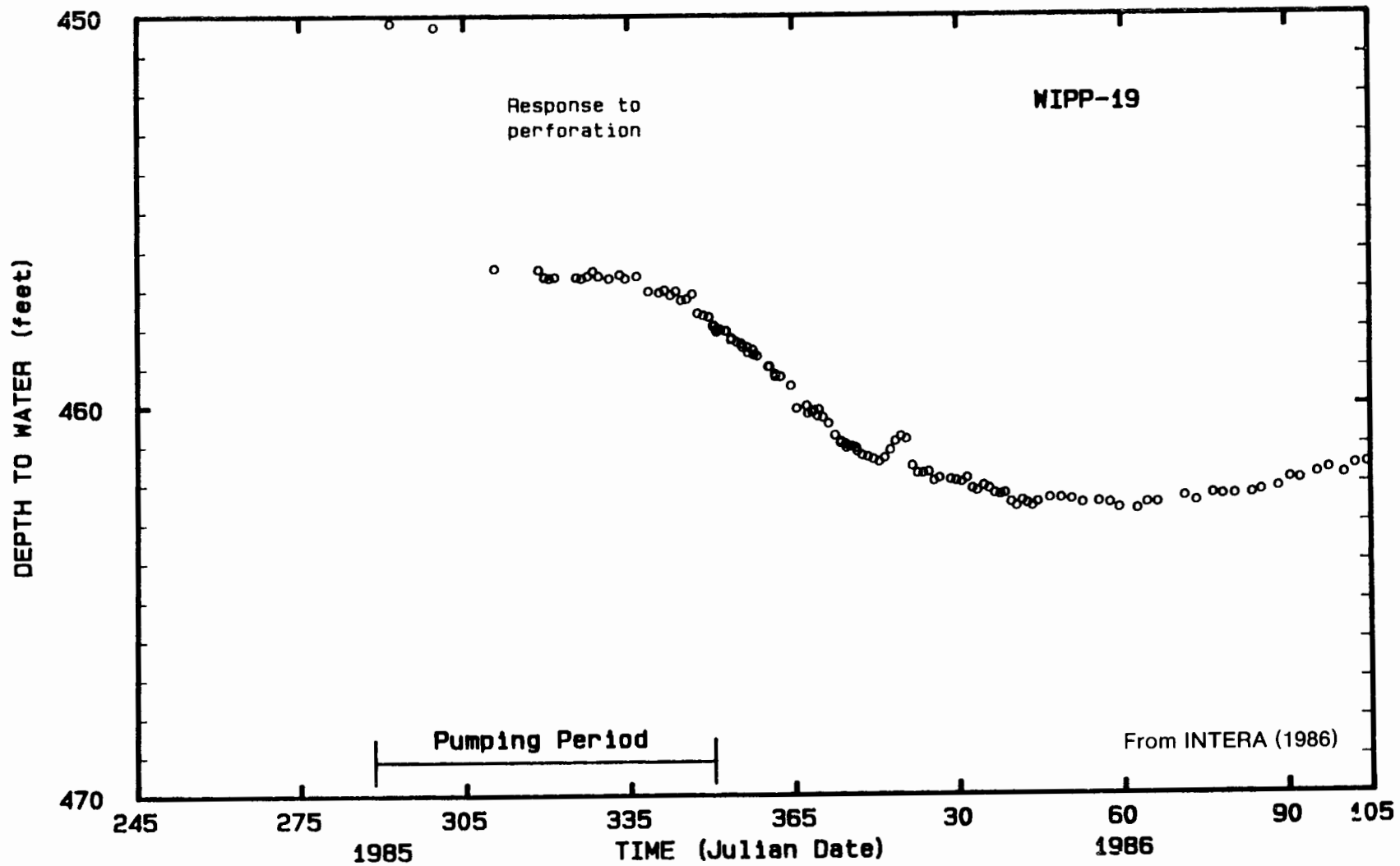


Figure 5-14. Water Levels Measured in Observation Well WIPP-19 During the H-3 Multipad Pumping Test

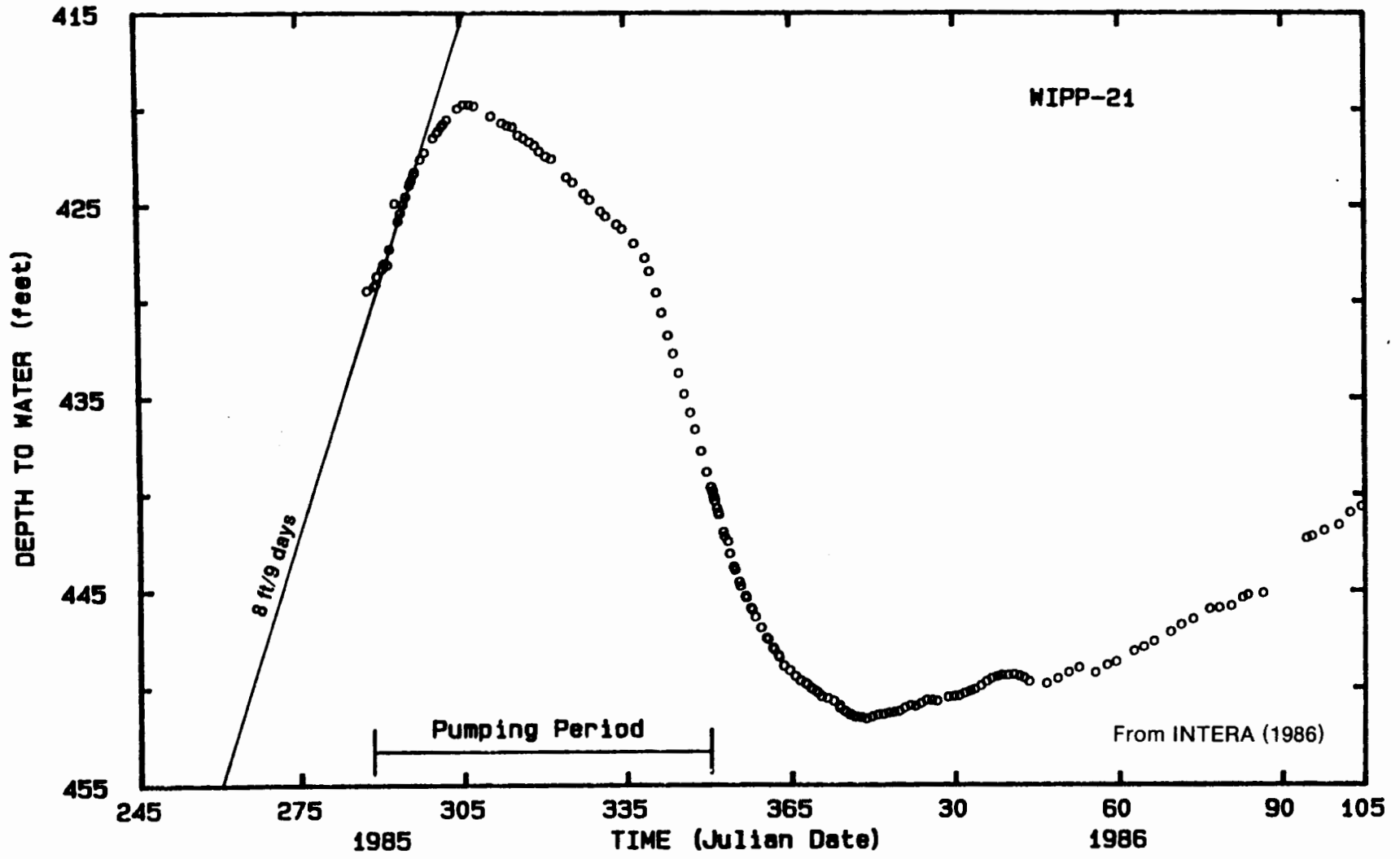
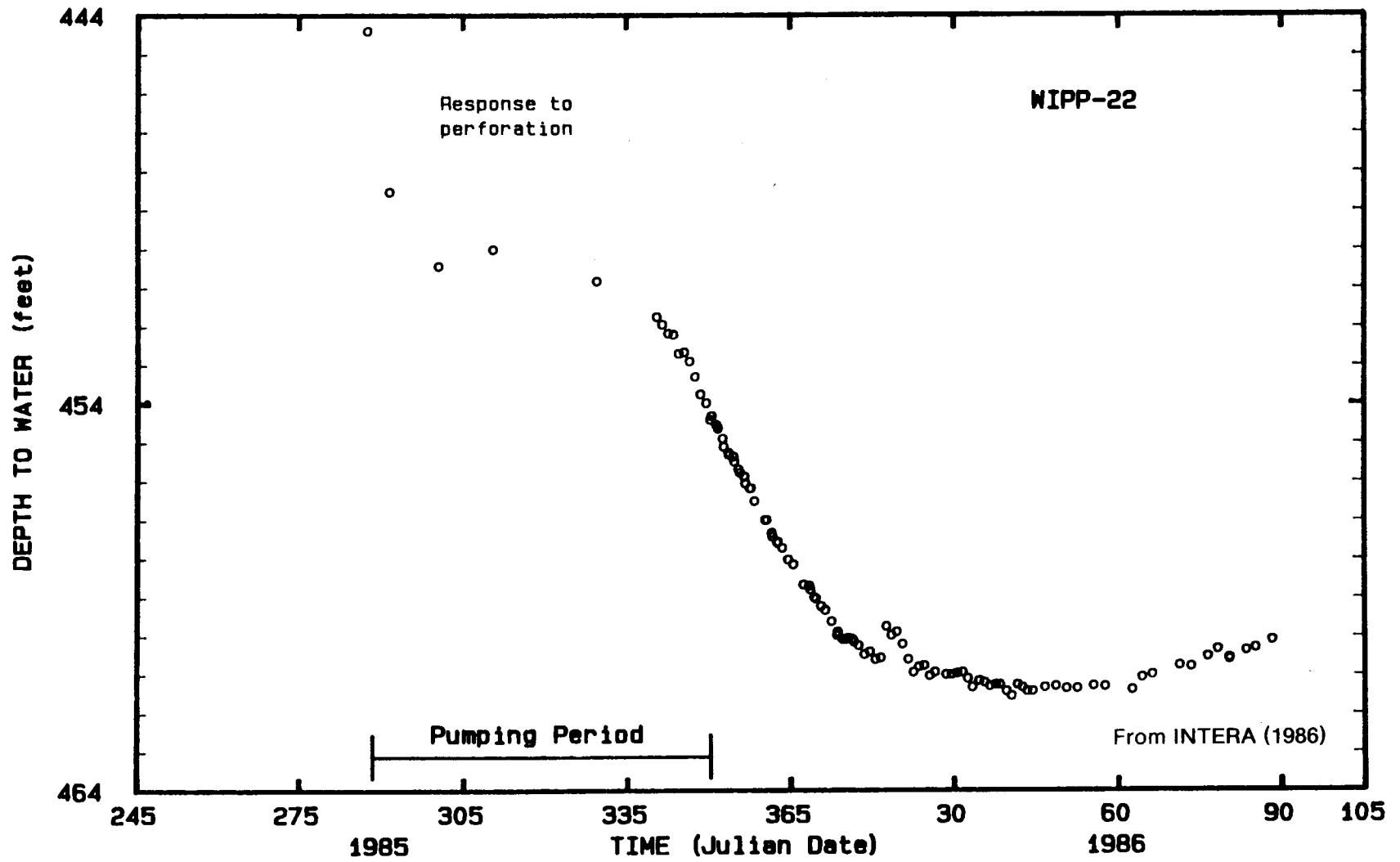


Figure 5-15. Water Levels Measured in Observation Well WIPP-21 During the H-3 Multipad Pumping Test



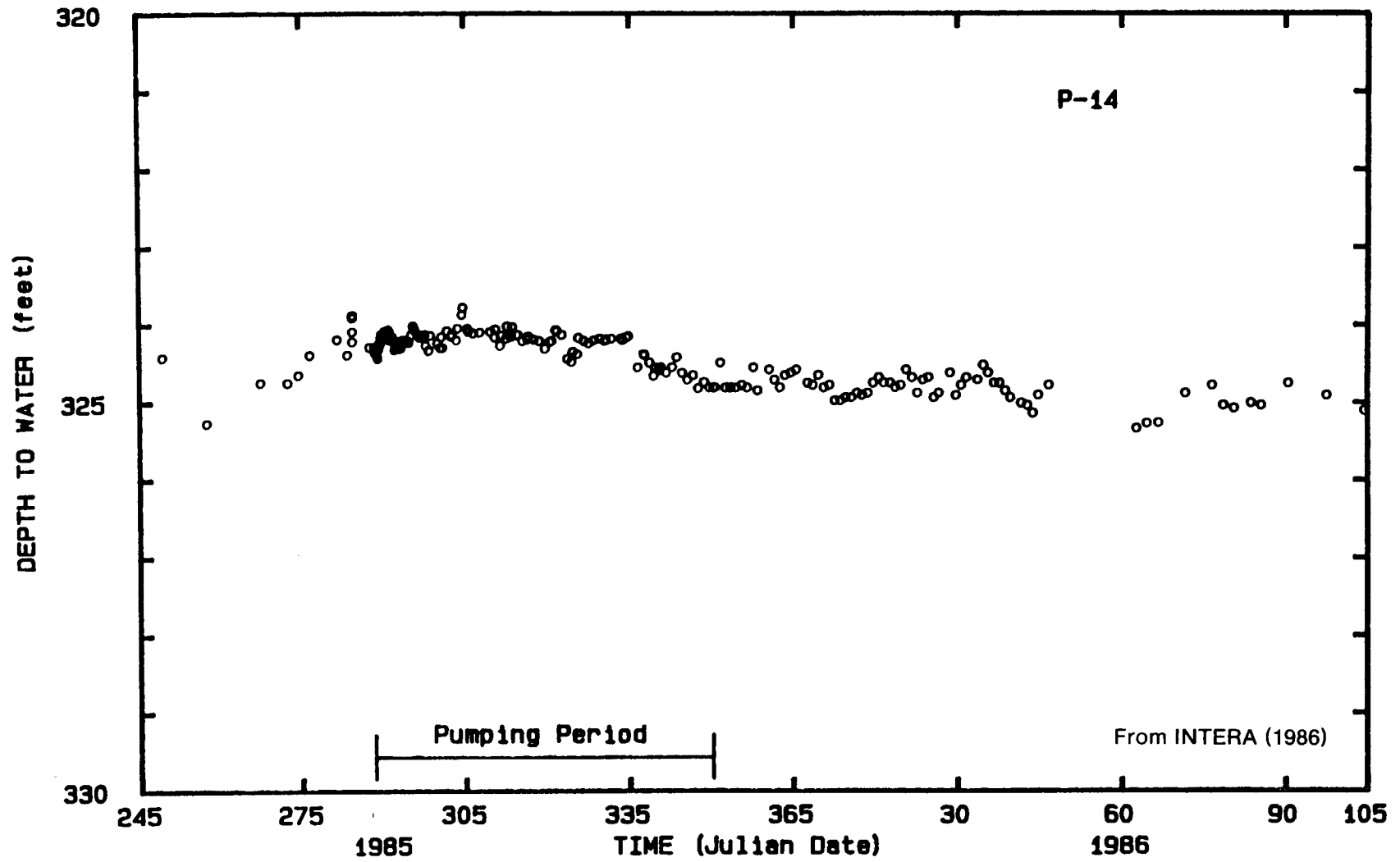


Figure 5-17. Water Levels Measured in Observation Well P-14 During the H-3 Multipad Pumping Test

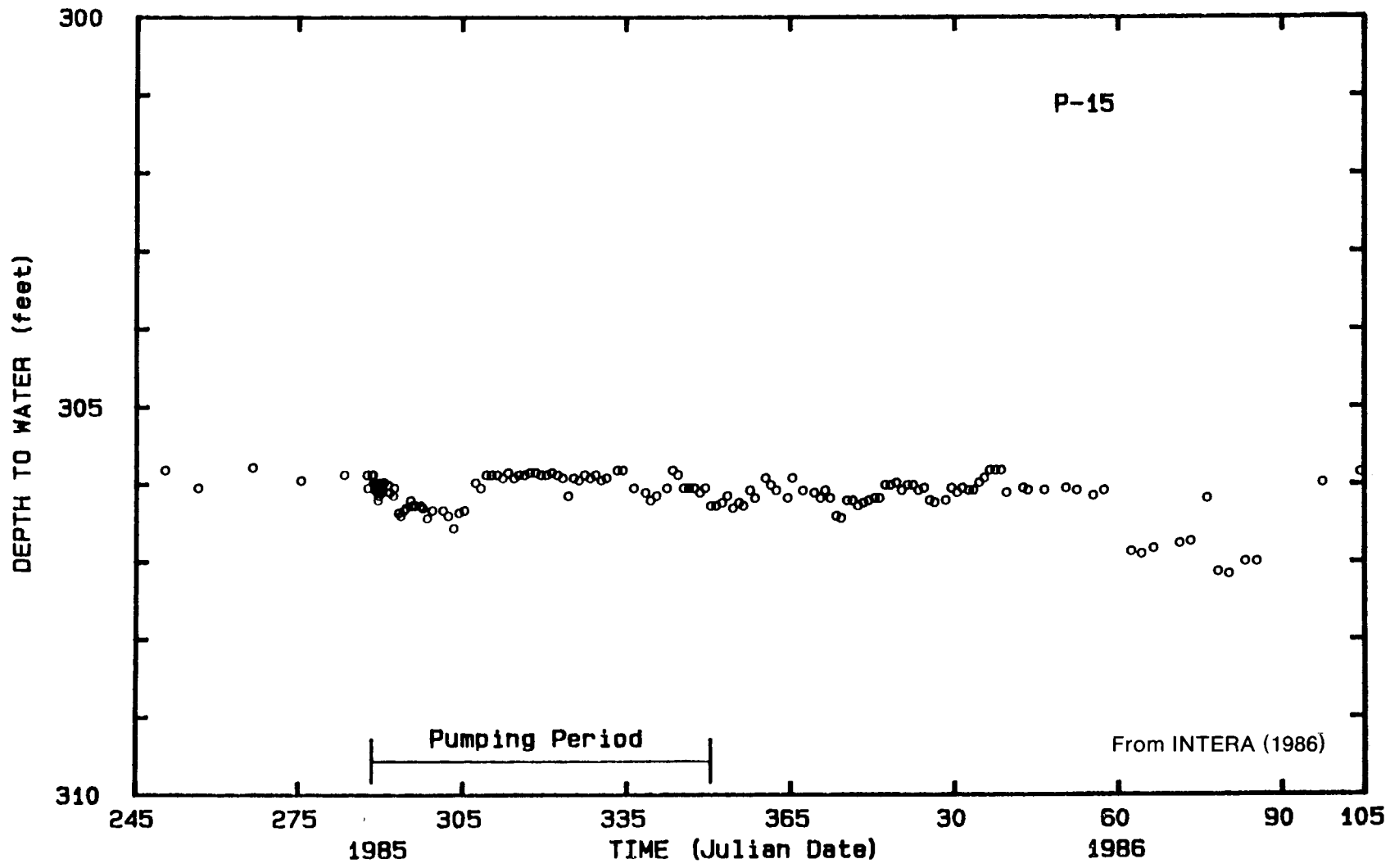


Figure 5-18. Water Levels Measured in Observation Well P-15 During the H-3 Multipad Pumping Test

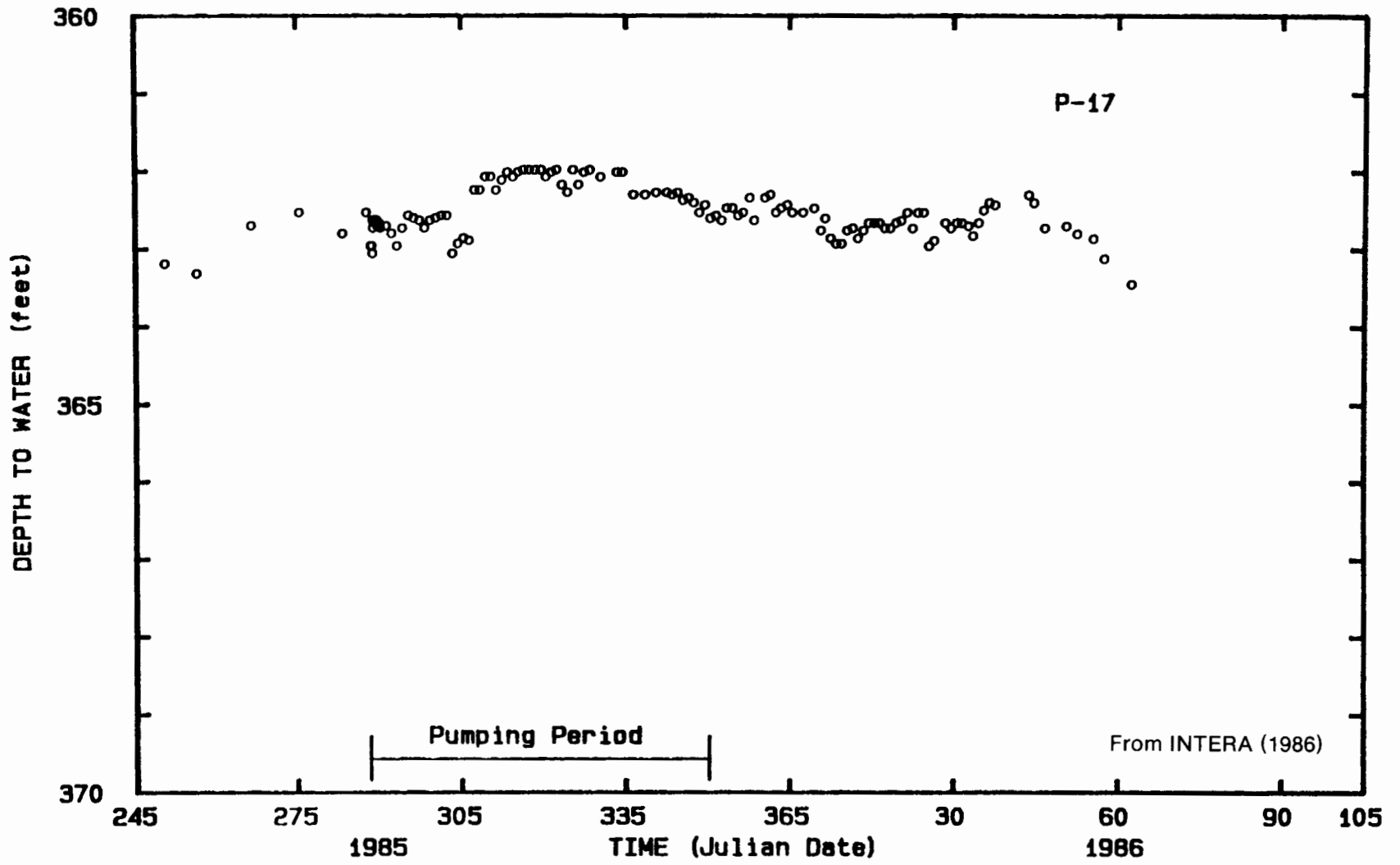


Figure 5-19. Water Levels Measured in Observation Well P-17 During the H-3 Multipad Pumping Test

Table 5-1. Response Times and Maximum Drawdowns at Multipad-Test Observation Wells

Well	Time After Pump On Until First Drawdown Observed (hr)	Maximum Drawdown Observed	Time After Pump On Until Maximum Drawdown Observed (hr)*
H-1	488	23.8 ft	2911
H-2b2	433	8.6 ft	2881
H-11b1	79	9.2 ft	1539
DOE-1	57	6.7 psi	1536
WIPP-19	1207 [†]	6.0 ft	3343
WIPP-21	437 [‡]	31.8 ft	2166
WIPP-22	990 [§]	10.6 ft	2215

*Pump was turned off after 1488 hr

[†]Previous reading at 1157 hr

[‡]Previous reading at 412 hr

[§]Previous reading at 533 hr

Wells P-14 (Figure 5-17), P-15 (Figure 5-18), P-17 (Figure 5-19), and H-6b (Figure 5-11) showed slight downward trends that may have been related to the multipad test and/or to other pumping activities performed under the WIPP Water Quality Sampling Program (WQSP). WIPP-18 water levels (Figure 5-13) declined very slightly.

At the end of the recovery monitoring period, the water level in H-11b1 (Figure 5-12) was still ~1 ft below its pretest level, even though the pressure recorded in H-11b3 (Figure 5-7) was ~2 psi (~4 ft) higher than its pretest level. Water levels measured in H-11b2 as part of the regional water-level monitoring (Figure 5-12) confirm the H-11b1 observations, and not the H-11b3 measurements. The apparent over-recovery at H-11b3 may be the result of a problem with the DAS; all analysis was performed using the data from H-11b1.

Culebra pressure data from the time of the H-3 multipad test are also available from the piezometers (transducers) installed behind the liner in the Waste-Handling Shaft. A sharp decrease of ~57 psi in the Culebra pressure was noted by the pressure transducer denoted "piezometer" PE-208 during the pumping period, followed by a slow increase during the recovery period (Figure 5-20). The relevance of these observations to the multipad test interpretation is discussed in Section 6.2.

Magenta water levels or pressures were measured in three wells during the H-3 multipad pumping test: H-1 (Figure 5-21), H-2b1 (Figure 5-22), and H-3b1

(Figure 5-4). The Culebra pumping did not appear to affect Magenta water levels/pressures in any of these wells.

5.2.2 Extraneous Trends and Modified Data

Pretest water-level/pressure trends were identified at all seven locations off the H-3 hydropad where drawdown was observed: H-1, the H-2 hydropad, the H-11 hydropad, DOE-1, WIPP-19, WIPP-21, and WIPP-22. Except at WIPP-19 and WIPP-22, water levels/pressures were rising before the test. If pretest water-level/pressure trends are believed to continue into the test period, the test data must be adjusted to separate the test-induced water-level/pressure changes from those caused by the trends.

H-1: At H-1, pretest water levels showed several trends (Figure 5-9). From 1985 Julian day 245 to about day 275, the water level was rising ~2.75 ft/15 days. The rate of rise then decreased until about day 291, when it began to increase. The rate of rise increased until about day 300, when the rate was ~1.3 ft/15 days. After day 300, the rising trend decreased, becoming a declining trend on about day 308.

For analysis purposes, two sets of data for H-1 were considered. One set consisted of the observed data, with multipad-test drawdown considered to begin on day 308 when the H-1 water level peaked. The other set consisted of the day 300 water-level trend of 1.3 ft/15 days added to the observed data beginning 280 hr into the test on day 300; this time is considered to be the beginning of multipad-test drawdown. For analysis, both sets of water-level data were converted to pressures by subtracting the depths to water from an arbitrary datum of 500 ft, then multiplying the remainders by 0.4403 psi/ft (Table B-2)—the conversion factor for H-1 water with a specific gravity of 1.016 (Mercer, 1983).

H-2: The pressure response at H-2c and the water-level response at H-2b2 were virtually identical (compare Figures 5-5 and 5-10). Consequently, only the H-2b2 data were analyzed. At H-2b2, water levels were rising at an approximate rate of 0.57 ft/15 days from 1985 Julian day 268 to about day 305 (Figure 5-10). Day 305 marks the absolute peak in H-2b2 water level before apparent drawdown began in response to the multipad test. For purposes of analysis, two sets of data for H-2b2 were considered. One consisted of the observed data. The other set consisted of the water-level trend of 0.57 ft/15 days added to the observed

data beginning 408 hr into the test on day 305. In both cases, multipad test drawdown is considered to begin on day 305.

For analysis, both sets of water-level data were converted to pressures by subtracting the depths to water from an arbitrary datum of 400 ft then multiplying the remainders by 0.436 psi/ft (Table B-3)—the conversion factor for H-2b2 water with a specific gravity of 1.006 (INTERA Technologies and Hydro-GeoChem, 1985).

H-11: As discussed above, the observed H-11b3 response (Figure 5-7) is believed to have been affected by a DAS malfunction; hence the data from H-11b1 (Figure 5-12) were chosen for analysis. At H-11b1, water levels were rising at an approximate rate of 0.425 ft/15 days from 1985 Julian day 250 to about day 291 (Figure 5-12). Day 291 marks the absolute peak in H-11b1 water level before apparent drawdown began in response to the multipad test. For purposes of analysis, two sets of data for H-11b1 were considered. One consisted of the observed data. The other consisted of the water-level trend of 0.425 ft/15 days added to the observed data beginning 73 hr into the test on day 291. In both cases, multipad test drawdown is considered to begin on day 291.

For analysis, both sets of water-level data were converted to pressures by subtracting the depths to water from an arbitrary datum of 500 ft, and multiplying the remainders by 0.473 psi/ft (Table B-4)—the conversion factor for H-11 water with a specific gravity of 1.0915 (Fischer, 1985).

DOE-1: At DOE-1, the Culebra pressure was rising at an approximate rate of 0.27 psi/15 days from 1985 Julian day 265 to about day 290 (Figure 5-8). The pressure peaked on day 290 before apparent drawdown began in response to the multipad test. For purposes of analysis, two sets of data for DOE-1 were considered. One set consisted of the observed data. The other set consisted of the pressure trend of 0.27 psi/15 days subtracted from the observed data beginning 59 hr into the test on day 290 (Table B-5). In both cases, multipad test drawdown is considered to begin on day 290.

WIPP-19: When the H-3 multipad test began, water levels in WIPP-19 were dropping after perforation of the casing across the Culebra interval on 1985

Julian day 282. This drop appears to have ended by about 1985 Julian day 319 (Figure 5-14). Drawdown induced by the H-3 pumping appears to have begun between Julian days 336 and 338. For analysis, the observed WIPP-19 water levels were converted to equivalent pressures by subtracting the depths to water from an arbitrary datum of 500 ft, and multiplying the remainders by 0.511 psi/ft (Table B-6)—the conversion factor for water with a specific gravity of 1.18 standing in the wellbore (Saulnier et al., 1987).

WIPP-21: At WIPP-21, the Culebra water level was rising at an approximate rate of 8 ft/9 days between 1985 Julian days 290 and 296 (Figure 5-15). The rise then began to slow, with the water level reaching a peak on days 305 and 306, and declining thereafter. Why the water level was rising so rapidly between days 290 and 296 is unknown, but this trend could not possibly have been sustained over the 6-mo duration of the multipad test. Consequently, the observed data were not adjusted to compensate for this trend.

For analysis, the observed WIPP-21 water levels were converted to equivalent pressures by subtracting the depths to water from an arbitrary datum of 500 ft, and multiplying the remainders by 0.438 psi/ft (Table B-7)—the conversion factor for water with a specific gravity of 1.01 standing in the wellbore (Saulnier et al., 1987).

WIPP-22: When the H-3 multipad test began, water levels in WIPP-22 were dropping after perforation of the casing across the Culebra interval on 1985 Julian day 281. This drop appears to have ended, followed by a slight water-level rise, before WIPP-22 felt the effects of the H-3 pumping (Figure 5-16). Drawdown might have begun between 1985 Julian days 310 and 329; it certainly began by day 340. For analysis, the observed WIPP-22 water levels were converted to equivalent pressures by subtracting the depths to water from an arbitrary datum of 500 ft, and multiplying the remainders by 0.498 psi/ft (Table B-8)—the conversion factor for water with a specific gravity of 1.15 standing in the wellbore (Saulnier et al., 1987).

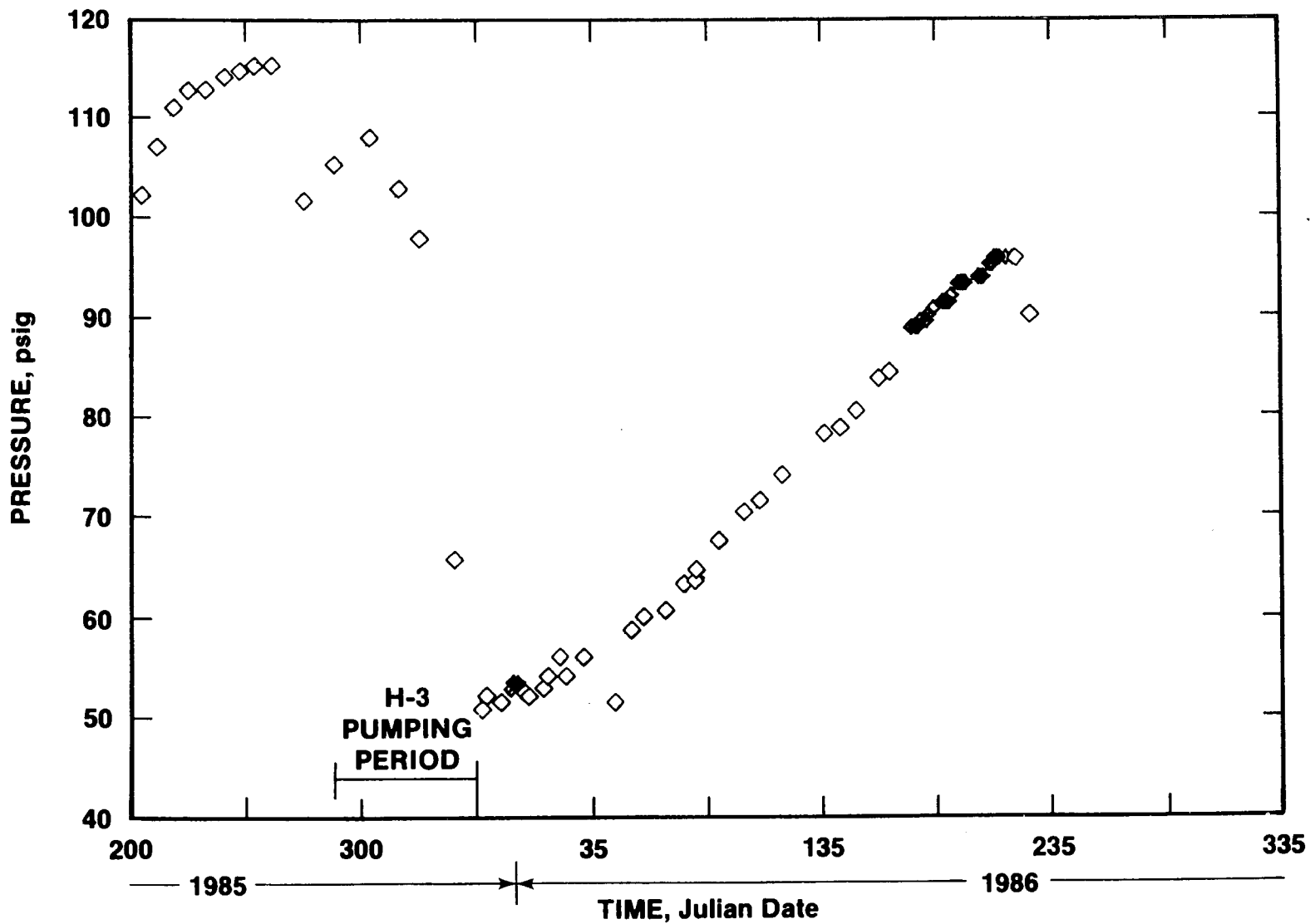


Figure 5-20. Pressure Response of the Culebra Transducer in the Waste-Handling Shaft During the H-3 Multipad Pumping Test

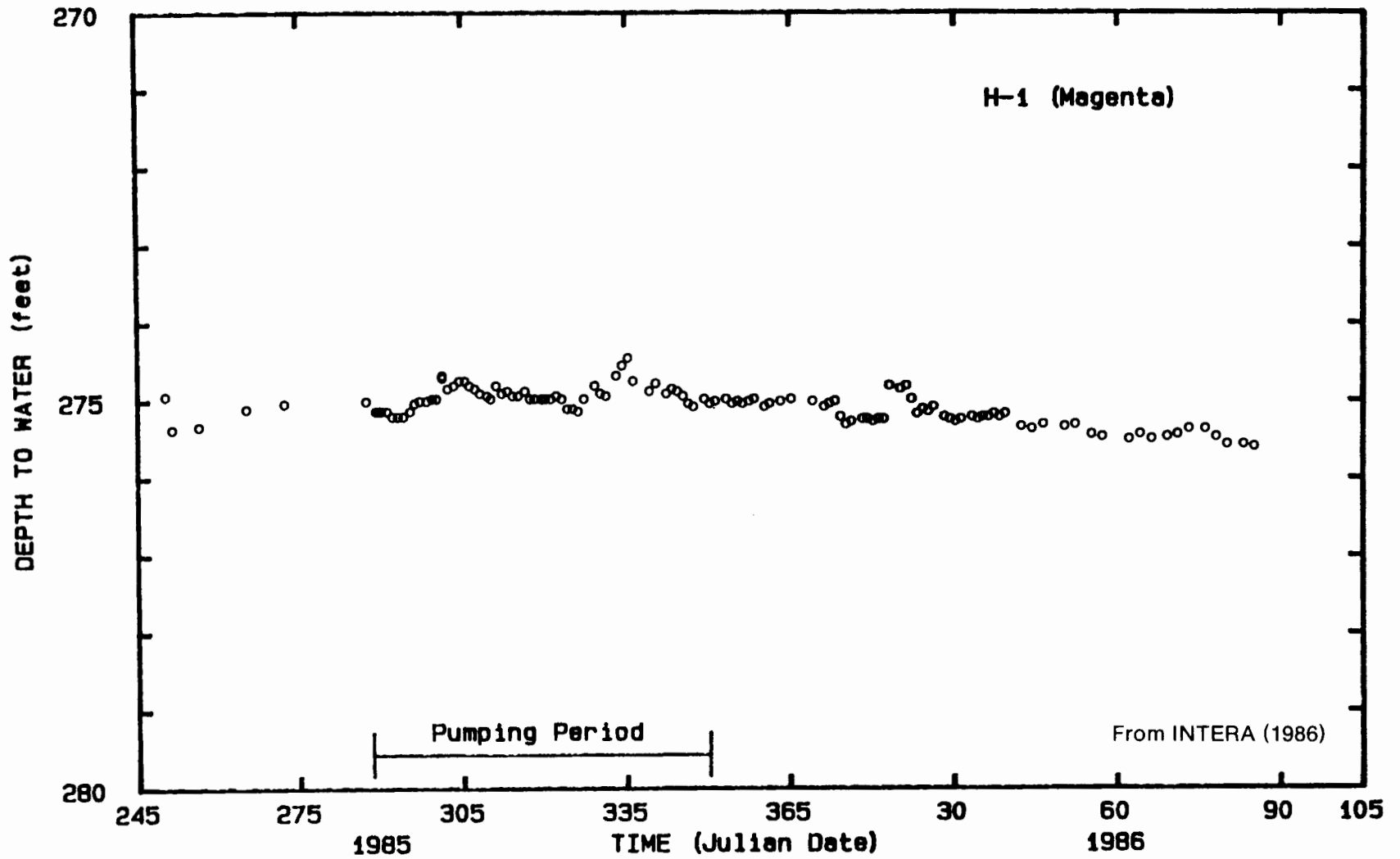


Figure 5-21. Water Levels Measured in Observation Well H-1 (Magenta) During the H-3 Multipad Pumping Test

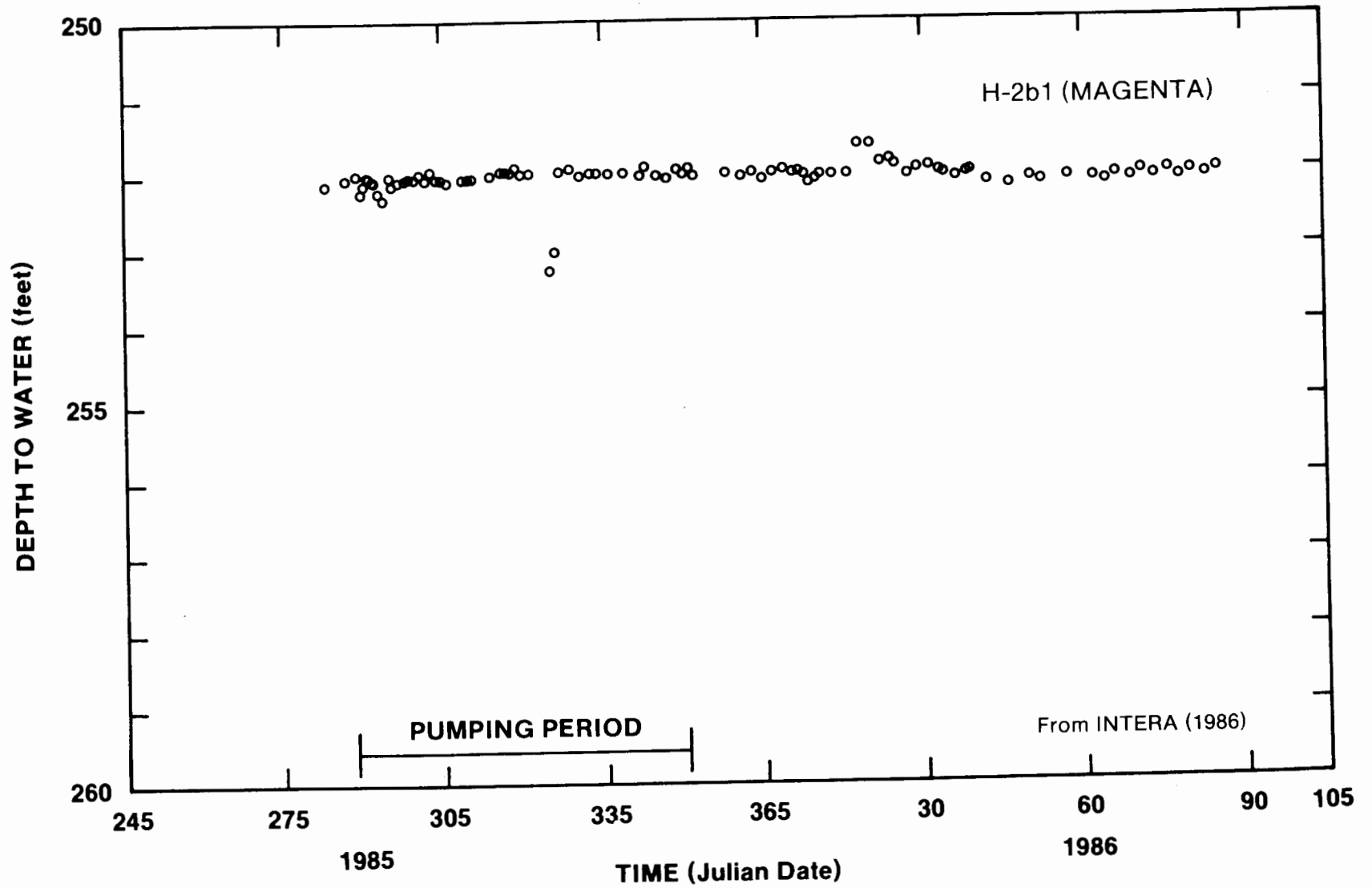


Figure 5-22. Water Levels Measured in Observation Well H-2b1 (Magenta) During the H-3 Multipad Pumping Test

6. Test Results

The hydraulic test data were analyzed to produce answers to the following questions:

- What is the most appropriate conceptualization of the nature of the Culebra flow system around H-3?
- What are the hydraulic properties of the Culebra dolomite in the vicinity of the H-3 hydropad?
- What are the average hydraulic properties of the Culebra dolomite between the H-3 hydropad and more-distant observation wells?

Analytical methods used to answer these questions, and the symbols used in the following text and figures, are discussed in Appendix C, which was adapted from a discussion presented in Beauheim (1986). Familiarity on the part of the reader with the material in Appendix C is assumed in the following chapter.

Results of the analyses are presented below, divided first by test, and second by wells on and off the H-3 hydropad. All analyses were performed with the INTERPRET well-test interpretation code developed by A. C. Gringarten and Scientific Software-Intercomp (SSI), which is described briefly in Appendix C.

6.1 Test 1

Hydraulic properties for the Culebra dolomite were interpretable from drawdown data from wells H-3b1, H-3b2, H-3b3, and DOE-1 from the 1984 H-3 pumping test. Because of the tracer test that followed immediately after the pumping test, no recovery data are available.

6.1.1 H-3b3 (Pumping Well)

The pumping-well (H-3b3) pressure response during the 1984 test appears to be that of a well completed in a double-porosity medium. Double-porosity media have two porosity sets that differ in terms of storage volume and permeability. Typically, the two porosity sets are a fracture network, with higher permeability and lower storage, and the primary porosity of the rock matrix, with lower permeability and higher storage. Double-porosity media are discussed more fully in Appendix C.

Figures 6-1 and 6-2 show linear-linear and log-log plots, respectively, of the H-3b3 data along with

double-porosity simulations of these data generated by INTERPRET. The data, particularly the pressure derivatives, are somewhat noisy because of pumping-rate fluctuations. The best INTERPRET simulations were achieved by assuming unrestricted interporosity flow (Appendix C), and using a transmissivity of 2.9 ft²/day (Table 6-1). This transmissivity is representative of the total system (i.e., fractures and matrix), but is derived almost entirely from the fractures. The storativity ratio, ω , was 0.07 for this test, an approximate measure of the percentage of water produced during the test coming from the fractures as opposed to from the matrix.

Table 6-1. Summary of Interpretive Results From 1984 H-3 Pumping Test

Well	Transmissivity (ft ² /day)	Skin Factor	Storativity	Storativity Ratio, ω
H-3b3	2.9	-7.8	NA	0.07
H-3b1	3.0	-7.3	—	0.25
H-3b2	3.0	-7.6	—	0.04
DOE-1	12	NA	1.2×10 ⁻⁵	NA

If we assume that the matrix porosity of the Culebra at H-3 is ~20%, that the fluid viscosity is ~1.0 cp, and that the total-system compressibility is ~2×10⁻⁵ psi⁻¹, the skin factor (s) for this well is ~-7.8. This is an extreme value for skin, lower (more negative) than Gringarten (1984) considers reasonable for a well that has not been acidized (see Appendix C for a discussion of skin factors). Because skin factor is proportional to total-system compressibility, this low value for skin may indicate that a higher value of Culebra compressibility is appropriate at H-3. In any case, a highly negative skin factor indicates that the wellbore is directly intersected by fractures. High-permeability fractures in direct connection with a wellbore may act as additional production surfaces to the well (in addition to the wellbore itself). Jenkins and Prentice (1982) term this type of wellbore-fracture system an "extended" well. Earlougher (1977) relates skin factor to an "effective" wellbore radius quantitatively by the following equation:

$$r_e = r_w e^{-s}, \quad (6-1)$$

where

r_e = effective wellbore radius

r_w = actual wellbore radius

s = skin factor.

This equation indicates that a well with a positive skin factor (wellbore damage) behaves hydraulically like a well with a smaller radius. A well with a negative skin factor should behave like a well with a larger radius. H-3b3, with a skin factor of -7.8 and a radius of 0.198 ft, behaves like a well with a radius of ~ 480 ft. The wellbore-storage coefficient calculated for H-3b3, 50 gal/psi, also indicates that the well is in direct connection with a much larger volume of water than that contained within the wellbore.

6.1.2 H-3b1 and H-3b2

The H-3b3 skin factor and effective wellbore radius help to explain the responses of the two observation wells on the H-3 hydropad. As discussed in Section 5.1, wells H-3b1 and H-3b2 responded very rapidly when the pump was turned on in H-3b3, and showed nearly the same amounts of drawdown as the pumping well. Figures 6-3 and 6-4 show log-log plots of the pressure and pressure-derivative data from H-3b1 and H-3b2, respectively. These responses are typical of pumping wells, not observation wells. Observation-well responses, even in double-porosity media, should show the general shape of a Theis curve (see Figure 6-3 and Appendix C), which represents the response observed at some distance from a (vertical) line source (or sink). H-3b1 and H-3b2 appear to be so well connected to H-3b3 hydraulically that they behave as if they are in fact part of the pumping well; i.e., on the scale of 100 ft, H-3b3 cannot be approximated as a line source. Judging from the skin factor calculated for H-3b3, direct connection of H-3b3 to

H-3b1 and H-3b2 by high-permeability fractures is not unreasonable.

Figures 6-3 and 6-4 show INTERPRET-generated simulations of the H-3b1 and H-3b2 data, respectively, treating those wells like pumping wells. This treatment is by no means rigorously correct, but it does provide some useful insight into the hydraulic behavior of the Culebra at the H-3 hydropad. Both sets of data are matched quite well using a double-porosity model with unrestricted interporosity flow. The analyses yield identical values of transmissivity of 3.0 ft²/day, and skin factors of -7.3 and -7.6 , for H-3b1 and H-3b2, respectively (Table 6-1). The calculated transmissivity values at H-3b1 and H-3b2 are slightly higher than that from H-3b3 because slightly less drawdown was measured at the two observation wells.

Some differences between the two observation-well responses are apparent. Because of the distances between H-3b1 and H-3b2 and the pump, data from those wells show less response to pumping-rate fluctuations than do the H-3b3 data. H-3b1 data, however, show less damping than the H-3b2 data (Figure 5-1), even though H-3b1 is farther from H-3b3. This may indicate a more direct connection between H-3b3 and H-3b1 than between H-3b3 and H-3b2. The storativity ratios estimated for the two observation wells also differed, with the 0.25 calculated for H-3b1 considerably larger than the 0.04 calculated for H-3b2 (Table 6-1). This difference points to a larger fracture volume in communication with H-3b1.

Because the damping discussed above reduces "noise" in the pressure derivative, the transition between water produced solely from the fractures and water produced by both the fractures and matrix is seen more clearly in the observation-well data, particularly from H-3b2 (Figure 6-4), than in the pumping-well data. This transition begins in the first 5 min of the test, indicating a high degree of interconnection between the matrix pores and the fractures.

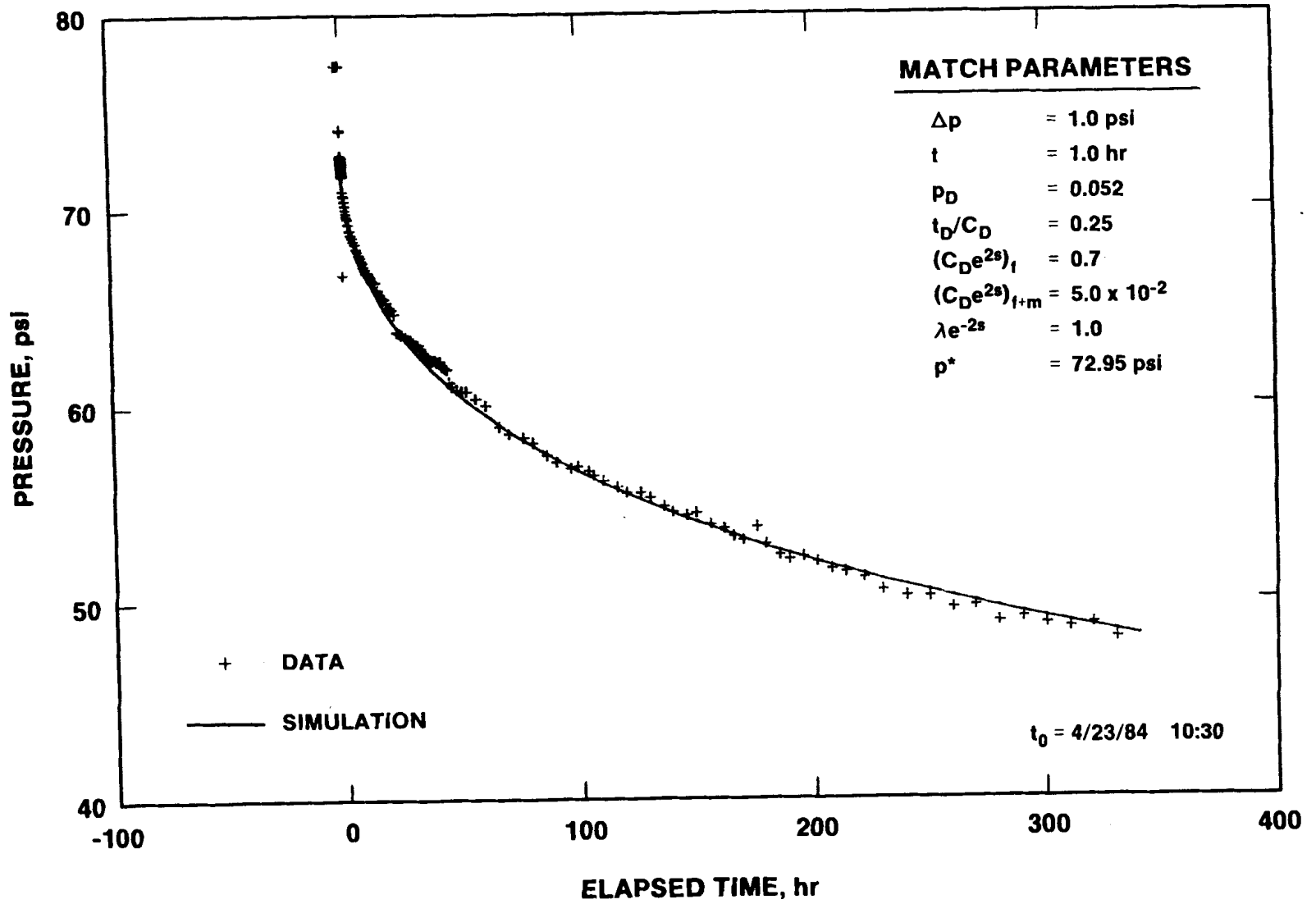


Figure 6-1. 1984 H-3 Pumping Test—H-3b3 Sequence Plot With INTERPRET Simulation

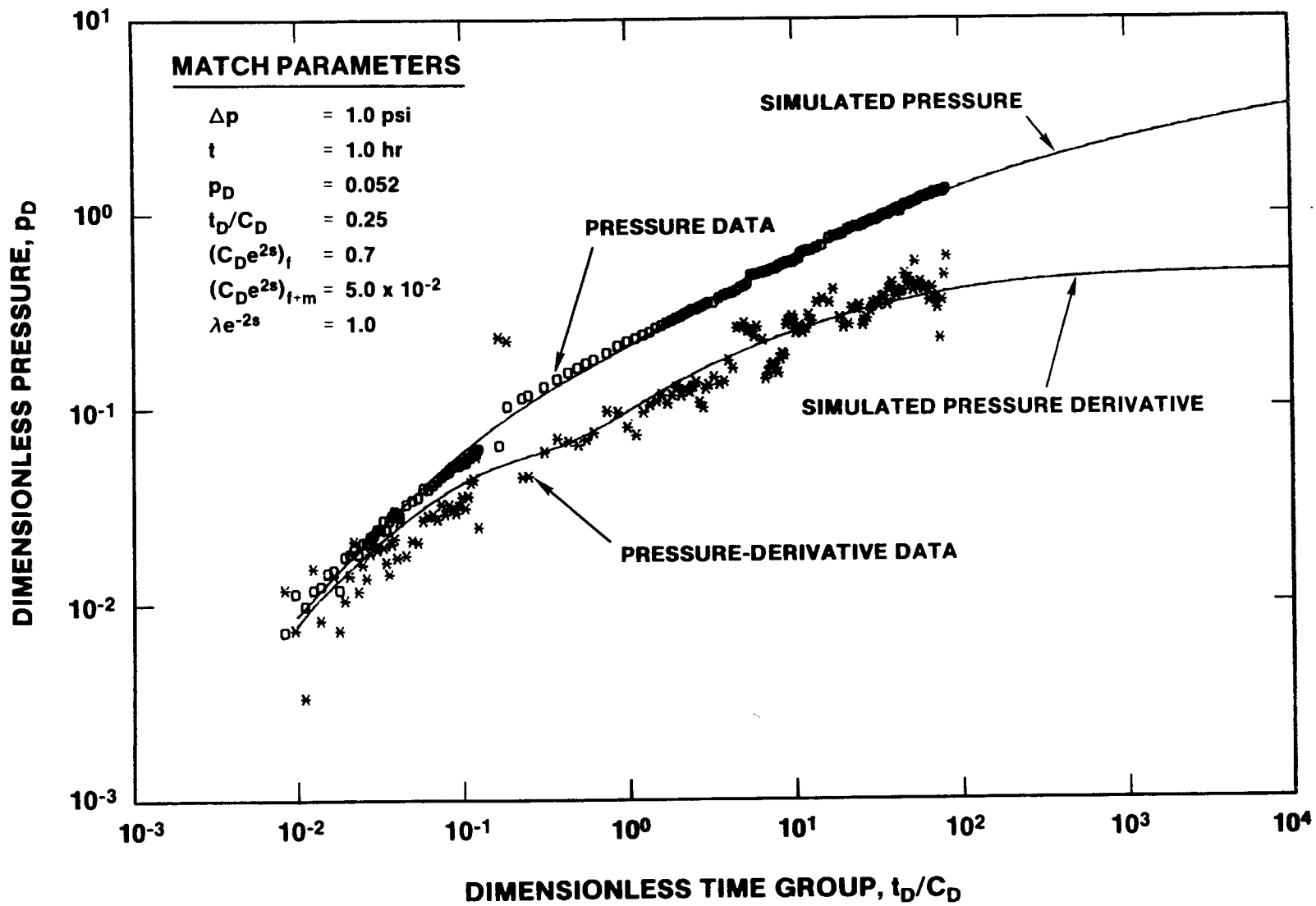


Figure 6-2. 1984 H-3 Pumping Test – H-3b3 Drawdown Log-Log Plot With INTERPRET Simulation

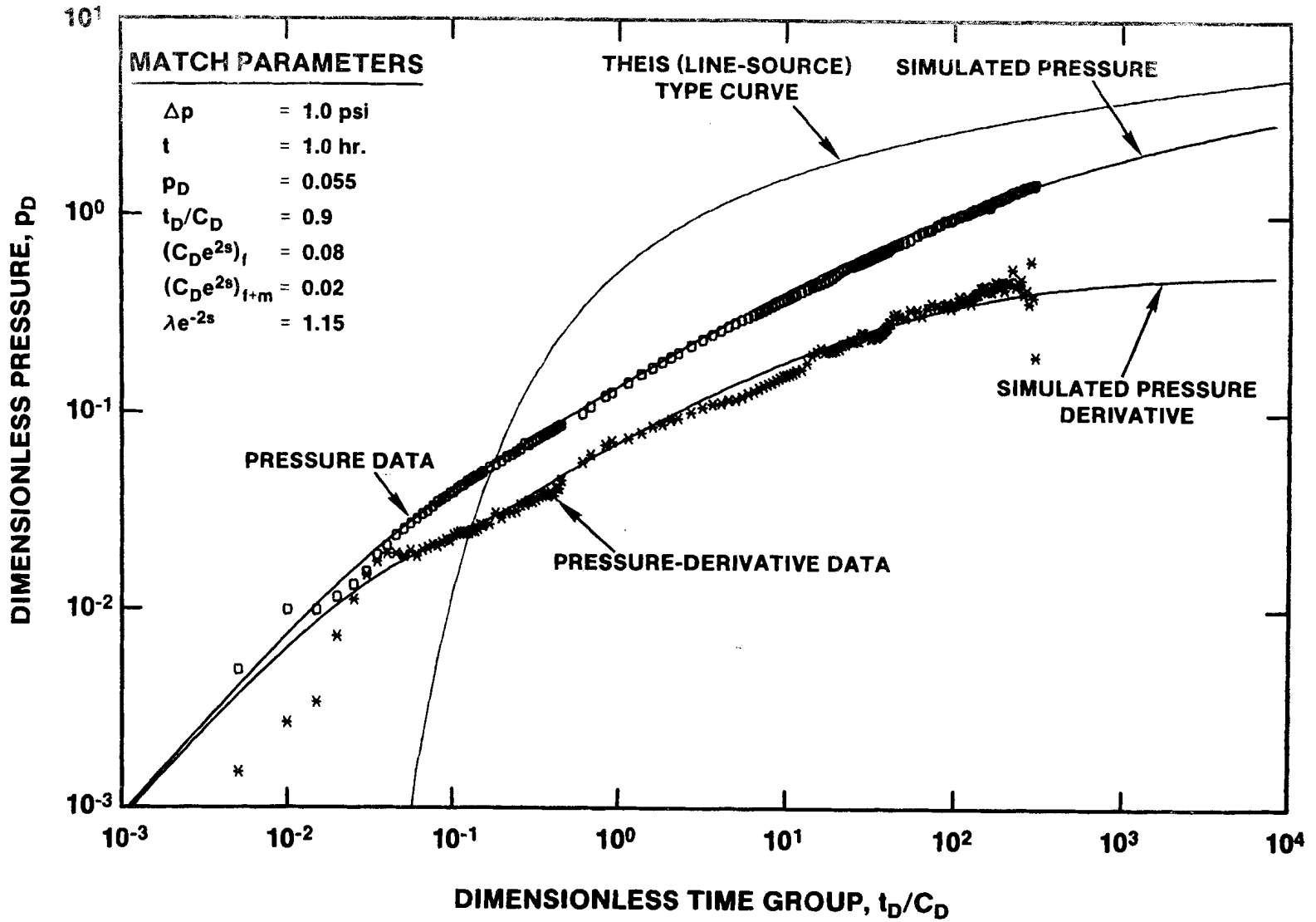


Figure 6-3. 1984 H-3 Pumping Test—H-3b1 Drawdown Log-Log Plot With INTERPRET Simulation

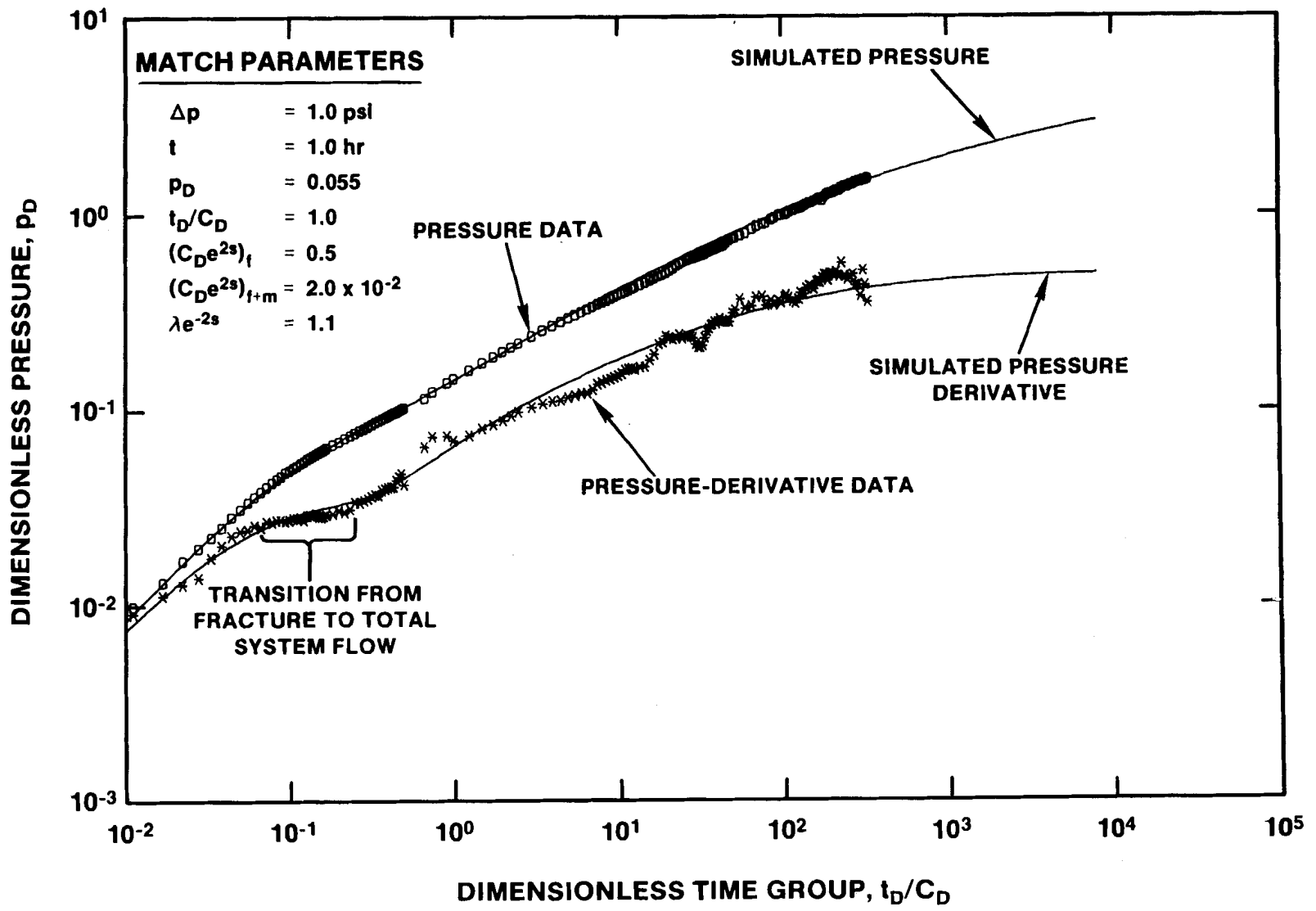


Figure 6-4. 1984 H-3 Pumping Test—H-3b2 Drawdown Log-Log Plot With INTERPRET Simulation

6.1.3 DOE-1

The DOE-1 data from the 1984 H-3 test were interpreted by fitting them to the line-source solution of Theis (1935) for flow in a porous medium, as implemented by INTERPRET (Appendix C). Several assumptions are implicit in the use of the line-source solution to simulate observation-well responses. One is that the aquifer is areally homogeneous. This means that water is contributed to the pumping well equally from all directions. In an inhomogeneous aquifer, less permeable regions will contribute less water, and more permeable regions will contribute more water. This will cause more drawdown in the more permeable regions than in a homogeneous system, and less drawdown in the less permeable regions. As a result, estimates of transmissivity for the more permeable regions will be too low, and estimates of transmissivity for the less permeable regions will be too high. Numerical modeling is required to evaluate the magnitude of these errors. In this report, the transmissivity and storativity values derived through an analytical approach are termed the "apparent" values.

A second assumption underlying the use of the line-source solution is that, on the areal scale of the observations, the aquifer behaves like a single-porosity medium. In a double-porosity medium, this assumption is justified when an observation well is far enough from the pumping well that only total-system responses are observed (Appendix C). The DOE-1 response exhibited no indications of double-porosity effects.

The calculated DOE-1 pressure data from before and during the 1984 H-3 pumping test are shown in Figure 6-5, along with a simulation of the pumping-period data generated by INTERPRET using a transmissivity of 12 ft²/day and a storativity of 1.2×10^{-5} . These apparent transmissivity and storativity values represent the gross or average hydraulic properties of the Culebra over the distance between H-3b3 and DOE-1, assuming that the Culebra is homogeneous in the region affected by pumping. An additional degree of uncertainty in these values is caused by the sparsity of the data and by the difficulty in defining a precise pretest static pressure (p^*).

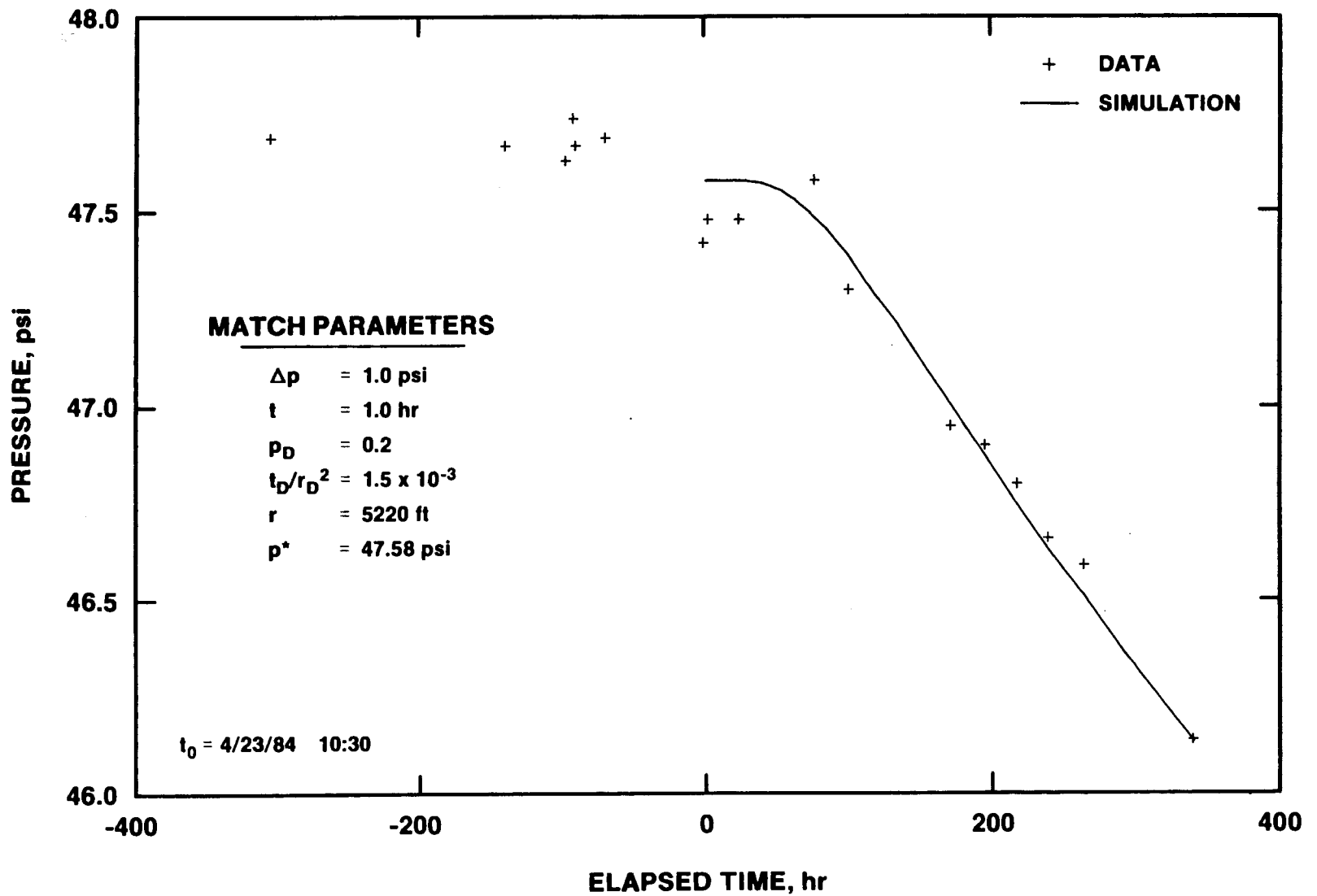


Figure 6-5. 1984 H-3 Pumping Test—DOE-1 Pressure Response With INTERPRET Simulation

6.2 Test 2 (Multipad Test)

Apparent responses to the H-3 multipad test were observed in the wells on the H-3, H-2, and H-11 hydropads, and at H-1, DOE-1, WIPP-19, WIPP-21, and WIPP-22. Pressure changes were also noted at the Culebra horizon behind the liner in the Waste-Handling Shaft during the test. Slight water-level changes were also noted at P-14, P-15, P-17, H-6b, and at WIPP-18 during the multipad-test monitoring period. These responses are interpreted and discussed below.

6.2.1 H-3 Hydropad

When the H-3 multipad test began, the wells on the H-3 hydropad were still recovering from several other pumping activities earlier in the year, and from the Exhaust Shaft sealing in July 1985. The most significant pre-multipad test pumping activity at the H-3 hydropad was the step-drawdown test conducted from June 20 to July 10, 1986 to determine the optimum pumping rate for the multipad test. This was followed by three brief pumping episodes related to testing of the pump and other instrumentation (INTERA Technologies, 1986). To simulate the responses on the H-3 hydropad to the multipad test, we had to include the residual responses to the four previous pumping episodes. This was done following the principle of superposition, which states most simply that responses to multiple pumping events are additive. Table 6-2 summarizes the pumping history used to simulate the responses of the H-3 wells to the multipad test. No attempt was made to include shaft effects in the pumping history.

Table 6-2. 1985 H-3b2 Pumping History

Event	Start Time (day:hr:min)	Duration (hr)	Rate (gpm)
Step-drawdown test	171:12:34	484.93	4.13
Recovery	191:17:30	2229.50	0.0
Pump test	284:15:00	0.25	4.79
Recovery	284:15:15	0.52	0.0
Pump test	284:15:46	0.14	4.79
Recovery	284:15:54	46.59	0.0
Pump test	286:14:30	0.27	4.36
Recovery	286:14:46	42.23	0.0
Multipad test	288:09:00	1488.00	4.82
Recovery	350:09:00	2800.00	0.0

H-3b2 (Pumping Well): The Culebra at H-3 behaved hydraulically like a double-porosity medium during the multipad pumping test, as it did during the 1984 test. Figure 6-6 shows a log-log plot of the pumping-well (H-3b2) drawdown data from the multipad test, along with simulations of those data generated by INTERPRET. The data, particularly the pressure derivatives, are somewhat noisy because of pumping-rate fluctuations. The INTERPRET simulations shown were obtained by assuming unrestricted interporosity flow (Appendix C), and using a transmissivity of 1.7 ft²/day. The storativity ratio (ω) was 0.03.

If we assume a Culebra porosity of 20%, a fluid viscosity of 1.0 cp, and a total-system compressibility of 2×10^{-5} psi⁻¹, the skin factor (s) for H-3b2 is ~ -8.1 . From Eq (6.1), this skin factor indicates that the well behaves hydraulically as though it had a radius of ~ 625 ft. Extremely negative skin factors, however, are better viewed qualitatively than quantitatively. Instead of attaching too much significance to a calculated effective well radius of 625 ft, H-3b2 should be viewed simply as intersected by fractures that increase the production surface of the well.

Figure 6-7 shows a linear-linear plot of both the drawdown and recovery data from H-3b2, along with a simulation of the test data generated by INTERPRET using the double-porosity model derived from the interpretation of the drawdown data. The drawdown-period data in this plot have been increased by 10.7 psi to compensate for the initial pump loss (see Section 5.2.1). Several features of this plot are noteworthy. First, the simulation is better during drawdown than during recovery. Toward the end of the recovery period, the simulation predicts increasingly less recovery than was observed. Second, the static formation pressure (p^*) specified for this simulation was 101.0 psig, several psi higher than the pressure measured at the beginning of the step-drawdown test in June 1985. Together, these observations indicate that at late time a significant portion of the well recovery was related to additional stresses apart from the multipad test.

Figure 6-8, the log-log plot and INTERPRET simulation of the recovery data, also shows the added recovery effects. The INTERPRET simulation was generated using the model derived from the drawdown-data analysis. In an ideal system with no stresses other than the test itself, this model should fit the recovery data perfectly. In this system, the fit is reasonably close until late time, indicating that the

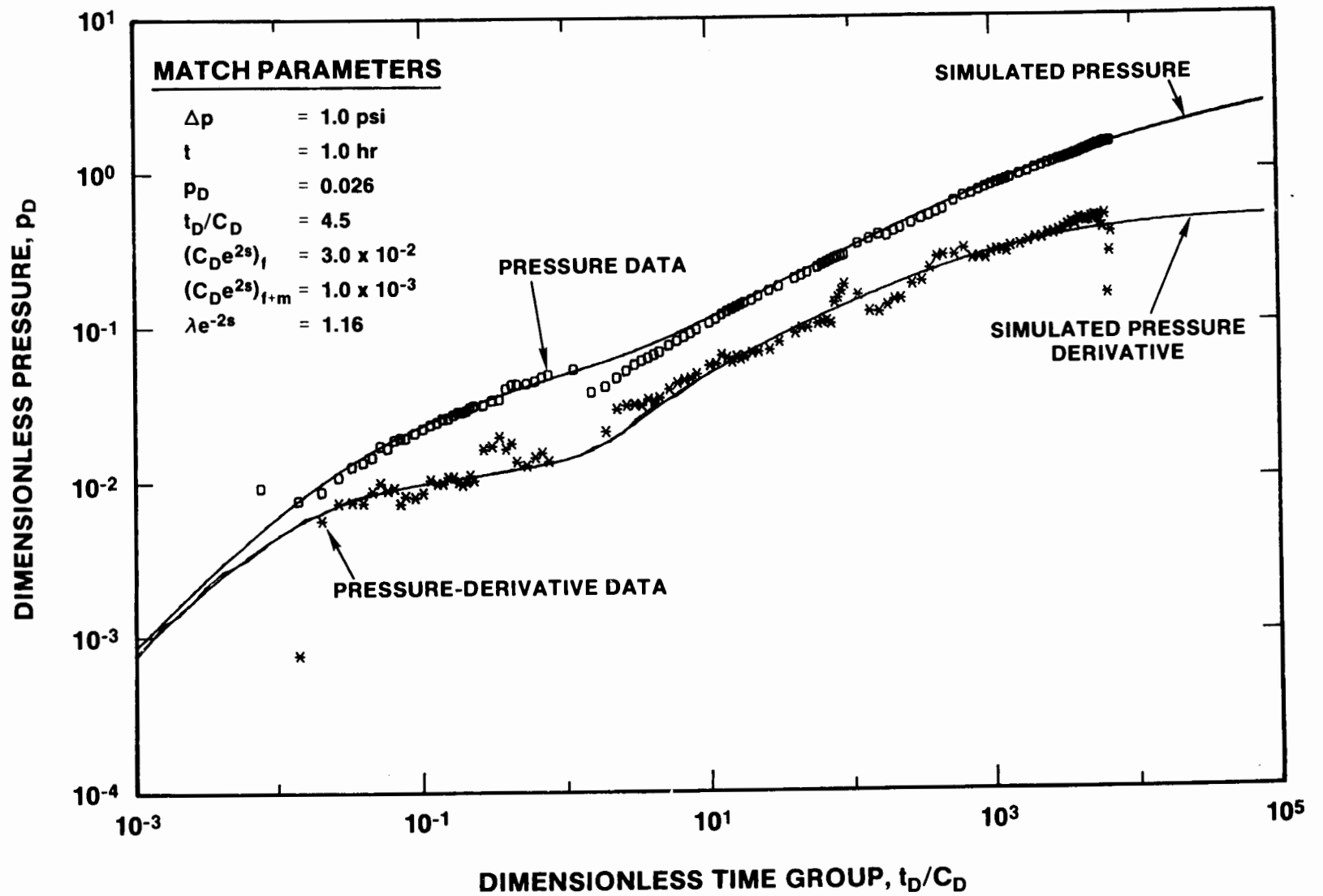


Figure 6-6. H-3 Multipad Pumping Test—H-3b2 Drawdown Log-Log Plot With INTERPRET Simulation

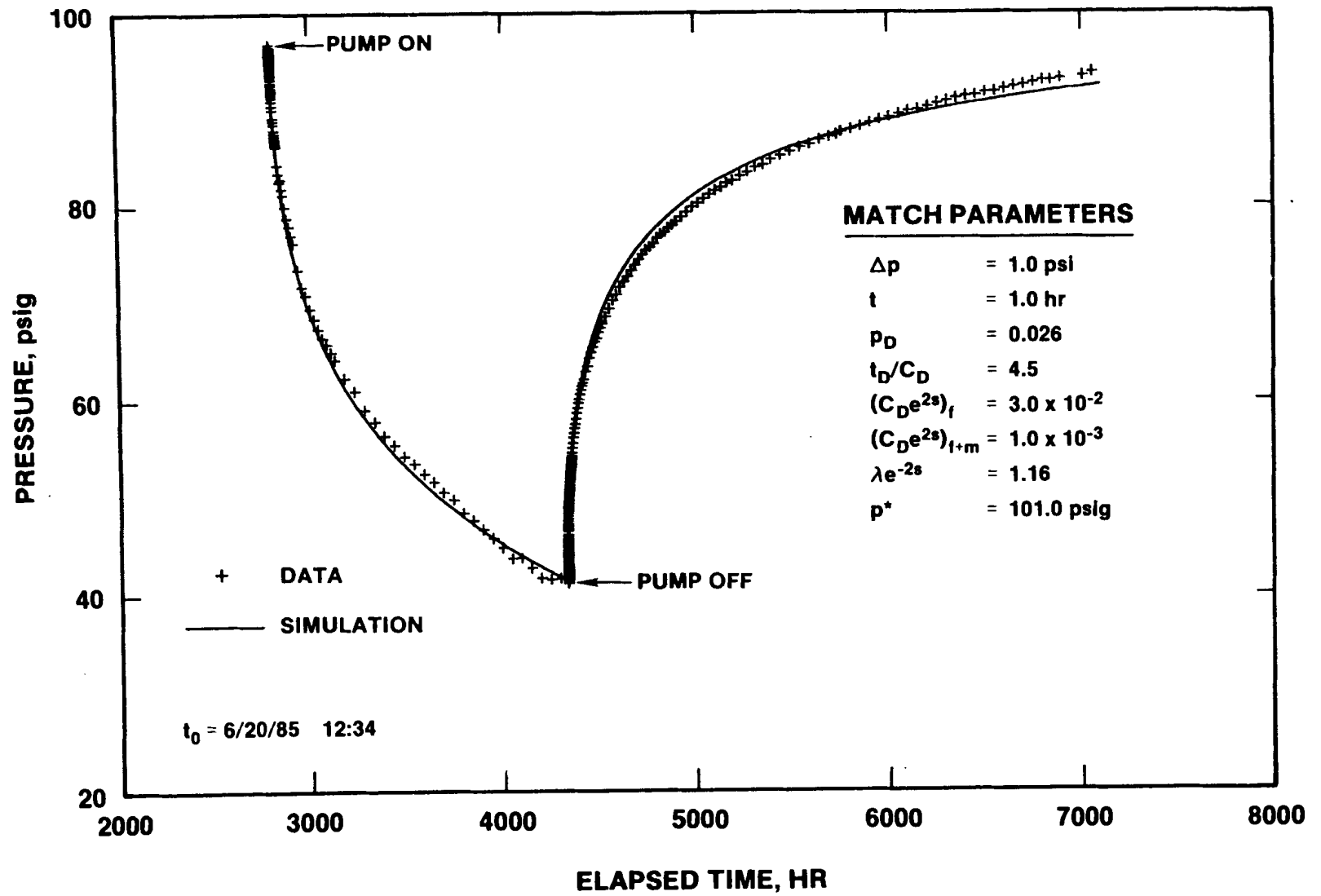


Figure 6-7. H-3 Multipad Pumping Test—H-3b2 Sequence Plot With INTERPRET Simulation

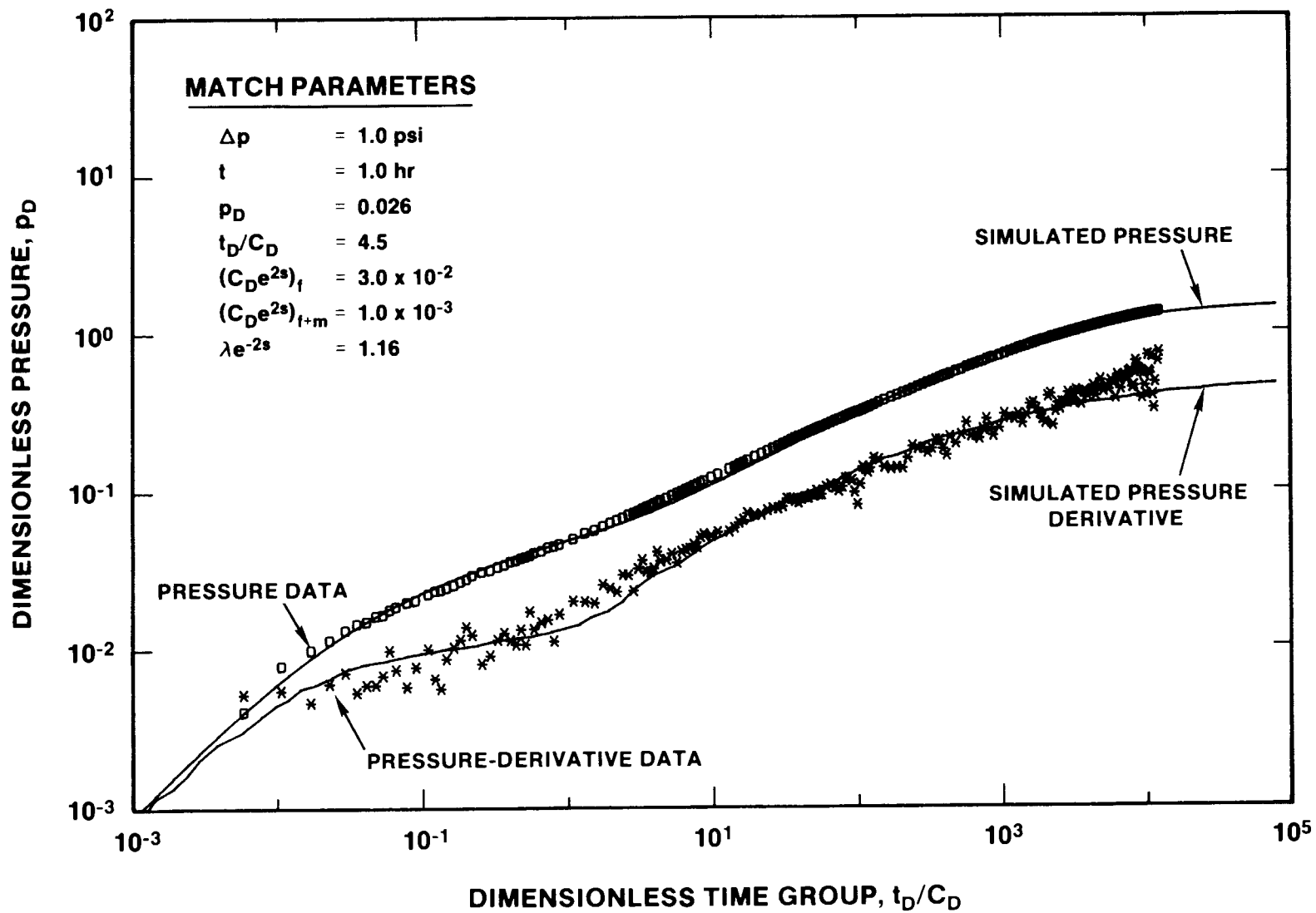


Figure 6-8. H-3 Multipad Pumping Test—H-3b2 Recovery Log-Log Plot With INTERPRET Simulation

model chosen appears to be an appropriate approximation to the actual system. At late time, the pressure and pressure-derivative data are rising above the simulations, apparently because of extra, nontest-related recovery.

Figures 6-9 and 6-10 show dimensionless Horner plots of the H-3b2 drawdown and recovery data, respectively, along with INTERPRET simulations. Like the log-log (Figure 6-6) and linear-linear (Figure 6-7) plots of the drawdown data, the dimensionless Horner plot shows excellent agreement between the observed drawdown data and the double-porosity simulation (Figure 6-9). The dimensionless Horner plot of the recovery data (Figure 6-10) has two important features: (1) the agreement between the data and the simulation at early time (the right side of the plot) shows the correctness of the selected pressure match (or transmissivity), and (2) the deviation of the data below the simulation at late time (lower left on the plot) shows that the pressure was recovering faster than it should have if it were recovering only from the five pumping periods included in the simulation. Most likely, some of the observed recovery was a regional response to the sealing of the Exhaust Shaft in July 1985.

H-3b1 and H-3b3: As in the 1984 test, the two nonpumping wells on the H-3 hydropad behaved like part of the pumping well, instead of like observation wells, during the multipad test. Consequently, even though not rigorously correct, the H-3b1 and H-3b3 responses were interpreted as if those wells were the pumping well to obtain additional insight into the Culebra behavior at H-3.

Figures 6-11 and 6-12 show log-log plots of the H-3b1 and H-3b3 drawdown data along with INTERPRET simulations. These simulations are based on a double-porosity model with unrestricted interporosity flow. The transmissivities used in the simulations were 1.8 ft²/day for both wells, and storativity ratios were 0.25 for H-3b1 and 0.10 for H-3b3 (Table 6-3).

Skin factors of -7.7 and -8.0 were calculated for H-3b1 and H-3b3, respectively. The calculated transmissivity values at H-3b1 and H-3b3 are slightly higher than that from H-3b2 because slightly less drawdown was measured at the two observation wells.

The two well responses were very similar. Neither well was significantly more sensitive to pumping-rate fluctuations than the other, perhaps indicating the absence of any preferred connection between either well and H-3b2. As in the 1984 test, H-3b1 has a higher storativity ratio than the other H-3 wells, probably indicating direct connection to a larger fracture volume. Both wells also show transition from fracture-only to fracture-plus-matrix flow during the first few minutes of pumping, indicating a high degree of interconnection between the matrix pores and the fractures.

The H-3b1 and H-3b3 recovery data show exactly the same additional recovery as do the H-3b2 data. As an example, Figure 6-13, the dimensionless Horner plot for the H-3b3 recovery, shows the pressure recovering more rapidly than the simulation at late time. As with the H-3b2 data, the best simulations of the H-3b1 and H-3b3 data were obtained using static formation pressures (p^*) several psi higher than those measured before testing began. Clearly, the wells were responding to some hydraulic stresses in addition to the multipad test.

Table 6-3. Summary of Multipad-Test Interpretive Results From H-3 Wells

Well	Transmissivity (ft ² /day)	Skin Factor	Storativity Ratio, ω
H-3b2	1.7	-8.1	0.03
H-3b1	1.8	-7.7	0.25
H-3b3	1.8	-8.0	0.10

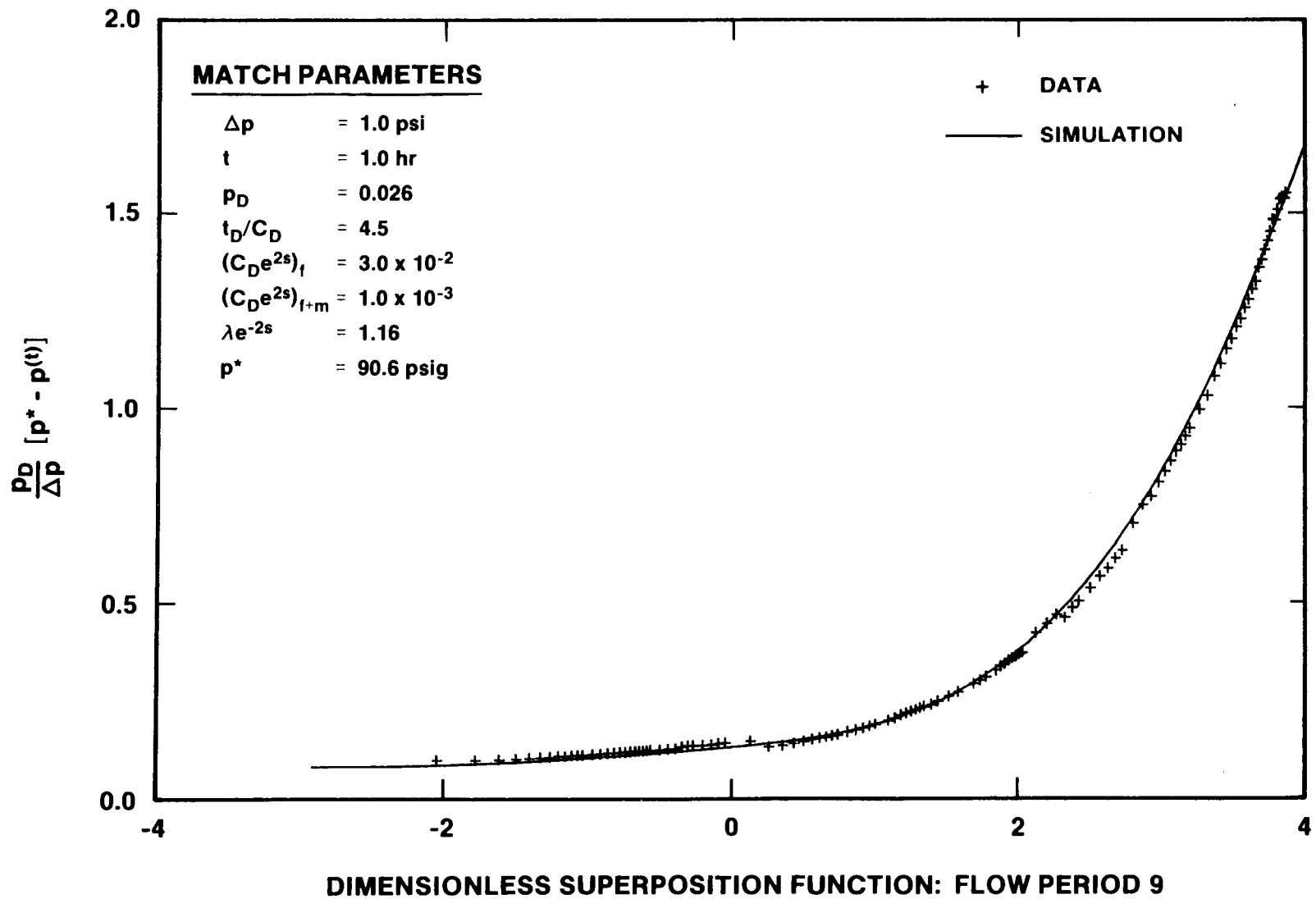


Figure 6-9. H-3 Multipad Pumping Test—H-3b2 Drawdown Dimensionless Horner Plot With INTERPRET Simulation

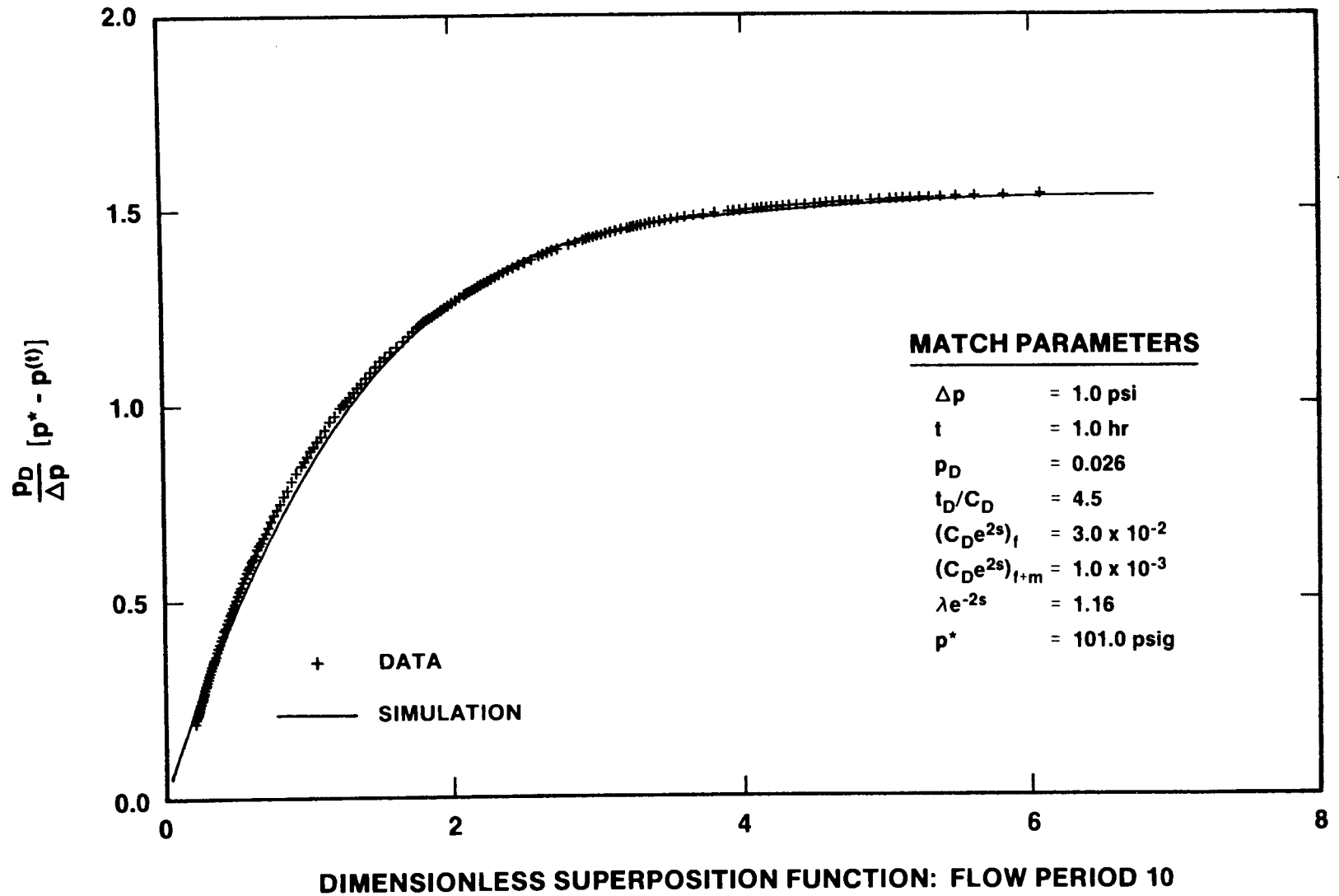


Figure 6-10. H-3 Multipad Pumping Test—H-3b2 Recovery Dimensionless Horner Plot With INTERPRET Simulation

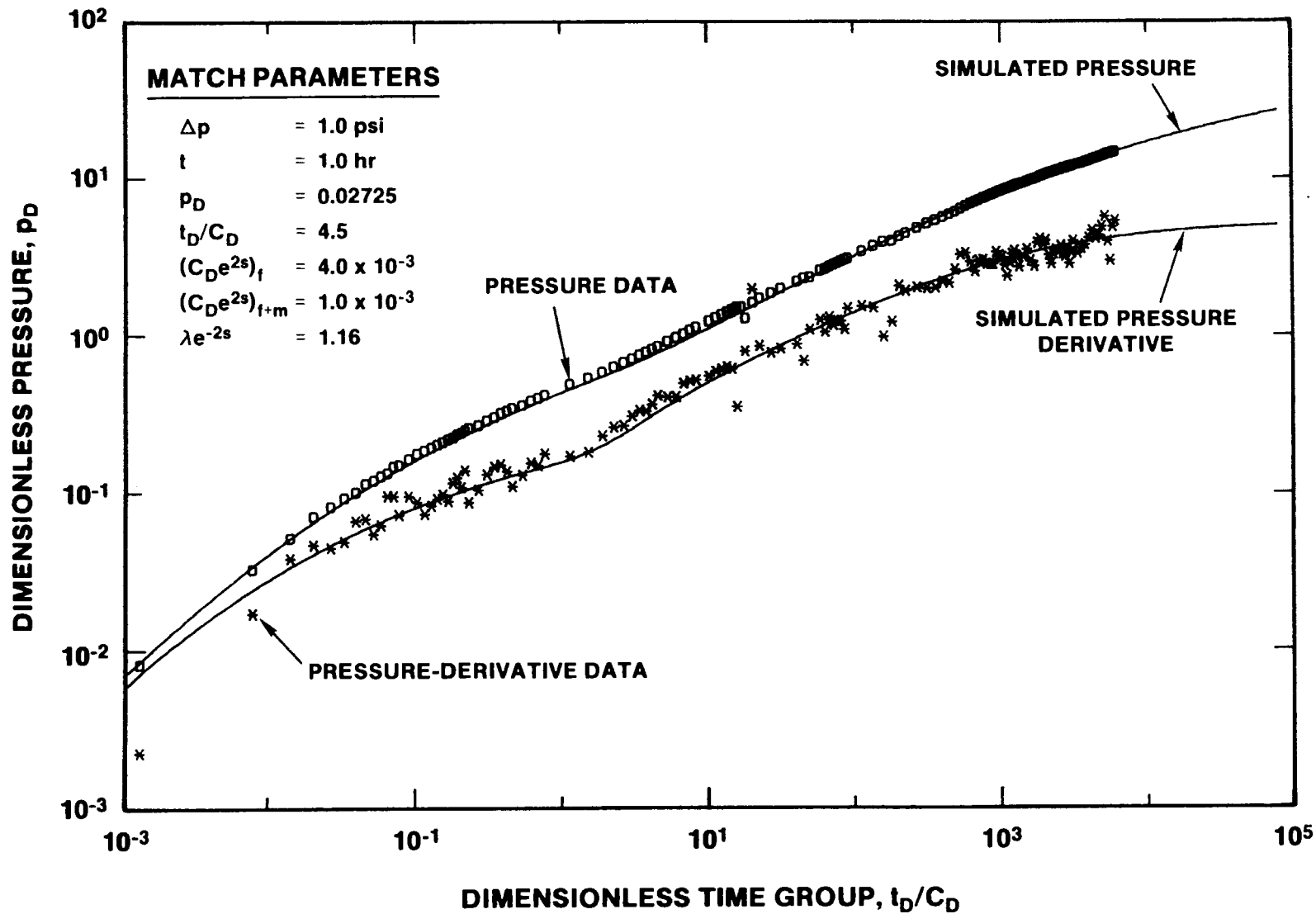


Figure 6-11. H-3 Multipad Pumping Test—H-3b1 Drawdown Log-Log Plot With INTERPRET Simulation

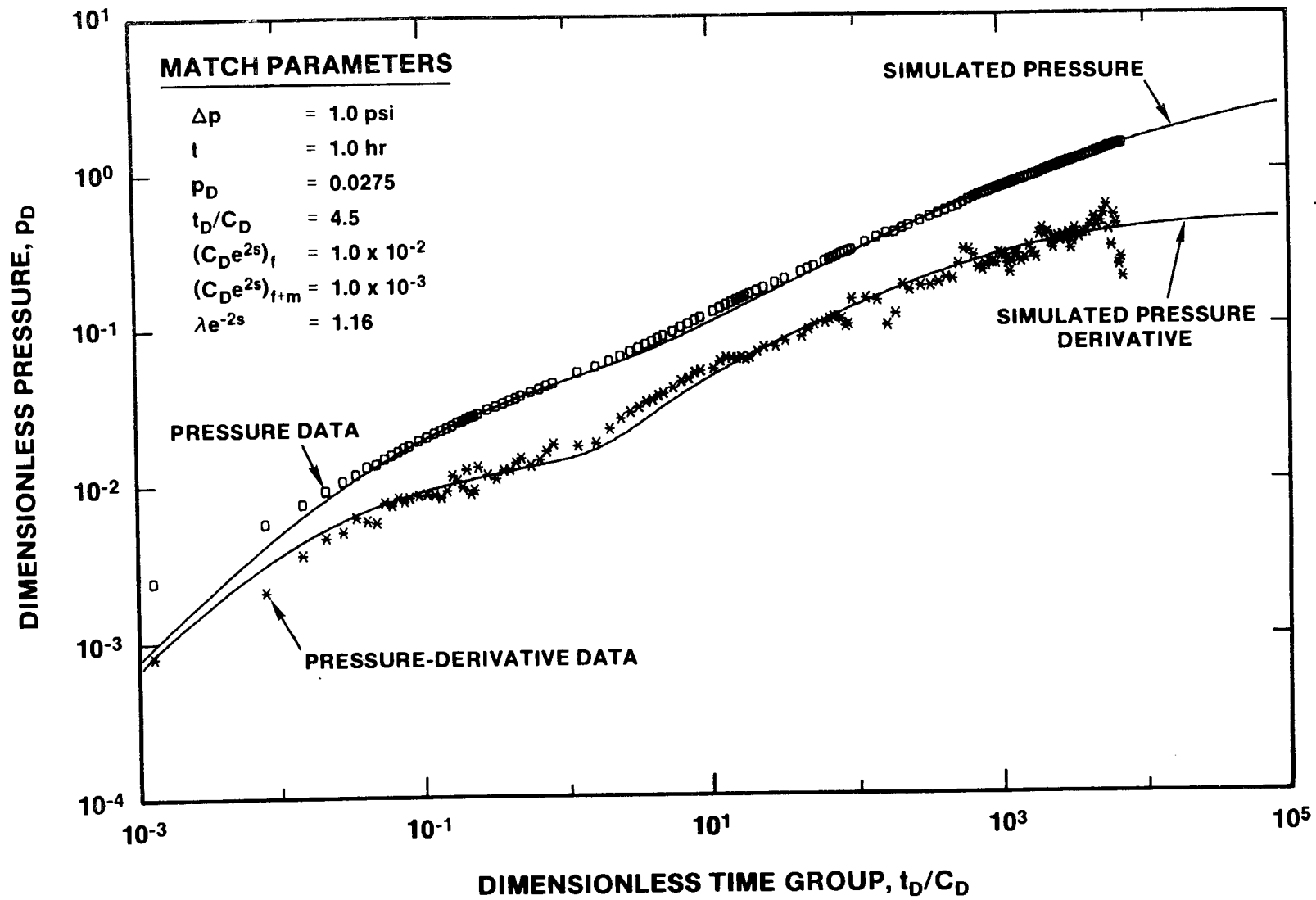


Figure 6-12. H-3 Multipad Pumping Test—H-3b3 Drawdown Log-Log Plot With INTERPRET Simulation

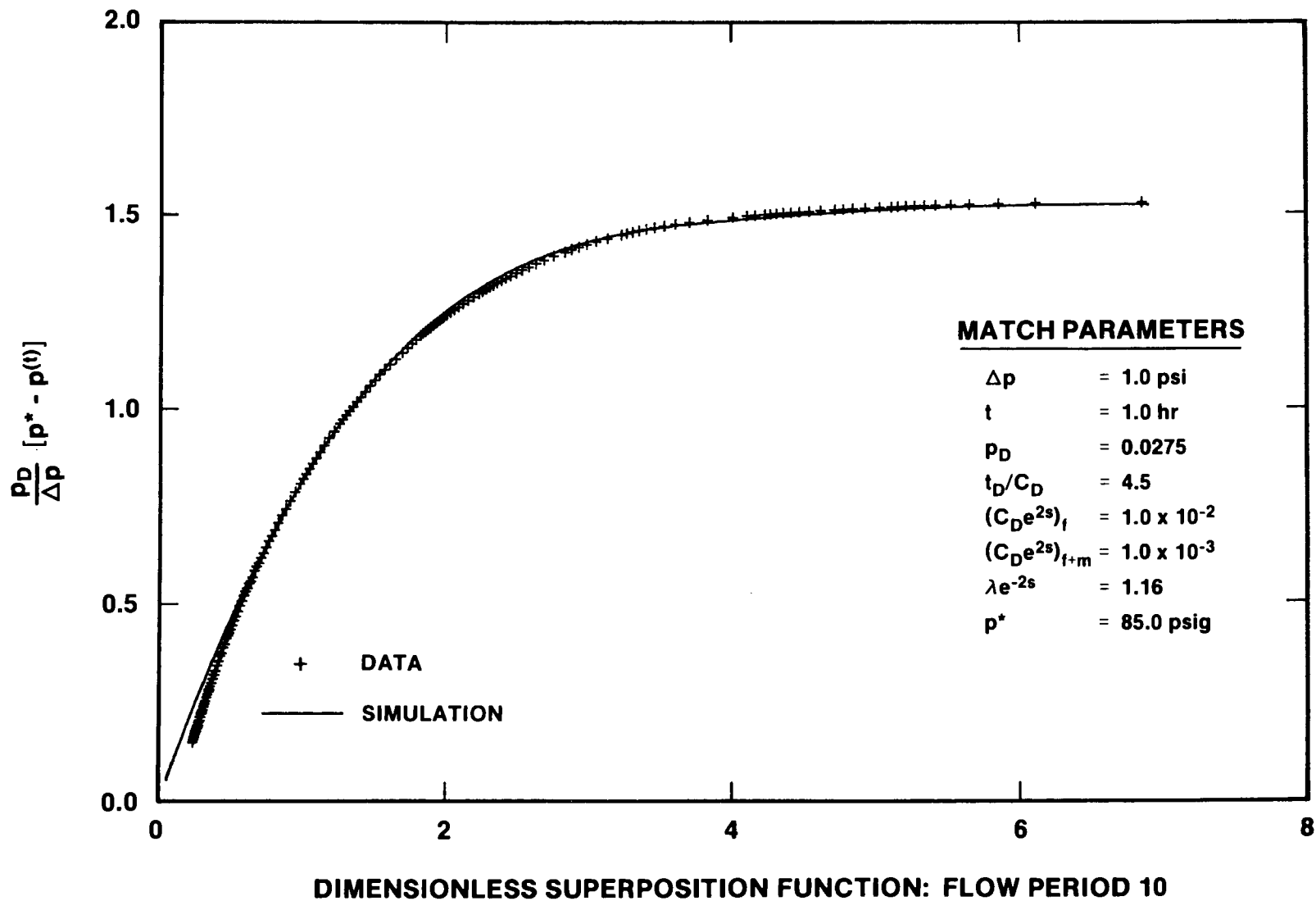


Figure 6-13. H-3 Multipad Pumping Test—H-3b3 Recovery Dimensionless Horner Plot With INTERPRET Simulation

6.2.2 Observation Wells

The observation-well responses were interpreted by fitting them to the line-source solution derived by Theis (1935) for flow in a porous medium, as implemented by INTERPRET (Appendix C). The limitations inherent in this approach were discussed in Section 6.1.3. Because INTERPRET can fit both the drawdown and recovery responses as a continuous record, two criteria were used in determining the best fit to the line-source solution. These were first to match the time at which pressure recovery began, and then to match the total magnitude of drawdown observed. The pressure match defines the transmissivity of the system, and the time match and pressure match together define the storativity of the system.

For the four wells for which the observed data were modified to compensate for pretest pressure/water-level trends (H-1, H-2b2, H-11b1, and DOE-1; Section 5.2.2), two interpretations are presented below. The first interpretation for each represents the best fit to the observed data with no modifications. Because the pretest trend of rising pressure/water level has not been compensated for in these data, the data show less drawdown and more rapid recovery than if the trend had been absent. As a result, the simulated fit to these data uses a slightly erroneous storativity and a transmissivity that is too high.

The second interpretation represents the best fit to the data including a linear compensation for the pretest trend. In most hydrologic systems, pressure/water-level trends follow exponential curves, decaying with time. Hence, applying a linear correction derived from pretest behavior to the observed test data probably represents some degree of overcompensation, particularly at late time. An exponentially decreasing compensation should be more accurate than a linear compensation, but the basis for such a compensation cannot be defined and defended with the available data, nor could the direction of the residual error be determined. When a linear compensation is employed, the simulated fit to these data uses a transmissivity that can reliably be considered a minimum, as well as a slightly erroneous storativity. Between them, the two interpretations presented should bound the apparent physical properties of the system being modeled.

Individual well responses are discussed and interpreted below. Quantitative results are summarized in Table 6-4.

H-1: Figure 6-14 presents pressure data calculated from the water levels observed at H-1 during the

multipad test, along with a simulation of those data generated by INTERPRET using a line-source solution. The simulation fits the data reasonably well until the recovery period, when the simulation predicts increasingly less recovery than was observed. The apparent transmissivity and storativity used for this simulation were $0.83 \text{ ft}^2/\text{day}$ and 3.9×10^{-5} , respectively.

Figure 6-15 presents the H-1 pressure data modified for the pretest water-level trend of $1.3 \text{ ft}/15 \text{ days}$, along with an INTERPRET-generated simulation. The simulation fits the entire data set very well, and particularly fits the recovery data much better than the simulation of the unmodified data (Figure 6-14). An apparent transmissivity of $0.46 \text{ ft}^2/\text{day}$ and an apparent storativity of 2.7×10^{-5} were used in this simulation.

H-2b2: Figure 6-16 presents pressure data calculated from the observed water levels at H-2b2 during the multipad test, along with a simulation of those data generated by INTERPRET using a line-source solution. The simulation is in reasonable agreement with the data until recovery begins, after which the simulation consistently predicts less recovery than was observed. The apparent transmissivity and storativity used for this simulation were $2.5 \text{ ft}^2/\text{day}$ and 4.5×10^{-5} , respectively.

Figure 6-17 presents the H-2b2 pressure data modified for the pretest water-level trend of $0.57 \text{ ft}/15 \text{ days}$, along with an INTERPRET-generated simulation. This simulation fits the entire data set very well, and provides a much better match to the recovery-period data than did the simulation of the unmodified data (Figure 6-16). An apparent transmissivity of $1.2 \text{ ft}^2/\text{day}$ and an apparent storativity of 3.0×10^{-5} were used in this simulation.

Table 6-4. Summary of Multipad-Test Observation-Well Response Interpretations

For the Flowpath Between H-3 and Well	Unmodified Data		Modified Data		Compensation
	T (ft^2/day)	S	T (ft^2/day)	S	
H-1	0.83	3.9×10^{-5}	0.46	2.7×10^{-5}	1.3 ft/15 days
H-2b2	2.5	4.5×10^{-5}	1.2	3.0×10^{-5}	0.57 ft/15 days
H-11b1	13	6.8×10^{-6}	6.8	7.4×10^{-6}	0.425 ft/15 days
DOE-1	9.2	9.2×10^{-6}	5.5	1.0×10^{-5}	0.27 psi/15 days
WIPP-19	2.9	2.9×10^{-6}	NA	NA	None
WIPP-21	1.1	9.0×10^{-6}	NA	NA	None
WIPP-22	1.6	1.7×10^{-6}	NA	NA	None

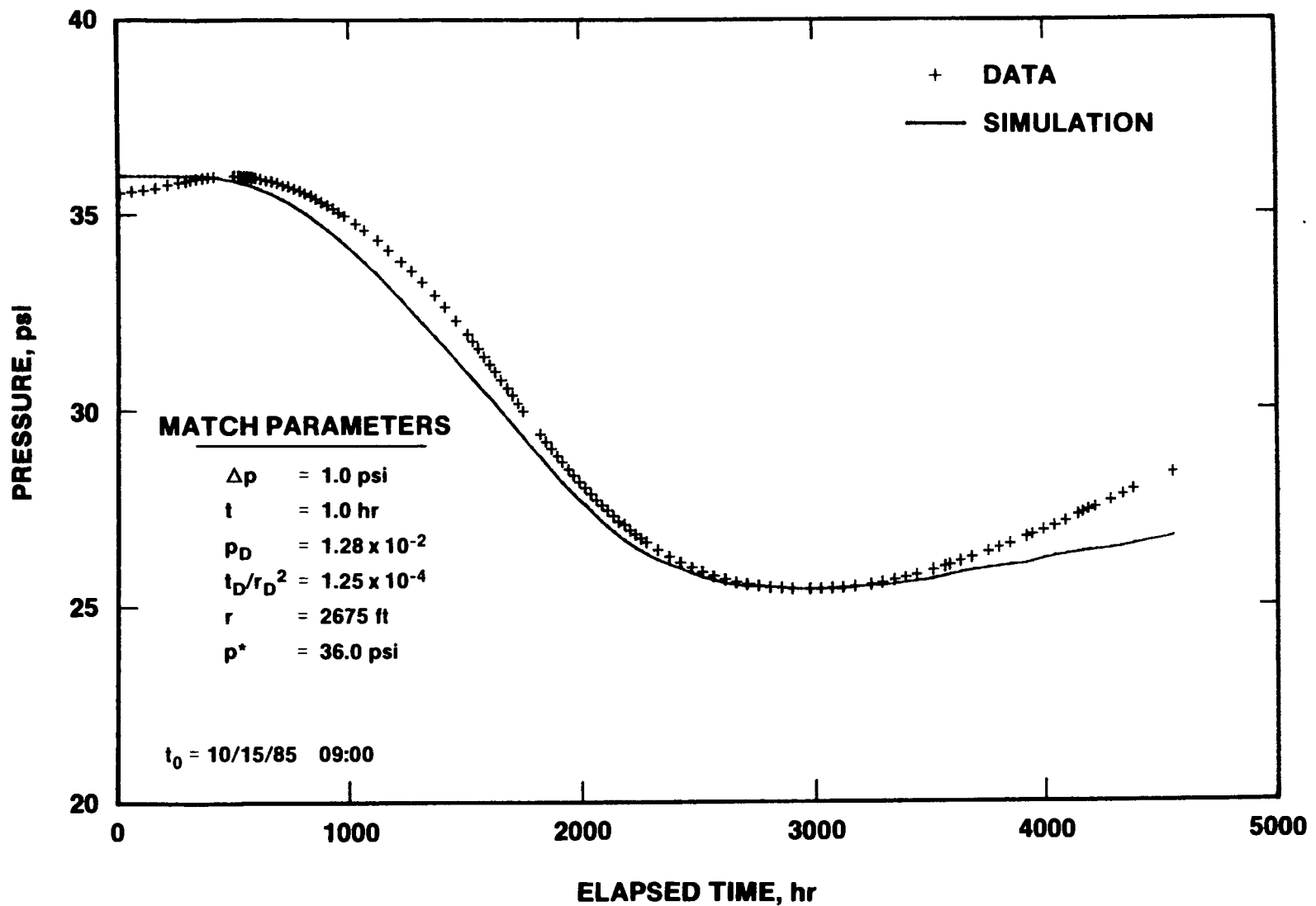


Figure 6-14. H-3 Multipad Pumping Test—H-1 Pressure Response With INTERPRET Simulation

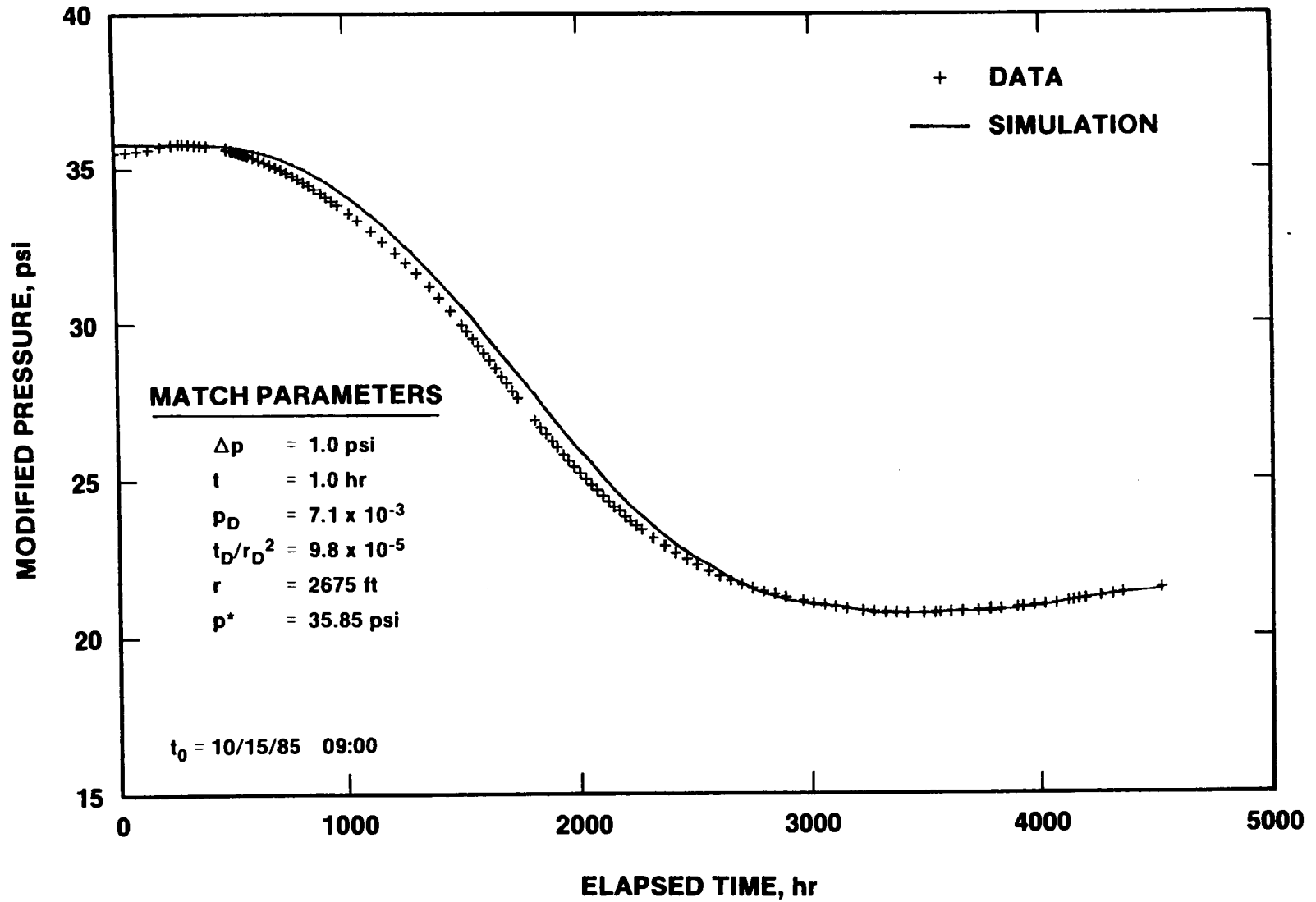


Figure 6-15. H-3 Multipad Pumping Test—H-1 Pressure Response Modified for 1.3 Ft/15 Days Water-Level Trend With INTERPRET Simulation

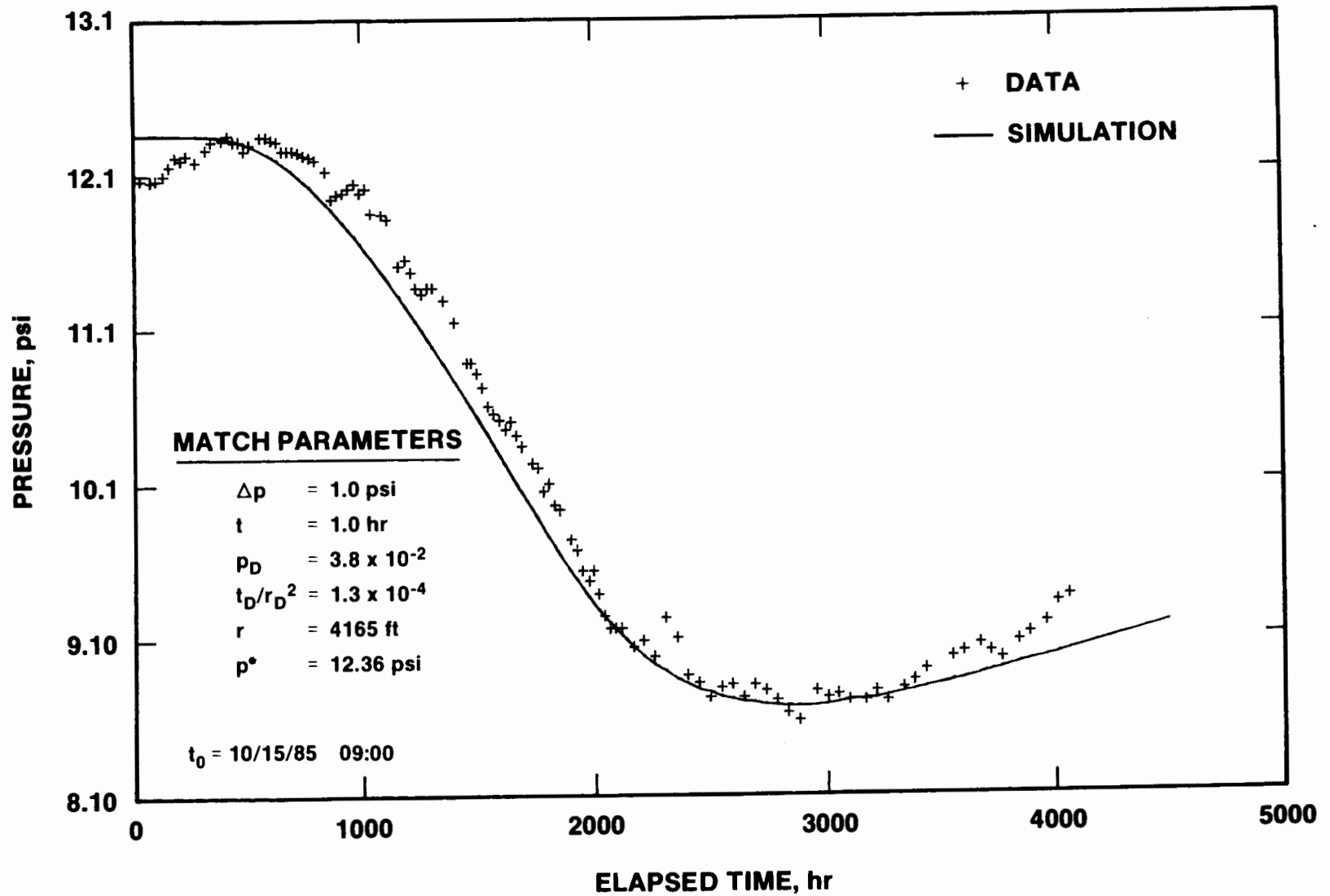


Figure 6-16. H-3 Multipad Pumping Test—H-2b2 Pressure Response With INTERPRET Simulation

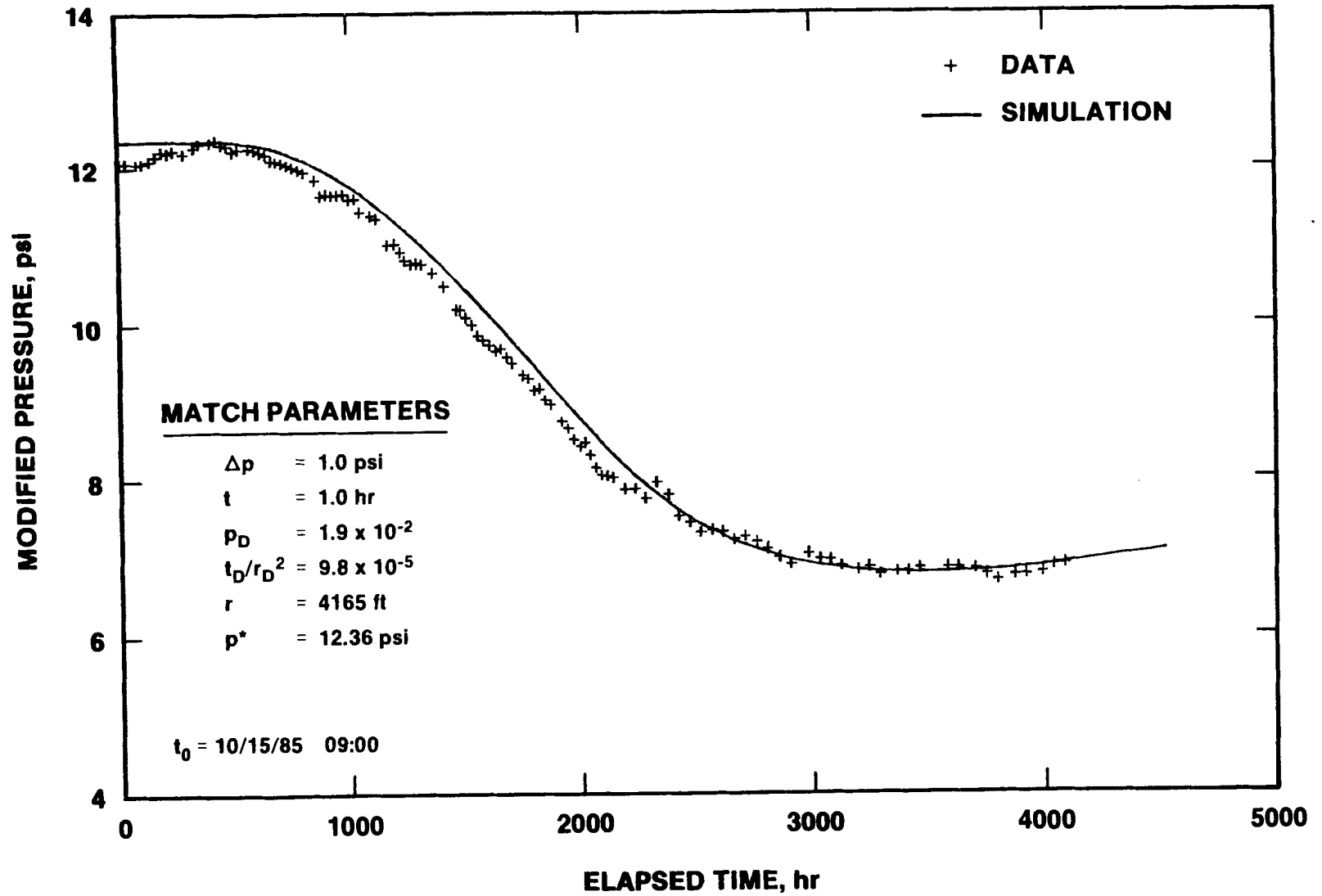


Figure 6-17. H-3 Multipad Pumping Test—H-2b2 Pressure Response Modified for 0.57 Ft/15 Days Water-Level Trend With INTERPRET Simulation

H-11b1: Figure 6-18 presents pressure data calculated from the observed water levels at H-11b1 during the multipad test, along with a simulation of those data generated by INTERPRET using a line-source solution. In general, the data show more linearity (less curvature) than does the simulation. The simulation further deviates from the data at late time, when the recovery data rise above the simulation. The apparent transmissivity and storativity used in this simulation were $13 \text{ ft}^2/\text{day}$ and 6.6×10^{-6} , respectively.

Figure 6-19 shows the H-11b1 pressure data modified for the pretest water-level trend of $0.425 \text{ ft}/15 \text{ days}$, along with an INTERPRET-generated simulation. This simulation fits the drawdown data very well, but predicts increasingly more recovery than is indicated by the data. The apparent transmissivity and storativity used for this simulation were $6.8 \text{ ft}^2/\text{day}$ and 7.4×10^{-6} , respectively.

Because of the pretest water-level trend compensation, the modified data in Figure 6-19 show considerably less recovery than the unmodified data in Figure 6-18. As discussed above, applying a linear correction to compensate for pretest trends represents a degree of overcompensation, particularly at late time. This definitely seems to be the case for the H-11b1 data, because a reasonably good simulation of the relatively early-time (drawdown) data deviates increasingly from the later time (recovery) data. In any case, the parameters derived from the simulations of the unmodified and modified data should bound the "correct" values of the apparent transmissivity and storativity of the Culebra between H-11 and H-3.

DOE-1: The DOE-1 response to the multipad test was very similar to that of H-11b1. Figure 6-20 presents the observed pressure data from DOE-1 during the multipad test, along with a simulation of those data generated by INTERPRET using a line-source solution. In general, the data show more linearity (less curvature) than does the simulation. The apparent transmissivity and storativity used in this simulation were $9.2 \text{ ft}^2/\text{day}$ and 9.2×10^{-6} , respectively.

Figure 6-21 shows the DOE-1 pressure data modified for the pretest pressure trend of $0.27 \text{ psi}/15 \text{ days}$, along with an INTERPRET-generated simulation. This simulation fits the drawdown data very well, but predicts increasingly more recovery than the data indicated. The apparent transmissivity and storativity used for this simulation were $5.5 \text{ ft}^2/\text{day}$ and 1.0×10^{-5} , respectively.

As with the H-11b1 data, the DOE-1 pretest pressure-trend compensation causes significantly less recovery than is apparent in the unmodified data

(Figure 6-20). The good agreement between the simulation and the modified drawdown data in Figure 6-21, and the increasingly poor agreement with the recovery data, indicate probable overcompensation of the pretest trend.

WIPP-19: Figure 6-22 presents pressure data calculated from the observed water levels at WIPP-19 during the multipad test, along with a simulation of those data generated by INTERPRET using a line-source solution. The simulation shows drawdown beginning more rapidly than was observed, and less recovery than was observed. These differences are discussed more fully below in connection with the observed pressure changes at the Waste-Handling Shaft. The apparent transmissivity and storativity used in the simulation in Figure 6-22 were $2.9 \text{ ft}^2/\text{day}$ and 2.9×10^{-5} , respectively.

WIPP-21: The pressure data calculated from the observed water levels at WIPP-21 during the multipad test, along with an INTERPRET-generated simulation of those data, are presented in Figure 6-23. The observed data show two distinct slopes during the drawdown period, neither of which is matched by the simulation. The fit between the observed data and the simulation is better during recovery, although the observed data show some fluctuations not represented by the simulation. The apparent transmissivity and storativity used in the simulation were $1.1 \text{ ft}^2/\text{day}$ and 9.0×10^{-6} , respectively. As with the WIPP-19 data, the WIPP-21 data are discussed below in connection with the observed pressure changes at the Waste-Handling Shaft.

WIPP-22: Figure 6-24 presents pressure data calculated from the observed water levels at WIPP-22 during the multipad test, along with a simulation of those data generated by INTERPRET using a line-source solution. As with the WIPP-19 data, the simulation shows drawdown beginning more rapidly than was observed, and less recovery than was observed. These differences are discussed below in connection with the Waste-Handling Shaft pressures. The WIPP-19 data were simulated using an apparent transmissivity of $1.6 \text{ ft}^2/\text{day}$ and an apparent storativity of 1.7×10^{-5} .

Waste-Handling Shaft: Culebra pressures measured in the Waste-Handling Shaft during the H-3 multipad pumping test were presented in Figure 5-20. From 1985 Julian days 304 to 352 (2 days after the pump was turned off at H-3b2), the Culebra pressure

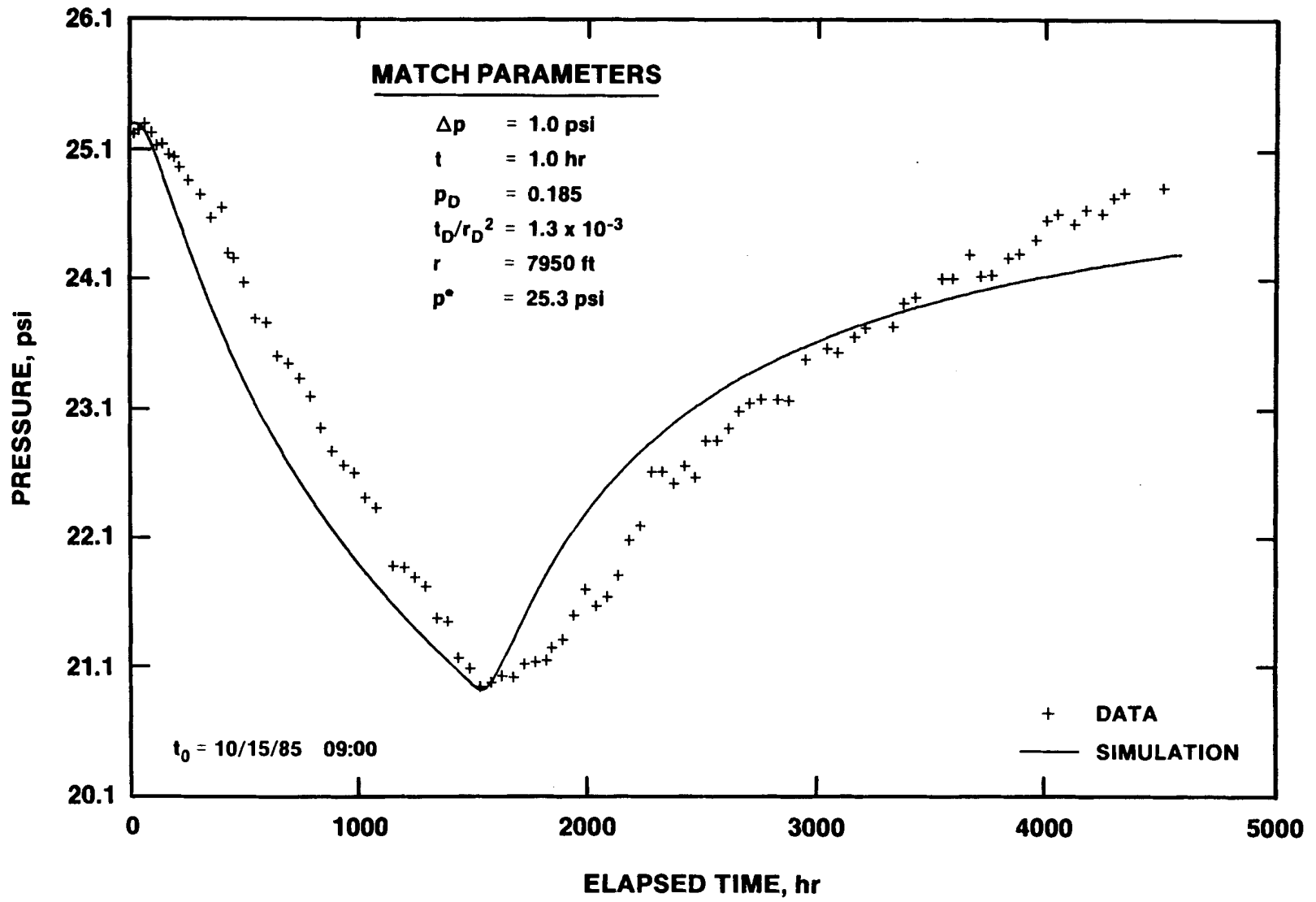


Figure 6-18. H-3 Multipad Pumping Test—H-11b1 Pressure Response With INTERPRET Simulation

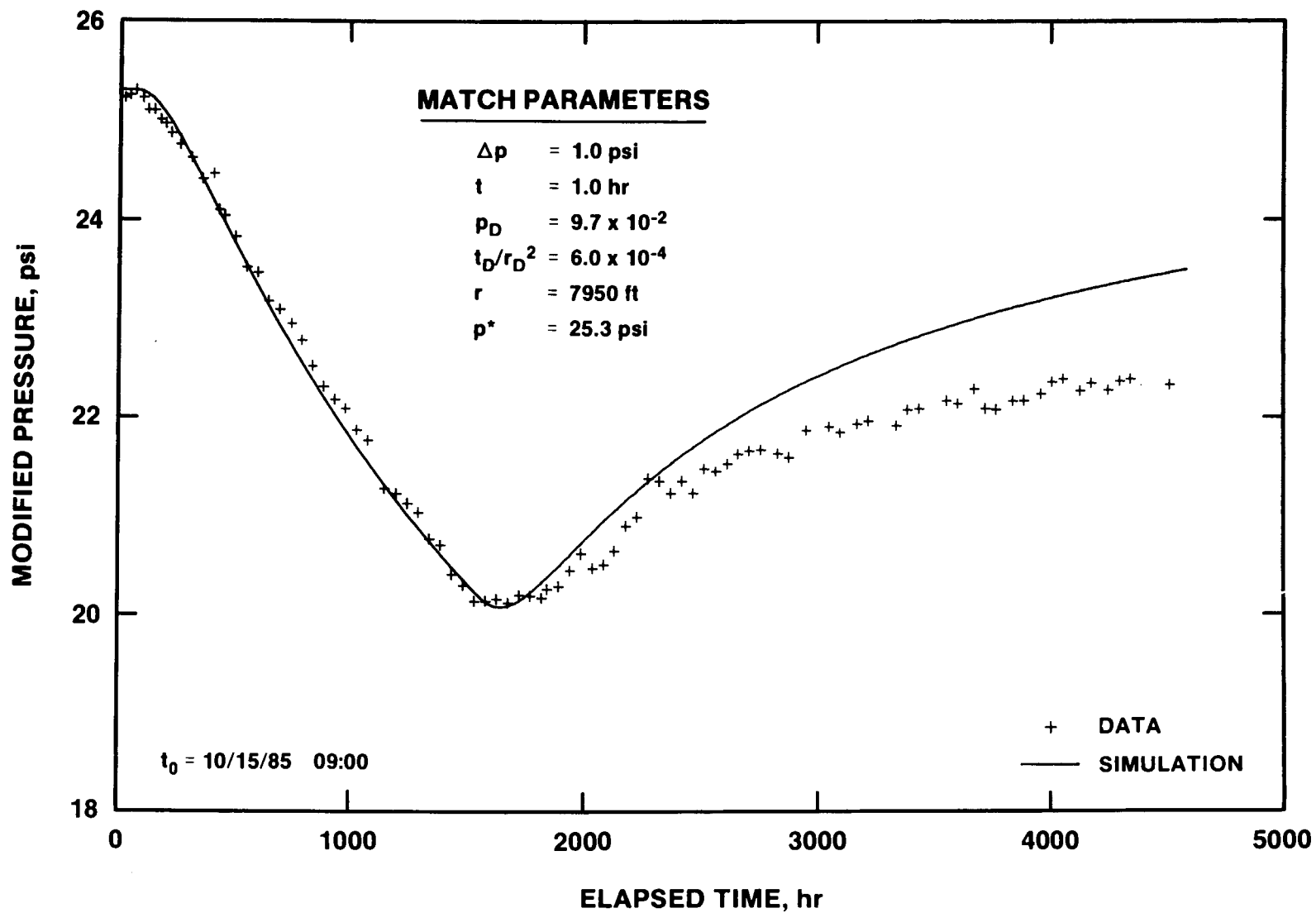


Figure 6-19. H-3 Multipad Pumping Test—H-11b1 Pressure Response Modified for 0.425 Ft/15 Days Water-Level Trend With INTERPRET Simulation

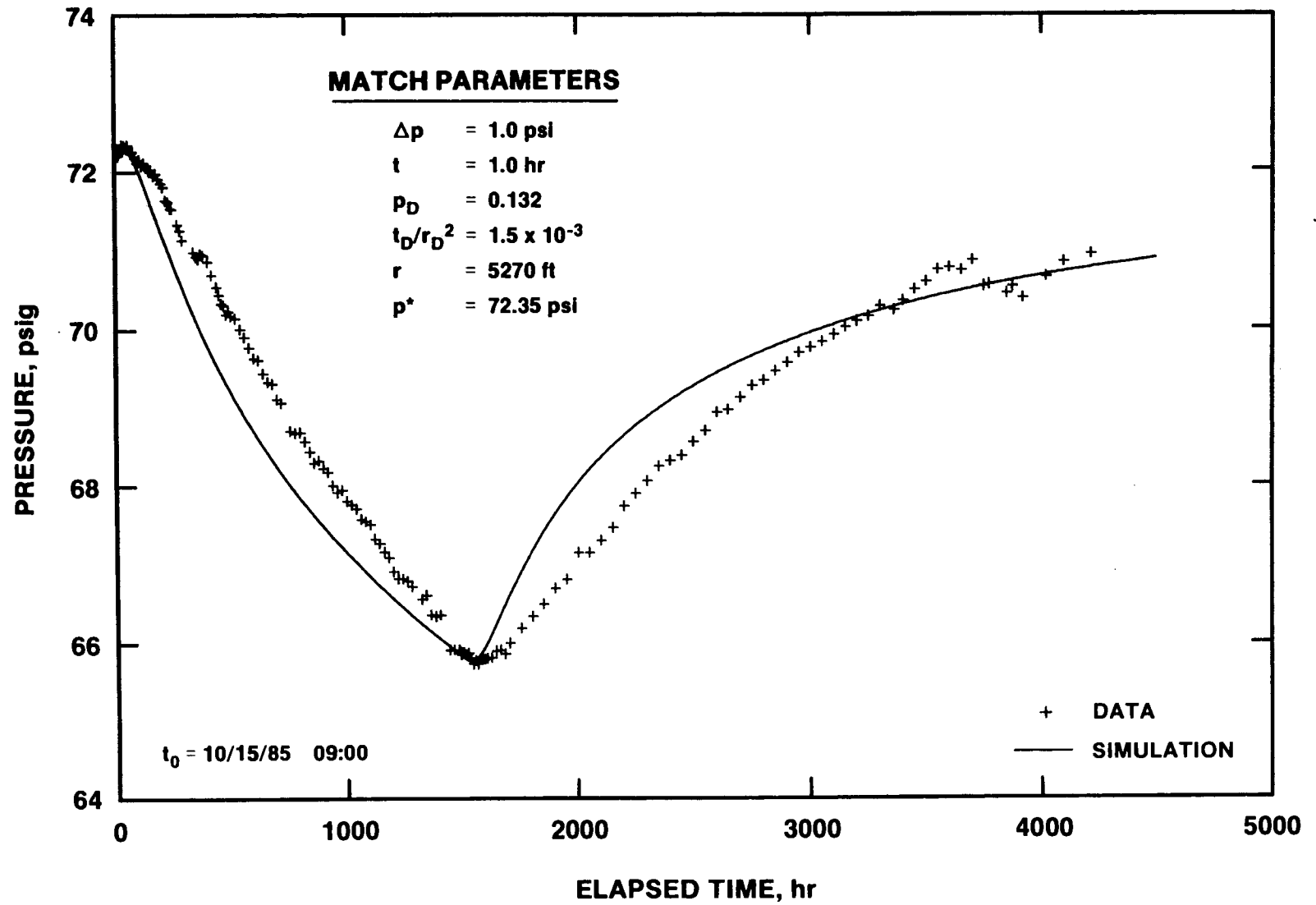


Figure 6-20. H-3 Multipad Pumping Test—DOE-1 Pressure Response With INTERPRET Simulation

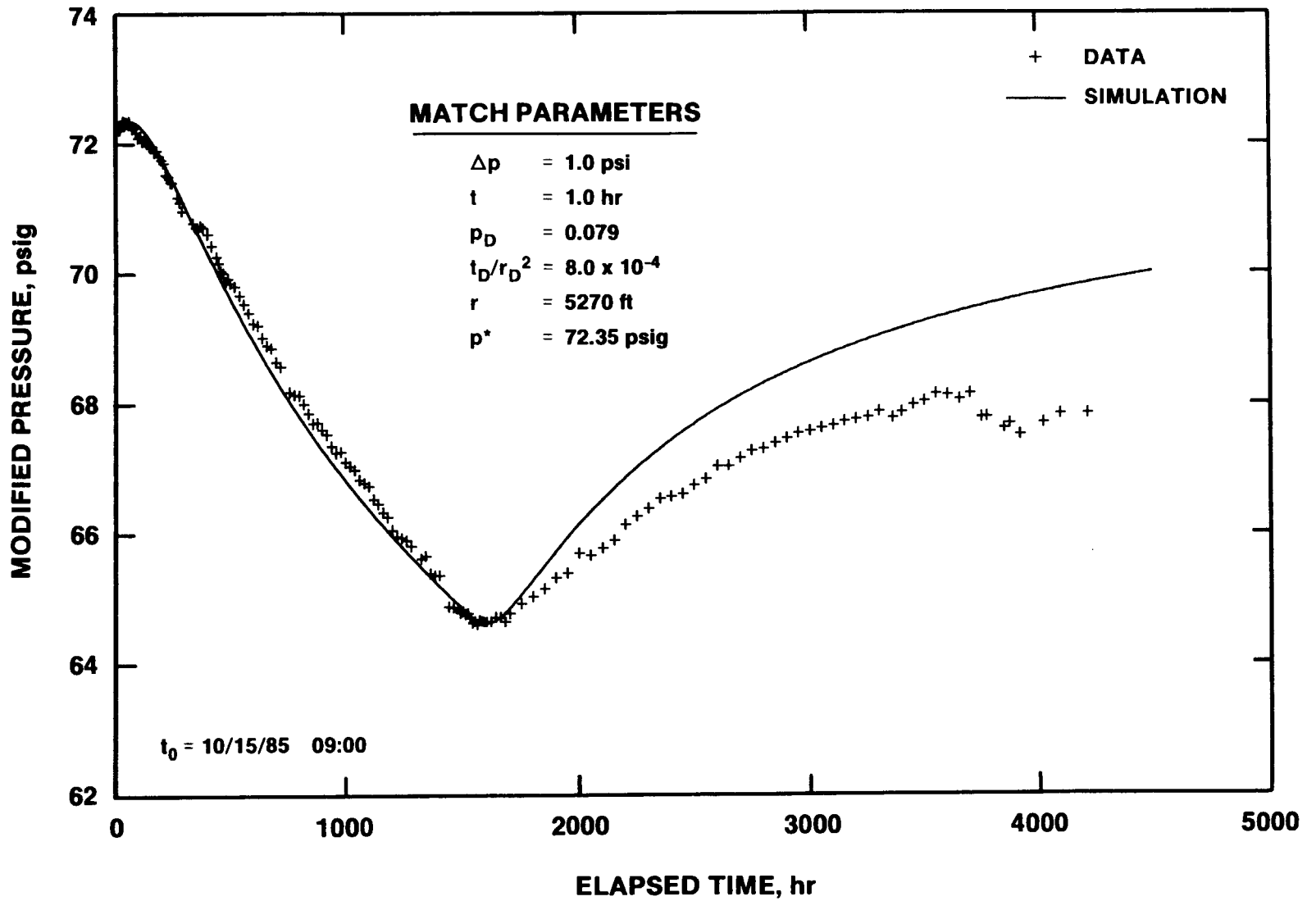


Figure 6-21. H-3 Multipad Pumping Test—DOE-1 Pressure Response Modified for 0.27 psi/15 Days Pressure Trend With INTERPRET Simulation

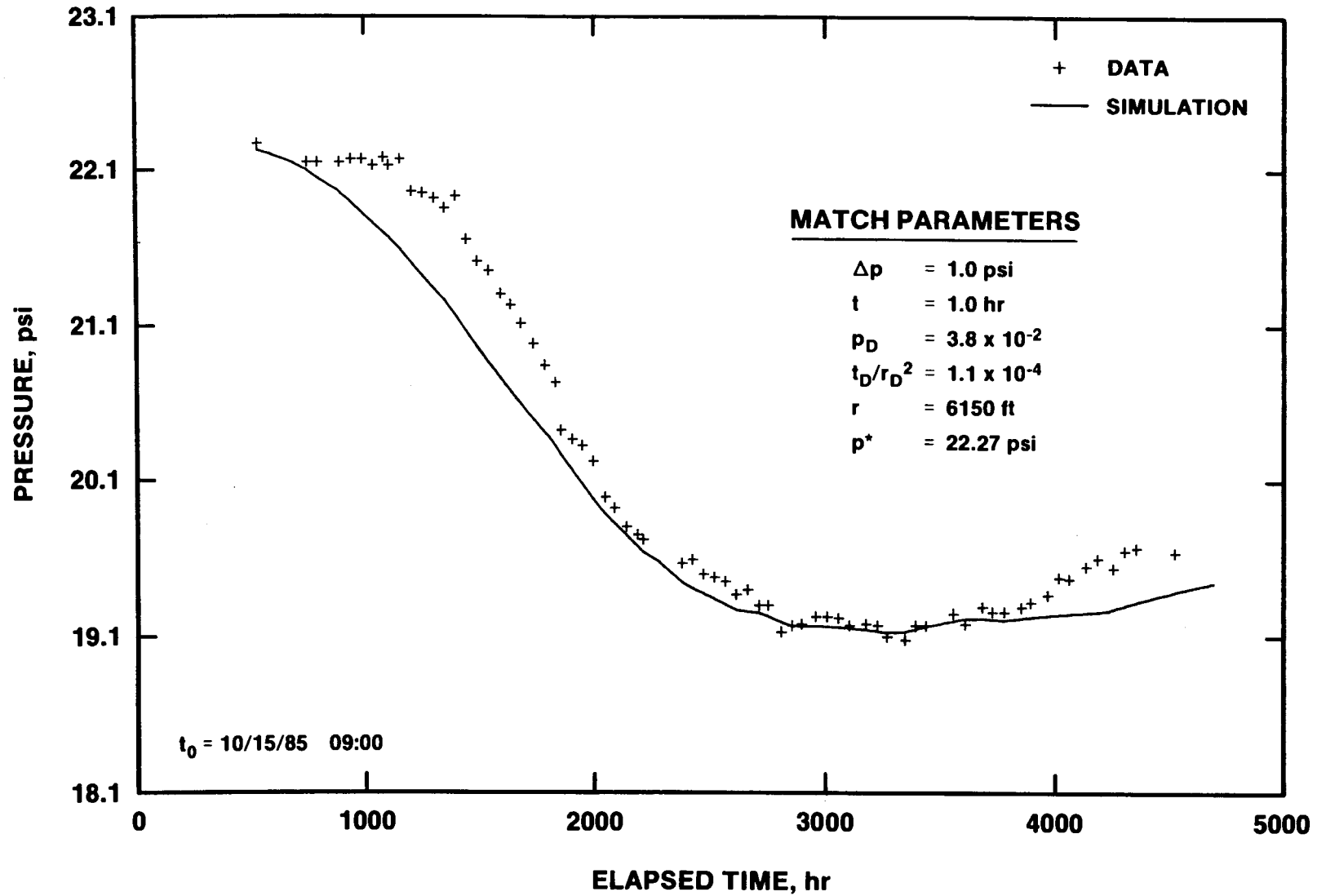


Figure 6-22. H-3 Multipad Pumping Test—WIPP-19 Pressure Response With INTERPRET Simulation

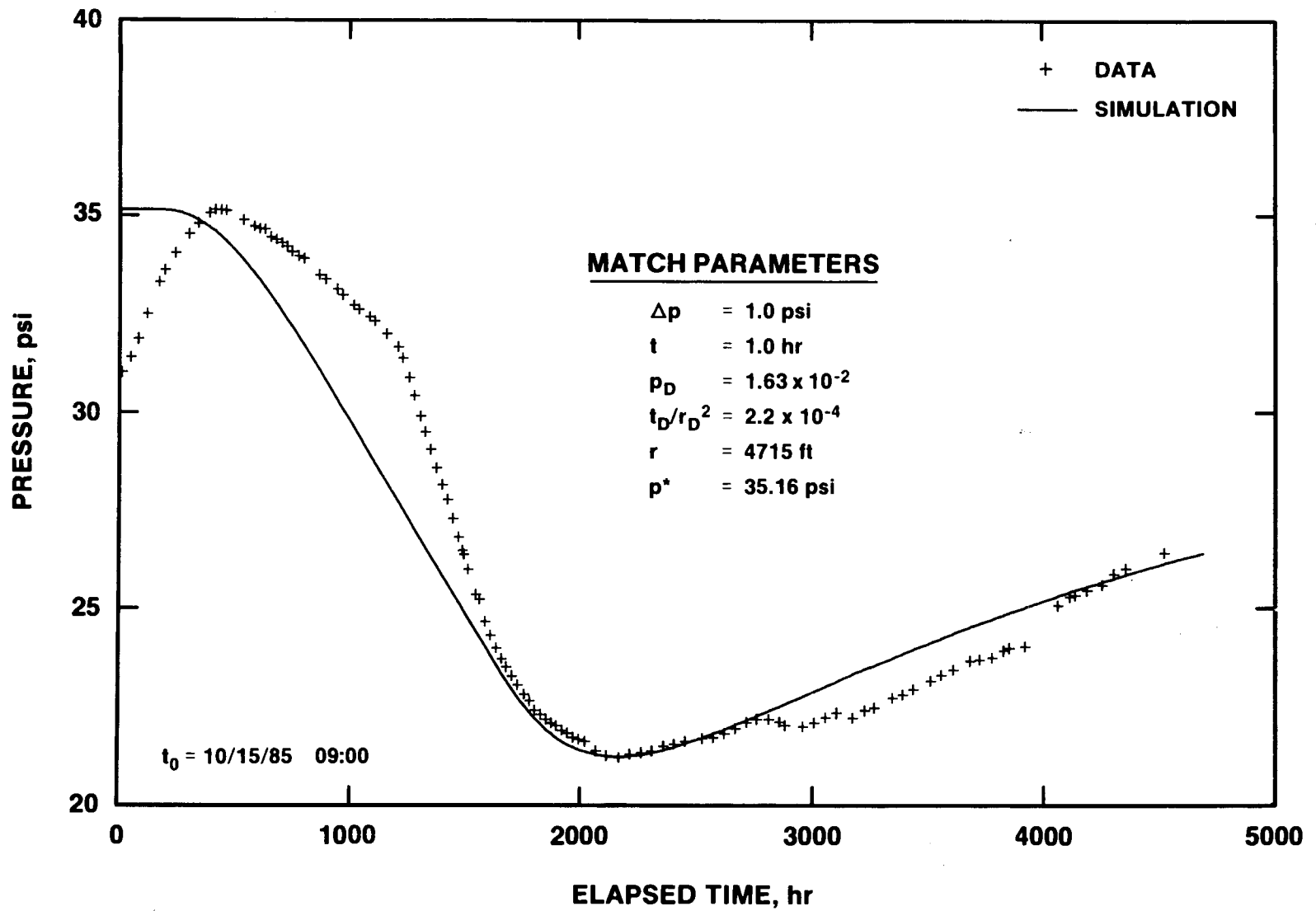


Figure 6-23. H-3 Multipad Pumping Test—WIPP-21 Pressure Response With INTERPRET Simulation

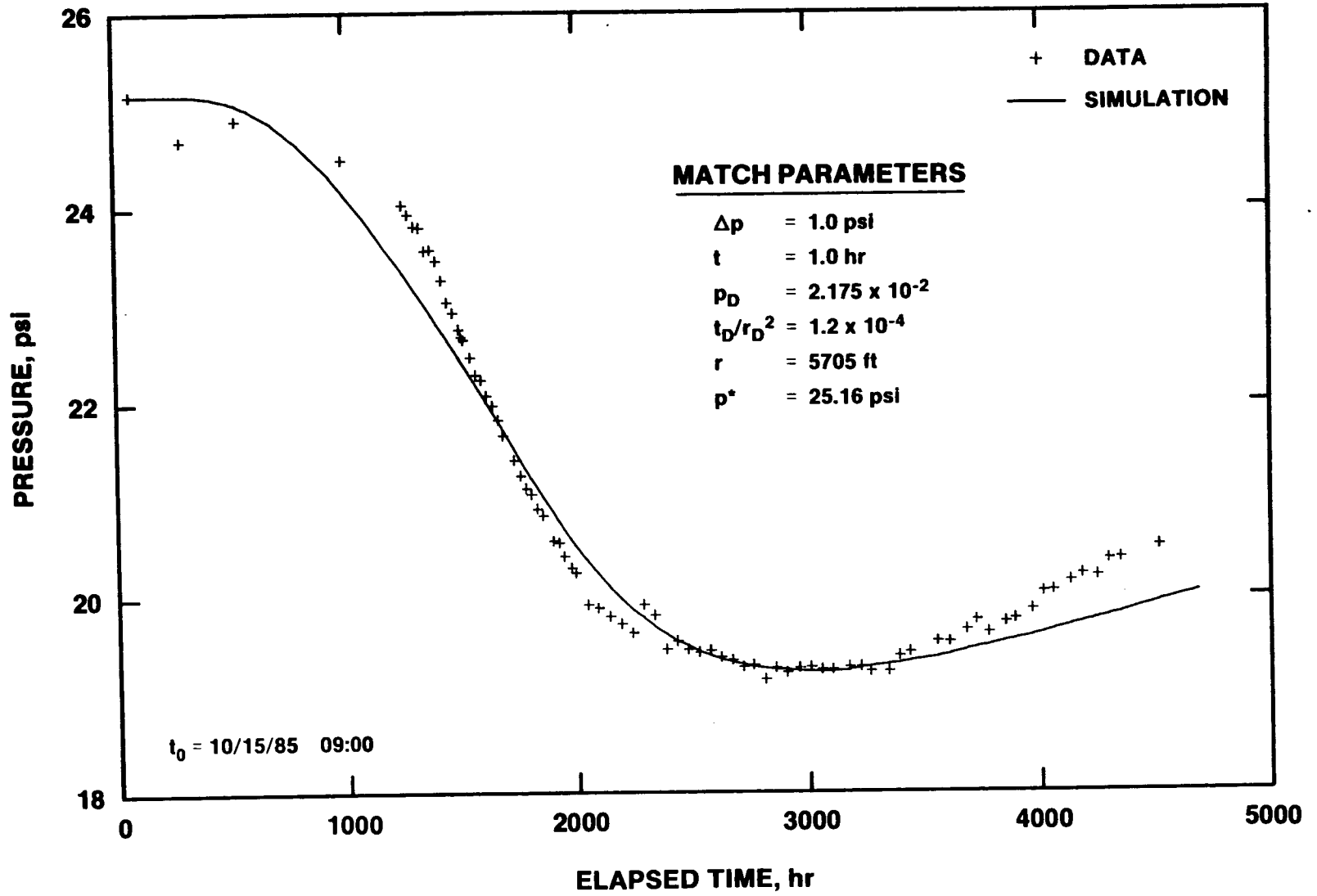


Figure 6-24. H-3 Multipad Pumping Test—WIPP-22 Pressure Response With INTERPRET Simulation

at the Waste-Handling Shaft measured by two separate transducers decreased by 53.4 to 57.1 psi. In contrast, the total drawdown at the pumping well H-3b2 was only ~56 psi. No credible mechanism can be postulated that would allow the same drawdown to be created 3840 ft from a pumping well as was observed at the pumping well itself.

If not related to the multipad test, however, the timing of the pressure changes at the Waste-Handling Shaft is highly coincidental. The pressure drop began during the first month of pumping at H-3b2, and stopped within several days of the end of pumping. Some connection between the H-3b2 pumping and the Waste-Handling Shaft pressure decline cannot be arbitrarily ruled out.

If the pressure drop at the Waste-Handling Shaft was in response to the H-3b2 pumping, the Culebra pressure at the Construction and Salt-Handling (C&SH) Shaft, 400 ft farther north, should have dropped by a similar amount (assuming homogeneous hydraulic properties on this scale). Pressure data from the C&SH Shaft are sparse, but some conclusions may still be drawn. From 1985 Julian days 288 to 343, a period covering all but the last 7 days of H-3b2 pumping, the Culebra pressure dropped 6.5 psi at the C&SH Shaft (Appendix B, Table B-10). In contrast, from 1985 Julian days 289 to 340, the Culebra pressure dropped 39.5 psi at the Waste-Handling Shaft. On 1986 Julian day 83, the Culebra pressure at the C&SH Shaft was 10.8 psi lower than at the start of the multipad test, whereas on 1986 Julian day 80, the Culebra pressure at the Waste-Handling Shaft was 40.8 psi lower than at the start of the multipad test. Thus, the available evidence indicates that the large pressure decline measured at the Waste-Handling Shaft did not occur at the C&SH Shaft. This indicates that the Waste-Handling Shaft pressure decline was probably not caused by the pumping at H-3b2, but may have had a more local origin.

The most plausible explanation for the pressure drop at the Waste-Handling Shaft is an increase in groundwater leakage from the Culebra into the shaft over this period. Unfortunately, no shaft-leakage data were collected from any of the shafts during the multipad-test pumping period. Thus, no direct evidence exists to support the assumed increase in leakage. Nor can a cause be found for the increase in leakage.

Discussion: The assumption of a separate event causing the pressure decline in the Waste-Handling Shaft has a significant bearing on the interpretation of the responses of nearby observation wells. Wells H-1, H-2b2, WIPP-19, WIPP-21, and WIPP-22 are closer

to the Waste-Handling Shaft than they are to H-3b2. If a separate drawdown event did occur in the Culebra at the Waste-Handling Shaft, then some, if not most, of the "multipad-test" responses observed at these wells may have been caused by the shaft event. If so, interpretations of the responses of these wells, presented above, are erroneous.

Figure 6-25 shows the similarities between the Waste-Handling Shaft pressure response during the H-3 multipad test and that at the closest observation well, WIPP-21. The pressure trends seen at the Waste-Handling Shaft appear to be mimicked very closely, with some lag time, at WIPP-21. The magnitude of the pressure changes was about four times greater at the Waste-Handling Shaft than at WIPP-21. If the drawdown event was centered at the Waste-Handling Shaft, a fourfold decrease in the magnitude of this pressure change as it propagated to WIPP-21, 1035 ft away, is not unreasonable.

The WIPP-19 (Figure 6-22) and WIPP-22 (Figure 6-24) responses also appear to be related to a separate drawdown event at the Waste-Handling Shaft. At both wells, water levels were fairly stable well into the multipad test, and then began dropping off quite rapidly, later and more rapidly than predicted using the line-source solution. These rapid declines began shortly after the large pressure decline began at the Waste-Handling Shaft.

Finally, recent testing at wells WIPP-19, WIPP-21, WIPP-22, and ERDA-9 (located between WIPP-21 and H-3, and completed after the multipad test) indicates the Culebra transmissivity in that vicinity is $\leq 0.6 \text{ ft}^2/\text{day}$ (Beauheim, in preparation). Thus, even allowing for the higher transmissivity of 1.7 to 1.8 ft^2/day at H-3, the average apparent transmissivity values between H-3 and the WIPP wells (Table 6-4) appear to be too high. Some shaft influence on the responses of these wells must be considered a strong possibility.

Apart from the potential shaft effects, other general features of the responses observed during the multipad test are noteworthy. Similarities are evident in the responses of observation wells that are generally in the same direction from H-3b2. DOE-1 and H-11b1, which are southeast of H-3b2, both showed rapid, relatively high-magnitude responses to the H-3b2 pumping. The responses are also more linear than a porous-flow model predicts (see Figures 6-18 and 6-20). Coupled with the relatively low storativities calculated for these wells, these observations indicate possible preferential fracture connection between H-3 and the southeast portion of the WIPP site.

H-1 and H-2b2, to the north and northwest of H-3b2, also responded similarly. Both wells, although

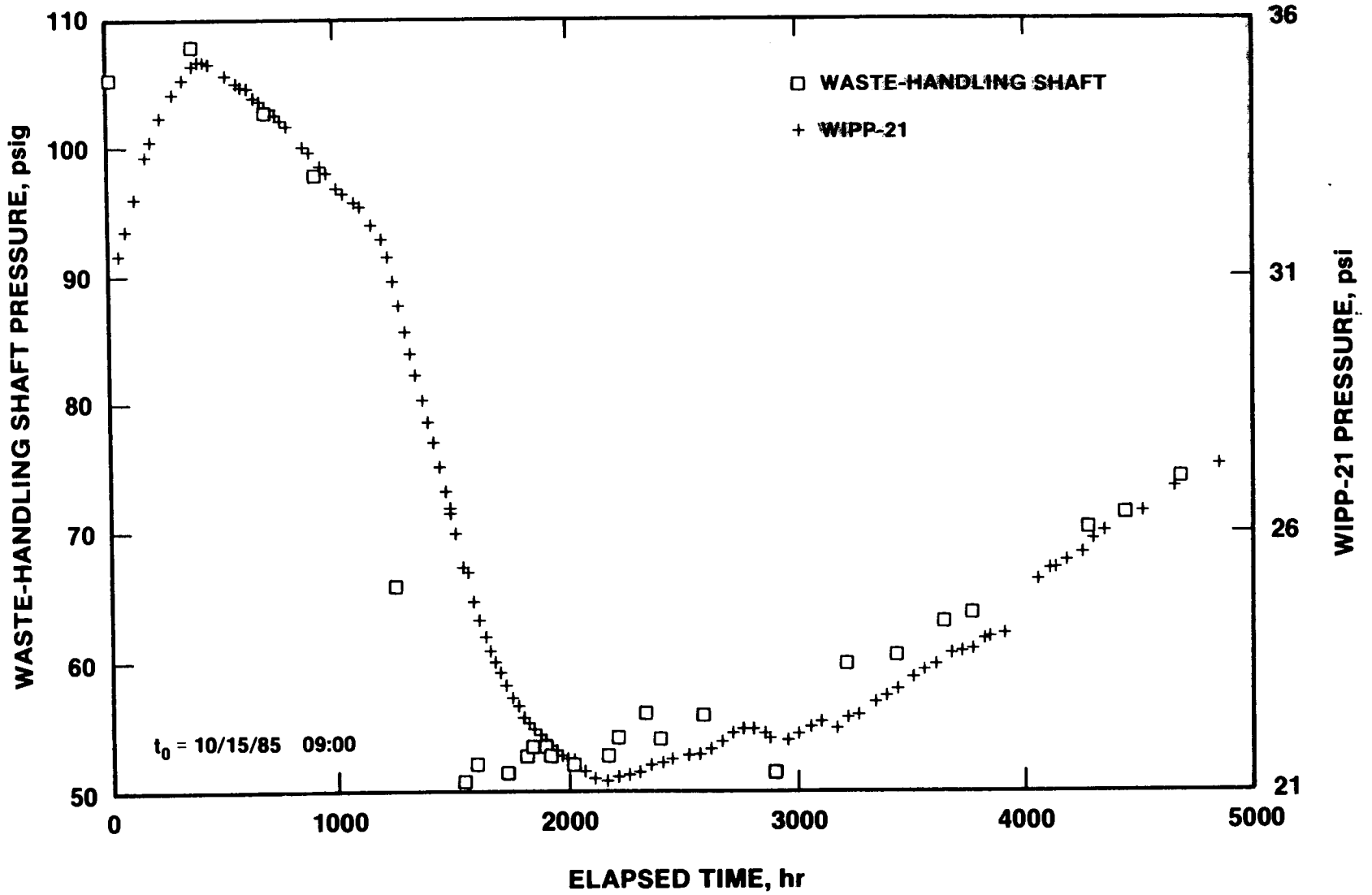


Figure 6-25. Comparison of Culbra Pressure Trends at the Waste-Handling Shaft and WIPP-21

closer to H-3b2 than DOE-1 or H-11b1, showed delayed responses and relatively little recovery. The data from these wells, particularly after modification for pretest trends, are well matched by the porous-flow model. On the scale of thousands of feet, the Culebra in the vicinity of H-1 and H-2b2 appears to behave hydraulically as a relatively simple porous medium.

Farther to the north from H-3b2, wells WIPP-19, WIPP-21, and WIPP-22 had pressure responses similar to those at H-1 and H-2b2 during the multipad test. Because of uncertainties about the event(s) to which these wells were responding, however, no general conclusions are drawn regarding their behavior other than that they appear to lack the type of fracture connection to H-3 postulated for DOE-1 and H-11.

With regard to the more-distant wells monitored during the multipad test, at which either ambiguous responses or no responses were measured, the follow-

ing observations may be made. The fracture system that appears to connect H-3 with DOE-1 and H-11 does not extend to H-4; if it did, H-4b should have shown a response to the multipad test. The fact that no response was observed at H-4b (Figure 5-6) indicates a fairly low average transmissivity ($<1 \text{ ft}^2/\text{day}$) for the Culebra between H-3 and H-4.

The slight decline in water level at P-17 (Figure 5-19), if related to the multipad test, may indicate a small degree of communication with the H-3 to H-11 fracture system. A small drop in water level at WIPP-18 (Figure 5-13) may have been related to the multipad test or to whatever caused the pressure decline in the Waste-Handling Shaft. Slight declines in water levels at P-14 (Figure 5-17), P-15 (Figure 5-18), and H-6b (Figure 5-11) may have been caused by WQSP pumping at WIPP-26 in November 1985, or later by WQSP pumping at WIPP-25 in January and February 1986. In any event, the magnitudes of these drawdowns are too low to allow quantitative interpretation.

6.3 Comparison of 1984 and Multipad Test Results

On the H-3 hydropad, the overall hydraulic behavior of the Culebra during the 1984 and multipad pumping tests was very similar. In both instances, the Culebra appeared to behave as a double-porosity medium, with unrestricted flow between the fractures and the matrix. The observation wells responded as rapidly as could be measured to events at the pumping wells, and the magnitudes of drawdown were virtually identical at both the pumping wells and the observation wells. In both tests, this resulted in the unusual condition wherein the observation-well responses could not be interpreted using the standard techniques for observation wells, but instead had to be interpreted using the techniques for pumping wells. This is a clear indication of substantial direct fracture connection between the wells on the H-3 hydropad.

The 1984 test indicated a potential preferential hydraulic connection between wells H-3b3 and H-3b1, an observation borne out from interpretation of the subsequent tracer test (Kelley and Pickens, 1986). No evidence was noted of a preferential hydraulic connection between H-3b2 and either H-3b1 or H-3b3 during the multipad test. In both tests, H-3b1 had a less-negative skin factor and a higher storativity ratio than the other two wells. H-3b1 probably has a less-negative skin because that well is cased and perforated, causing less-direct connection with the aquifer than exists at H-3b2 and H-3b3, which are simply open holes through the Culebra.

The primary difference between the interpretations of the 1984 and multipad tests lies in the transmissivity assigned to the Culebra. From the 1984 test when H-3b3 was pumped, a transmissivity of 2.9 ft²/day was obtained. From the multipad test when H-3b2 was pumped, a transmissivity of 1.7 ft²/day was

obtained. This difference could be caused by two nonexclusive factors: (1) H-3b3 may be slightly better connected to fractures than H-3b2, as evidenced by the preferential H-3b1-to-H-3b3 flow path, resulting in slightly less drawdown (which translates to higher transmissivity) when that well is pumped, and (2) the multipad test, substantially longer than the 1984 test, stressed a much larger volume of Culebra that might have a slightly lower average transmissivity than the volume stressed during the 1984 test. Regardless of the exact reason for the difference, the two transmissivity values are quite similar, differing by less than a factor of 2.

Mercer (1983) reported the Culebra transmissivity at H-3b1 (then known simply as H-3) as 19 ft²/day. This value represents an average of results from a short bailing test and a slug test. Because of the short-term and local-scale nature of these tests, the major fractures on the H-3 hydropad may have been the only portion of the Culebra tested. The two H-3 pumping tests discussed in this report stressed the Culebra on a larger scale over a longer term, and this should provide more representative transmissivity values on a scale larger than the hydropad (i.e., >100 ft).

Off the H-3 hydropad, the only well for which comparisons can be made between the 1984 and multipad tests is DOE-1. The DOE-1 data from the 1984 test were very sparse (Figure 6-5), with a poorly defined starting static formation pressure. The interpretation of these data resulted in a transmissivity (12 ft²/day) slightly higher than the values obtained from both the observed and modified (for the pretest trend) multipad-test data (9.2 and 5.5 ft²/day). The multipad-test interpretations are probably more reliable, because the multipad-test data are more complete than those from the 1984 test. The storativity values obtained from the two tests are in good agreement.

7. Summary and Conclusions

Two pumping tests were conducted in the Culebra dolomite at the H-3 hydropad. In the first, performed in 1984, H-3b3 was pumped for 14 days at a rate of ~ 4 gpm. In the second, the H-3 multipad test performed in late 1985 and early 1986, H-3b2 was pumped for 62 days at a rate of ~ 4.8 gpm. Both tests provided information on the hydraulic properties of the Culebra in the vicinity of the H-3 hydropad; the second test also provided information on average Culebra hydraulic properties on a much larger scale.

The interpretation of these tests had three principal objectives. The first was to determine the most appropriate conceptualization of the nature of the Culebra flow system around the H-3 hydropad. The pumping well responses during the H-3 tests appear to be those of wells completed in a double-porosity medium with unrestricted interporosity flow. In such a system, fractures provide the bulk of the permeability, and matrix pores provide the majority of the storage capacity. The importance of fracture flow is indicated by the rapidity with which the observation wells on the H-3 hydropad respond to pumping, and the nearly identical behaviors of those wells and the pumping well. The similarity between pumping- and observation-well behavior on the H-3 hydropad is so pronounced that the responses of all three wells on the hydropad can be interpreted only with pumping-well analytical techniques, and not observation-well analytical techniques. H-3b1 and H-3b3, in particular, appear to be very well connected by fractures.

The second objective was to quantify the hydraulic properties of the Culebra in the vicinity of the H-3 hydropad. The total-system (fractures plus matrix) transmissivity of the Culebra derived from the first test is $2.9 \text{ ft}^2/\text{day}$; that from the second test is $1.7 \text{ ft}^2/\text{day}$. The lower value derived from the second test probably represents lower transmissivity (lower fracture connectivity) at H-3b2 than at H-3b3, and/or lower average transmissivity of the volume of Culebra stressed in the multipad test as opposed to the smaller volume stressed in the first test. The fracture-to-total-system storativity ratios derived from the various analyses range from 0.03 to 0.25, indicating a relatively high degree of storage within the fractures. The highest storativity ratios were consistently found at H-3b1. Wellbore skin values are highly negative, indicating direct wellbore connection with fractures.

The third objective was to quantify the average hydraulic properties of the Culebra between the H-3

hydropad and more-distant observation wells. Meeting this objective was complicated by the effects of an apparent increase in groundwater leakage from the Culebra into the Waste-Handling Shaft on the data from wells near that shaft, and by water-level/pressure trends already existing at many of the observation wells when the multipad test began. Between H-3 and wells DOE-1 and H-11 to the southeast, the average apparent Culebra transmissivity is between 5.5 and $13 \text{ ft}^2/\text{day}$, and the apparent storativity is between 6.6×10^{-6} and 1.0×10^{-5} . The rapid responses observed at DOE-1 and H-11 during the multipad test, and the associated relatively high transmissivities, indicate a preferential hydraulic connection, probably related to fractures, between H-3 and the southeast portion of the WIPP site.

Between H-3 and wells H-1 and H-2 to the north-northwest, the apparent transmissivity is between 0.46 and $2.5 \text{ ft}^2/\text{day}$, and the apparent storativity is between 2.7×10^{-5} and 4.5×10^{-5} . Ignoring possible shaft-leakage effects, the apparent transmissivity between H-3 and WIPP-19, 21, and 22 to the north is between 1.1 and $2.9 \text{ ft}^2/\text{day}$, and the apparent storativity is between 9.0×10^{-6} and 2.9×10^{-6} . If shaft leakage did, as we think, affect the responses observed at WIPP-19, 21, and 22, then the transmissivity values listed above are not representative. The wells to the north of H-3 are not as well connected hydraulically to H-3 as are DOE-1 and H-11, and provided no indications that groundwater was flowing primarily through fractures.

The interpretations presented in this report represent an analytical approach to the understanding of large-scale tests. In an aquifer with considerable areal heterogeneity, an analytical approach has significant limitations. Calculated transmissivities and storativities are only "apparent" values, representing the average response of large volumes of aquifer to a stress imposed at a certain location. These interpretations are most useful in qualitatively defining areas of "higher" and "lower" transmissivity. Quantitative evaluation/simulation of heterogeneous systems on a large scale is best attempted using numerical models, which allow the heterogeneity of the system to be directly incorporated. Such a modeling effort is under way, and will be reported by Haug et al. (in preparation).

APPENDIX A
1984 H-3 Pumping Test Data

Table A-1. H-3 Calculated Water Levels and Pressures During the 1984 H-3 Pumping Test

Day	Hr	Min	S	Elapsed Pumping Time (hr)	Depths to Water (ft)			Pressures* (psi)		
					H-3B3	H-3B2	H-3B1	H-3B3	H-3B2	H-3B1
114	8	51	0	-1.6500	421.24	422.07	420.20	77.40	77.04	77.85
114	9	0	0	-1.5000	421.24	422.07	420.20	77.40	77.04	77.85
114	9	15	0	-1.2500	421.25	422.07	420.21	77.40	77.04	77.85
114	9	30	0	-1.0000	421.25	422.09	420.19	77.40	77.04	77.86
114	9	45	0	-0.7500	421.24	422.09	420.22	77.40	77.04	77.84
114	10	0	0	-0.5000	421.22	422.09	420.21	77.41	77.04	77.85
114	10	15	0	-0.2500	421.19	422.09	420.17	77.42	77.04	77.87
114	10	30	0	0.0000	421.24	422.07	420.17	77.40	77.04	77.87
114	10	30	20	0.0056	445.93	422.20	420.90	66.71	76.99	77.55
114	10	30	40	0.0111	428.77	422.49	421.10	74.14	76.86	77.46
114	10	31	0	0.0167	428.86	422.64	421.12	74.10	76.80	77.46
114	10	31	20	0.0222	428.87	422.79	421.17	74.10	76.73	77.43
114	10	32	0	0.0333	431.84	423.02	421.34	72.81	76.63	77.36
114	10	32	19	0.0386	432.03	423.15	421.48	72.73	76.58	77.30
114	10	32	39	0.0442	431.97	423.27	421.58	72.76	76.52	77.26
114	10	33	0	0.0500	432.05	423.40	421.68	72.72	76.47	77.21
114	10	33	20	0.0556	432.07	423.50	421.75	72.71	76.42	77.19
114	10	33	40	0.0611	432.17	423.60	421.82	72.67	76.38	77.15
114	10	34	0	0.0667	432.20	423.70	421.90	72.66	76.34	77.12
114	10	34	20	0.0722	432.06	423.79	421.96	72.72	76.30	77.09
114	10	34	40	0.0778	432.32	423.87	422.01	72.61	76.26	77.07
114	10	35	0	0.0833	432.33	423.95	422.09	72.60	76.23	77.04
114	10	35	19	0.0886	432.37	424.03	422.14	72.58	76.20	77.01
114	10	35	39	0.0942	432.34	424.10	422.19	72.60	76.16	76.99
114	10	36	0	0.1000	432.45	424.16	422.25	72.55	76.14	76.97
114	10	36	20	0.1056	432.45	424.22	422.31	72.55	76.11	76.94
114	10	36	40	0.1111	432.51	424.28	422.34	72.52	76.09	76.93
114	10	37	0	0.1167	432.54	424.34	422.41	72.51	76.06	76.90
114	10	37	20	0.1222	432.60	424.39	422.44	72.48	76.04	76.88
114	10	37	40	0.1278	432.61	424.45	422.48	72.48	76.01	76.87
114	10	38	0	0.1333	432.72	424.50	422.53	72.43	75.99	76.84
114	10	38	19	0.1386	432.62	424.55	422.57	72.48	75.97	76.83
114	10	38	39	0.1442	432.73	424.60	422.61	72.43	75.95	76.81
114	10	39	0	0.1500	432.79	424.65	422.65	72.40	75.93	76.79
114	10	39	20	0.1556	432.86	424.69	422.69	72.37	75.91	76.78
114	10	39	40	0.1611	432.85	424.73	422.73	72.38	75.89	76.76
114	10	40	0	0.1667	432.80	424.77	422.76	72.40	75.87	76.74
114	10	41	0	0.1833	432.98	424.89	422.88	72.32	75.82	76.69
114	10	42	0	0.2000	433.05	425.00	422.96	72.29	75.78	76.66
114	10	43	0	0.2167	433.09	425.10	423.05	72.27	75.73	76.62
114	10	44	0	0.2333	433.28	425.20	423.16	72.19	75.69	76.57

(continued)

*Pressure = (600 ft - Depth to Water) × 0.433 psi/ft

Table A-1. (continued)

Day	Hr	Min	S	Elapsed Pumping Time (hr)	Depths to Water (ft)			Pressures (psi)		
					H-3B3	H-3B2	H-3B1	H-3B3	H-3B2	H-3B1
114	10	45	0	0.2500	433.26	425.28	423.24	72.20	75.65	76.54
114	10	46	0	0.2667	433.36	425.38	423.33	72.16	75.61	76.50
114	10	47	0	0.2833	433.45	425.46	423.42	72.12	75.58	76.46
114	10	48	0	0.3000	433.54	425.55	423.57	72.08	75.54	76.39
114	10	49	0	0.3167	433.61	425.64	423.56	72.05	75.50	76.40
114	10	50	0	0.3333	433.65	425.72	423.65	72.03	75.46	76.36
114	10	51	0	0.3500	433.78	425.80	423.71	71.97	75.43	76.33
114	10	52	0	0.3667	433.81	425.87	423.79	71.96	75.40	76.30
114	10	53	0	0.3833	433.80	425.94	423.86	71.96	75.37	76.27
114	10	54	0	0.4000	433.92	426.01	423.93	71.91	75.34	76.24
114	10	55	0	0.4167	433.88	426.08	423.99	71.93	75.31	76.21
114	10	56	0	0.4333	434.02	426.15	424.05	71.87	75.28	76.19
114	10	57	0	0.4500	434.06	426.20	424.12	71.85	75.26	76.16
114	10	58	0	0.4667	434.16	426.27	424.19	71.81	75.23	76.13
114	10	59	0	0.4833	434.20	426.33	424.24	71.79	75.20	76.10
114	11	0	0	0.5000	434.29	426.39	424.30	71.75	75.17	76.08
114	11	10	0	0.6667	434.42	426.91	424.82	71.70	74.95	75.85
114	11	15	0	0.7500	436.10	427.27	425.18	70.97	74.79	75.70
114	11	25	0	0.9167	436.56	427.86	425.74	70.77	74.54	75.45
114	11	30	0	1.0000	436.73	428.12	425.98	70.70	74.42	75.35
114	11	40	0	1.1667	437.14	428.57	426.44	70.52	74.23	75.15
114	11	45	0	1.2500	437.26	428.77	426.63	70.47	74.14	75.07
114	11	50	0	1.3333	437.47	428.99	426.85	70.38	74.05	74.97
114	11	55	0	1.4167	437.62	429.17	427.04	70.31	73.97	74.89
114	12	0	0	1.5000	437.78	429.38	427.25	70.24	73.88	74.80
114	12	5	0	1.5833	437.92	429.55	427.41	70.18	73.80	74.73
114	12	10	0	1.6667	438.13	429.72	427.57	70.09	73.73	74.66
114	12	15	0	1.7500	438.30	429.91	427.75	70.02	73.65	74.58
114	12	20	0	1.8333	438.43	430.08	427.92	69.96	73.58	74.51
114	12	25	0	1.9167	438.54	430.24	428.09	69.91	73.51	74.44
114	12	30	0	2.0000	438.67	430.39	428.24	69.86	73.44	74.37
114	12	35	0	2.0833	438.76	430.54	428.39	69.82	73.38	74.31
114	12	40	0	2.1667	438.85	430.68	428.53	69.78	73.32	74.25
114	12	45	0	2.2500	439.06	430.83	428.66	69.69	73.25	74.19
114	12	50	0	2.3333	439.13	430.97	428.81	69.66	73.19	74.13
114	12	55	0	2.4167	439.29	431.12	428.95	69.59	73.13	74.06
114	13	0	0	2.5000	439.35	431.25	429.09	69.56	73.07	74.00
114	13	10	0	2.6667	439.63	431.52	429.37	69.44	72.95	73.88
114	13	20	0	2.8333	439.91	431.79	429.60	69.32	72.83	73.78
114	13	30	0	3.0000	440.00	432.03	429.84	69.28	72.73	73.68
114	13	40	0	3.1667	440.29	432.25	430.06	69.15	72.64	73.58

(continued)

Table A-1 (continued)

Day	Hr	Min	S	Elapsed Pumping Time (hr)	Depths to Water (ft)			Pressures (psi)		
					H-3B3	H-3B2	H-3B1	H-3B3	H-3B2	H-3B1
114	13	50	0	3.3333	440.60	432.49	430.31	69.02	72.53	73.48
114	14	0	0	3.5000	440.76	432.72	430.49	68.95	72.43	73.40
114	14	10	0	3.6667	440.90	432.93	430.72	68.89	72.34	73.30
114	14	20	0	3.8333	441.05	433.13	430.92	68.83	72.25	73.21
114	14	30	0	4.0000	441.25	433.32	431.13	68.74	72.17	73.12
114	14	40	0	4.1667	441.43	433.53	431.33	68.66	72.08	73.03
114	15	0	30	4.5083	441.59	433.89	431.67	68.59	71.93	72.89
114	15	10	0	4.6667	441.76	434.06	431.85	68.52	71.85	72.81
114	15	20	0	4.8333	441.92	434.23	432.01	68.45	71.78	72.74
114	15	30	0	5.0000	442.00	434.38	432.19	68.41	71.71	72.66
114	15	40	0	5.1667	442.21	434.55	432.34	68.32	71.64	72.60
114	15	50	0	5.3333	442.29	434.69	432.48	68.29	71.58	72.54
114	16	0	0	5.5000	442.36	434.83	432.63	68.26	71.52	72.47
114	16	30	0	6.0000	442.90	435.27	433.07	68.02	71.33	72.28
114	17	0	0	6.5000	443.24	435.69	433.47	67.88	71.15	72.11
114	17	30	0	7.0000	443.63	436.08	433.86	67.71	70.98	71.94
114	18	0	0	7.5000	443.95	436.46	434.21	67.57	70.81	71.79
114	18	30	0	8.0000	444.30	436.78	434.56	67.42	70.67	71.64
114	19	0	0	8.5000	444.54	437.09	434.86	67.31	70.54	71.51
114	19	30	0	9.0000	444.96	437.44	435.21	67.13	70.39	71.35
114	20	0	0	9.5000	445.29	437.81	435.57	66.99	70.23	71.20
114	20	30	0	10.0000	445.67	438.19	435.95	66.82	70.06	71.03
114	21	0	0	10.5000	445.73	438.48	436.27	66.80	69.94	70.90
114	21	30	0	11.0000	446.05	438.78	436.59	66.66	69.81	70.76
114	22	0	0	11.5000	446.23	439.07	436.88	66.58	69.68	70.63
114	22	30	0	12.0000	446.58	439.36	437.17	66.43	69.56	70.51
114	23	0	0	12.5000	446.84	439.63	437.44	66.32	69.44	70.39
115	0	0	0	13.5000	446.89	440.11	437.91	66.30	69.23	70.18
115	1	0	0	14.5000	447.75	440.65	438.46	65.92	69.00	69.95
115	2	0	0	15.5000	448.22	441.12	438.95	65.72	68.80	69.73
115	3	0	0	16.5000	448.62	441.50	439.34	65.55	68.63	69.57
115	4	0	0	17.5000	448.80	441.98	439.80	65.47	68.42	69.37
115	5	0	0	18.5000	449.23	442.36	440.19	65.28	68.26	69.20
115	6	0	0	19.5000	449.81	442.81	440.61	65.03	68.06	69.02
115	7	0	0	20.5000	450.10	443.38	441.13	64.91	67.82	68.79
115	8	0	0	21.5000	450.60	443.92	441.75	64.69	67.58	68.52
115	9	0	0	22.5000	452.67	444.69	442.49	63.79	67.25	68.20
115	10	0	0	23.5000	452.84	445.24	443.00	63.72	67.01	67.98
115	11	0	0	24.5000	453.00	445.64	443.40	63.65	66.84	67.81
115	12	54	21	26.4058	453.32	446.18	443.95	63.51	66.60	67.57
115	14	0	0	27.5000	453.55	446.52	444.26	63.41	66.46	67.44

(continued)

Table A-1. (continued)

Day	Hr	Min	S	Elapsed Pumping Time (hr)	Depths to Water (ft)			Pressures (psi)		
					H-3B3	H-3B2	H-3B1	H-3B3	H-3B2	H-3B1
115	15	0	0	28.5000	453.65	446.73	444.45	63.37	66.37	67.35
115	16	0	0	29.5000	453.94	446.98	444.73	63.24	66.26	67.23
115	17	0	0	30.5000	454.25	447.27	445.01	63.11	66.13	67.11
115	18	0	0	31.5000	454.27	447.54	445.27	63.10	66.02	67.00
115	19	0	0	32.5000	454.66	447.76	445.49	62.93	65.92	66.90
115	20	0	0	33.5000	455.14	448.07	445.79	62.72	65.79	66.77
115	21	0	0	34.5000	455.43	448.45	446.17	62.60	65.62	66.61
115	22	0	0	35.5000	455.75	448.77	446.51	62.46	65.48	66.46
115	23	0	0	36.5000	456.01	449.05	446.82	62.35	65.36	66.33
116	0	0	0	37.5000	456.13	449.34	447.09	62.30	65.24	66.21
116	1	0	0	38.5000	456.05	449.52	447.32	62.33	65.16	66.11
116	2	0	0	39.5000	456.28	449.78	447.54	62.23	65.05	66.02
116	3	0	0	40.5000	456.18	449.99	447.78	62.27	64.95	65.91
116	3	15	0	40.7500	456.51	450.04	447.83	62.13	64.93	65.89
116	3	30	0	41.0000	456.46	450.11	447.91	62.15	64.90	65.85
116	3	45	0	41.2500	456.69	450.17	447.97	62.05	64.88	65.83
116	4	0	0	41.5000	456.78	450.25	448.02	62.01	64.84	65.81
116	4	15	0	41.7500	456.82	450.31	448.09	62.00	64.82	65.78
116	4	30	0	42.0000	456.98	450.36	448.15	61.93	64.79	65.75
116	4	45	0	42.2500	457.06	450.42	448.20	61.89	64.77	65.73
116	5	0	0	42.5000	456.94	450.47	448.24	61.94	64.75	65.71
116	5	15	0	42.7500	456.90	450.51	448.29	61.96	64.73	65.69
116	5	30	0	43.0000	457.01	450.55	448.33	61.91	64.71	65.67
116	5	45	0	43.2500	457.12	450.60	448.38	61.87	64.69	65.65
116	6	0	0	43.5000	457.15	450.71	448.47	61.85	64.64	65.61
116	6	15	0	43.7500	458.29	450.99	448.70	61.36	64.52	65.51
116	6	30	0	44.0000	458.62	451.16	448.86	61.22	64.45	65.44
116	6	45	0	44.2500	458.76	451.32	449.03	61.16	64.38	65.37
116	7	0	0	44.5000	458.63	451.44	449.14	61.21	64.33	65.32
116	7	15	0	44.7500	458.74	451.58	449.29	61.17	64.27	65.26
116	7	30	0	45.0000	459.04	451.71	449.44	61.04	64.21	65.19
116	7	45	0	45.2500	459.06	451.83	449.55	61.03	64.16	65.14
116	8	0	0	45.5000	459.11	451.91	449.67	61.01	64.12	65.09
116	10	0	0	47.5000	459.49	452.57	450.29	60.84	63.84	64.82
116	12	0	0	49.5000	459.75	452.98	450.67	60.73	63.66	64.66
116	14	0	0	51.5000	459.77	453.25	450.96	60.72	63.54	64.53
116	16	0	0	53.5000	460.26	453.59	451.26	60.51	63.40	64.40
116	18	0	0	55.5000	460.65	453.97	451.66	60.34	63.23	64.23
116	20	0	0	57.5000	461.07	454.40	452.10	60.16	63.04	64.04
116	22	0	0	59.5000	461.42	454.86	452.56	60.01	62.85	63.84
117	0	0	0	61.5000	462.01	455.37	453.07	59.75	62.62	63.62

(continued)

Table A-1 (continued)

Day	Hr	Min	S	Elapsed Pumping Time (hr)	Depths to Water (ft)			Pressures (psi)		
					H-3B3	H-3B2	H-3B1	H-3B3	H-3B2	H-3B1
117	2	0	0	63.5000	463.35	455.86	453.58	59.17	62.41	63.40
117	4	0	0	65.5000	463.94	456.53	454.22	58.91	62.12	63.12
117	6	0	0	67.5000	464.29	457.11	454.78	58.76	61.87	62.88
117	8	0	23	69.5064	464.81	457.79	455.49	58.54	61.58	62.57
117	10	0	23	71.5064	464.97	458.17	455.85	58.47	61.41	62.42
117	12	0	23	73.5064	465.10	458.43	456.05	58.41	61.30	62.33
117	14	0	23	75.5064	465.25	458.66	456.25	58.35	61.20	62.24
117	16	0	23	77.5064	465.31	458.84	456.43	58.32	61.12	62.17
117	18	0	23	79.5064	465.86	459.07	456.72	58.08	61.02	62.04
117	20	0	23	81.5064	466.58	459.63	457.23	57.77	60.78	61.82
117	22	0	23	83.5064	467.04	460.16	457.81	57.57	60.55	61.57
118	0	0	23	85.5064	467.36	460.60	458.24	57.43	60.36	61.38
118	2	0	23	87.5064	467.82	460.98	458.62	57.23	60.20	61.22
118	4	0	23	89.5064	468.16	461.32	458.94	57.09	60.05	61.08
118	6	0	23	91.5064	468.48	461.72	459.32	56.95	59.88	60.91
118	8	0	23	93.5064	468.73	462.34	459.97	56.84	59.61	60.63
118	10	0	23	95.5064	468.87	462.66	460.23	56.78	59.47	60.52
118	12	0	23	97.5064	468.68	462.73	460.27	56.86	59.44	60.50
118	13	0	23	98.5064	468.66	462.73	460.28	56.87	59.44	60.50
118	18	0	0	103.5000	469.22	463.12	460.56	56.63	59.27	60.38
118	20	0	0	105.5000	469.73	463.49	460.90	56.41	59.11	60.23
118	22	0	0	107.5000	470.07	463.91	461.39	56.26	58.93	60.02
119	0	0	0	109.5000	470.35	464.22	461.76	56.14	58.79	59.86
119	2	0	0	111.5000	470.80	464.49	461.99	55.94	58.68	59.76
119	4	0	0	113.5000	471.06	464.76	462.31	55.83	58.56	59.62
119	6	0	0	115.5000	471.10	465.00	462.53	55.81	58.45	59.52
119	8	0	0	117.5000	471.64	465.40	463.00	55.58	58.28	59.32
119	10	0	0	119.5000	471.79	465.73	463.40	55.51	58.14	59.15
119	12	0	0	121.5000	471.92	465.96	463.60	55.46	58.04	59.06
119	14	0	0	123.5000	471.83	466.02	463.63	55.50	58.01	59.05
119	16	0	0	125.5000	471.85	466.06	463.58	55.49	58.00	59.07
119	18	0	0	127.5000	472.11	466.26	463.69	55.38	57.91	59.02
119	20	0	0	129.5000	472.42	466.52	463.94	55.24	57.80	58.91
119	22	0	0	131.5000	472.75	466.79	464.24	55.10	57.68	58.78
120	0	0	0	133.5000	473.08	467.08	464.56	54.96	57.55	58.65
120	2	0	0	135.5000	473.47	467.37	464.81	54.79	57.43	58.54
120	4	0	0	137.5000	473.79	467.73	465.16	54.65	57.27	58.39
120	6	0	0	139.5000	474.09	468.04	465.47	54.52	57.14	58.25
120	8	0	0	141.5000	474.44	468.38	465.94	54.37	56.99	58.05
120	10	0	0	143.5000	474.54	468.69	466.26	54.32	56.86	57.91
120	12	0	0	145.5000	474.51	468.84	466.38	54.34	56.79	57.86

(continued)

Table A-1. (continued)

Day	Hr	Min	S	Elapsed Pumping Time (hr)	Depths to Water (ft)			Pressures (psi)		
					H-3B3	H-3B2	H-3B1	H-3B3	H-3B2	H-3B1
120	14	0	0	147.5000	474.43	468.91	466.41	54.37	56.76	57.84
120	16	0	0	149.5000	474.22	468.90	466.33	54.46	56.77	57.88
120	18	0	0	151.5000	474.25	469.04	466.41	54.45	56.71	57.84
120	20	0	0	153.5000	475.03	469.38	466.65	54.11	56.56	57.74
120	22	0	0	155.5000	475.54	469.77	467.12	53.89	56.39	57.54
121	0	0	0	157.5000	475.35	469.90	467.32	53.97	56.33	57.45
121	4	0	0	161.5000	476.03	470.29	467.70	53.68	56.16	57.29
121	6	0	0	163.5000	476.12	470.53	467.98	53.64	56.06	57.16
121	8	0	0	165.5000	476.96	470.99	468.51	53.28	55.86	56.94
121	10	0	0	167.5000	477.13	471.39	468.93	53.20	55.69	56.75
121	12	0	0	169.5000	477.40	471.55	469.10	53.09	55.62	56.68
121	14	0	0	171.5000	477.42	471.77	469.20	53.08	55.52	56.64
121	18	0	0	175.5000	475.84	470.18	467.46	53.76	56.21	57.39
121	19	0	0	176.5000	476.58	470.82	468.04	53.44	55.93	57.14
121	21	0	0	178.5000	477.48	471.64	468.92	53.05	55.58	56.76
121	22	0	0	179.5000	477.87	471.98	469.32	52.88	55.43	56.58
122	0	0	0	181.5000	478.57	472.51	469.87	52.58	55.20	56.35
122	2	0	0	183.5000	478.92	472.91	470.26	52.43	55.03	56.18
122	4	0	0	185.5000	479.15	473.20	470.54	52.33	54.90	56.06
122	6	0	0	187.5000	479.37	473.51	470.83	52.23	54.77	55.93
122	8	0	0	189.5000	479.66	473.87	471.31	52.11	54.61	55.72
122	14	0	0	195.5000	479.40	474.24	471.62	52.22	54.45	55.59
122	20	0	0	201.5000	480.01	474.61	471.79	51.96	54.29	55.51
123	2	0	0	207.5000	480.85	475.38	472.67	51.59	53.96	55.13
123	8	0	0	213.5000	481.25	475.97	473.37	51.42	53.70	54.83
123	12	15	48	217.7633	481.12	476.21	473.56	51.48	53.60	54.75
123	16	0	0	221.5000	481.85	476.44	473.65	51.16	53.50	54.71
123	18	0	0	223.5000	482.28	476.73	473.89	50.97	53.38	54.61
123	20	0	0	225.5000	482.61	477.02	474.16	50.83	53.25	54.49
123	22	0	0	227.5000	482.97	477.38	474.56	50.67	53.09	54.32
124	0	0	0	229.5000	483.36	477.73	474.94	50.51	52.94	54.15
124	2	0	0	231.5000	483.69	478.02	475.20	50.36	52.82	54.04
124	4	0	0	233.5000	483.89	478.24	475.43	50.28	52.72	53.94
124	10	18	32	239.8089	484.06	478.87	476.21	50.20	52.45	53.60
124	14	18	32	243.8089	483.90	478.99	476.20	50.27	52.40	53.61
124	20	18	32	249.8089	484.18	479.08	476.15	50.15	52.36	53.63
125	0	18	32	253.8089	484.89	479.64	476.82	49.84	52.12	53.34
125	6	18	33	259.8092	485.48	480.24	477.45	49.59	51.86	53.06
125	10	18	32	263.8089	484.84	480.33	477.69	49.86	51.82	52.96
125	16	18	32	269.8089	485.23	480.63	477.71	49.70	51.69	52.95
125	20	18	32	273.8089	485.89	480.93	477.96	49.41	51.56	52.84

(continued)

Table A-1. (concluded)

Day	Hr	Min	S	Elapsed Pumping Time (hr)	Depths to Water (ft)			Pressures (psi)		
					H-3B3	H-3B2	H-3B1	H-3B3	H-3B2	H-3B1
126	2	18	32	279.8089	487.08	481.76	478.94	48.89	51.20	52.42
126	6	18	32	283.8089	487.19	482.12	479.33	48.85	51.04	52.25
126	12	50	0	290.3333	486.55	482.22	479.44	49.12	51.00	52.20
126	16	50	0	294.3333	486.52	482.16	479.26	49.14	51.02	52.28
126	22	50	0	300.3333	487.39	482.69	479.74	48.76	50.80	52.07
127	2	50	0	304.3333	488.00	483.09	480.23	48.50	50.62	51.86
127	8	50	0	310.3333	487.82	483.44	480.71	48.57	50.47	51.65
127	12	50	0	314.3333	487.37	483.41	480.58	48.77	50.48	51.71
127	18	50	0	320.3333	487.38	483.44	480.42	48.76	50.47	51.78
127	22	50	0	324.3333	488.41	483.93	480.98	48.32	50.26	51.54
128	4	50	0	330.3333	489.07	484.52	481.69	48.03	50.00	51.23

Table A-2. Water Levels in Observation Well H-1 During the 1984 H-3 Pumping Test

Day	Hr	Min	Elapsed Time (hr)	Depth to Water (ft)	Comments
110	9	17	-97.217	444.72	
110	16	0	-90.500	444.72	
114	9	0	-1.500	444.67	
114	12	35	2.083	444.67	PUMP ON AT H-3B3
115	10	3	23.550	444.53	114:10:30
118	14	12	99.700	444.40	
119	13	16	122.767	444.45	
121	14	26	171.933	444.40	
124	9	44	239.233	443.82	
128	13	29	338.983	443.53	

Table A-3. Water Levels and Pressures in Observation Well DOE-1 During the 1984 H-3 Pumping Test

Day	Hr	Min	Elapsed Time (hr)	Depth to Water (ft)	Pressure* (psi)	Comments
101	16	32	-305.970	499.18	47.69	
108	14	10	-140.330	499.21	47.67	
110	8	55	-97.583	499.31	47.63	
110	14	5	-92.417	499.08	47.74	
110	15	44	-90.767	499.21	47.67	
111	12	45	-69.750	499.18	47.69	
114	8	45	-1.750	499.74	47.42	
114	12	7	1.617	499.61	47.48	PUMP ON AT H-3B3
115	9	42	23.200	499.61	47.48	114:10:30
117	13	46	75.267	499.41	47.58	
118	13	40	99.167	500.00	47.30	
121	13	17	170.783	500.75	46.95	
122	13	20	194.833	500.85	46.90	
123	11	52	217.367	501.05	46.80	
124	9	24	238.900	501.35	46.66	
125	10	6	263.600	501.51	46.59	
128	13	48	339.300	502.46	46.14	

*Pressure = (600 ft - Depth to Water) × 0.473 psi/ft

APPENDIX B
H-3 Multipad Pumping Test Data

Table B-1. H-3 Pressures During the 1985 H-3 Multipad Pumping Test

Day	Hr	Min	S	Elapsed Pumping Time (hr)	H-3B3 (psig)	H-3B2 (psig)	H-3B1 (psig)	H-3B1 Magenta (psig)	Comments
288	8	59	55	-0.0014	81.74	98.24	62.25	64.52	
288	9	0	0	0.0000	81.65	87.51	62.22	64.31	PUMP ON
288	9	0	5	0.0014	81.53	87.16	62.13	64.31	
288	9	0	10	0.0028	81.46	87.22	62.06	64.32	
288	9	0	15	0.0042	81.40	87.18	61.99	64.32	
288	9	0	20	0.0056	81.35	87.10	61.95	64.31	
288	9	0	25	0.0069	81.31	87.03	61.91	64.31	
288	9	0	30	0.0083	81.26	87.00	61.88	64.31	
288	9	0	35	0.0097	81.24	86.96	61.84	64.32	
288	9	0	40	0.0111	81.20	86.86	61.81	64.31	
288	9	0	45	0.0125	81.17	86.88	61.78	64.31	
288	9	0	50	0.0139	81.14	86.80	61.76	64.32	
288	9	0	55	0.0153	81.11	86.78	61.71	64.32	
288	9	1	0	0.0167	81.09	86.78	61.70	64.31	
288	9	1	10	0.0194	81.04	86.72	61.65	64.33	
288	9	1	20	0.0222	81.00	86.67	61.60	64.33	
288	9	1	30	0.0250	80.96	86.62	61.57	64.33	
288	9	1	40	0.0278	80.93	86.59	61.54	64.33	
288	9	1	50	0.0306	80.90	86.54	61.51	64.34	
288	9	2	0	0.0333	80.87	86.53	61.48	64.33	
288	9	2	10	0.0361	80.83	86.48	61.45	64.32	
288	9	2	20	0.0389	80.81	86.44	61.43	64.33	
288	9	2	30	0.0417	80.78	86.44	61.39	64.33	
288	9	2	40	0.0444	80.75	86.42	61.37	64.34	
288	9	2	50	0.0472	80.74	86.37	61.34	64.34	
288	9	3	0	0.0500	80.71	86.34	61.31	64.33	
288	9	3	30	0.0583	80.64	86.32	61.27	64.34	
288	9	4	0	0.0667	80.59	86.24	61.20	64.35	
288	9	4	30	0.0750	80.54	86.22	61.15	64.36	
288	9	5	0	0.0833	80.49	86.00	61.08	64.37	
288	9	5	30	0.0917	80.45	85.91	61.04	64.38	
288	9	6	0	0.1000	80.40	85.90	60.99	64.38	
288	9	7	0	0.1167	80.32	85.88	60.94	64.41	
288	9	8	0	0.1333	80.26	85.82	60.85	64.44	
288	9	9	0	0.1500	80.19	85.72	60.80	64.46	
288	9	10	0	0.1667	80.13	85.66	60.73	64.49	
288	9	15	0	0.2500	79.86	85.50	60.47	64.54	
288	9	20	0	0.3333	79.69	86.08	60.30	64.55	
288	9	25	0	0.4167	79.52	85.96	60.13	64.55	
288	9	30	0	0.5000	79.36	85.75	59.96	64.54	
288	9	35	0	0.5833	79.20	85.56	59.81	64.53	
288	9	40	0	0.6667	79.06	85.37	59.68	64.54	
288	9	45	0	0.7500	78.92	85.24	59.53	64.54	

(continued)

Table B-1. (continued)

Day	Hr	Min	S	Elapsed Pumping Time (hr)	H-3B3 (psig)	H-3B2 (psig)	H-3B1 (psig)	H-3B1 Magenta (psig)	Comments
288	9	50	0	0.8333	78.79	85.15	59.41	64.54	
288	9	55	0	0.9167	78.67	85.04	59.29	64.54	
288	10	0	0	1.0000	78.55	84.94	59.17	64.53	
288	10	10	0	1.1667	78.34	84.68	58.93	64.53	
288	10	20	0	1.3333	78.12	84.49	58.75	64.53	
288	10	30	0	1.5000	77.93	84.30	58.56	64.53	
288	10	40	0	1.6667	77.74	84.12	58.35	64.50	
288	10	50	0	1.8333	77.56	83.93	58.19	64.50	
288	11	15	0	2.2500	77.17	83.56	57.79	64.48	
288	11	30	0	2.5000	76.95	83.33	57.57	64.48	
288	11	45	0	2.7500	76.73	83.05	57.36	64.41	
288	12	0	0	3.0000	76.53	82.85	57.17	64.41	
288	12	15	0	3.2500	76.35	82.68	56.98	64.38	
288	12	30	0	3.5000	76.18	82.53	56.83	64.41	
288	12	45	0	3.7500	76.02	82.37	56.80	64.39	
288	13	0	0	4.0000	75.88	82.21	57.64	64.41	
288	13	30	0	4.5000	75.60	82.02	56.46	64.44	
288	14	0	0	5.0000	75.32	81.68	56.07	64.48	
288	14	59	0	5.9833	74.84	81.19	55.57	64.44	
288	15	59	0	6.9833	74.42	80.78	55.14	64.49	
288	18	1	0	9.0167	73.64	79.96	54.36	64.49	
288	19	1	0	10.0167	73.29	79.62	53.99	64.56	
288	20	1	0	11.0167	72.95	79.30	53.87	64.58	
288	22	1	0	13.0167	72.32	78.65	53.01	64.57	
288	23	1	0	14.0167	72.03	78.29	52.82	64.56	
289	0	1	0	15.0167	71.75	78.03	52.47	64.56	
289	1	1	0	16.0167	71.48	77.72	52.20	64.56	
289	2	1	0	17.0167	71.23	77.48	51.95	64.53	
289	3	1	0	18.0167	71.01	77.27	51.68	64.54	
289	4	1	0	19.0167	70.83	77.10	51.46	64.53	
289	5	1	0	20.0167	70.62	76.92	51.27	64.56	
289	10	1	0	25.0167	69.38	74.98	50.03	64.52	
289	15	2	0	30.0333	68.41	74.09	49.05	64.56	
289	20	0	0	35.0000	67.61	73.21	48.23	64.58	
290	1	0	0	40.0000	67.38	73.50	48.06	64.64	
290	6	0	0	45.0000	66.51	72.52	47.12	64.68	
290	11	0	0	50.0000	65.91	71.88	46.42	64.55	
290	21	5	0	60.0833	64.75	70.64	45.15	64.64	
291	7	0	3	70.0008	63.73	69.48	44.00	64.59	
291	17	0	0	80.0000	62.89	68.66	43.13	64.61	
292	3	0	0	90.0000	62.02	67.71	42.20	64.63	
292	13	5	0	100.0833	61.26	66.93	41.38	64.53	
292	23	0	0	110.0000	60.59	66.22	40.66	64.62	

(continued)

Table B-1 (continued)

Day	Hr	Min	S	Elapsed Pumping Time (hr)	H-3B3 (psig)	H-3B2 (psig)	H-3B1 (psig)	H-3B1 Magenta (psig)	Comments
293	9	0	0	120.0000	59.64	64.22	39.69	64.62	
294	5	0	0	140.0000	57.95	62.43	37.87	64.71	
295	1	14	0	160.2333	56.82	61.58	36.65	64.75	
295	21	15	0	180.2500	55.80	60.20	35.40	64.76	
296	17	1	53	200.0314	54.86	59.14	34.36	64.72	
297	13	30	0	220.5000	53.85	58.02	33.21	64.65	
298	9	23	0	240.3833	52.98	57.18	32.24	64.70	
299	5	15	0	260.2500	52.36	56.50	31.57	64.73	
300	1	15	0	280.2500	51.61	55.68	30.71	64.75	
300	21	0	0	300.0000	50.92	54.90	29.96	64.75	
302	23	10	0	350.1667	49.31	53.02	28.19	64.79	
305	1	25	0	400.4167	47.99	51.66	26.83	64.90	
307	3	0	0	450.0000	46.23	49.74	25.11	64.91	
309	5	15	0	500.2500	44.92	48.49	23.84	64.85	
311	7	6	0	550.1000	43.62	47.02	22.64	64.88	
313	9	0	0	600.0000	42.56	46.06	21.62	64.80	
315	11	34	45	650.5792	41.50	44.88	20.65	64.90	
317	13	50	0	700.8333	40.58	44.09	19.81	64.88	
319	15	30	0	750.5000	39.60	43.03	18.89	64.92	
321	17	15	0	800.2500	38.85	42.18	18.26	65.04	
323	19	0	0	850.0000	37.86	41.16	17.32	65.05	
325	21	50	0	900.8333	37.19	40.40	16.69	65.04	
327	23	0	0	950.0000	36.11	39.02	15.68	65.06	
330	1	51	19	1000.8553	35.34	38.23	14.97	65.15	
332	3	50	0	1050.8333	34.54	37.28	14.21	65.17	
334	5	50	0	1100.8333	33.76	36.38	13.52	65.24	
336	7	50	0	1150.8333	32.84	35.42	12.63	65.19	
338	9	52	38	1200.8772	31.92	34.27	11.77	65.04	
340	11	45	0	1250.7500	31.62	34.34	11.47	65.06	
342	13	19	0	1300.3167	31.00	33.29	10.93	65.11	
344	15	5	0	1350.0833	30.22	32.25	10.15	65.29	REPLACED H-3B1 TRANSDUCER
346	17	42	0	1400.7000	29.81	32.07	0.00	65.30	
348	19	4	0	1450.0667	29.60	32.20	18.76	65.29	
350	8	59	50	1487.9972	29.21	31.66	18.27	65.16	
350	9	0	0	1488.0000	29.26	41.37	18.29	65.15	PUMP OFF
350	9	0	5	1488.0014	29.37	42.16	18.36	65.15	
350	9	0	9	1488.0025	29.45	42.31	18.41	65.14	
350	9	0	14	1488.0039	29.51	42.39	18.48	65.15	
350	9	0	19	1488.0053	29.56	42.45	18.52	65.15	
350	9	0	24	1488.0067	29.60	42.52	18.56	65.14	
350	9	0	29	1488.0081	29.65	42.57	18.59	65.15	
350	9	0	34	1488.0094	29.68	42.59	18.63	65.15	
350	9	0	39	1488.0108	29.71	42.64	18.66	65.16	

(continued)

Table B-1 (continued)

Day	Hr	Min	S	Elapsed Pumping Time (hr)	H-3B3 (psig)	H-3B2 (psig)	H-3B1 (psig)	H-3B1 Magenta (psig)	Comments
350	9	0	44	1488.0122	29.75	42.65	18.70	65.14	
350	9	0	49	1488.0136	29.77	42.70	18.72	65.16	
350	9	0	54	1488.0150	29.80	42.73	18.74	65.15	
350	9	1	4	1488.0178	29.85	42.78	18.79	65.15	
350	9	1	14	1488.0206	29.89	42.80	18.83	65.15	
350	9	1	30	1488.0250	29.95	42.88	18.89	65.14	
350	9	1	40	1488.0278	29.98	42.92	18.92	65.15	
350	9	1	50	1488.0306	30.01	42.93	18.96	65.16	
350	9	2	0	1488.0333	30.04	42.96	18.99	65.15	
350	9	2	15	1488.0375	30.09	43.00	19.03	65.15	
350	9	2	30	1488.0417	30.11	43.05	19.07	65.15	
350	9	2	45	1488.0458	30.16	43.09	19.10	65.16	
350	9	3	0	1488.0500	30.19	43.15	19.13	65.16	
350	9	3	30	1488.0583	30.25	43.21	19.20	65.15	
350	9	4	0	1488.0667	30.30	43.24	19.25	65.15	
350	9	4	30	1488.0750	30.36	43.30	19.31	65.15	
350	9	5	0	1488.0833	30.40	43.34	19.35	65.16	
350	9	5	30	1488.0917	30.44	43.40	19.38	65.15	
350	9	6	0	1488.1000	30.48	43.42	19.43	65.15	
350	9	6	30	1488.1083	30.52	43.47	19.47	65.15	
350	9	7	0	1488.1167	30.55	43.50	19.50	65.16	
350	9	7	30	1488.1250	30.60	43.53	19.54	65.15	
350	9	8	0	1488.1333	30.62	43.59	19.56	65.16	
350	9	9	0	1488.1500	30.69	43.63	19.63	65.15	
350	9	10	0	1488.1667	30.75	43.72	19.69	65.16	
350	9	11	0	1488.1833	30.81	43.75	19.75	65.16	
350	9	12	0	1488.2000	30.85	43.80	19.81	65.16	
350	9	15	0	1488.2500	31.00	43.95	19.95	65.17	
350	9	18	0	1488.3000	31.12	44.12	20.07	65.17	
350	9	21	0	1488.3500	31.24	44.21	20.20	65.18	
350	9	24	0	1488.4000	31.36	44.34	20.30	65.17	
350	9	27	0	1488.4500	31.46	44.46	20.41	65.17	
350	9	30	0	1488.5000	31.56	44.55	20.51	65.17	
350	9	33	0	1488.5500	31.65	44.64	20.60	65.18	
350	9	36	0	1488.6000	31.74	44.76	20.69	65.17	
350	9	39	0	1488.6500	31.83	44.83	20.78	65.17	
350	9	42	0	1488.7000	31.92	44.90	20.87	65.18	
350	9	45	0	1488.7500	31.99	45.01	20.95	65.18	
350	9	48	0	1488.8000	32.08	45.09	21.02	65.18	
350	9	51	0	1488.8500	32.15	45.16	21.10	65.18	
350	9	54	0	1488.9000	32.22	45.23	21.18	65.17	
350	9	57	0	1488.9500	32.29	45.30	21.25	65.19	
350	10	0	0	1489.0000	32.37	45.40	21.32	65.19	

(continued)

Table B-1. (continued)

Day	Hr	Min	S	Elapsed Pumping Time (hr)	H-3B3 (psig)	H-3B2 (psig)	H-3B1 (psig)	H-3B1 Magenta (psig)	Comments
350	10	6	0	1489.1000	32.50	45.51	21.46	65.20	
350	10	12	0	1489.2000	32.64	45.66	21.58	65.19	
350	10	18	0	1489.3000	32.76	45.77	21.70	65.18	
350	10	24	0	1489.4000	32.87	45.87	21.82	65.17	
350	10	30	0	1489.5000	32.99	46.00	21.91	65.17	
350	10	36	0	1489.6000	33.08	46.09	22.04	65.13	
350	10	42	0	1489.7000	33.20	46.21	22.15	65.15	
350	10	48	0	1489.8000	33.30	46.30	22.26	65.16	
350	10	54	0	1489.9000	33.41	46.40	22.36	65.18	
350	11	0	0	1490.0000	33.50	46.51	22.45	65.17	
350	11	15	0	1490.2500	33.73	46.75	22.68	65.17	
350	11	30	0	1490.5000	33.96	46.96	22.91	65.16	
350	12	0	0	1491.0000	34.34	47.36	23.29	65.15	
350	12	15	0	1491.2500	34.53	47.52	23.47	65.13	
350	12	30	0	1491.5000	34.72	47.71	23.65	65.15	
350	12	45	0	1491.7500	34.88	47.87	23.83	65.15	
350	13	0	0	1492.0000	35.04	48.05	23.99	65.15	
350	13	30	0	1492.5000	35.36	48.38	24.30	65.16	
350	14	0	0	1493.0000	35.64	48.66	24.59	65.15	
350	14	30	0	1493.5000	35.92	48.93	24.87	65.16	
350	15	0	0	1494.0000	36.17	49.19	25.14	65.18	
350	15	30	0	1494.5000	36.41	49.43	25.38	65.20	
350	16	0	0	1495.0000	36.64	49.65	25.62	65.21	
350	16	30	0	1495.5000	36.85	49.87	25.84	65.22	
350	17	0	0	1496.0000	37.07	50.11	26.06	65.26	
350	17	30	0	1496.5000	37.27	50.30	26.28	65.26	
350	18	0	0	1497.0000	37.46	50.50	26.46	65.25	
350	18	30	0	1497.5000	37.64	50.66	26.64	65.27	
350	19	0	0	1498.0000	37.82	50.86	26.82	65.26	
350	19	30	0	1498.5000	37.99	51.01	26.99	65.24	
350	20	0	0	1499.0000	38.15	51.19	27.16	65.26	
350	20	30	0	1499.5000	38.32	51.34	27.34	65.26	
350	21	0	0	1500.0000	38.47	51.50	27.48	65.25	
350	21	30	0	1500.5000	38.62	51.66	27.64	65.25	
350	22	0	0	1501.0000	38.78	51.79	27.77	65.24	
350	23	0	0	1502.0000	39.07	52.07	28.08	65.24	
351	0	0	0	1503.0000	39.34	52.37	28.34	65.26	
351	1	0	0	1504.0000	39.59	52.63	28.60	65.28	
351	2	0	0	1505.0000	39.84	52.87	28.85	65.27	
351	3	0	0	1506.0000	40.08	53.08	29.10	65.26	
351	4	0	0	1507.0000	40.32	53.32	29.34	65.25	
351	5	0	0	1508.0000	40.56	53.56	29.58	65.26	
351	6	0	0	1509.0000	40.79	53.78	29.80	65.27	

(continued)

Table B-1 (continued)

Day	Hr	Min	S	Elapsed Pumping Time (hr)	H-3B3 (psig)	H-3B2 (psig)	H-3B1 (psig)	H-3B1 Magenta (psig)	Comments	
351	7	0	0	1510.0000	41.00	53.98	30.04	65.27		
351	8	0	0	1511.0000	41.18	54.12	30.20	65.18		
351	9	0	0	1512.0000	41.37	54.25	30.40	65.13		
351	10	0	0	1513.0000	41.59	54.47	30.61	65.14		
351	11	0	0	1514.0000	41.77	54.68	30.81	65.12		
351	12	4	0	1515.0667	41.98	54.88	31.02	65.11		
351	13	0	0	1516.0000	42.17	55.05	31.20	65.10		
351	14	55	0	1517.9167	42.52	55.40	31.55	65.11		
351	17	10	0	1520.1667	42.92	55.89	31.99	65.27		
351	20	11	47	1523.1964	43.41	56.37	32.48	65.26		
352	0	11	47	1527.1964	43.98	56.94	33.06	65.27		
352	4	11	47	1531.1964	44.49	57.43	33.57	65.22		
352	8	11	47	1535.1964	44.98	57.91	34.06	65.21		
352	12	11	47	1539.1964	45.46	58.31	34.55	65.11		
352	16	11	47	1543.1964	45.97	58.86	35.06	65.17		
352	21	4	0	1548.0667	46.52	59.45	35.62	65.22		
353	2	4	0	1553.0667	47.07	59.98	36.16	65.22		
353	7	4	0	1558.0667	47.58	60.50	36.68	65.24		
353	12	1	0	1563.0167	48.03	60.89	37.10	65.09		
353	17	1	0	1568.0167	48.48	61.40	37.61	65.23		
353	22	1	0	1573.0167	48.87	61.84	37.98	65.23		
354	3	1	0	1578.0167	49.29	62.29	38.40	65.26		
354	8	1	0	1583.0167	49.66	62.58	38.75	65.16		
354	13	11	0	1588.1833	50.08	62.94	39.18	65.11		
354	23	11	0	1598.1833	50.78	63.73	39.90	65.24		
355	9	20	0	1608.3333	51.40	64.25	40.49	65.10		
355	19	20	0	1618.3333	52.09	65.09	41.22	65.24		
356	5	20	0	1628.3333	52.74	65.71	41.87	65.27		
356	15	20	0	1638.3333	53.28	66.20	42.39	65.20		
357	1	20	0	1648.3333	53.78	66.75	42.90	65.31		
357	11	0	5	1658.0014	54.26	67.11	43.35	65.11		
357	21	0	5	1668.0014	54.78	67.73	43.90	65.29		
358	7	0	5	1678.0014	55.21	68.19	44.34	65.33		
358	17	0	5	1688.0014	55.67	68.60	44.81	65.29		
359	13	0	5	1708.0014	56.41	69.30	45.53	65.18		
360	9	1	0	1728.0167	57.27	70.13	46.36	65.18		
361	5	1	0	1748.0167	57.99	70.99	47.12	65.35		
362	1	1	0	1768.0167	58.62	71.58	47.73	65.32		
362	21	1	0	1788.0167	59.31	72.31	48.44	65.35		
363	17	1	0	1808.0167	59.96	72.88	49.09	65.31		
364	13	28	0	1828.4667	60.51	73.38	49.61	65.22		
365	9	28	0	1848.4667	61.01	74.01	50.12	65.32		
	1	5	28	0	1868.4667	61.56	74.59	50.67	65.36	

(continued)

Table B-1 (continued)

Day	Hr	Min	S	Elapsed Pumping Time (hr)	H-3B3 (psig)	H-3B2 (psig)	H-3B1 (psig)	H-3B1 Magenta (psig)	Comments
2	1	28	0	1888.4667	62.11	75.16	51.22	65.39	
2	21	20	0	1908.3333	62.54	75.58	51.64	65.44	
3	17	5	0	1928.0833	63.03	76.03	52.13	65.38	
4	13	5	0	1948.0833	63.36	76.34	52.43	65.29	
5	9	5	0	1968.0833	63.75	76.72	52.81	65.26	
6	5	5	0	1988.0833	64.33	77.31	50.93	65.39	
7	1	23	0	2008.3833	64.73	77.67	53.66	65.44	
7	21	23	0	2028.3833	64.89	77.88	53.80	65.43	
8	17	23	0	2048.3833	65.35	78.34	54.27	65.40	
9	13	4	0	2068.0667	65.67	78.59	54.57	65.27	
10	9	4	0	2088.0667	66.02	78.97	54.93	65.32	
11	15	18	0	2118.3000	66.55	79.42	55.44	65.24	
12	21	18	0	2148.3000	66.98	79.91	55.90	65.36	
14	3	0	0	2178.0000	67.53	80.43	56.42	65.40	
15	9	0	0	2208.0000	67.98	80.79	56.84	65.35	
16	15	0	0	2238.0000	68.36	81.21	57.25	65.34	
17	21	0	0	2268.0000	68.81	81.68	57.70	65.47	
19	3	30	0	2298.5000	69.18	82.04	58.05	65.49	
20	10	0	0	2329.0000	69.53	82.35	58.40	65.35	
21	16	0	0	2359.0000	69.80	82.79	58.81	66.80	
22	22	0	0	2389.0000	70.02	83.06	59.05	66.86	
24	13	15	59	2428.2664	70.54	83.52	59.56	66.79	
26	4	43	1	2467.7169	70.87	83.90	59.89	66.88	
27	20	43	0	2507.7167	71.40	84.40	60.41	66.87	
29	13	23	0	2548.3833	71.65	84.63	60.65	66.83	
31	5	23	0	2588.3833	72.16	85.17	61.16	66.93	
33	7	23	0	2638.3833	72.55	85.56	61.56	66.93	
35	9	6	0	2688.1000	73.06	85.99	62.03	66.92	
37	10	41	0	2737.6833	73.43	86.38	62.55	66.96	
39	12	41	0	2787.6833	73.77	86.73	62.76	66.97	
41	15	59	0	2838.9833	74.20	87.19	63.09	67.02	
43	17	0	0	2888.0000	74.50	87.46	63.42	66.99	
45	8	34	0	2927.5667	74.76	87.69	63.67	66.94	
46	6	29	0	2949.4833	74.95	87.94	63.88	67.01	
48	10	0	0	3001.0000	75.24	88.21	64.18	66.98	
50	12	0	0	3051.0000	75.54	88.52	64.49	66.94	
52	14	20	0	3101.3333	75.86	88.86	64.80	66.97	
54	15	24	0	3150.4000	76.14	89.14	65.08	66.93	
56	17	24	0	3200.4000	76.39	89.44	65.33	66.94	
58	19	34	0	3250.5667	76.70	89.74	65.61	67.26	
60	21	27	0	3300.4500	76.94	90.03	65.89	67.07	
62	22	55	0	3349.9167	77.05	90.18	66.01	67.08	
65	1	55	11	3400.9197	77.33	90.47	66.28	67.09	

(continued)

Table B-1 (concluded)

Day	Hr	Min	S	Elapsed Pumping Time (hr)	H-3B3 (psig)	H-3B2 (psig)	H-3B1 (psig)	H-3B1 Magenta (psig)	Comments
67	3	50	0	3450.8333	77.65	90.79	66.60	67.15	
69	5	50	0	3500.8333	77.86	91.02	66.81	67.19	
71	7	54	0	3550.9000	78.12	91.28	67.06	67.27	
73	10	24	0	3601.4000	78.28	91.48	67.23	67.29	
75	10	58	0	3649.9667	78.41	91.58	67.35	67.17	
77	12	42	0	3699.7000	78.69	91.89	67.64	67.32	
79	15	43	0	3750.7167	78.69	91.92	67.59	67.18	
81	17	30	0	3800.5000	78.94	92.18	67.85	67.14	
83	19	30	0	3850.5000	79.16	92.41	68.04	67.24	
85	21	30	0	3900.5000	79.27	92.55	68.12	67.26	
87	23	30	0	3950.5000	79.47	92.76	68.30	67.25	
90	1	30	0	4000.5000	79.70	92.99	68.52	67.29	
91	17	51	22	4040.8561	79.80	92.97	68.69	67.40	
93	20	12	3	4091.2008	79.99	93.16	68.98	67.65	
98	15	22	54	4206.3817	80.17	93.43	69.01	67.59	
100	18	2	21	4257.0392	80.61	93.80	69.36	67.87	

Table B-2. Water Levels and Pressures in Observation Well H-1 During the 1985 H-3 Multipad Pumping Test

Day	Hr	Min	Elapsed Time (hr)	Depth to Water (ft)	Pressure* (psi)	Modified Pressure† (psi)
288	9	0	0.00	419.26	35.55	--
290	11	20	50.33	419.18	35.59	--
292	12	0	99.00	419.08	35.63	--
294	15	6	150.10	418.96	35.68	--
296	18	15	201.25	418.75	35.77	--
298	19	8	250.13	418.65	35.82	--
300	1	6	280.10	418.57	35.85	35.85
300	20	7	299.12	418.51	35.88	35.85
301	21	6	324.14	418.45	35.91	35.84
302	23	7	350.12	418.39	35.93	35.82
303	22	6	373.14	418.34	35.95	35.81
304	23	30	398.50	418.30	35.97	35.78
308	15	0	486.00	418.23	36.00	35.68
309	10	15	505.25	418.24	36.00	35.64
309	15	0	510.00	418.25	35.99	35.63
309	20	44	515.73	418.26	35.99	35.62
310	10	33	529.55	418.27	35.99	35.59
310	20	59	539.98	418.28	35.98	35.57
310	23	5	542.08	418.29	35.98	35.56
311	10	12	553.20	418.30	35.97	35.54
311	16	0	559.00	418.31	35.97	35.52
311	20	0	563.00	418.32	35.96	35.51
311	21	11	564.18	418.33	35.96	35.51
312	9	44	576.73	418.35	35.95	35.48
313	9	8	600.13	418.41	35.92	35.42
314	9	34	624.57	418.48	35.89	35.35
315	8	40	647.67	418.55	35.86	35.28
316	9	48	672.80	418.65	35.82	35.19
317	10	9	697.15	418.75	35.77	35.11
318	9	4	720.07	418.86	35.73	35.03
319	9	56	744.93	418.99	35.67	34.93
320	9	36	768.60	419.13	35.61	34.83
321	8	21	791.35	419.27	35.55	34.73
322	10	20	817.33	419.42	35.48	34.63
323	9	15	840.25	419.57	35.41	34.52
324	8	47	863.78	419.75	35.33	34.41
325	10	43	889.72	419.95	35.25	34.28
326	9	48	912.80	420.13	35.17	34.16
327	9	30	936.50	420.34	35.07	34.03
328	10	30	961.50	420.54	34.99	33.90

(continued)

*Pressure = (500 ft - Depth to Water) × 0.4403 psi/ft

†Modified Pressure = (500 ft - [Depth to Water + [1.3 ft/360 hr × (Elapsed Time - 280 hr)]) × 0.4403 psi/ft

Table B-2 (continued)

Day	Hr	Min	Elapsed Time (hr)	Depth to Water (ft)	Pressure (psi)	Modified Pressure (psi)
330	10	22	1009.37	421.00	34.78	33.62
332	0	8	1047.13	421.38	34.62	33.40
334	8	40	1103.67	421.97	34.36	33.05
336	8	48	1151.80	422.53	34.11	32.72
338	16	20	1207.33	423.17	33.83	32.35
340	12	33	1251.55	423.72	33.59	32.04
342	10	17	1297.28	424.33	33.32	31.70
344	16	15	1351.25	425.10	32.98	31.28
346	10	15	1393.25	425.75	32.69	30.92
348	11	0	1442.00	426.54	32.34	30.50
350	10	0	1489.00	427.33	32.00	30.07
351	8	11	1511.18	427.72	31.82	29.87
352	8	45	1535.75	428.17	31.63	29.63
353	9	18	1560.30	428.63	31.42	29.39
354	9	1	1584.02	429.07	31.23	29.16
355	8	47	1607.78	429.51	31.04	28.93
356	9	15	1632.25	429.97	30.83	28.68
357	11	33	1658.55	430.47	30.61	28.42
358	8	12	1679.20	430.88	30.43	28.21
359	8	17	1703.28	431.35	30.23	27.96
360	7	45	1726.75	431.80	30.03	27.73
363	8	53	1799.88	433.15	29.43	27.02
364	9	45	1824.75	433.60	29.24	26.78
365	8	35	1847.58	433.99	29.06	26.57
1	11	20	1874.33	434.43	28.87	26.34
2	8	29	1895.48	434.78	28.72	26.15
3	11	0	1922.00	435.21	28.53	25.92
4	9	0	1944.00	435.55	28.38	25.73
5	9	15	1968.25	435.93	28.21	25.53
6	10	16	1993.27	436.28	28.06	25.33
7	9	30	2016.50	436.61	27.91	25.15
8	9	35	2040.58	436.95	27.76	24.96
9	9	13	2064.22	437.26	27.62	24.79
10	9	24	2088.40	437.57	27.49	24.61
11	10	1	2113.02	437.89	27.35	24.43
12	9	48	2136.80	438.17	27.22	24.27
13	10	34	2161.57	438.35	27.14	24.15
14	9	38	2184.63	438.70	26.99	23.96
15	8	49	2207.82	438.94	26.88	23.82
16	9	4	2232.07	439.17	26.78	23.68

(continued)

Table B-2 (continued)

Day	Hr	Min	Elapsed Time (hr)	Depth to Water (ft)	Pressure (psi)	Modified Pressure (psi)
17	8	45	2255.75	439.39	26.69	23.55
19	10	14	2305.23	439.81	26.50	23.28
21	11	52	2354.87	440.20	26.33	23.03
23	10	24	2401.40	440.54	26.18	22.81
25	10	50	2449.83	440.82	26.06	22.61
27	9	20	2496.33	441.06	25.95	22.43
29	9	0	2544.00	441.31	25.84	22.24
31	9	26	2592.43	441.50	25.76	22.08
33	9	22	2640.37	441.65	25.69	21.94
35	9	29	2688.48	441.77	25.64	21.81
37	9	34	2736.57	441.86	25.60	21.69
39	9	57	2784.95	441.92	25.57	21.59
41	10	5	2833.08	441.96	25.56	21.50
43	9	14	2880.23	441.99	25.54	21.41
46	11	26	2954.43	442.00	25.54	21.29
48	9	37	3000.62	441.99	25.54	21.22
50	9	35	3048.58	441.95	25.56	21.16
52	9	46	3096.77	441.91	25.58	21.10
54	11	0	3146.00	441.84	25.61	21.05
57	9	20	3216.33	441.72	25.66	20.99
59	8	17	3263.28	441.60	25.71	20.97
61	12	0	3315.00	441.46	25.78	20.95
63	10	15	3361.25	441.32	25.84	20.94
65	10	0	3409.00	441.16	25.91	20.93
68	10	5	3481.08	440.89	26.03	20.94
70	11	30	3530.50	440.68	26.12	20.95
71	8	29	3551.48	440.59	26.16	20.96
73	8	29	3599.48	440.37	26.26	20.98
75	10	0	3649.00	440.14	26.36	21.00
78	8	41	3719.68	439.81	26.50	21.03
80	8	45	3767.75	439.58	26.60	21.06
82	8	55	3815.92	439.35	26.70	21.08
85	9	0	3888.00	438.97	26.87	21.13
86	8	45	3911.75	438.86	26.92	21.15
88	10	10	3961.17	438.58	27.04	21.19
90	9	30	4008.50	438.31	27.16	21.23
92	9	16	4056.27	438.07	27.27	21.26
94	12	57	4107.95	437.70	27.43	21.34
95	9	25	4128.42	437.58	27.48	21.36
96	9	10	4152.17	437.44	27.55	21.39

(continued)

Table B-2 (concluded)

Day	Hr	Min	Elapsed Time (hr)	Depth to Water (ft)	Pressure (psi)	Modified Pressure (psi)
97	15	8	4182.13	437.26	27.62	21.42
100	9	0	4248.00	436.87	27.80	21.49
102	12	35	4299.58	436.53	27.95	21.55
104	9	0	4344.00	436.25	28.07	21.61
111	9	0	4512.00	435.25	28.51	21.78

Table B-3. Water Levels and Pressures in Observation Well H-2B2 During the 1985 H-3 Multipad Pumping Test

Day	Hr	Min	Elapsed Time (hr)	Depth to Water (ft)	Pressure* (psi)	Modified Pressure† (psi)
288	9	0	0.00	372.31	12.07	--
289	9	35	24.58	372.31	12.07	--
291	8	19	71.32	372.34	12.06	--
292	7	42	94.70	372.31	12.07	--
293	16	17	127.28	372.24	12.10	--
294	17	14	152.23	372.11	12.16	--
295	20	0	179.00	371.98	12.22	--
296	20	38	203.63	372.01	12.20	--
297	18	21	225.35	371.94	12.23	--
299	12	9	267.15	372.04	12.19	--
301	9	48	312.80	371.85	12.27	--
302	9	19	336.32	371.75	12.32	--
304	8	46	383.77	371.71	12.33	--
305	8	54	407.90	371.65	12.36	--
306	9	34	432.57	371.75	12.32	12.30
307	9	30	456.50	371.75	12.32	12.28
308	9	23	480.38	371.88	12.26	12.21
309	9	55	504.92	371.78	12.30	12.24
311	9	0	552.00	371.68	12.35	12.25
312	10	9	577.15	371.68	12.35	12.23
313	9	24	600.40	371.71	12.33	12.20
314	9	33	624.55	371.75	12.32	12.17
315	8	50	647.83	371.88	12.26	12.09
316	9	4	672.07	371.88	12.26	12.08
317	8	50	695.83	371.88	12.26	12.06
318	9	8	720.13	371.91	12.25	12.03
319	9	9	744.15	371.94	12.23	12.00
320	9	38	768.63	371.98	12.22	11.97
321	9	39	792.65	372.01	12.20	11.94
323	8	50	839.83	372.17	12.13	11.84
324	9	0	864.00	372.60	11.95	11.63
325	9	24	888.40	372.53	11.98	11.65
326	8	47	911.78	372.50	11.99	11.64
327	9	48	936.80	372.44	12.02	11.65
328	11	7	962.12	372.37	12.05	11.66
329	9	50	984.83	372.50	11.99	11.59
330	10	26	1009.43	372.44	12.02	11.60
331	10	11	1033.18	372.80	11.86	11.43
333	8	45	1079.75	372.83	11.85	11.38
334	8	57	1103.95	372.90	11.82	11.34

(continued)

*Pressure = (400 ft - Depth to Water) × 0.436 psi/ft

†Modified Pressure = (400 ft - {Depth to Water + [0.57 ft/360 hr × (Elapsed Time - 408 hr)]) × 0.436 psi/ft

Table B-3 (continued)

Day	Hr	Min	Elapsed Time (hr)	Depth to Water (ft)	Pressure (psi)	Modified Pressure (psi)
336	9	8	1152.13	373.58	11.52	11.01
337	15	15	1182.25	373.49	11.56	11.02
338	15	50	1206.83	373.68	11.48	10.92
339	10	35	1225.58	373.91	11.38	10.81
340	12	45	1251.75	373.98	11.34	10.76
341	13	58	1276.97	373.91	11.38	10.78
342	10	41	1297.68	373.91	11.38	10.76
344	10	30	1345.50	374.08	11.30	10.65
346	10	25	1393.42	374.40	11.16	10.48
348	15	30	1446.50	375.00	10.90	10.18
349	9	1	1464.02	375.00	10.90	10.17
350	9	17	1488.28	375.16	10.83	10.08
351	9	34	1512.57	375.36	10.74	9.98
352	9	40	1536.67	375.65	10.62	9.84
353	9	11	1560.18	375.75	10.57	9.78
354	11	8	1586.13	375.85	10.53	9.72
355	14	6	1613.10	375.98	10.47	9.64
356	12	45	1635.75	375.88	10.52	9.67
357	13	52	1660.87	376.08	10.43	9.56
358	12	55	1683.92	376.24	10.36	9.48
360	10	25	1729.42	376.50	10.25	9.33
361	9	53	1752.88	376.57	10.22	9.29
362	10	1	1777.02	376.90	10.07	9.13
363	9	17	1800.28	376.80	10.12	9.15
364	10	13	1825.22	377.10	9.98	9.01
365	9	8	1848.13	377.19	9.95	8.95
	2	8	1895.73	377.62	9.76	8.73
	3	10	1921.83	377.78	9.69	8.64
	4	10	1945.13	378.08	9.56	8.50
	5	15	1974.65	378.24	9.49	8.41
	6	11	1994.20	378.08	9.56	8.46
	7	9	2016.83	378.41	9.41	8.30
	8	10	2041.22	378.74	9.27	8.14
	9	9	2064.88	378.93	9.19	8.04
	10	9	2088.70	378.93	9.19	8.03
	11	10	2113.95	378.93	9.19	8.01
	13	14	2165.93	379.19	9.07	7.86
	15	11	2210.45	379.10	9.11	7.87
	17	9	2256.40	379.33	9.01	7.74
	19	10	2305.75	378.77	9.26	7.95

(continued)

Table B-3 (concluded)

Day	Hr	Min	Elapsed Time (hr)	Depth to Water (ft)	Pressure (psi)	Modified Pressure (psi)
21	12	1	2355.02	379.06	9.13	7.79
23	10	35	2401.58	379.62	8.89	7.51
25	11	12	2450.20	379.72	8.84	7.43
27	9	31	2496.52	379.92	8.75	7.31
29	10	52	2545.87	379.79	8.81	7.34
31	9	45	2592.75	379.75	8.83	7.32
33	10	34	2641.57	379.92	8.75	7.21
35	9	34	2688.57	379.75	8.83	7.25
37	9	47	2736.78	379.85	8.79	7.18
39	10	18	2785.30	379.98	8.73	7.09
41	10	16	2833.27	380.15	8.65	6.98
43	10	2	2881.03	380.28	8.60	6.89
46	11	43	2954.72	379.85	8.79	7.03
48	14	37	3005.62	379.92	8.75	6.96
50	10	0	3049.00	379.88	8.77	6.95
52	10	7	3097.12	379.98	8.73	6.87
55	10	6	3169.10	379.98	8.73	6.82
57	9	50	3216.83	379.85	8.79	6.85
59	8	30	3263.50	379.98	8.73	6.76
62	10	37	3337.62	379.79	8.81	6.79
64	9	25	3384.42	379.69	8.86	6.80
66	10	56	3433.93	379.52	8.93	6.84
71	9	44	3552.73	379.33	9.01	6.84
73	8	50	3599.83	379.26	9.04	6.84
76	9	30	3672.50	379.16	9.09	6.83
78	9	53	3720.88	379.26	9.04	6.76
80	9	10	3768.17	379.36	9.00	6.68
83	9	32	3840.53	379.10	9.11	6.74
85	10	30	3889.50	379.00	9.16	6.75
88	10	30	3961.50	378.83	9.23	6.78
90	9	40	4008.67	378.54	9.36	6.87
92	10	16	4057.27	378.44	9.40	6.88

Table B-4. Water Levels and Pressures in Observation Well H-11B1 During the 1985 H-3 Multipad Pumping Test

Day	Hr	Min	Elapsed Time (hr)	Depth to Water (ft)	Pressure* (psi)	Modified Pressure† (psi)
288	18	25	9.42	446.65	25.23	--
289	10	2	25.03	446.68	25.22	--
290	9	15	48.25	446.62	25.25	--
291	10	3	73.05	446.52	25.30	25.30
292	16	50	103.83	446.65	25.23	25.22
293	15	53	126.88	446.88	25.13	25.10
294	16	49	151.82	446.84	25.14	25.10
295	20	35	179.58	447.01	25.06	25.00
296	19	20	202.33	447.07	25.04	24.96
297	17	48	224.80	447.24	24.96	24.87
299	9	4	264.07	447.44	24.86	24.75
301	11	1	314.02	447.67	24.75	24.62
303	10	2	361.03	448.06	24.57	24.41
305	10	17	409.28	447.89	24.65	24.46
306	11	20	434.33	448.62	24.30	24.10
307	11	25	458.42	448.72	24.26	24.04
309	9	50	504.83	449.11	24.07	23.83
311	10	0	553.00	449.70	23.79	23.52
313	10	45	601.75	449.76	23.76	23.47
315	10	0	649.00	450.32	23.50	23.18
317	10	46	697.77	450.45	23.44	23.09
319	13	30	748.50	450.68	23.33	22.95
321	11	19	794.32	450.98	23.19	22.78
323	10	15	841.25	451.48	22.95	22.52
325	10	41	889.68	451.86	22.77	22.31
327	11	13	938.22	452.09	22.66	22.18
329	11	7	986.12	452.23	22.60	22.09
331	11	15	1034.25	452.62	22.41	21.87
333	10	7	1081.12	452.79	22.33	21.77
336	10	16	1153.27	453.74	21.88	21.28
338	13	40	1204.67	453.77	21.87	21.23
340	13	53	1252.88	453.94	21.79	21.13
342	12	0	1299.00	454.07	21.72	21.04
344	11	42	1346.70	454.59	21.48	20.77
346	11	19	1394.32	454.66	21.45	20.71
348	11	33	1442.55	455.24	21.17	20.41
350	11	26	1490.43	455.41	21.09	20.30
352	11	44	1538.73	455.70	20.95	20.14
354	11	46	1586.77	455.64	20.98	20.14
356	10	45	1633.75	455.54	21.03	20.16

(continued)

*Pressure = (500 ft - Depth to Water) × 0.473 psi/ft

†Modified Pressure = (500 ft - [Depth to Water + [0.425 ft/360 hr × (Elapsed Time - 73 hr)]) × 0.473 psi/ft

Table B-4 (continued)

Day	Hr	Min	Elapsed Time (hr)	Depth to Water (ft)	Pressure (psi)	Modified Pressure' (psi)
358	11	30	1682.50	455.57	21.02	20.12
360	11	52	1730.87	455.34	21.12	20.20
362	11	27	1778.45	455.31	21.14	20.19
364	12	15	1827.25	455.28	21.15	20.17
365	10	46	1849.77	455.08	21.25	20.26
2	11	0	1898.00	454.95	21.31	20.29
4	11	23	1946.38	454.55	21.50	20.45
6	12	24	1995.40	454.13	21.70	20.62
8	12	28	2043.47	454.39	21.57	20.47
10	11	59	2090.98	454.26	21.64	20.51
12	11	20	2138.33	453.90	21.81	20.65
14	11	4	2186.07	453.31	22.08	20.90
16	10	26	2233.43	453.08	22.19	20.99
18	10	47	2281.78	452.19	22.61	21.38
20	11	43	2330.72	452.19	22.61	21.35
22	12	46	2379.77	452.39	22.52	21.23
24	13	15	2428.25	452.09	22.66	21.35
26	10	48	2473.80	452.29	22.57	21.23
28	11	9	2522.15	451.70	22.85	21.48
30	13	21	2572.35	451.69	22.85	21.45
32	14	56	2621.93	451.47	22.95	21.53
34	11	45	2666.75	451.21	23.08	21.63
36	11	7	2714.12	451.08	23.14	21.66
38	12	0	2763.00	451.01	23.17	21.67
41	11	22	2834.37	451.01	23.17	21.63
43	11	9	2882.15	451.04	23.16	21.59
46	12	47	2955.78	450.39	23.47	21.86
50	11	45	3050.75	450.19	23.56	21.90
52	11	20	3098.33	450.26	23.53	21.84
55	11	30	3170.50	449.99	23.65	21.93
57	11	10	3218.17	449.86	23.72	21.96
62	12	45	3339.75	449.83	23.73	21.91
64	10	23	3385.38	449.44	23.91	22.07
66	13	47	3436.78	449.34	23.96	22.08
71	10	48	3553.80	449.04	24.10	22.16
73	9	55	3600.92	449.04	24.10	22.13
76	11	5	3674.08	448.65	24.29	22.28
78	10	53	3721.88	449.01	24.12	22.08
80	10	10	3769.17	448.98	24.13	22.07
83	11	10	3842.17	448.71	24.26	22.16

(continued)

Table B-4 (concluded)

Day	Hr	Min	Elapsed Time (hr)	Depth to Water (ft)	Pressure (psi)	Modified Pressure (psi)
85	11	25	3890.42	448.65	24.29	22.16
88	11	15	3962.25	448.42	24.40	22.23
90	11	10	4010.17	448.09	24.55	22.35
92	10	56	4057.93	447.99	24.60	22.38
95	10	20	4129.33	448.16	24.52	22.26
97	11	18	4178.30	447.93	24.63	22.34
100	10	59	4249.98	447.99	24.60	22.27
102	12	15	4299.25	447.73	24.72	22.36
104	10	25	4345.42	447.65	24.76	22.38
111	10	45	4513.75	447.56	24.80	22.32

Table B-5. Pressures in Observation Well DOE-1 During the 1985 H-3 Multipad Pumping Test

Day	Hr	Min	S	Elapsed Time (hr)	Pressure (psig)	Modified Pressure* (psig)
288	9	0	0	0.000000	72.25	--
288	11	0	0	2.000000	72.20	--
288	13	4	1	4.066890	72.20	--
288	15	4	1	6.066890	72.25	--
288	17	4	1	8.066900	72.29	--
288	19	4	1	10.066900	72.29	--
288	21	5	1	12.083500	72.27	--
288	23	5	1	14.083500	72.24	--
289	1	5	1	16.083500	72.21	--
289	3	5	1	18.083500	72.22	--
289	5	5	1	20.083500	72.28	--
289	7	5	1	22.083500	72.30	--
289	9	5	1	24.083500	72.29	--
289	11	0	0	26.000000	72.28	--
289	13	0	0	28.000000	72.29	--
289	14	0	0	29.000000	72.30	--
289	19	0	0	34.000000	72.35	--
290	0	0	0	39.000000	72.30	--
290	5	0	0	44.000000	72.34	--
290	10	0	0	49.000000	72.32	--
290	20	5	1	59.083500	72.35	72.35
291	10	25	59	73.433100	72.24	72.23
291	16	51	0	79.850100	72.27	72.25
292	2	51	0	89.850100	72.20	72.18
292	12	17	59	99.299810	72.12	72.09
292	22	0	0	109.000000	72.16	72.12
293	8	0	0	119.000000	72.08	72.03
293	18	0	0	129.000000	72.12	72.07
294	4	0	0	139.000000	72.06	72.00
294	14	6	0	149.100100	72.03	71.96
295	0	6	0	159.100100	72.03	71.95
295	11	36	0	170.600100	71.95	71.87
295	20	6	0	179.100100	71.98	71.89
296	6	6	0	189.100100	71.91	71.81
296	16	6	0	199.100100	71.86	71.75
297	2	6	0	209.100100	71.81	71.70
297	12	6	0	219.100100	71.64	71.52
297	22	6	0	229.100100	71.62	71.49
298	8	15	0	239.250000	71.54	71.40

(continued)

*Modified Pressure = Pressure - [0.27 psi/360 hr × (elapsed time - 59 hr)]

Table B-5 (continued)

Day	Hr	Min	S	Elapsed Time (hr)	Pressure (psig)	Modified Pressure (psig)
298	14	15	0	245.250000	71.53	71.39
299	14	0	0	269.000000	71.33	71.17
300	0	0	0	279.000000	71.26	71.09
300	10	0	0	289.000000	71.13	70.96
302	11	13	1	338.216800	70.98	70.77
302	23	13	1	350.216800	70.92	70.70
303	9	13	0	360.216800	70.89	70.66
303	19	13	0	370.216800	70.96	70.73
304	5	13	1	380.216800	70.94	70.70
305	1	30	0	400.500000	70.86	70.60
305	18	39	59	417.666500	70.69	70.42
306	16	20	1	439.333500	70.54	70.25
307	2	20	1	449.333500	70.44	70.15
307	12	13	0	459.216800	70.33	70.03
307	22	13	0	469.216800	70.31	70.00
308	9	13	13	480.220210	70.19	69.87
308	19	22	48	490.379880	70.23	69.91
309	5	22	48	500.379880	70.17	69.84
310	1	0	0	520.000000	70.14	69.79
310	21	25	49	540.430180	70.01	69.65
311	17	4	48	560.080080	69.90	69.52
312	13	0	0	580.000000	69.77	69.38
313	9	0	0	600.000000	69.63	69.22
314	5	0	0	620.000000	69.61	69.19
315	1	0	0	640.000000	69.44	69.00
315	21	10	12	660.169920	69.33	68.88
316	17	9	37	680.160160	69.31	68.84
317	13	40	12	700.669920	69.11	68.63
318	9	19	48	720.330080	69.06	68.56
320	0	1	12	759.020020	68.70	68.17
320	21	19	48	780.330080	68.67	68.13
321	17	46	47	800.779790	68.68	68.12
322	13	13	48	820.229980	68.56	67.99
323	9	37	12	840.620120	68.43	67.84
324	5	37	12	860.620120	68.29	67.69
325	1	40	12	880.669920	68.32	67.70
325	21	0	0	900.000000	68.22	67.59
326	16	10	59	919.183110	68.17	67.52
327	12	10	59	939.183110	68.00	67.34

(continued)

Table B-5 (continued)

Day	Hr	Min	S	Elapsed Time (hr)	Pressure (psig)	Modified Pressure (psig)
328	8	10	59	959.183110	67.91	67.23
329	4	10	59	979.183110	67.94	67.25
330	0	35	1	999.583500	67.80	67.09
330	20	9	59	1019.166500	67.75	67.03
331	16	0	0	1039.000000	67.70	66.97
332	12	55	59	1059.933100	67.57	66.82
333	8	55	59	1079.933100	67.54	66.77
334	4	55	59	1099.933100	67.50	66.72
335	0	39	59	1119.666500	67.32	66.52
335	20	35	1	1139.583500	67.26	66.45
336	16	49	59	1159.833000	67.15	66.32
337	12	13	0	1179.216800	67.08	66.24
338	8	13	1	1199.216800	66.90	66.04
339	4	31	59	1219.533200	66.81	65.94
340	0	32	0	1239.533200	66.81	65.92
340	20	1	0	1259.016600	66.78	65.88
341	16	1	0	1279.016600	66.71	65.79
343	11	30	49	1322.513700	66.55	65.60
344	4	50	59	1339.849600	66.60	65.64
345	0	56	1	1359.933600	66.35	65.37
345	20	56	1	1379.933600	66.33	65.34
346	16	58	0	1399.966800	66.35	65.34
348	8	58	1	1439.966800	65.90	64.86
349	4	30	0	1459.500000	65.90	64.85
350	0	56	1	1479.933600	65.90	64.83
350	8	57	1	1487.950200	65.84	64.77
350	9	0	0	1488.000000	65.85	64.78
350	10	0	0	1489.000000	65.87	64.80
350	11	0	0	1490.000000	65.86	64.79
350	21	1	48	1500.030000	65.87	64.79
351	7	1	48	1510.030000	65.84	64.75
351	17	4	12	1520.069900	65.86	64.76
352	3	4	12	1530.069900	65.79	64.69
352	13	12	0	1540.200000	65.72	64.61
352	23	12	0	1550.200000	65.76	64.64
353	9	12	0	1560.200000	65.72	64.59
353	19	12	0	1570.200000	65.78	64.65
354	5	12	0	1580.200000	65.78	64.64
354	15	12	0	1590.200000	65.78	64.63

(continued)

Table B-5 (continued)

Day	Hr	Min	S	Elapsed Time (hr)	Pressure (psig)	Modified Pressure (psig)
355	1	12	0	1600.200000	65.79	64.63
355	21	6	0	1620.100000	65.80	64.63
356	17	6	0	1640.100000	65.89	64.70
357	13	6	0	1660.100000	65.90	64.70
358	9	10	12	1680.170000	65.85	64.63
359	5	10	12	1700.170000	65.99	64.76
361	7	10	12	1750.170000	66.18	64.91
363	9	10	12	1800.170000	66.33	65.02
365	11	10	12	1850.170000	66.48	65.14
367	13	10	12	1900.170000	66.69	65.31
369	15	21	0	1950.350000	66.80	65.38
371	18	18	0	2001.300000	67.14	65.68
373	20	37	48	2051.629900	67.14	65.65
375	22	49	12	2101.820100	67.30	65.77
378	0	49	12	2151.820100	67.46	65.89
380	2	37	12	2201.620100	67.74	66.13
382	4	37	12	2251.620100	67.90	66.26
384	6	37	12	2301.620100	68.06	66.38
386	8	37	12	2351.620100	68.25	66.53
388	8	37	12	2399.620100	68.32	66.56
390	10	12	0	2449.200000	68.39	66.60
392	12	12	0	2499.200000	68.56	66.73
394	15	55	12	2550.919900	68.70	66.83
396	18	34	48	2601.580100	68.94	67.03
398	18	46	48	2649.780000	68.97	67.03
400	21	42	0	2700.700000	69.13	67.15
402	23	42	0	2750.700000	69.28	67.26
405	1	42	0	2800.700000	69.35	67.29
407	3	31	48	2850.530000	69.47	67.38
409	5	31	48	2900.530000	69.58	67.45
411	7	24	0	2950.399900	69.70	67.53
413	9	34	48	3000.580100	69.77	67.56
415	11	34	48	3050.580100	69.84	67.60
417	13	34	48	3100.580100	69.93	67.65
419	15	34	48	3150.580100	70.03	67.71
421	17	34	48	3200.580100	70.10	67.74
423	18	55	12	3249.919900	70.16	67.77
425	20	43	48	3299.730000	70.29	67.86
428	10	35	24	3361.590100	70.24	67.76

(continued)

Table B-5 (concluded)

Day	Hr	Min	S	Elapsed Time (hr)	Pressure (psig)	Modified Pressure (psig)
430	1	4	48	3400.080100	70.36	67.85
432	2	22	12	3449.370100	70.50	67.96
434	4	51	0	3499.850100	70.60	68.02
436	7	0	0	3550.000000	70.75	68.13
438	8	40	12	3599.669900	70.78	68.12
440	11	30	0	3650.500000	70.74	68.05
442	12	27	0	3699.450000	70.87	68.14
444	14	4	48	3749.080100	70.54	67.77
445	12	52	48	3771.879900	70.56	67.78
448	16	28	12	3847.470000	70.45	67.61
449	17	4	48	3872.080100	70.54	67.68
451	14	4	12	3917.070100	70.39	67.50
455	18	12	36	4017.210000	70.66	67.69
458	20	0	36	4091.010000	70.85	67.83
463	16	19	48	4207.330100	70.95	67.84

**Table B-6. Water Levels and Pressures in Observation Well WIPP-19
During the 1985 H-3 Multipad Pumping Test**

Day	Hr	Min	Elapsed Time (hr)	Depth to Water (ft)	Pressure* (psi)
287	15	15	-17.75	410.82	45.57
291	16	10	79.17	450.16	25.47
299	15	48	270.80	450.26	25.42
310	14	10	533.17	456.42	22.27
319	16	0	751.00	456.65	22.15
321	14	20	797.33	456.65	22.15
325	13	25	892.42	456.65	22.15
327	14	50	941.83	456.62	22.17
329	15	5	990.08	456.62	22.17
331	13	20	1036.33	456.69	22.13
333	12	15	1083.25	456.59	22.18
334	12	0	1107.00	456.69	22.13
336	13	38	1156.63	456.62	22.17
338	15	38	1206.63	457.02	21.96
340	16	0	1255.00	457.05	21.95
342	17	22	1304.37	457.11	21.92
344	14	16	1349.27	457.25	21.85
346	14	48	1397.80	457.08	21.93
348	14	20	1445.33	457.64	21.65
350	13	57	1492.95	457.90	21.51
352	13	50	1540.83	458.03	21.45
354	16	40	1591.67	458.32	21.30
356	13	10	1636.17	458.45	21.23
358	9	24	1680.40	458.69	21.11
360	14	50	1733.83	458.95	20.98
362	16	20	1783.33	459.21	20.84
364	13	52	1828.87	459.44	20.73
365	13	55	1852.92	460.03	20.42
2	16	29	1903.48	460.16	20.36
2	16	29	1903.48	460.16	20.36
4	9	32	1944.53	460.23	20.32
6	10	50	1993.83	460.43	20.22
8	16	40	2047.67	460.89	19.99
10	10	3	2089.05	461.02	19.92
12	13	19	2140.32	461.25	19.80
14	14	29	2189.48	461.35	19.75
15	15	28	2214.47	461.41	19.72
22	15	14	2382.23	461.71	19.57
24	15	7	2430.12	461.67	19.59
26	13	47	2476.78	461.84	19.50

(continued)

*Pressure = (500 ft - Depth to Water) × 0.511 psi/ft

Table B-6. (concluded)

Day	Hr	Min	Elapsed Time (hr)	Depth to Water (ft)	Pressure (psi)
28	15	3	2526.05	461.87	19.48
30	15	19	2574.32	461.94	19.45
32	13	30	2620.50	462.10	19.37
34	14	36	2669.60	462.03	19.40
36	14	7	2717.12	462.23	19.30
38	5	54	2756.90	462.23	19.30
40	12	55	2811.92	462.56	19.13
42	10	48	2857.80	462.49	19.17
44	20	0	2897.00	462.46	19.18
46	14	54	2957.90	462.36	19.23
48	15	19	3006.32	462.36	19.23
50	14	25	3053.42	462.39	19.22
52	13	50	3100.83	462.49	19.17
55	14	2	3173.03	462.46	19.18
57	16	5	3223.08	462.49	19.17
59	9	0	3264.00	462.63	19.10
62	15	42	3342.70	462.66	19.08
64	12	53	3387.88	462.49	19.17
66	10	13	3433.22	462.49	19.17
71	9	6	3552.10	462.33	19.25
73	12	24	3603.40	462.46	19.18
76	13	50	3676.83	462.26	19.29
78	9	25	3720.42	462.30	19.26
80	13	45	3772.75	462.30	19.26
83	15	45	3846.75	462.26	19.29
85	9	37	3888.62	462.20	19.32
88	12	20	3963.33	462.10	19.37
90	13	33	4012.55	461.87	19.48
92	9	49	4056.82	461.90	19.47
95	11	40	4130.67	461.74	19.55
97	14	33	4181.55	461.64	19.60
100	9	32	4248.53	461.77	19.54
102	10	40	4297.67	461.54	19.65
104	14	25	4349.42	461.51	19.67
111	14	13	4517.22	461.57	19.64

Table B-7. Water Levels and Pressures in Observation Well WIPP-21 During the 1985 H-3 Multipad Pumping Test

Day	Hr	Min	Elapsed Time (hr)	Depth to Water (ft)	Pressure* (psi)
288	23	40	14.67	429.19	31.01
290	12	10	51.17	428.31	31.40
291	20	21	83.35	427.24	31.87
293	10	32	121.53	425.81	32.50
295	14	13	173.22	423.94	33.31
296	12	45	195.75	423.25	33.62
298	9	53	240.88	422.23	34.06
300	22	24	301.40	421.15	34.54
302	13	28	340.47	420.53	34.81
304	13	0	388.00	419.94	35.07
305	13	18	412.30	419.73	35.16
306	14	0	437.00	419.75	35.15
307	13	20	460.33	419.79	35.13
310	14	32	533.53	420.34	34.89
312	13	43	580.72	420.70	34.73
313	12	55	603.92	420.84	34.67
314	12	30	627.50	420.89	34.65
315	12	41	651.68	421.34	34.45
316	14	0	677.00	421.48	34.39
317	15	0	702.00	421.70	34.30
318	13	50	724.83	421.89	34.21
319	10	2	745.03	422.19	34.08
320	14	0	773.00	422.44	33.97
321	14	6	797.10	422.57	33.91
324	8	45	863.75	423.53	33.49
325	13	6	892.10	423.78	33.38
327	14	31	941.52	424.37	33.13
328	14	30	965.50	424.70	32.98
330	14	10	1013.17	425.29	32.72
331	13	2	1036.03	425.55	32.61
333	12	0	1083.00	425.98	32.42
334	11	46	1106.77	426.21	32.32
336	13	30	1156.50	426.96	31.99
338	15	22	1206.37	427.72	31.66
339	10	10	1225.17	428.41	31.36
340	15	41	1254.68	429.52	30.87
341	14	29	1277.48	430.57	30.41
342	17	6	1304.10	431.75	29.89
343	14	46	1325.77	432.67	29.49
344	13	52	1348.87	433.69	29.04

(continued)

*Pressure = (500 ft - Depth to Water) × 0.438 psi/ft

Table B-7 (continued)

Day	Hr	Min	Elapsed Time (hr)	Depth to Water (ft)	Pressure (psi)
345	13	45	1372.75	434.77	28.57
346	15	10	1398.17	435.72	28.15
347	13	8	1420.13	436.61	27.76
348	13	30	1444.50	437.72	27.28
349	14	3	1469.05	438.81	26.80
350	7	23	1486.38	439.59	26.46
350	13	42	1492.70	439.82	26.36
351	8	44	1511.73	440.68	25.98
352	18	17	1545.28	442.15	25.34
353	9	30	1560.50	442.42	25.22
354	11	5	1586.08	443.73	24.65
355	11	5	1610.08	444.52	24.30
356	13	40	1636.67	445.24	23.98
357	13	0	1660.00	445.86	23.71
358	8	50	1679.83	446.34	23.50
359	8	49	1703.82	446.88	23.27
360	9	35	1728.58	447.40	23.04
361	13	50	1756.83	447.93	22.81
362	13	55	1780.92	448.32	22.64
363	12	25	1803.42	448.85	22.40
364	14	10	1829.17	449.08	22.30
365	14	40	1853.67	449.37	22.18
1	12	1	1875.02	449.60	22.08
2	10	20	1897.33	449.73	22.02
3	11	16	1922.27	449.99	21.90
4	9	10	1944.17	450.16	21.83
5	9	30	1968.50	450.42	21.72
6	10	29	1993.48	450.52	21.67
7	14	7	2021.12	450.65	21.62
9	13	14	2068.23	451.18	21.38
11	10	32	2113.53	451.45	21.26
13	14	40	2165.67	451.57	21.21
15	15	52	2214.87	451.37	21.30
17	16	8	2263.13	451.27	21.34
19	14	30	2309.50	451.18	21.38
21	16	32	2359.53	450.88	21.51
23	15	13	2406.22	450.78	21.56
25	14	30	2453.50	450.62	21.63
28	15	24	2526.40	450.44	21.71
30	15	37	2574.62	450.39	21.73

(continued)

Table B-7 (concluded)

Day	Hr	Min	Elapsed Time (hr)	Depth to Water (ft)	Pressure (psi)
32	15	21	2622.35	450.16	21.83
34	14	58	2669.97	449.86	21.96
36	14	30	2717.50	449.50	22.12
38	10	13	2761.22	449.32	22.20
40	13	18	2812.30	449.31	22.20
42	11	6	2858.10	449.47	22.13
43	9	47	2880.78	449.67	22.04
46	14	33	2957.55	449.76	22.01
48	14	53	3005.88	449.50	22.12
50	15	0	3054.00	449.21	22.25
52	13	25	3100.42	448.94	22.36
55	13	37	3172.62	449.24	22.23
57	16	38	3223.63	448.81	22.42
59	9	20	3264.33	448.65	22.49
62	16	8	3343.13	448.09	22.74
64	12	28	3387.47	447.89	22.82
66	10	36	3433.60	447.60	22.95
69	12	50	3507.83	447.11	23.17
71	8	44	3551.73	446.75	23.32
73	12	45	3603.75	446.45	23.45
76	14	25	3677.42	445.93	23.68
78	9	0	3720.00	445.86	23.71
80	14	20	3773.33	445.76	23.76
82	16	30	3823.50	445.34	23.94
83	16	10	3847.17	445.20	24.00
86	12	25	3915.42	445.11	24.04
92	9	28	4056.47	442.73	25.08
94	13	8	4108.13	442.24	25.30
95	12	0	4131.00	442.14	25.34
97	15	0	4182.00	441.87	25.46
100	9	15	4248.25	441.55	25.60
102	11	0	4298.00	440.92	25.88
104	15	0	4350.00	440.60	26.02
111	14	55	4517.92	439.68	26.42

Table B-8. Water Levels and Pressures in Observation Well WIPP-22 During the 1985 H-3 Multipad Pumping Test

Day	Hr	Min	Elapsed Time (hr)	Depth to Water (ft)	Pressure* (psi)
287	14	50	-18.17	443.96	27.91
291	15	45	78.75	449.47	25.16
300	14	0	293.00	450.42	24.69
310	14	18	533.30	449.99	24.90
329	15	20	990.33	450.81	24.50
340	14	37	1253.62	451.73	24.04
341	14	45	1277.75	451.93	23.94
342	17	12	1304.20	452.16	23.82
343	15	40	1326.67	452.19	23.81
344	14	26	1349.43	452.68	23.57
345	14	22	1373.37	452.65	23.58
346	15	0	1398.00	452.88	23.47
347	14	10	1421.17	453.28	23.27
348	13	43	1444.72	453.73	23.04
349	14	15	1469.25	453.96	22.93
350	14	11	1493.18	454.29	22.76
350	23	45	1502.75	454.45	22.68
351	9	15	1512.25	454.52	22.65
352	14	0	1541.00	454.88	22.47
353	15	15	1566.25	455.24	22.29
354	13	4	1588.07	455.34	22.24
355	11	16	1610.27	455.67	22.08
356	13	20	1636.33	455.87	21.98
357	13	4	1660.07	456.16	21.83
358	9	11	1680.18	456.49	21.67
360	9	25	1728.42	456.98	21.42
361	14	25	1757.42	457.31	21.26
362	14	25	1781.42	457.57	21.13
363	12	43	1803.72	457.70	21.07
364	14	1	1829.02	458.00	20.92
365	14	24	1853.40	458.13	20.85
	2	10	1897.17	458.66	20.59
	3	11	1922.87	458.69	20.57
	4	9	1944.68	458.98	20.43
	5	16	1975.75	459.21	20.31
	6	11	1994.00	459.31	20.26
	8	14	2045.87	459.97	19.93
	10	10	2089.17	460.07	19.89
	12	13	2140.62	460.23	19.81
	14	14	2189.62	460.39	19.73
	16	15	2238.32	460.56	19.64

(continued)

*Pressure = (500 ft - Depth to Water) × 0.498 psi/ft

Table B-8 (concluded)

Day	Hr	Min	Elapsed Time (hr)	Depth to Water (ft)	Pressure (psi)
18	14	22	2285.37	459.97	19.93
20	14	36	2333.60	460.20	19.82
22	15	27	2382.45	460.92	19.46
24	15	18	2430.30	460.75	19.55
26	13	55	2476.92	460.92	19.46
28	15	12	2526.20	460.98	19.43
30	15	26	2574.43	460.95	19.45
32	13	40	2620.67	461.08	19.38
34	14	45	2669.75	461.15	19.35
36	14	17	2717.28	461.28	19.28
38	10	59	2761.98	461.25	19.30
40	13	8	2812.13	461.54	19.15
42	10	57	2857.95	461.31	19.27
44	9	27	2904.45	461.41	19.22
46	15	4	2958.07	461.31	19.27
48	15	9	3006.15	461.28	19.28
50	14	40	3053.67	461.35	19.25
52	14	0	3101.00	461.35	19.25
55	13	51	3172.85	461.28	19.28
57	16	18	3223.30	461.28	19.28
59	9	10	3264.17	461.38	19.23
62	15	55	3342.92	461.38	19.23
64	13	3	3388.05	461.06	19.39
66	10	23	3433.38	460.98	19.43
71	8	55	3551.92	460.76	19.54
73	12	34	3603.57	460.79	19.53
76	14	10	3677.17	460.52	19.66
78	9	14	3720.23	460.33	19.76
80	13	55	3772.92	460.59	19.63
83	15	55	3846.92	460.36	19.74
85	9	28	3888.47	460.30	19.77
88	12	30	3963.50	460.10	19.87
90	13	50	4012.83	459.74	20.05
92	9	39	4056.65	459.71	20.06
95	11	50	4130.83	459.51	20.16
97	14	48	4181.80	459.38	20.23
100	9	23	4248.38	459.41	20.21
102	10	50	4297.83	459.08	20.38
104	14	40	4349.67	459.05	20.39
111	14	35	4517.58	458.79	20.52

Table B-9. Pressures in the Culebra at the Waste-Handling Shaft Before, During, and After the 1985 H-3 Multipad Pumping Test

Day	Hr	Min	S	Pressure* (psig)
205	9	27	39	102.20
212	9	36	3	107.20
219	9	15	56	111.00
226	10	18	40	112.80
233	9	15	54	112.80
241	9	15	33	114.10
248	12	46	31	114.70
254	9	15	57	115.30
261	9	15	57	115.30
275	9	15	57	101.60
289	11	55	43	105.30
304	8	26	20	107.90
317	12	14	33	102.80
326	9	4	57	97.80
340	12	52	5	65.80
346	8	22	6	50.80
348	15	37	6	52.10
354	10	51	54	51.40
358	7	52	29	52.70
359	7	33	13	53.40
2	7	42	43	53.40
3	15	32	55	52.70
7	7	47	44	52.10
13	7	36	8	52.70
15	8	32	16	54.10
20	10	56	58	56.00
23	9	31	49	54.10
31	8	4	2	56.00
44	8	4	17	51.40
52	13	38	12	58.60
57	9	0	25	59.90
66	13	34	7	60.60
75	9	0	43	63.20
80	10	30	18	63.84
80	15	33	53	64.50
90	11	47	18	67.70
101	11	45	4	70.30
108	14	16	16	71.60
118	14	46	5	74.20
136	13	22	44	78.10
143	12	53	28	78.70

(continued)

*PE-208

Table B-9 (concluded)

Day	Hr	Min	S	Pressure (psig)
150	9	46	42	80.60
160	12	59	39	83.80
164	11	15	43	84.50
174	10	17	29	88.90
176	14	0	0	88.93
177	13	5	37	88.93
178	9	16	26	89.56
181	15	33	30	89.56
182	8	25	1	90.20
184	8	18	15	90.83
188	13	29	4	91.47
189	13	28	59	91.47
190	8	7	38	91.47
191	10	51	39	91.47
192	10	44	47	92.10
195	13	51	39	93.37
196	13	50	35	93.37
197	13	4	57	93.37
198	12	20	26	93.37
204	13	55	14	94.00
205	12	34	59	94.00
206	13	19	39	94.00
209	12	56	44	95.27
210	13	48	8	95.27
211	13	0	49	95.90
212	13	19	19	95.90
213	13	57	23	95.90
216	14	2	11	95.90
219	12	36	44	95.90
226	14	26	31	90.20

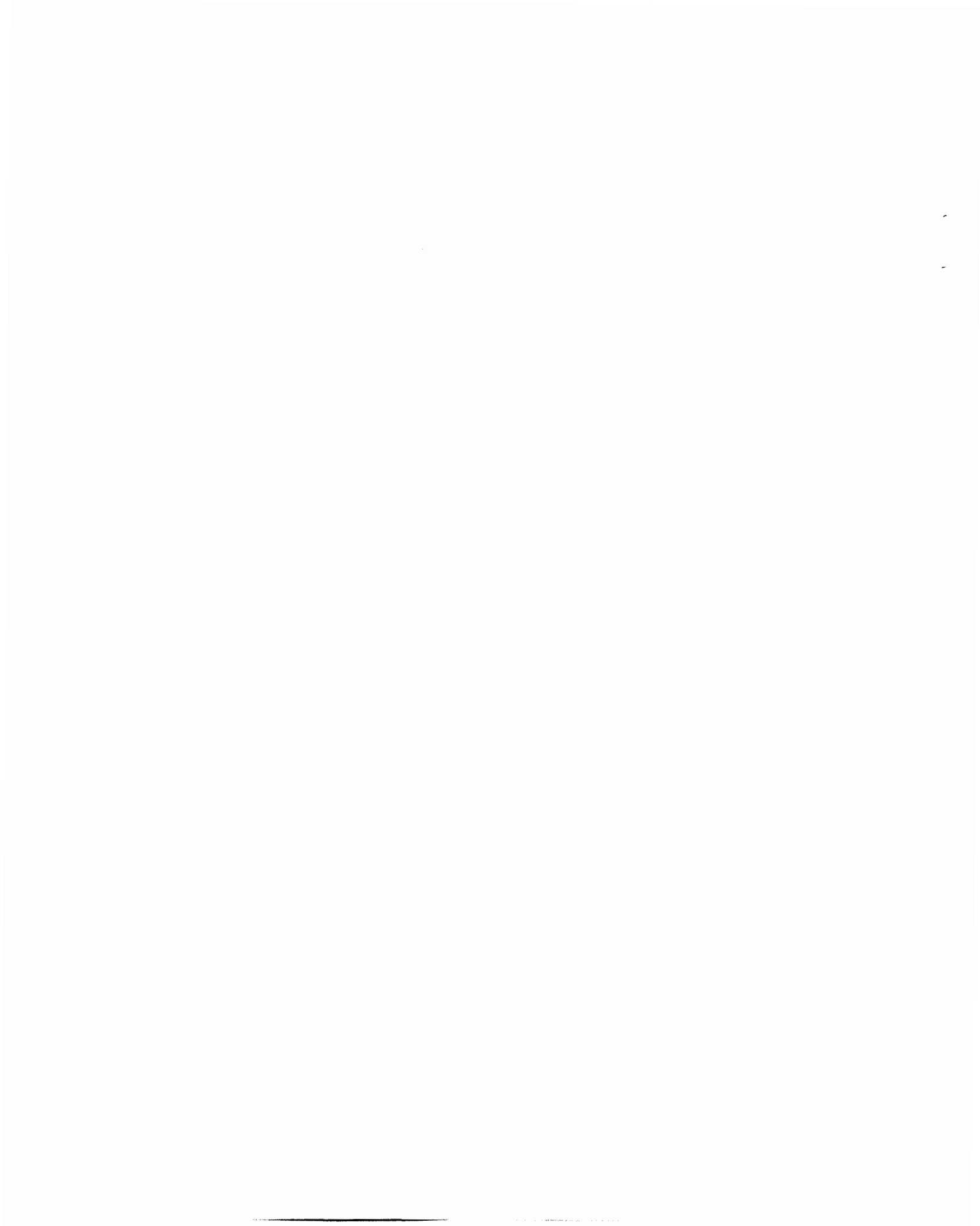
Table B-10. Pressures in the Culebra at the Construction and Salt-Handling Shaft Before, During, and After the 1985 H-3 Multipad Pumping Test

Date	Day	Hr	Min	Pressure* (psig)
06/29/85	180	12	00	104.1
10/15/85	288	16	50	114.9
12/09/85	343	17	00	108.4
03/24/86	83	17	00	104.1
06/02/86	153	19	15	108.4

*PE-207

APPENDIX C

Techniques for Analyzing Multiwell Pumping Test Data



Techniques for Analyzing Multiwell Pumping Test Data

The analysis of data from multiwell pumping tests may be divided into analysis of the pumping-well data and analysis of the observation-well data. The different techniques that may be used for these analyses are presented below. The well-test interpretation code INTERPRET is also described.

C.1 Pumping-Well Data Analysis

Pumping-well data, from both the drawdown and recovery periods, may be analyzed with either single-porosity or double-porosity interpretation techniques, and with log-log and semilog plotting techniques. These are described below. The drawdown and recovery analyses should provide nearly identical results. Consistency of results validates the conceptual model used in the analysis.

C.1.1 Single-Porosity Log-Log Analysis

Single-porosity log-log analysis of drawdown and buildup (recovery) data may be performed using a method presented by Gringarten et al. (1979) and modified to include the pressure-derivative technique of Bourdet et al. (1984). This method applies to both the drawdown and buildup during or after a constant-rate flow period of a well that fully penetrates a homogeneous, isotropic, horizontal, confined porous medium. When used to interpret a test performed in a heterogeneous, anisotropic aquifer, the method provides volumetrically averaged results.

Gringarten et al. (1979) constructed a family of log-log type curves of dimensionless pressure, p_D , versus a dimensionless time group defined as dimensionless time, t_D , divided by dimensionless wellbore storage, C_D , where

$$p_D = \frac{kh}{141.2qB\mu} \Delta p \quad (C-1)$$

$$t_D = \frac{0.000264 kt}{\phi\mu c_t r_w^2} \quad (C-2)$$

$$C_D = \frac{0.8936 C}{\phi c_t h r_w^2} \quad (C-3)$$

$$\frac{t_D}{C_D} = \frac{0.000295 kht}{\mu C} \quad (C-4)$$

and

- k = permeability, millidarcies (md)
- h = test interval thickness, ft
- Δp = change in pressure, psi
- q = flow rate, barrels/day (BPD)
- B = formation volume factor (B = 1.0 in single-phase water reservoir)
- μ = fluid viscosity, centipoises (cp)
- t = elapsed time, hr
- ϕ = porosity
- c_t = total-system compressibility, 1/psi
- r_w = wellbore radius, ft
- C = wellbore storage coefficient, barrels/psi.

Each type curve in the family of curves (Figure C-1) is characterized by a distinct value of the parameter $C_D e^{2s}$, where s = skin factor.

A positive value of s indicates wellbore damage, or a wellbore with a lower permeability than the formation as a whole as a result of drilling effects. A negative value of s indicates a wellbore with enhanced permeability, usually caused by one or more fractures intersecting the wellbore.

The type curves begin with an initial segment having a unit slope corresponding to early-time wellbore storage and skin effects. The duration of this unit slope segment is proportional to the amount of wellbore storage and skin that are present. At late time, the curves flatten as infinite-acting radial-flow effects dominate.

Bourdet et al. (1984) added the pressure derivative to the analytical procedure by constructing a family of type curves of the semilog slope of the dimensionless pressure response versus the same dimensionless time group, t_D/C_D . The semilog slope of the dimensionless pressure response is defined as

$$\frac{dp_D}{d \ln(t_D/C_D)} = \frac{t_D}{C_D} \frac{dp_D}{d(t_D/C_D)} = \frac{t_D}{C_D} p'_D \quad (C-5)$$

where p'_D = dimensionless pressure derivative.

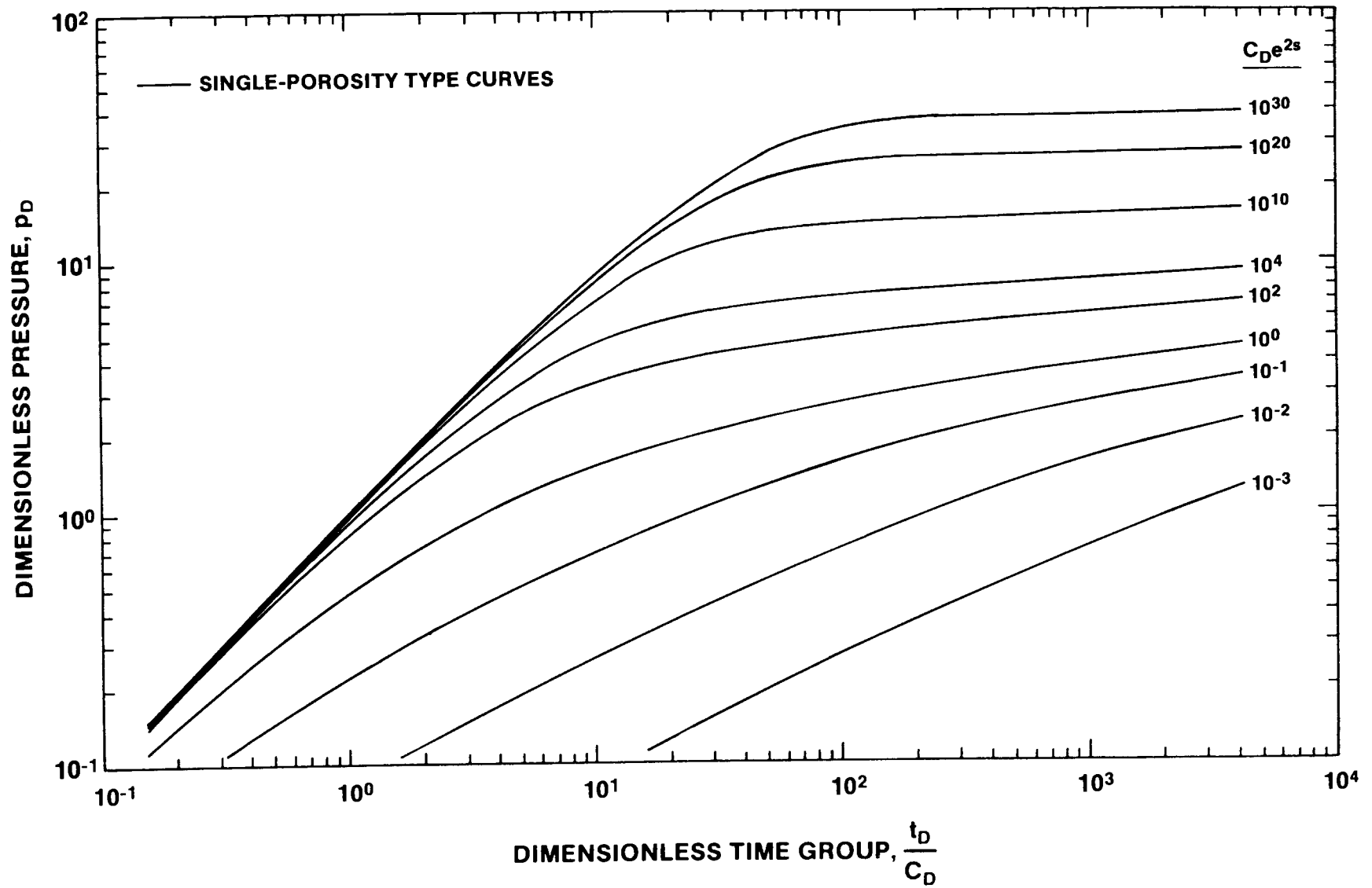


Figure C-1. Single-Porosity Type Curves for Wells With Wellbore Storage and Skin

These curves are plotted on the same log-log graphs as the type curves of Gringarten et al. (1979), with the vertical axis now also labeled $(t_D/C_D) p'_D$ (Figure C-2). Again, each individual type curve is characterized by a distinct value of C_{De}^{2s} . Pressure-derivative type curves begin with an initial segment with unit slope corresponding to early-time wellbore storage and skin effects. This segment reaches a maximum that is proportional to the amount of wellbore storage and skin, and then the curve declines and stabilizes at a dimensionless pressure/semilog slope value of 0.5 corresponding to late-time, infinite-acting, radial-flow effects.

Pressure-derivative data in combination with pressure data are much more sensitive indicators of double-porosity effects, boundary effects, nonstatic antecedent test conditions, and other phenomena than are pressure data alone. For this reason, pressure-derivative data are useful in choosing between conflicting phenomenological models that often cannot be differentiated on the basis of pressure data alone. Pressure-derivative data are also useful in determining when infinite-acting, radial-flow conditions occur during a test, because these conditions cause the pressure derivative to stabilize at a constant value.

For any given point, the pressure derivative is calculated as the linear-regression slope of a semilog line fit through that point and any chosen number of neighboring points on either side. The equation for the derivative follows:

$$p' = \frac{n \sum_{i=1}^n x_i y_i - \sum_{i=1}^n x_i \sum_{i=1}^n y_i}{n \sum_{i=1}^n x_i^2 - \sum_{i=1}^n x_i^2}, \quad (C-6)$$

where, for a single constant-rate flow period

- n = number of points to be fitted
- x_i = $\ln \Delta t_i$
- y_i = Δp_i
- Δt_i = elapsed test time at point i , hr
- Δp_i = pressure change at Δt_i , psi

For a multirate flow period or a buildup period, the time parameter is a superposition function calculated as

$$x_i = \left\{ \sum_{i=1}^{n-1} (q_i - q_{i-1}) \log \left[\left(\sum_{j=i}^{n-1} \Delta t_j \right) + \Delta t \right] \right\} + (q_n - q_{n-i}) \log \Delta t, \quad (C-7)$$

where

- q = flowrate, BPD
- Δt = elapsed time during a flow period, hr

with subscripts

- i = individual flow period
- j = individual flow period
- n = number of flow periods considered.

In general, the fewer the number of points used in calculating the derivative, the more accurate it will be. Three-point derivatives, calculated using only the nearest neighbor on either side of a point, usually provide enough resolution to distinguish most important features. However, excessive noise in the data sometimes makes it necessary to use five- or seven-point derivatives, or various "windowing" procedures, to obtain a smooth curve. Unfortunately, this may also smooth out some of the features sought.

The type curves published by both Gringarten et al. (1979) and Bourdet et al. (1984) were derived for flow-period (drawdown) analysis. In general, the curves can also be used for buildup-period analysis, so long as it is recognized that, at late time, buildup data will fall below the drawdown type curves because of superposition effects.

If the test analysis is to be done manually, the buildup data are plotted as *pressure change* since buildup began (Δp) versus *elapsed time* since buildup began (t) on log-log paper of the same scale as the type curves. The derivative of the pressure change is also plotted using the same vertical axis as the Δp data. The data plot is then laid over the type curves and moved both laterally and vertically, so long as the axes remain parallel, until a fit is achieved between the data and pressure and pressure-derivative curves with the same C_{De}^{2s} value. When the data fit the curves, an arbitrary match point is selected, and the coordinates of that point on both the data plot, t and Δp , and on the type-curve plot, p_D and t_D/C_D , are noted. The permeability-thickness product is then calculated from a rearrangement of Eq (C-1):

$$kh = 141.2qB\mu \frac{p_D}{\Delta p} \quad (C-8)$$

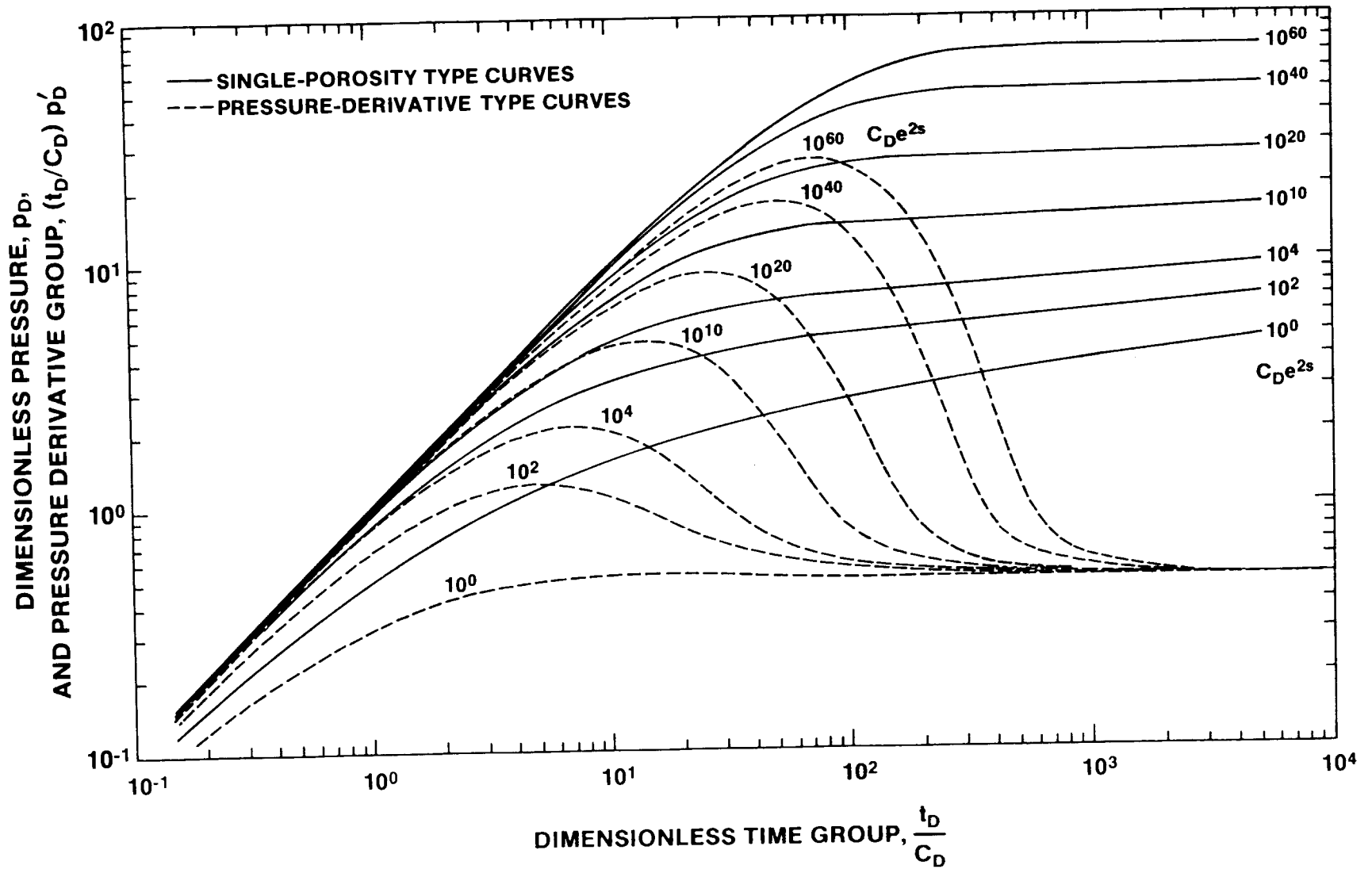


Figure C-2. Single-Porosity Type Curves and Pressure-Derivative Type Curves for Wells With Wellbore Storage and Skin

The groundwater-hydrology parameter transmissivity, T , is related to the permeability-thickness product by the following relationship, modified from Freeze and Cherry (1979):

$$T = kh\rho g/\mu \quad , \quad (C-9)$$

where

$$\begin{aligned} \rho &= \text{fluid density, M/L}^3 \\ g &= \text{gravitational acceleration, L/T}^2 \\ \mu &= \text{fluid viscosity, M/LT.} \end{aligned}$$

When T is given in ft^2/day , kh is given in millidarcy-feet, ρ is given in g/cm^3 , g is set equal to $980.665 \text{ cm}/\text{s}^2$, and μ is given in centipoises, Eq (C-9) becomes

$$T = 2.7435 \times 10^{-3} kh\rho/\mu \quad . \quad (C-10)$$

The wellbore storage coefficient is calculated from a rearrangement of Eq (C-4):

$$C = \frac{0.000295 kht}{\mu t_D/C_D} \quad . \quad (C-11)$$

Finally, if estimates of porosity and total-system compressibility are available, the skin factor can be calculated from the value of the $C_D e^{2s}$ curve selected and Eq (C-3):

$$s = 0.5 \ln \left[\frac{C_D e^{2s}}{0.8936C/\phi c_t \text{hr}_w^2} \right] \quad . \quad (C-12)$$

C.1.2 Double-Porosity Log-Log Analysis

Double-porosity media have two porosity sets that differ in terms of storage volume and permeability. Typically, the two porosity sets are (1) a fracture network with higher permeability and lower storage, and (2) the primary porosity of the rock matrix with lower permeability and higher storage. During a hydraulic test, these two porosity sets respond differently. With high-quality test data, the hydraulic parameters of both porosity sets can be quantified.

During a hydraulic test in a double-porosity medium, the fracture system responds first. Initially, most of the water pumped comes from the fractures, and the pressure in the fractures drops accordingly. With time, the matrix begins to supply water to the fractures, causing the fracture pressure to stabilize and the matrix pressure to drop. As the pressures in the fractures and matrix equalize, both systems produce water to the well. The total-system response is then observed for the balance of the test.

The initial fracture response and the final total-system response both follow the single-porosity type curves described above. By simultaneously fitting the fracture response and the total-system response to two different $C_D e^{2s}$ curves, we can derive fracture-system and total-system properties. Information on the matrix, and additional information on the fracture system, can be obtained by interpretation of the data from the transition period when the matrix begins to produce to the fractures. Two different sets of type curves can be used to try to fit the transition-period data.

Transition-period data are affected by the nature, or degree, of interconnection between the matrix and the fractures. Warren and Root (1963) published the first line-source solution for well tests in double-porosity systems. They assumed that flow from the matrix to the fractures (interporosity flow) occurred under *pseudosteady-state* conditions; that is, that the flow between the matrix and the fractures was directly proportional to the average head difference between those two systems. Other authors, such as Kazemi (1969) and de Swaan (1976), derived solutions using the diffusivity equation to govern interporosity flow. These are known as *transient* interporosity flow solutions. Mavor and Cinco-Ley (1979) added wellbore storage and skin to the double-porosity solution, but still used pseudosteady-state interporosity flow. Bourdet and Gringarten (1980) modified Mavor and Cinco-Ley's (1979) theory to include transient interporosity flow, and generated type curves for double-porosity systems with both pseudosteady-state and transient interporosity flow.

Pseudosteady-state and transient interporosity flow represent two extremes; all intermediate behaviors are also possible. Gringarten (1984), however, indicates that the majority of tests he has seen exhibit pseudosteady-state interporosity flow behavior.

In recent years, Gringarten (1984, 1986) has suggested that the terms "restricted" and "unrestricted" interporosity flow replace the terms "pseudosteady-state" and "transient" interporosity flow. He believes that all interporosity flow is transient in the sense that it is governed by the diffusivity equation. But in the case where the fractures possess a positive skin similar to a wellbore skin (caused, for example, by secondary mineralization on the fracture surfaces) that restricts the flow from the matrix to the fractures, the observed behavior is similar to that described by the pseudosteady-state formulation (Moench, 1984; Cinco-Ley et al., 1985). "Transient" interporosity flow is observed when there are no such restrictions. Hence, the terms "restricted" and "unrestricted" more accurately

describe conditions than do the terms "pseudosteady-state" and "transient." The recent terminology of Gringarten is followed in this report.

Restricted Interporosity Flow. Warren and Root (1963) defined two parameters to aid in characterizing double-porosity behavior. These are the storativity ratio, ω , and the interporosity flow coefficient, λ . The storativity ratio is defined as

$$\omega = \frac{(\phi V c_t)_f}{(\phi V c_t)_{f+m}} \quad (\text{C-13})$$

where

- ϕ = ratio of the pore volume in the system to the total-system volume
- V = the ratio of the total volume of one system to the bulk volume
- c_t = total compressibility of the system,

with subscripts

- f = fracture system
- m = matrix.

The interporosity flow coefficient is defined as

$$\lambda = \alpha r_w^2 \frac{k_m}{k_f} \quad (\text{C-14})$$

where α is a shape factor characteristic of the geometry of the system and other terms are as defined above.

The shape factor, α , is defined as

$$\alpha = \frac{4n(n+2)}{\ell^2} \quad (\text{C-15})$$

where

- n = number of normal sets of planes limiting the matrix
- ℓ = characteristic dimension of a matrix block (ft).

Bourdet and Gringarten (1980) constructed a family of transition type curves for restricted interporosity flow on the same axes as the $C_D e^{2s}$ curves of Gringarten et al. (1979), with each transition curve characterized by a distinct value of the parameter λe^{-2s} . Together, the single-porosity type curves and the transition type curves make up the double-porosity type curves.

In manual double-porosity type-curve matching, a log-log plot of the data is prepared as in single-porosity type-curve matching. The data plot is then laid over the double-porosity type curves and moved both laterally and vertically, so long as the axes remain parallel, until (1) the early-time (fracture flow only) data fall on one $C_D e^{2s}$ curve, (2) the middle portion of the transition data falls on a λe^{-2s} curve, and (3) the late-time (total-system) data fall on a lower $C_D e^{2s}$ curve (Figure C-3). In computer-aided analysis, pressure-derivative curves for double-porosity systems may also be prepared (Gringarten, 1986). The number of possible curve combinations, however, precludes preparation of generic pressure-derivative curves for manual double-porosity curve fitting.

When a fit of the data plot to the type curves is achieved, an arbitrary match point is selected, and the coordinates of that point on both the data plot, t and Δp , and the type-curve plot, t_D/C_D and p_D , are noted. The values of $C_D e^{2s}$ and λe^{-2s} of the matched curves are also noted. The permeability-thickness product of the fracture system (and also of the total system because fracture permeability dominates) and the wellbore storage coefficient are calculated from Eqs (C-8) and (C-11). The storativity ratio, ω , is calculated from

$$\omega = \frac{(C_D e^{2s})_{f+m}}{(C_D e^{2s})_f} \quad (\text{C-16})$$

The dimensionless wellbore storage coefficient for the matrix is calculated as

$$(C_D)_m = \frac{0.8936 C}{(V \phi c_t)_m h r_w^2} \quad (\text{C-17})$$

This leads to the dimensionless wellbore storage coefficient for the total system:

$$(C_D)_{f+m} = (C_D)_m \times (1-\omega) \quad (\text{C-18})$$

Then the skin factor is calculated as

$$s = 0.5 \ln \left[\frac{(C_D e^{2s})_{f+m}}{(C_D)_{f+m}} \right] \quad (\text{C-19})$$

The interporosity flow coefficient is calculated from

$$\lambda = \frac{\lambda e^{-2s}}{e^{-2s}} \quad (\text{C-20})$$

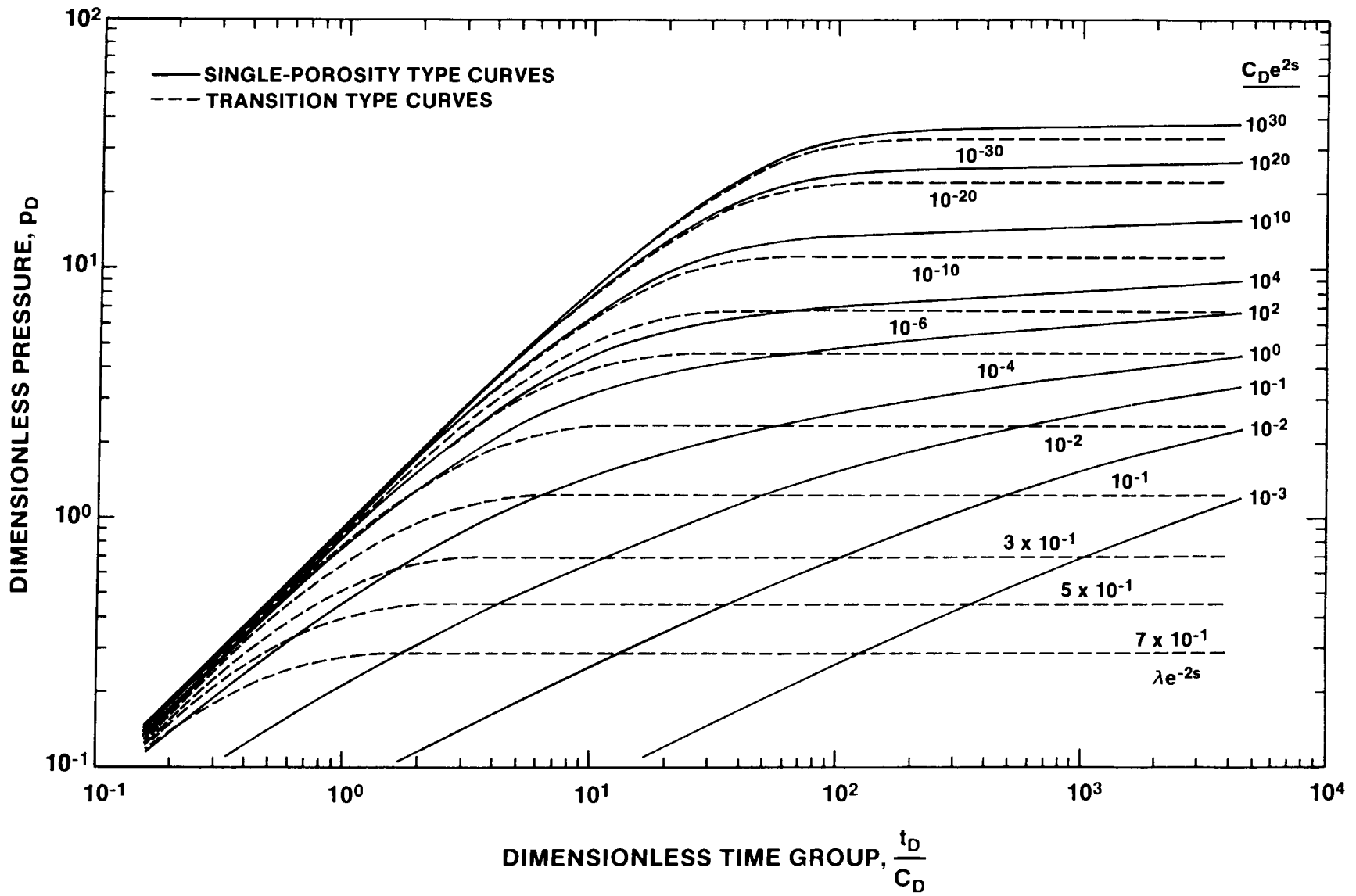


Figure C-3. Double-Porosity Type Curves for Wells With Wellbore Storage, Skin, and Restricted Interporosity Flow

If matrix permeability and geometry are known independently, Eqs (C-14) and (C-15) can be used to determine the effective dimensions of the matrix blocks.

Unrestricted Interporosity Flow. Matrix geometry is more important for unrestricted interporosity flow than for restricted interporosity flow, because the former is governed by the diffusivity equation. A different set of type curves is used, therefore, to match transition-period data when unrestricted interporosity flow conditions exist (Figure C-4). Bourdet and Gringarten (1980) characterize each curve with a different value of the parameter β , the exact definition of which is a function of the matrix geometry. For example, for slab-shaped matrix blocks, they give

$$\beta = \frac{6}{\gamma^2} \frac{(C_D e^{2s})_{f+m}}{\lambda e^{-2s}}, \quad (\text{C-21})$$

and for spherical blocks they give

$$\beta = \frac{10}{3\gamma^2} \frac{(C_D e^{2s})_{f+m}}{\lambda e^{-2s}}, \quad (\text{C-22})$$

where $\gamma =$ exponential of Euler's constant ($=1.781$).

Moench (1984) provides an extensive discussion on the effects of matrix geometry on unrestricted interporosity flow.

Manual double-porosity type-curve matching with unrestricted-interporosity-flow transition curves is performed in exactly the same manner as with restricted-interporosity-flow transition curves, described above. The same equations are used to derive the fracture and matrix parameters, except that the matrix geometry must now be known or assumed to obtain the interporosity flow coefficient, λ , from rearrangement of Eq (C-21) or (C-22).

C.1.3 Semilog Analysis

Horner (1951) provided a method of checking the permeability value obtained from log-log type-curve matching. Horner's method applies to the buildup (recovery) of the pressure after a constant-rate flow period in a well that fully penetrates a homogeneous, isotropic, horizontal, infinite, confined reservoir. For a recovery after a single flow period, Horner's solution is

$$p(t) = p^* - \frac{162.6qB\mu}{kh} \log \left[\frac{t_p + dt}{dt} \right], \quad (\text{C-23})$$

where

$p(t)$ = pressure at time t , psi
 p^* = static formation pressure, psi
 t_p = duration of previous flow period, hr
 dt = time elapsed since end of flow period, hr,

and other terms are as defined above under Eq (C-4). For a recovery after multiple flow periods, the time group in Eq (C-23) is replaced by the superposition function given in the right-hand side of Eq (C-7).

The permeability-thickness product (kh) is obtained by (1) plotting $p(t)$ versus $\log [(t_p + dt)/dt]$ (or the superposition function), (2) drawing a straight line through the data determined from the log-log pressure-derivative plot to be representative of infinite-acting radial flow, and (3) measuring the change in $p(t)$ on this line over one log cycle of time (m). Equation (C-23) can then be rearranged and reduced to

$$kh = 162.6qB\mu/m. \quad (\text{C-24})$$

Static formation pressure is estimated by extrapolating the radial-flow straight line to the pressure axis where $\log [(t_p + dt)/dt] = 1$, representing infinite recovery time. In the absence of reservoir boundaries, the pressure intercept at that time should equal the static formation pressure.

Horner (1951) also suggested a modification of his method for the case where the flow rate was not held constant. This modification was later theoretically verified for the case of constant-pressure, variable-rate production by Ehlig-Economides (1979). The modification entails calculating a modified production time

$$t_p^* = V/q_f, \quad (\text{C-25})$$

where

V = total flow produced, bbl
 q_f = final flow rate, bbl/hr.

The modified production time, t_p^* , is substituted for the actual production time, t_p , in Eq (C-23), and the analysis proceeds as before. The modified production time can also be used for calculation of buildup type curves for log-log analysis.

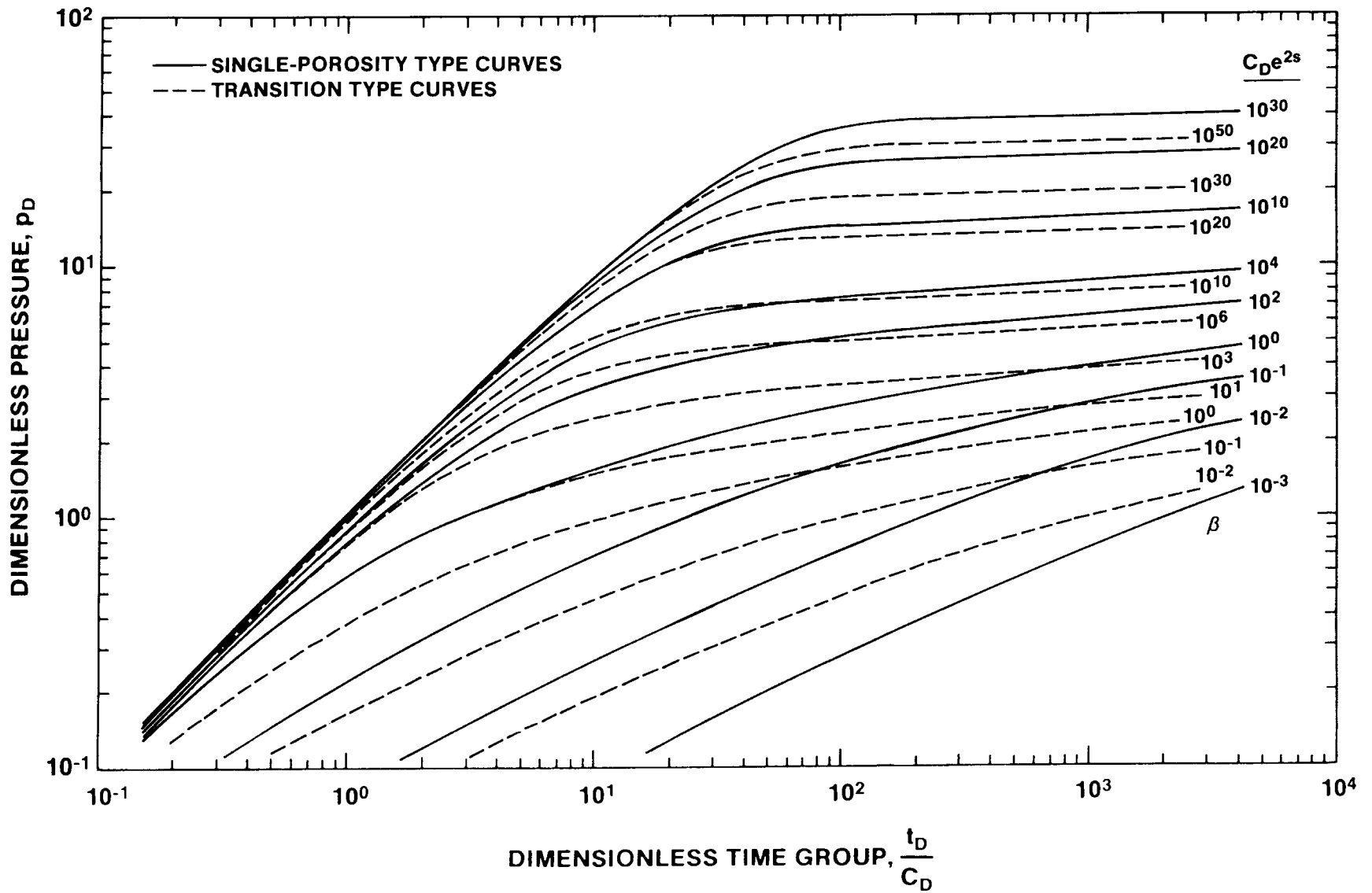


Figure C-4. Double-Porosity Type Curves for Wells With Wellbore Storage, Skin, and Unrestricted Interporosity Flow

C.2 Observation-Well Data Analysis

For observation wells monitored during pumping tests, the drawdown and recovery data can be analyzed using a method first described by Theis (1935) for single-porosity systems. Use of a single-porosity interpretation technique for an observation well in a double-porosity aquifer is justified when the observation well is far enough from the pumping well that only total-system responses are observed. Deruyck et al. (1982) provide the following criterion for being able to measure double-porosity responses at an observation well:

$$\ln \left[\frac{2}{\gamma(\lambda r_D^2)^{0.5}} \right] > \text{gauge resolution} + \text{noise} , \quad (\text{C-26})$$

where

$$r_D = r/r_w , \quad (\text{C-27})$$

r = radial distance to pumping well, ft,

and other terms are as defined above. Generally, this criterion limits observable double-porosity responses to a maximum distance of tens to perhaps hundreds of feet from the pumping well.

Theis (1935) created a log-log drawdown type curve of p_D versus r_D^2 using an exponential integral (Ei) solution for drawdown caused by a line-source well in a porous medium:

$$p_D = -0.5 \text{Ei}(-r_D^2/4t_D) , \quad (\text{C-28})$$

where

$$\frac{t_D}{r_D^2} = \frac{0.000264 \text{ kht}}{\phi \mu c_t \text{ hr}^2} . \quad (\text{C-29})$$

The terms p_D and t_D are defined by Eqs (C-1) and (C-2), respectively; other terms are as defined above in Section C.1.1. This type curve applies to the analysis of drawdown at both pumping wells (assuming no wellbore storage) and observation wells.

Elapsed pumping time (t) and drawdown (Δp) are plotted on log-log paper of the same scale as the type curve. The observed data are matched to the line-source type curve, thus defining a match point. The two sets of coordinates of that point, t and Δp , and t_D/r_D^2 and p_D , are used with Eqs (C-8) and (C-29) to calculate the permeability-thickness product and the porosity-compressibility-thickness product, respectively.

The permeability-thickness product is related to transmissivity through Eqs (C-9) and (C-10). Narasimhan and Kinehiro (1980) give the relationship between the porosity-compressibility-thickness product and the groundwater-hydrology parameter storativity, S , in consistent units as

$$S = \phi c_t h \rho g . \quad (\text{C-30})$$

When total compressibility, c_t is in units of 1/psi; thickness, h , is in units of ft; fluid density, ρ , is in units of g/cm^3 ; and gravitational acceleration, g , is set equal to 980.665 cm/s^2 , Eq (C-30) becomes

$$S = 0.4335 \phi c_t h \rho . \quad (\text{C-31})$$

C.3 INTERPRET Well-Test Interpretation Code

Manual type-curve fitting is a time-consuming process limited by the published type curves available, and by the degree of resolution/differentiation obtainable in manual curve fitting. The analyses presented in this report were not performed manually but by using the well-test analysis code INTERPRET developed by A. C. Gringarten and Scientific Software-Intercomp (SSI). INTERPRET is a proprietary code that uses analytical solutions. It can be leased from SSI.

INTERPRET can analyze drawdown (flow) and recovery (buildup) tests in single-porosity, double-porosity, and fractured media. It incorporates the analytical techniques discussed above, and additional techniques discussed in Gringarten et al. (1974), Bourdet and Gringarten (1980), and Gringarten (1984). Rather than relying on a finite number of drawdown type curves, INTERPRET calculates the precise drawdown or buildup type curve corresponding to the match point and data point selected by the user.

After type-curve selection, INTERPRET simulates the test with the chosen parameters so that the user can see how good the match truly is. Through an iterative parameter-adjustment process, the user fine-tunes the simulation until satisfied with the results. Both log-log and semilog (Horner and dimensionless Horner) plotting techniques are employed to ensure consistency of the final model with the data in every respect. Once the final model is selected, INTERPRET carries out all necessary calculations and provides final parameter values. Analyses obtained using INTERPRET have been verified by manual checks.

In addition to standard type-curve analysis, INTERPRET allows the incorporation of constant-pressure and no-flow boundaries in analysis, using the theory of superposition and image wells discussed by Lohman (1979) and others. A constant-pressure boundary can be simulated by adding a recharge (image) well to the model. A no-flow boundary can be simulated by adding a discharge (image) well to the model. Drawdowns/rises from multiple discharge/recharge wells are additive. In INTERPRET, an image well (either discharge or recharge) is included by specifying a dimensionless distance for the image well from the production well, and by using the line-source solution of Theis (1935; see Section C.2) to calculate the drawdown or recovery caused by that well at the production well. The dimensionless distance is related to the actual distance, d , by the following:

$$d = \frac{(C_D D_D)^{0.5} r_w}{2}, \quad (\text{C-32})$$

where D_D = dimensionless distance, and other terms are as defined above.

For observation-well data analysis, the INTERPRET code uses the solution of Theis (1935) and the principle of superposition to calculate a combined drawdown-recovery response with the parameters derived from the log-log drawdown match. The calculated solution is displayed in a linear-linear plot along with the observed data. Through an iterative match-point-adjustment procedure, the user fine-tunes the simulation until an acceptable fit of the simulation to both the drawdown and recovery data is obtained.

References

- Beauheim, R. L. 1986. *Hydraulic-Test Interpretations for Well DOE-2 at the Waste Isolation Pilot Plant (WIPP) Site*, SAND86-1364 (Albuquerque, NM: Sandia National Laboratories).
- Beauheim, R. L. In preparation. *Interpretations of Single-Well Hydraulic Tests Conducted At and Near the Waste Isolation Pilot Plant (WIPP) Site, 1983-1987*, SAND87-0039 (Albuquerque, NM: Sandia National Laboratories).
- Bourdet, D., and Gringarten, A. C. 1980. *Determination of Fissure Volume and Block Size in Fractured Reservoirs by Type-Curve Analysis*, SPE 9293 (Richardson, TX: Soc Pet Eng).
- Bourdet, D.; Ayoub, J. A.; and Pirard, Y. M. 1984. *Use of Pressure Derivative in Well Test Interpretation*, SPE 12777 (Richardson, TX: Soc Pet Eng).
- Cinco-Ley, H.; Samaniego-V., F.; and Kucuk, F. 1985. *The Pressure Transient Behavior for Naturally Fractured Reservoirs With Multiple Block Size*, SPE 14168 (Richardson, TX: Soc Pet Eng).
- Deruyck, B. G.; Bourdet, D. P.; DaPrat, G.; and Ramey, H. J., Jr. 1982. *Interpretation of Interference Tests in Reservoirs with Double Porosity Behavior—Theory and Field Examples*, SPE 11025 (Richardson, TX: Soc Pet Eng).
- de Swaan, A. O. 1976. "Analytical Solutions for Determining Naturally Fractured Reservoir Properties by Well Testing," *Soc Pet Eng J* (June 1976):117-22.
- Earlougher, R. C., Jr. 1977. "Advances in Well Test Analysis," *Monograph Volume 5* (Dallas, TX: Soc Pet Eng of AIME).
- Ehlig-Economides, C. A. 1979. *Well Test Analysis for Wells Produced at a Constant Pressure*, PhD Dissertation (Palo Alto, CA: Stanford Univ Dept of Pet Eng).
- Fischer, N. T., ed., 1985. *Ecological Monitoring Program Semiannual Report, January-June, 1985*, DOE/WIPP-85-002 (Carlsbad, NM: Waste Isolation Pilot Plant).
- Freeze, R. A., and Cherry, J. A. 1979. *Groundwater* (Englewood Cliffs, NJ: Prentice-Hall, Inc.).
- Gringarten, A. C. 1984. "Interpretation of Tests in Fissured and Multilayered Reservoirs with Double-Porosity Behavior: Theory and Practice," *J Pet Tech* 36(4):549-64.
- Gringarten, A. C. 1986. *Computer-Aided Well Test Analysis*, SPE 14099 (Richardson, TX: Soc Pet Eng).
- Gringarten, A. C.; Ramey, H. J., Jr.; and Raghavan, R. 1974. "Unsteady-State Pressure Distributions Created by a Well with a Single Infinite-Conductivity Vertical Fracture," *Soc Pet Eng J* 14(4):347-60.
- Gringarten, A. C.; Bourdet, D. P.; Landel, P. A.; and Kniazeff, V. J. 1979. *A Comparison Between Different Skin and Wellbore Storage Type-Curves for Early-Time Transient Analysis*, SPE 8205 (Richardson, TX: Soc Pet Eng).
- Haug, A.; Kelley, V. A.; LaVenue, A. M.; and Pickens, J. F. In preparation. *Modeling of Ground-Water Flow in the Culebra Dolomite at the Waste Isolation Pilot Plant (WIPP) Site: Interim Report*, SAND86-7167 (Albuquerque, NM: Sandia National Laboratories).
- Horner, D. R. 1951. "Pressure Buildup in Wells," *Proc Third World Pet Cong* 2:503-23 (The Hague, Netherlands). Reprinted 1967. *Pressure Analysis Methods*, AIME Reprint Series 9:45-50 (Richardson, TX: Soc Pet Eng).
- HydroGeoChem, Inc. 1985. *WIPP Hydrology Program, Waste Isolation Pilot Plant, SENM, Hydrologic Data Report #1*, SAND85-7206 (Albuquerque, NM: Sandia National Laboratories).
- INTERA Technologies, Inc. 1986. *WIPP Hydrology Program, Waste Isolation Pilot Plant, SENM, Hydrologic Data Report #3*, SAND86-7109 (Albuquerque, NM: Sandia National Laboratories).
- INTERA Technologies, Inc., and HydroGeoChem, Inc. 1985. *WIPP Hydrology Program, Waste Isolation Pilot Plant, SENM, Hydrologic Data Report #2*, SAND85-7263 (Albuquerque, NM: Sandia National Laboratories).
- Jenkins, D. N., and Prentice, J. K. 1982. "Theory for Aquifer Test Analysis in Fractured Rocks Under Linear (Non-radial) Flow Conditions," *Ground Water* 20(1):12-21.
- Kazemi, H. 1969. "Pressure Transient Analysis of Naturally Fractured Reservoirs with Uniform Fracture Distribution," *Soc Pet Eng J* (Dec 1969):451-62.
- Kelley, V. A., and Pickens, J. F. 1986. *Interpretation of the Convergent-Flow Tracer Tests Conducted in the Culebra Dolomite at the H-3 and H-4 Hydropads, Waste Isolation Pilot Plant (WIPP)*, SAND86-7161 (Albuquerque, NM: Sandia National Laboratories).
- Lohman, S. W. 1979. *Ground-Water Hydraulics*. USGS Prof Paper 708 (Washington, DC: US GPO).
- Mavor, M. J., and Cinco-Ley, H. 1979. *Transient Pressure Behavior of Naturally Fractured Reservoirs*, SPE 7977 (Richardson, TX: Soc Pet Eng).
- Mercer, J. W. 1983. *Geohydrology of the Proposed Waste Isolation Pilot Plant Site, Los Medanos Area, Southeastern New Mexico*. USGS Water-Resources Investigations Rpt 83-4016 (Albuquerque, NM).
- Mercer, J. W., and Orr, B. R. 1979. *Interim Data Report on the Geohydrology of the Proposed Waste Isolation Pilot Plant Site, Southeast New Mexico*. USGS Water-Resources Investigations Rpt 79-98 (Albuquerque, NM).

- Moench, A. F. 1984. "Double-Porosity Models for a Fissured Groundwater Reservoir with Fracture Skin," *Water Resources Research* 20(7):831-46.
- Narasimhan, T. N., and Kanehiro, B. Y. 1980. "A Note on the Meaning of Storage Coefficient," *Water Resources Research* 16(2):423-29.
- Robinson, K. L. In preparation. *Analysis of Solutes in Groundwaters From the Rustler Formation At and Near the WIPP Site*, SAND86-0917 (Albuquerque, NM: Sandia National Laboratories).
- Saulnier, G. J., Jr.; Freeze, G. A.; and Stensrud, W. A. 1987. *WIPP Hydrology Program, Waste Isolation Pilot Plant, SENM, Hydrologic Data Report #4*, SAND86-7166 (Albuquerque, NM: Sandia National Laboratories).
- Theis, C. V. 1935. "The Relation Between the Lowering of the Piezometric Surface and the Rate and Duration of Discharge of a Well Using Ground-water Storage," *Trans AGU* 2:519-24.
- Warren, J. E., and Root, P.J. 1963. "The Behavior of Naturally Fractured Reservoirs," *Soc Pet Eng J* (Sept 1963):245-55.

DISTRIBUTION:

US Department of Energy (5)
Office of Civilian Radioactive Waste Management
Office of Geologic Repositories
Attn: Associate Director
 W. J. Purcell, RW-20
 Director, Repository Coordination Div.
 T. H. Isaacs, RW-22
 Director, Engineering & Licensing
 R. Stein, RW-23
 Director, Geosciences & Technology
 R. Stein, Actg., RW-24
 Director, Siting Division
 E. Burton, RW-25
Forrestal Building
Washington, DC 20585

US Department of Energy (3)
Albuquerque Operations
Attn: R. G. Romatowski
 D. L. Krenz
 D. G. Jackson, Director, Public Affairs Division
PO Box 5400
Albuquerque, NM 87185

US Department of Energy (6)
Attn: J. Tillman,
 WIPP Project Office (Carlsbad) (2)
 G. Pappas, WPO (Carlsbad)
 A. Hunt, WPO (Carlsbad)
 R. Eastmond, WPO (Carlsbad) (2)
PO Box 3090
Carlsbad, NM 88221

US Department of Energy, SRPO (4)
Office of Nuclear Waste Isolation
Attn: J. O. Neff
 R. Wunderlich
 G. Appel
 J. Sherwin
505 King Avenue
Columbus, OH 43201

US Department of Energy (2)
Idaho Operations Office
Nuclear Fuel Cycle Division
Attn: R. M. Nelson
 J. Whitsett
550 Second Street
Idaho Falls, ID 83401

US Department of Energy (2)
Savannah River Operations Office
Waste Management Project Office
Attn: S. Cowan
 W. J. Brumley
PO Box A
Aiken, SC 29801

US Department of Energy (3)
Office of Defense Waste and
 Transportation Management
Attn: J. E. Dieckhoner, DP-122
 L. H. Harmon, DP-121
 A. Follett, DP-121
Washington, DC 20545

US Department of Energy
Research & Technical Support Division
Attn: D. E. Large
PO Box E
Oak Ridge, TN 37830

US Department of the Interior
Attn: E. Roedder
959 National Center
Geological Survey
Reston, VA 22092

US Nuclear Regulatory Commission (2)
Division of Waste Management
Attn: M. Bell
 H. Miller
Mail Stop 623SS
Washington, DC 20555

US Geological Survey
Special Projects
Attn: R. Snyder
MS954, Box 25046
Denver Federal Center
Denver, CO 80255

US Geological Survey
Conservation Division
Attn: W. Melton
PO Box 1857
Roswell, NM 88201

DISTRIBUTION (Continued):

US Geological Survey (2)
Water Resources Division
Attn: H. L. Case
P. Davies
Western Bank Bldg.
505 Marquette NW, #720
Albuquerque, NM 87102

State of New Mexico (3)
Environmental Evaluation Group
Attn: R. H. Neill, Director
320 Marcy Street
PO Box 968
Santa Fe, NM 87503

NM Department of Energy & Minerals
Attn: K. LaPlante, Librarian
PO Box 2770
Santa Fe, NM 87501

New Mexico Bureau of Mines and Mineral
Resources (2)
Attn: F. E. Kottolowski, Director
J. Hawley
Socorro, NM 87801

Battelle Pacific Northwest Laboratories
Attn: D. J. Bradley
Battelle Boulevard
Richland, WA 99352

Battelle Memorial Institute (13)
Project Management Division
Attn: W. Carbiener, General Manager (3)
J. Treadwell
T. Naymik
J. Kirchner
V. Adams
O. Swanson
A. Razem
S. Gupta
W. Newcomb
A. LaSala
ONWI Library
505 King Avenue
Columbus, OH 43201

Bechtel Inc. (2)
Attn: E. Weber
M. Bethard
PO Box 3965
45-11-B34
San Francisco, CA 94119

IT Corporation (2)
Attn: W. E. Coons
J. E. Zurkoff
2340 Alamo, SE
Suite 306
Albuquerque, NM 87106

IT Corporation (4)
Attn: W. Patrick
R. McKinney
D. Deal
D. Winstanley
PO Box 2078
Carlsbad, NM 88221

INTERA Technologies, Inc. (7)
Attn: G. E. Grisak
J. F. Pickens
G. J. Saulnier
V. A. Kelley
G. E. Freeze
A. Haug
INTERA Library
6850 Austin Center Blvd., #300
Austin, TX 78731

INTERA Technologies, Inc.
Attn: W. Stensrud
PO Box 2123
Carlsbad, NM 88221

Martin Marietta Energy Systems, Inc.
Oak Ridge National Laboratory
Attn: J. A. Carter
Box Y
Oak Ridge, TN 37830

Martin Marietta Energy Systems, Inc.
Oak Ridge National Laboratory
Environmental Science
Attn: E. Bondietti
X10 Area, Bldg. 1505, Rm. 322
Oak Ridge, TN 37831

RE/SPEC Inc.
Attn: P. Gnirk
PO 725
Rapid City, SD 57701

RE/SPEC Inc.
Attn: S. W. Key
PO Box 14984
Albuquerque, NM 87191

DISTRIBUTION (Continued):

Rockwell International
Atomics International Division
Rockwell Hanford Operations
Attn: W. W. Schultz
PO Box 800
Richland, WA 99352

Serata Geomechanics
Attn: S. Serata
4124 Lakeside Drive
Richmond, CA 94806-1941

G. O. Bachman
Star Route Box 1028
Corrales, NM 87048

Leonard Minerals Co.
Attn: B. Donegan
3202 Candelaria NE
Albuquerque, NM 87107

Peters Technology Transfer
Attn: L. Lantz
PO Box 216
Swarthmore, PA 19081

Stanford University
Department of Geology
Attn: K. B. Krauskopf
Stanford, CA 94305

Vanderbilt University
Department of Environmental and
Water Resources Engineering
Attn: F. L. Parker
Nashville, TN 37235

Oak Ridge National Laboratory
Attn: J. O. Blomeke
PO Box X
Oak Ridge, TN 37830

US Geological Survey
Water Resources Division
Attn: J. D. Bredehoeft
Western Region Hydrologist
345 Middlefield Road
Menlo Park, CA 94025

K. P. Cohen
928 N. California Avenue
Palo Alto, CA 94303

F. M. Ernsberger
1325 NW 10th Avenue
Gainesville, FL 32601

Johns Hopkins University
Department of Earth Sciences
Attn: H. P. Eugster
Baltimore, MD 21218

University of New Mexico
Department of Geology
Attn: R. C. Ewing
Albuquerque, NM 87131

University of Minnesota
Department of Geological Sciences
Attn: C. Fairhurst
Minneapolis, MN 55455

University of Texas at Austin
Department of Geological Sciences
Attn: W. R. Muehlberger
Austin, TX 78712

D. A. Shock
233 Virginia
Ponca City, OK 74601

National Academy of Sciences
Committee on Radioactive Waste Management
Attn: P. Meyers
2101 Constitution Avenue, NW
Washington, DC 20418

New Mexico Junior College
Pannell Library
Attn: R. Hill
Lovington Highway
Hobbs, NM 88240

New Mexico Tech
Martin Speere Memorial Library
Campus Street
Socorro, NM 87810

DISTRIBUTION (Continued):

New Mexico Tech (3)
Department of Geoscience
Attn: J. Wilson
D. Stephens
C. S. Chen
Socorro, NM 87801

New Mexico State Library
Attn: I. Vollenhofer
PO Box 1629
Santa Fe, NM 87503

US Geological Survey (2)
Water Resources Division
Attn: P. Hsieh
A. F. Moench
345 Middlefield Rd.
Menlo Park, CA 94025

University of New Mexico
Zimmerman Library
Attn: Z. Vivian
Albuquerque, NM 87131

Atomic Museum
WIPP Public Reading Room
Attn: G. Schreiner
Kirtland East AFB
Albuquerque, NM 87185

Carlsbad Municipal Library
WIPP Public Reading Room
Attn: L. Hubbard, Head Librarian
101 S. Hallagueno St.
Carlsbad, NM 88220

Thomas Brannigan Library
Attn: D. Dresp, Head Librarian
106 W. Hadley St.
Las Cruces, NM, 88001

Roswell Public Library
Attn: N. Langston
301 N. Pennsylvania Avenue
Roswell, NM 88201

University of Minnesota
Dept. of Energy and Materials Science
Attn: R. Oriani
151 Amundson Hall
421 Washington Ave SE
Minneapolis, MN 55455

Texas A&M University
Center of Tectonophysics
Attn: J. Handin
College Station, TX 77840

Texas A&M University
Department of Geology
Attn: P. A. Domenico
College Station, TX 77843

University of British Columbia
Department of Geological Sciences
Attn: R. A. Freeze
Vancouver, British Columbia V6T 1W5
CANADA

University of Arizona (2)
Department of Nuclear Engineering
Attn: J. G. McCray
J. J. K. Daemen
Tucson, AZ 85721

University of Arizona
Department of Hydrology
Attn: S. P. Neuman
Tucson, AZ 85721

University of New Mexico (2)
Geology Department
Attn: D. G. Brookins
Library
Albuquerque, NM 87131

University of Texas at El Paso
Department of Geological Sciences
Attn: D. W. Powers
El Paso, TX 79968

DISTRIBUTION (Continued):

Princeton University
Department of Civil Engineering
Attn: G. Pinder
Princeton, NJ 08504

Scientific Software-Intercomp
Attn: A. C. Gringarten
1801 California, 3rd Floor
Denver, CO 80202

University of California (2)
Lawrence W. Berkeley Laboratory
Attn: J. Long
S. M. Benson
Berkeley, CA 94720

University of Wisconsin-Madison
Department of Geology and Geophysics
Attn: M. P. Anderson
1215 W. Dayton St.
Madison, WI 53706

Emcon Associates
Attn: F. W. Fenzel
1921 Ringwood Ave.
San Jose, CA 95131

Gartner-Lee Associates
Attn: K. G. Kennedy
Toronto-Buttonville Airport
Markham, Ontario L3P3J9
CANADA

Netherlands Energy Research Foundation ECN (2)
Attn: T. Deboer, Mgr.
L. H. Vons
3 Westerduinweg
PO Box 1
1755 ZG Petten
THE NETHERLANDS

Nationale Genossenschaft für die
Lagerung Radioaktiver Abfälle (3)
Attn: P. Hufschmied
C. McCombie
M. Thury
Parkstrasse 23
CH5401 Baden
SWITZERLAND

1540 W. C. Luth
6000 D. L. Hartley
6300 R W. Lynch
6310 T. O. Hunter
6311 L. W. Scully
6312 F. W. Bingham
6314 J. R. Tillerson
6330 W. D. Weart
6330 Sandia WIPP Central Files (700H IND) (2)
6331 A. R. Lappin
6331 R. L. Beauheim (2)
6331 D. J. Borns
6331 M. M. Gonzales
6331 A. L. Jensen
6331 S. J. Lambert
6331 K. L. Robinson
6331 C. L. Stein
6331 D. Tomasko
6332 L. D. Tyler
6332 F. G. Yost
6416 P. A. Davis
6416 K. Brinster
6416 M. D. Siegel
6431 C. D. Updegraff
7100 C. D. Broyles
7120 M. J. Navratil
7125 R. L. Rutter
7130 J. D. Kennedy
7133 R. D. Statler
7133 J. W. Mercer
7135 P. D. Seward
8024 P. W. Dean
3141 S. A. Landenberger (5)
3151 W. L. Garner (3)
3154-1 C. H. Dalin (28)
For DOE/OSTI (Unlimited Release)